UNIVERSITY OF WOLVERHAMPTON
KNOWLEDGE • INNOVATION • ENTERPRISE

# MiRNA Influences in Mesenchymal Stem Cell Commitment to Neuroblast Lineage Development

VANESSA ZAMMIT M.Sc.

A thesis submitted in partial fulfilment of the requirements of the University of Wolverhampton for the degree of Professional Doctorate in Biomedical Science

November 2019



Signature.. [redacted] Date 15·11·2019

## Disclaimer

This is a statement to confirm that this dissertation 'MiRNA Influences in Mesenchymal Stem Cell Commitment to Neuroblast Lineage Development' is solely the work of Vanessa Zammit M.Sc.

Sections from Chapter 1, Chapter 2 and Chapter 3 have been presented to the University of Wolverhampton in the form of an Interim Report as part of module 8BM004.

The procedure for the collection and processing of cord samples and method for culturing of Mesenchymal Stem Cells has been published in the Malta's Midwives Journal: The Stork. The candidate contributed to most of the writing. Refer to:

Zammit, V. and Baron. B (2017) Points of Good Practice for the Sampling of Cords and Culturing of Mesenchymal Stem Cells, *Malta's Midwife Journal: The Stork*, **10**, p. 26.

Sections from Chapter 1 have been published as a review paper in *Genes* (doi: 10.3390/genes9010026). The candidate contributed to most of the writing. Refer to:

Zammit, V., Baron, B. and Ayers, D. (2018) MiRNA Influences in Neuroblast Modulation: An Introspective Analysis, *Genes*, **9**(1).

Sections from Chapters 1, 2, 3 and 4 have been published as an original article in the journal Non-coding RNA Research (doi: 10.10.1016/j.ncrna.2018.11.002). The candidate contributed to most of the writing. Refer to:

Zammit, V., Brincat, M. R., Cassar, V., Muscat-Baron, Y., Ayers, D. and Baron, B. (2018) MiRNA influences in mesenchymal stem cell commitment to neuroblast lineage development, *Non-coding RNA research*, **3**(4), pp. 232–242.

Sections from Chapters 2, 3 and 4 have been published as an original article in the Journal of Clinical and Translational Research (doi: 10.18053/jctres.05.201902.001). Authors contributed equally to the writing of the article. Refer to:

Zammit, V., Farrugia, M. and Baron, B. (2019) Redirection of transfusion waste and by-products for xeno-free research applications, *J Clin Transl Res*, **5**(2): 1.

# Consent Request

I am in the process of creating a thesis entitled "MIRNA influences in mesenchymal stem cell commitment to neuroblast lineage development", and I am writing to ask your permission to include the following material in this project:

"Points of good practice for the sampling of cords and culturing of mesenchymal stem cells" published in the Malta Midwives Journal, Issue 10, dated July 2017.

The thesis shall be submitted to the University of Wolverhampton in partial fulfilment for the attainment of a Doctorate in Biomedical Science. The thesis shall be used both for academic and research purposes and shall be available to my thesis supervisor, examiners and other students. The thesis will be accessed online through the University's official website.

I request non-exclusive world rights to use this material in my work, in all languages and for all editions and formats, including digital/electronic formats. These rights will in no way restrict republication of the material in any other form by you or by others authorised by you.

---

Permission granted for the use of the material as described above:

| Name and Title: | Signature: | Date: |
|---|---|---|
| Dr Byron Baron | [redacted] | 3/7/19 |
| Ms Vanessa Zammit | [redacted] | 03.07.2019 |

# Consent Request

I am in the process of creating a thesis entitled "MIRNA influences in mesenchymal stem cell commitment to neuroblast lineage development", and I am writing to ask your permission to include the following material in this project:

"Points of good practice for the sampling of cords and culturing of mesenchymal stem cells" published in the Malta Midwives Journal, Issue 10, dated July 2017.

The thesis shall be submitted to the University of Wolverhampton in partial fulfilment for the attainment of a Doctorate in Biomedical Science. The thesis shall be used both for academic and research purposes and shall be available to my thesis supervisor, examiners and other students. The thesis will be accessed online through the University's official website.

I request non-exclusive world rights to use this material in my work, in all languages and for all editions and formats, including digital/electronic formats. These rights will in no way restrict republication of the material in any other form by you or by others authorised by you.

---

Permission granted for the use of the material as described above:

| Name and Title: | Signature: | Date: |
|---|---|---|
| Dr Byron Baron | [redacted] | 3/7/19 |
| Ms Vanessa Zammit | [redacted] | 03-07-2019 |

# Consent Request

I am in the process of submitting a thesis entitled "MIRNA influences in mesenchymal stem cell commitment to neuroblast lineage development", and I request your permission to include the following material in this project:

"MiRNA influences in mesenchymal stem cell commitment to neuroblast lineage development" having reference DOI10.1016/j.ncrna.2018.11.002

The thesis shall be submitted to the University of Wolverhampton in partial fulfilment for the attainment of a Doctorate in Biomedical Science. The thesis shall be used both for academic and research purposes and shall be available to my supervisors, examiners and other students. The thesis will be accessed online through the University's official website.

I request non-exclusive world rights to use this material in my work, in all languages and for all editions and formats, including digital/electronic formats. These rights will in no way restrict republication of the material in any other form by you or by others authorised by you.

---

Permission granted for the use of the material as described above:

| Name and Title: | Signature: | Date: |
|---|---|---|
| Prof Yves Muscat Baron | [redacted] | 5/6/19 |
| Dr Viktor Cassar | | 5/6/19 |
| Dr Mark R. Brincat | | 6/6/19 |
| Dr Duncan Ayers | | 3/7/19 |
| Dr Byron Baron | | 4/6/19 |
| Ms Vanessa Zammit | | 06.06.2019 |

# Consent Request

I am in the process of submitting a thesis entitled "MIRNA influences in mesenchymal stem cell commitment to neuroblast lineage development", and I request your permission to include the following material in this project:

"Redirection of transfusion waste and by-products for xeno-free research applications" having reference DOI10.18053/jctres.05.201902.001

The thesis shall be submitted to the University of Wolverhampton in partial fulfilment for the attainment of a Doctorate in Biomedical Science. The thesis shall be used both for academic and research purposes and shall be available to my supervisors, examiners and other students. The thesis will be accessed online through the University's official website.

I request non-exclusive world rights to use this material in my work, in all languages and for all editions and formats, including digital/electronic formats. These rights will in no way restrict republication of the material in any other form by you or by others authorised by you.

---

Permission granted for the use of the material as described above:

| Name and Title: | Signature: | Date: |
|---|---|---|
| Dr Byron Baron | [redacted] | 28/02/2020 |
| Mr Mark Farrugia | [redacted] | 01/12/2019 |
| Ms Vanessa Zammit | [redacted] | 20-02-2020 |

## Acknowledgements

I would like to sincerely thank my supervisors, Dr Byron Baron and Dr Duncan Ayers. Their patience, determination, enthusiasm towards research, attention to detail, advice and guidance throughout these years were essential for the completion of this study. Their sense of purpose when what seemed insurmountable problems cropped up certainly encouraged me to persevere.

I cannot let this opportunity pass without making special reference to my indebtedness towards my Director of Studies Professor Tracy Warr, Dr James Vickers and other staff in various Departments at the University of Wolverhampton for their courteousness and support during my visits to the university.

I am grateful to Professor Yves Muscat Baron, Dr Viktor Cassar, Dr Mark Brincat and all the staff of the Obstetrics and Gynaecology Department at Mater Dei Hospital for their precious support in recruiting donors and collecting cord samples that made this research possible.

My thanks to Professor Anthony Fenech for allowing me to use the facilities of the Allied Research Unit at the Department of Clinical Pharmacology at the University of Malta, as well as all members of his staff for putting their resources at my disposal to pursue this research project.

My thanks go also to Dr Christian Saliba, for his unfailing advice; Ms Josette Zammit B.Sc. for dedicating much of her time to proofreading and for her valuable suggestions; Ms Dorianne Buttigieg and Ms Sharon Falzon from the Pathology Department, Mater Dei Hospital, Malta for assisting with staining protocols and equipment; Professor Liberato Camilleri from the Statistics & Operations Research, Faculty of Science, University of Malta for his statistical guidance. Thanks also to the Management and my close colleagues at the National Blood Transfusion Centre for their interest and encouragement.

I would like to acknowledge the financial support obtained through the Malta Government Scholarship Scheme.

Last but certainly not least thanks go to my family for all their love, encouragement and constant support.

## Abstract

Mesenchymal Stem Cells (MSCs) are multipotent stromal cells that can self-renew and differentiate into cells from the mesodermal cell lineage. Under specific conditions, MSCs are known to transdifferentiate into the neuronal cell lineage. The aim of this study was to investigate if specific microRNAs (miRNAs) are responsible for neural induction, differentiation and fate specification and if they can induce MSCs to commit to a neuroblast and/or mature neuron cell lineage. The selected miRNAs were miR-107, miR-124 and miR-381, which respectively are known to promote neurogenesis, neural differentiation and neural proliferation. Targeting protein expression by transiently destroying the messenger RNA using miRNAs is an alternative to destroying the gene permanently and, being a transient process, the cells being differentiated should not retain any permanent evidence of this process. The objectives of this study were to culture MSCs from the Wharton's Jelly, transform these MSCs into neural-like cells using the spent medium from the neuroblastoma cell line SH-SY5Y, and further treat these

conditioned cells with retinoic acid to induce further maturation. MSCs were characterised by trilineage differentiation and all three cell types were tested for a series of CD and neural markers. Once characterised, the three cell types were transfected with one of the three selected miRNAs and a target gene for each miRNA was analysed but results were sub-optimal. The MSCs and neural-like derivatives were then tested for a selection of neural markers. Once again results provided limited information, however it was observed that miR-107 and miR-124 have the potential to induce MSCs to differentiate into neural-like cells and that these miRNAs may also induce intermediate neural progenitors and immature neuron cell types to differentiate further.

# Table of Contents

# List of Tables

# List of Figures

# List of Abbreviations

| | |
|---|---|
| AgNP | Silver nanoparticles |
| AKT2 | V-akt murine thymoma viral oncogene homolog 2 |
| BDNF | Brain-derived Neurotrophic Factor |
| BM | Bone Marrow |
| BMP | Bone Morphogenetic Proteins |
| $CaCl_2$ | Calcium Chloride |
| CC | Conditioned Cells |
| CD | Cluster of differentiation |
| cDNA | Complementary DNA |
| CNS | Central Nervous System |
| CPP | Cryo Poor Plasma |
| Cq | Quantification cycle |
| dlx-2 | Distal-less Homebox 2 |
| DMEM/F-12 | Dulbecco's Modified Eagle Medium: Nutrient Mixture F-12 |
| DMSO | Dimethyl Sulfoxide |
| E2F3 | E2F Transcription Factor 3 |
| EDTA | Ethylenediaminetetraacetic acid disodium salt dihydrate |
| EGF | Epidermal Growth Factor |
| EPHB2 | Ephrin type-B receptor 2 |
| FBS | Foetal Bovine Serum |
| FGF | Fibroblast Growth Factor |
| FLNA | Filmin Alpha |
| FOXO | Forkhead Transcription Factor Family O |
| GAPDH | Glyceraldehyde-3-phosphate dehydrogenase, |
| GFP | Green Fluorescent Protein |
| GO | Graphene Oxide |
| HES1 | Hairy and Enhancer of Split 1 |
| HES1/3 | Hairy and Enhancer of Split 1/3 |
| HNF4A | Hepatocyte Nuclear Factor 4 Alpha |
| HSC | Haematopoietic Stem Cells |
| IGF | Insulin-like Growth Factor 1 |
| iPSCs | Induced Pluripotent Stem Cells |
| ISCT | International Society for Cellular Therapy |
| LB | Luria Broth |
| KCNQ2 | Potassium Voltaged-Gated Channel Subfamily Q Member 2 |
| MAP2 | Microtubule-associated protein *2* |

| | |
|---|---|
| MASH-1 | Mammalian Achaete-Scute Homolog-1 |
| MiRNAs | MicroRNAs |
| mRNA | Messenger RNA |
| MSC | Mesenchymal Stem Cell |
| ND1 | NeuroD1 |
| NEFM | Neurofilament Medium Polypeptide |
| NES | Nestin |
| NEU | Neuronal-specific Nuclear Protein 1 |
| NGF | Neural Growth Factor |
| NSCs | Neural Stem Cells |
| NTC | Non-Template Control |
| OCT4 | Octamer-binding Transcription Factor 4 |
| P/S | Penicillin/streptomycin |
| PAX 6 | Paired-box Protein 6 |
| PBS | Phosphate buffer saline |
| PCR | Polymerase Chain Reaction |
| Pre-miRNA | Precursor miRNA |
| PSD95 | Postsynaptic Density Protein 95 |
| PTP1B | Polypyrimidine Tract-Binding Protein 1 |
| RA | Retinoic Acid |
| RA-CCs | RA-treated CCs |
| REST | RE-1 silencing transcription factor |
| RT | Reverse Transcription |
| RT-qPCR | Real Time Polymerase Chain Reaction |
| Runx2 | Runt-related Transcription Factor 2 |
| SCNBA | Sodium Channel Protein Type 1 Subunit Alpha |
| SCP1 | Small C-terminal domain Phosphatase 1 |
| Shh | Sonic Hedgehog |
| SiRNA/SiR | MicroRNA antagonist |
| SOX10 | Sex Determining Region Y-Box 10 |
| SOX2 | Sex Determining Region Y-Box 2 |
| SOX9 | Sex Determining Region Y-box 9 |
| SYN2 | Synapsin II |
| TAE | Tris-acetate-EDTA |
| TB Fix | Tokuda-Baron Fixative |
| TBR1 | T-box brain protein 1 |
| TBR2 | T-box brain protein 2 |
| TGF | Transforming Growth Factor |
| TGF-β | Transforming Growth Factor- beta |
| Th | Tyrosine hydroxylase |
| TUBB3 | Beta III Tubulin |
| Wnt | Wingless-type MMTV integration site |
| ZIC | Zinc Finger Marker |

# Chapter 1
# Introduction

## 1.1. Stem Cells

Stem cells are undifferentiated cells with the unique property to become specific cells that make up tissues and organs. The term "Stem Cell" is a generalised terminology for cells displaying two fundamental characteristics defined as stemness properties i.e. self-renewal, where cells create identical copies of themselves; and differentiation, during which these cells become specialised and are then committed to one specific cell lineage. Stemness markers such as Nanog a transcription factor which regulates stem cell pluripotency (Allouba *et al*., 2015), Octamer-binding Transcription Factor 4 (OCT4) a gene essential for somatic cell reprogramming (Zeineddine *et al*., 2014) and Sex Determining Region Y Box 2 (SOX2), a transcription factor that plays an important role in the maintenance of pluripotency (Park *et al*., 2012), also characterise these cells (Yu *et al.*, 2016). Stem cells maybe (i) totipotent and so may give rise to any type of cell; (ii) pluripotent meaning that they may become any cell type apart from those of extraembryonic origin; (iii) or multipotent, which may

develop into cell types of a specific lineage (Singh *et al*., 2016). Cells which pertain to the stem cell category include:

- Embryonic Stem Cells which originate from the blastocyte and appear only during the early stages of development. These are termed as pluripotent stem cells since they lack the ability to differentiate into non-embryonic cells such as placenta (Singh *et al*., 2016).
- Tissue Specific Stem Cells or adult stem cells consisting of more specialised cells such as Hematopoietic Stem Cells (HSCs). These cells are multipotent stem cells (Cheng, Zheng and Cheng, 2020). They have a limited differential potential and are normally committed into becoming a predefined cell type and do not differentiate into other cell types.
- Mesenchymal Stem Cells (MSCs) which are traditionally found in the bone marrow (BM) stroma. These cells are considered to be multipotent stem cells (Caplan, 2017) and may differentiate into cells of the mesodermal germ layer but may also transdifferentiate into cell types pertaining to

endodermal and ectodermal origin. Transdifferentiation is when a cell type pertaining to one particular tissue or organ is able to convert itself into a cell of a completely different tissue or organ without the need of reverting back to a pluripotent stage (Mollinari *et al*., 2018). MSC cells were first isolated and described in 1976 by Friendenstrein *et al.*, as fibroblast-like cells belonging to the hematopoietic group of cells that functioned as supportive cells of the BM (Zhang *et al.*, 2018). MSCs were subsequently isolated from BM cultures as plastic adherent stromal cells capable of differentiating into mesoderm-derived cells.

- Induced Pluripotent Stem Cells (iPSCs) are *in-vitro* modified somatic cells which have reverted to their embryonic stage. As the name implies these cells are of the pluirpotent type.

## 1.2. Mesenchymal Stem Cells

MSCs are multipotent stromal cells that are capable of self-renewal and may differentiate into a variety of cell types which include osteoblasts, chondrocytes, myocytes and adipocytes (Ullah, Subbarao and Rho, 2015). Originally, these cells where thought to originate from the BM as a sub-population which supports the function of BM cells. However, these stromal cells are today recognised as multi-linage cells which are also found in adipose tissue, amnion, synovial fluids, muscles, dermis, teeth pulp and umbilical tissue (Lv *et al.*, 2014). The functions of MSCs are related to immunomodulation and regeneration (Caplan and Hariri, 2015), and involves both the paracrine and endocrine systems (Hoogduijn and Dor, 2013).

Isolation of MSCs from BM samples is met with reluctance in terms of ethical approval, availability and collection, since sampling may result in pain, bleeding or infection (Berebichez-Fridman and Montero-Olvera, 2018). Furthermore, in Malta, it is very difficult to obtain BM samples for research purposes and most of the donated are

in the form of a few grams of BM scrapings. These samples are obtained by scrapping off some BM from the thorax during open heart surgery and mainly consist of bone which, in conjunction with the small amount collected, are not suitable for cell culture. Due to the limitation of securing adequate BM samples, for this project Wharton's Jelly was chosen as the source for the isolation of MSCs.

Non-foetal derived MSCs may also differentiate into several cell lineages (West *et al*., 2016) and this differentiation method provided an alternative solution to somatic cell transfection with the added advantage of having both a lower tumorigenic risk and a lower risk of grafting rejection (Cortés-Medina *et al.*, 2019). In this project, once MSCs were isolated from the Wharton's Jelly, transdifferentiation of these cells into neural-like cells was induced by a selection of microRNAs (miRNAs). Transdifferentiaiton of MSCs is the result of the combined effort of several factors. Knowing whether miRNAs directly involved in neurogenesis may induce such a change would help better elucidate such mechanisms. In a similar study conducted by Cortés-

Medina *et al*. (2019), MSCs cultured from BM, umbilical cord and placenta, dental tissue and skin were induced to transdifferentiate into neural-like cells by supplementing cell culture medium with ICFRYA, a small molecule cocktail. Transdifferentiation of the MSCs was then confirmed via neuronal morphology and function, neuronal marker analysis and downregulation of CD90 and CD105. The transdifferentiation of adult-derived MSCs is, however, very limited. Although Cortés-Medina *et al*., demonstrated that it is possible to induce the neural differentiation of MSCs, they were not able to induce this change from all the different sources tested. A full differentiation was achieved in MSCs isolated from BM and umbilical cord blood and a partial differentiation was seen with the cells derived from the dental tissue and skin sources. No differentiation was reported from MSCs isolated from Wharton's Jelly. This demonstrated that although MSCs have the potential to transdifferentiate not all sources are ideal.

### 1.2.1. Characterisation of Mesenchymal Stem Cells

The standardised attributes defining MSCs were declared by the International Society for Cellular Therapy (ISCT) (Dominici *et al.*, 2006) and these are:

1. plastic adherence
2. expression of CD105, CD73 and CD90, and lack of expression of CD45, CD34, CD14, CD79alpha and HLA-DR surface molecules.
3. *in vitro* differentiation into osteoblasts, adipocytes and chondrocytes.

#### 1.2.1.1. Cluster of Differentiation Markers

Cluster of differentiation (CD) molecules perform a variety of cellular functions but are commonly referred to in terms of being membrane proteins found on the cell surface that identify the cell, monitor differentiation stages and sort cell sub-populations. These markers have been used both in research and diagnosis and recently have been employed in the treatment of several malignancies and autoimmune diseases (Engel *et al*., 2015). More than 400 CD markers have been identified and each is assigned a number which

identifies a group of surface antibodies (Dawson and Lunney, 2018).

In their position paper, Domenici *et al*. do not indicate how the ISCT establish how the selected CD markers may or may not identify a cell as an MSC in terms of a specific cellular function. However, CD73 expression regulates the phenotypes of T and Natural Killer Cells and also acts as a cell marker for progenitor stem cells (Monguió-Tortajada *et al*., 2017). CD105 is a component of the receptor complex of transforming growth factor-beta (TGF-β) which is involved in cell proliferation, differentiation and migration (Maleki *et al*., 2014). The role of CD90 in MSCs is still unknown *(*Moraes *et al.*, 2016), however it is postulated that this is a marker for MSC progenitors (Michelis *et al.*, 2018). CD45 and CD34 are markers of HSC and progenitor cells, and MSCs are not hematopoietic cells (Sidney *et al*., 2014). CD14 acts as a co-receptor expressed mainly by macrophages, neutrophils and dendritic cells (Jiang *et al.*, 2019). CD79 is a B-cell marker, and MSCs are not members of this family *(*Healy *et al.*, 2015); since one of the

properties of MSCs is their immune modulatory effect, these cells should be HLA-DR negative.

MSCs may be isolated from different sources and different species, so a wider range of CD markers are now being used, which allows for further cell differentiation. The CD marker characterisation established by the ISCT was based on BM-derived MSCs and does not take into consideration the source of origin or the isolation technique used (Okolicsanyi *et al*., 2015). However, identification of MSCs should not be limited to these CD markers since MSCs derived from other sources possess less defined characteristics (Ullah, Subbarao and Rho, 2015) and most importantly, no CD marker is specific for MSCs (Davies *et al*., 2015). Table 1.1 categorises the use of CD markers according to the source from where the MSCs were originally obtained.

| Source | Positive Markers | Negative Markers | Source |
|---|---|---|---|
| Bone marrow | CD73, CD90, CD105, STRO-1 | CD14, CD34, CD45, HLA-DR | Pittenger *et al*., 1999; Mamidi *et al*., 2012; Otsuru *et al*., 2013; Gronthos *et al*., 1994 |
| Adipose tissue | CD73, CD090, CD29, CD44, CD71, CD105, CD13, CD166, STRO-1 | CD14, CD31, CD34, CD45 | Wagner *et al*., 2005; Zhang *et al*., 2011; Pendleton *et al*., 2013; Gronthos *et al*., 2001; Baglioni *et al*., 2009 |
| Amniotic fluid and membrane | CD29, CD44, CD90, CD105, SH2, SH3, HLA-DR | CD10, CD14, CD34, HLA-DR | In 't Anker *et al*., 2003; Tsai *et al*., 2004; Cai *et al*., 2010 |
| Dental tissue | CD29, CD44, CD90, CD105 | CD14, CD34, CD45 | Huang, Gronthos and Shi, 2009; Seifrtová *et al*., 2012; Kadar *et al*., 2009 |
| Endometrium | CD73, CD90, CD105, CD146 | CD34, CD45 | Schüring *et al.*, 2011 |
| Limb bud | CD13, CD29, CD90, CD105, CD106 | CD3, CD4, CD14, CD15, CD34, CD45, HLA-DR | Jiao *et al*., 2012 |
| Peripheral blood | CD44, CD90, CD105, HLA-ABC | CD45, CD133 | Ab Kadir *et al*., 2012 |
| Placenta and foetal membrane | CD29, CD73, CD90, CD105 | CD34, CD45 | Raynaud *et al.*, 2012 |
| Salivary gland | CD13, CD29, CD44, CD90, STRO-1 | CD34, CD45 | Rotter *et al*., 2008; Riekstina *et al*., 2008 |
| Skin and Foreskin | CD44, CD73, CD90, CD105, CD166, SSEA-4, Vimentin | CD34, CD45, HLA-DR | Bartsch *et al*., 2005 |
| Sub amniotic umbilical cord lining membrane | CD29, CD44, CD73, CD90, CD105 | CD34, CD45 | Wagner *et al.*, 2005; Kita *et al*., 2010; Moretti *et al*., 2010 |
| Synovial fluid | CD44, CD90, CD105, CD147, STRO-1 | CD31, CD34, CD45, CD106 | Morito *et al*., 2008 |
| Wharton's jelly | CD73, CD90, CD105 | CD14, CD34, CD45, CD79, HLA-DR | Hou *et al*., 2009; Kuznetsov *et al*., 1997 |

**Table 1.1: Mesenchymal Stem Cells sources and cell surface markers** (adapted from Ullah, Subbarao and Rho, 2015)

In this project, MSCs were characterised by tri-lineage differentiation, followed by a panel of CD markers. As illustrated in Table 1.1, MSCs isolated from Wharton's Jelly are characterised as being positive for CD73, CD90, CD105 and negative for CD14, CD34, CD45 and CD79. All three recommended positive markers, that is, CD73, CD90 and CD105 were tested in this project. CD73 was chosen in view that neural cells are negative for CD73 and this would indicate that MSCs would have tansdifferentiaiton into neural-like cells. Both CD90 and CD105 are expressed by neural cells. Two negative markers, CD34 and CD45, were selected out of the recommended panel of negatives because CD34 may also be expressed by neuroblastoma and neural cells that are not fully mature, while CD45 is the most commonly used negative CD marker for the characterisation of MSCs and is also not expressed by neural cells.

As previously discussed, these markers do not pertain exclusively to the characterisation of the MSC lineage: CD73 is an ecto-enzyme and a key molecule that regulates cancer

progression (Buisseret *et al*., 2018); CD90 is a glycoprotein marker highly associated with brain, kidney and pancreatic tumours (Sauzay *et al*., 2019); CD105 is a marker for tumour-related vascular endothelial cells (Kasprzak and Adamek, 2018); CD34 a transmembrane phosphoglycoprotein that acts as a marker for different cell progenitors including muscle satellite cells, corneal keratocytes, interstitial cells, epithelial progenitors, and vascular endothelia progenitors but used primarily for the selection and enrichment of HSCs for BM transplants (Sidney *et al.*, 2014); and CD45 is a protein tyrosine phosphatase enzyme expressed by lymphoid cells responsible for cell proliferation and postulated to be a potential target for cancer drug treatment (Perron and Saragovi, 2018).

### 1.2.2. MSC differentiation and therapeutic potential

The three germ layers arise during the early stages of the embryonic development during the process of gastrulation. After an egg has been fertilised, the zygote eventually becomes a blastocyst. The blastocyst contains an inner cell

mass which eventually will develop into the organism. The outside of the blastocyst contains trophoblast cells and the inside contains an inner core known as the blastoseal. This inner core contains a fluid which nourishes the inner cells of the inner cell mass. As the blastocyst develops the trophoblasts differentiate into syncytial-trophoblasts and cyto-trophoblasts. The syncytial-trophoblasts become invasive and release digestive enzymes allowing the blastocyst to implant into the endometrium of the uterus. The syncytial-trophoblasts embedded in the endometrium lining will later develop into the placenta. Eventually the blastocytes will enter the endometrium of the uterus where the inner cell mass will begin to differentiate into two layers, which are composed of the epiblast (the lower layer) and the hypoblasts (the upper layer) cells. The two layers will continue to develop forming cavities within each other but will remain connected to the rest of the cells via the connecting stalk. The epiblast cells migrate into the midline to form the primitive streak. Some of the epiblast cells will migrate into the primitive streak and enter the hypoblast layer creating the endoderm. The epiblast cells which do not

migrate will differentiate and become the ectodermal layer. At this stage the majority of epiblast cells would be occupying the space between the epiblast and hypoblast layers. These cells will differentiate and form the mesodermal layer. The ectoderm layer will give rise to the outer cells of the body such as skin and hair but will also develop into the nervous system and the neural crest which eventually structures the face and brain. The endoderm is responsible for the development of the inner organ cells, while the mesoderm will form muscles and bones (Solnica-Krezel and Sepich, 2012).

MSCs differentiate into cells pertaining to the mesodermal germ layer, but under certain conditions, these cells may be induced to differentiate into cells belonging to the ectodermal and endodermal linages. This mechanism of transdifferentiation led to the development of promising cell-based therapies for the treatment of both neurological and endocrine disorders.

Ectoderm MSC differentiation produces cells of the nervous system and epidermis. MSCs are known to transdifferentiate into the cells of the ectodermal cell linage when treated with growth factors such as hepatocyte growth factor, Fibroblast Growth Factor (FGF) and Epidermal Growth Factor (EGF) (Datta *et al*., 2011). Other studies postulate that a combination of the transcription factor neurogenin-1 and LIM homoeobox transcription factor 1 (Barzilay *et al.*, 2009), β-Mercaptoethanol and nerve growth factor (Naghdi *et al*., 2009), and factors like insulin and retinoic acid (RA) enhance the differentiation of MSCs into neural-like cells (Ullah, Subbarao and Rho, 2015).

Endodermal differentiation causes MSCs to transdifferentiated into either pancreocytes or hepatocytes. The possibility of differentiating MSCs into pancreocytes has successfully resulted in the culturing of insulin producing β-cells (Tang *et al.*, 2012) which is intended to replace the standard drug therapeutic approach to Diabetes with a more tailored cell-based therapy. To a lesser degree of success, hepatocytes have also been obtained from MSCs, however

their ability to differentiate and thus be used for therapeutic applications requires further elucidation (Ullah, Subbarao and Rho, 2015).

Two properties of MSCs - their multipotentiality and ease of isolation - show the potential of using these cells for tissue engineering and therapeutic applications for ischemic, inflammatory, and immunological disorders such as sclerosis (Fellows *et al.*, 2016). The therapeutic effectiveness of MSCs is associated with their unique characteristic of homing to the site of tissue injury or inflammation after systemic administration (Karimineko*o et al.*, 2016), their ability to differentiate into various cell types, stimulate the recovery of damaged cells and inhibit inflammation by secreting multiple bioactive molecules such as cytokines, growth factors, and chemokines (Taran *et al*., 2014; Wang, Yuan and Xie, 2018) and the absence of immunogenicity, which makes performing immunomodulatory functions possible (Mukonoweshuro *et al*., 2014).

#### 1.2.2.1. Mechanism of differentiation

MSC differentiation entails (i) lineage commitment, during which MSCs transform into lineage-specific progenitors, and (ii) maturation, where the progenitors become specific cell types. Several signalling pathways regulate the lineage commitment of MSCs, including TGFβ/bone morphogenetic protein (BMP) signalling, Wingless-type MMTV integration site (Wnt) signalling, Sonic Hedgehog (Shh), Notch, and FGFs (Chen *et al.*, 2016). These pathways are activated via the interaction of MSCs and the microenvironment which is composed of various extracellular matrix components, growth factors, cytokines, and chemokines that consequently activate or inhibit cell lineage commitment. Transdifferentiation is the result of a change in the expression of a master regulator gene which is responsible for the normal development of one specific tissue (Li *et al*., 2005). This change is finely regulated by cellular signalling pathways which are in turn dependent on key transcription factors (Chen *et al.*, 2016). Transcription factors responsible for cell fate determination in MSCs are: PPAR*γ* for the adipocyte commitment; and Runt-related transcription

factor 2 (Runx2) for osteogenesis and chondrogenesis differentiation. The osteo/adipocyte balance is dependent on the expression of these factors where an increased PPARγ expression will inhibit osteogenesis (Moerman *et al*., 2004). *In vivo* this imbalance is mostly seen in osteoporosis patients and is described as an increase in BM adiposity. Similarly, an increased expression of Runx2 will sustain osteogenesis and suppress the production of adipocytes (Huang *et al.*, 2010).

To be able to differentiate into the desired cell lineage, stem cells are required to undergo several progression stages (Lee, Abdeen and Kilian, 2014). *In vivo*, transdifferentiation is a natural process. It is a vital mechanism during the development of the new cell lineage and plays a critical role during the developing and regenerative processes since functional cells of different lineages need to be formed from distinct stem cells (Sisakhtnezhad and Matin, 2012). During development, cell fate specification is determined by a complex set of transcription factors and epigenetic networks. This process is no longer considered as

irreversible and *in vitro* it is now possible to bring about transdifferentiation of certain cells by inserting lineage-specific transcription factors into these cells. However although highly efficient results have been seen, unlike iPSCs, transdifferentiaiton can be unstable and cells may lose their pluripotent properties.

There are two ways in which a cell may transdifferentiate. The first is a direct differentiation where the cell differentiates completely into a new cell type. The other method is known as a two-stage differentiation. In this case during transdifferentiation the cell will undergo partial differentiation. At this stage, the cell cycle is stopped so that the chromatin may be modified. This modification alters the cell-specific transcription and causes both epigenetic and chromosome architecture modifications. Once cell fate is committed, the cell will continue to differentiate into the desired cell lineage (Sisakhtnezhad and Matin, 2012). These transition intervals permit progenitors, which are not yet committed to a specific cell lineage, to be reprogrammed back to the multipotent stem cell state (Zhang and Kilian,

2013). Early differentiation *in vitro* is generally triggered by specific media formulations of small molecules and proteins, such as in the case of the tri-lineage characterisation of the MSCs, in which cells are forced to differentiate into osteocytes, adipocytes and chondrocytes using induction (differentiating) media. Synthetic matrices that modify the microenvironment have also been used to bring about cell differentiation (Bloom and Zaman, 2014); for example, culturing MSCs on scaffolds creates a 3D environment which mimics that found *in vivo* thus preserving their pluripotent gene expression (Zhou *et al*., 2017). This cell modulation is possible through signalling pathways responsible for cell specificity which are triggered by extracellular signals which activate transduction cascades that regulate gene expression and cell fate (Zhang and Kilian, 2013). In fact, early markers for osteogenesis and neurogenesis, such as Runx2 and Beta III Tubulin (TUBB3) respectively, are more likely to respond to the microenvironmental change than later markers like osteopontin and Microtubule-associated protein 2 (MAP2) (Lee, Abdeen and Kilian, 2014).

The changes seen during this transformation may not be the result of a true transdifferentiation but may be a consequence of external factors such as cell fusion. To determine that transdifferentiation has actually occurred the cells must satisfy two important criteria which are (i) the differentiation stage of the cell before and after transdifferentiaiton and, (ii) demonstrate the cell lineage of the two cells types (Li *et al*., 2005).

## 1.3. Neurogenesis

### 1.3.1. Neural cells

The neural cell lineages evolve from neuroectodermal progenitor cells which become Neural Stem Cells (NSCs) (Kessaris, Pringle and Richardson, 2008). Neuronal progenitors undergo an additional differential stage and subdivide into neurones and glia (Shenoy and Blelloch, 2014).

### 1.3.2. Neural differentiation

The *in vitro* transition from stem cells to neural cells (Figure 1.1.), involves several complex procedures including, but not limited to: cell proliferation, fate specification, differentiation and maturation. To proceed to ectodermal differentiation, stem cells need to lose their original characteristic feature markers such as Nanog, OCT4 and SOX2. This loss of stemness is brought about by inducing agents such as BMP signalling inhibitors Noggin and dorsomorphin, and TGFβ inhibitor SB431542 (Madhu *et al.*, 2016).

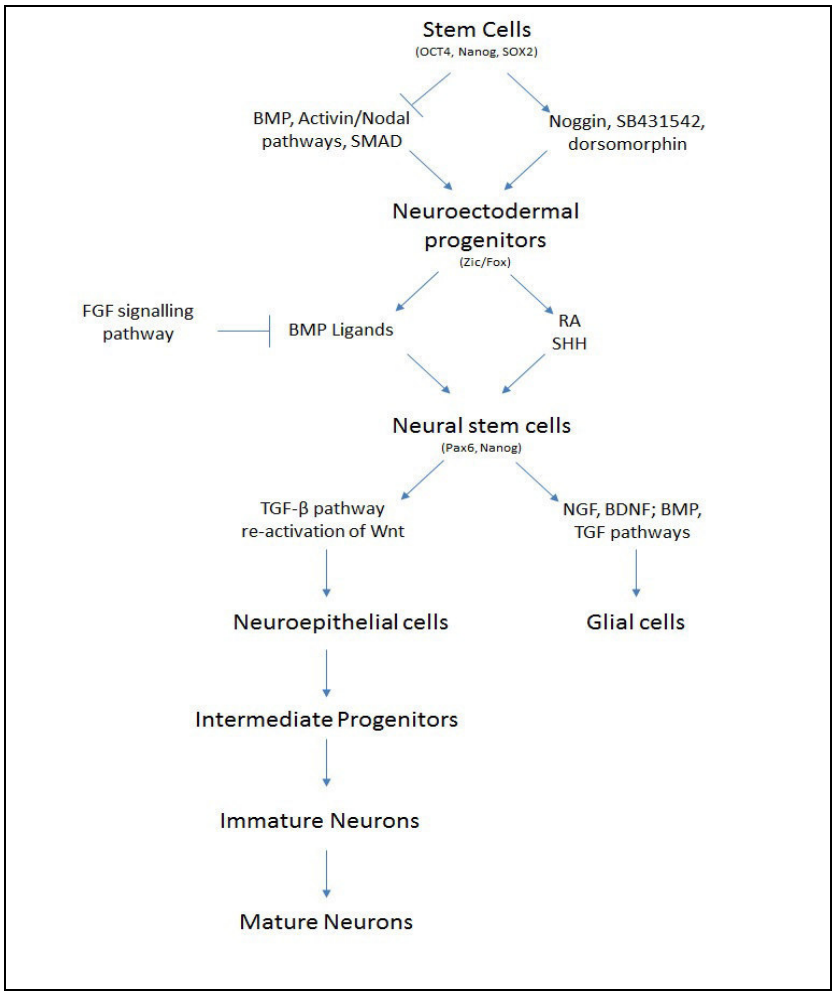


**Figure 1.1: Stem cells to neural cell lineage Transdifferentiation** (Mishra, Derynck and Mishra, 2005)

Stem cells differentiate into neuroectodermal progenitors in the presence of Noggin, SB431542 and dorsmorphin and subsequent interference of the TGF-β/Activin/NODAL pathways. FGF and Shh signalling pathways together with RA further differentiate these progenitors into NSCs which are influenced in turn by the reactivation of the TGF-β pathways that promote NSC proliferation and by the Wnt signalling pathway which determines cell specification.

Legend: OCT4 - Octamer-binding transcription factor 4, SOX2 - Sex determining region Y-Box 2, BMP - Bone Morphogenetic Proteins, ZIC – zinc finger marker, FOX - Forkhead transcription factor, FGF – Fibroblast Growth Factor, RA – Retinoic acid, Shh – Sonic Hedgehog, Pax6 - Paired box protein 6, NGF – neural growth factor, BDNF - Brain-derived neurotrophic factor, TGF – Transforming Growth Factor, PAX6 - paired-box protein 6 .

SB431542, a selective and potent inhibitor of the TGF-β/Activin/NODAL pathway (Taïhi *et al.*, 2019), replaces SOX2 during reprogramming (Zheng *et al.*, 2018), and in conjunction with Noggin, a protein responsible for neural growth, it promotes neural progenitor differentiation (Chambers *et al.*, 2012). Once neuroectodermal progenitors are formed, the original stemness markers are replaced with other neuro-ectoderm gene markers such as Zinc Finger Marker and Forkhead Transcription Factor (Wu et al., 2016). Dorsomorphin inhibits the BMP signalling pathway (Dasgupta and Seibel, 2018), halting embryogenesis and promoting neural differentiation (Feng *et al.*, 2016). Once the neuroectodermal progenitors are formed the FGF signalling pathway causes neural induction by inhibiting the expression of BMP ligands (Dorey and Amaya, 2010). Neural differentiation is further encouraged by the release of RA, a metabolite of Vitamin A and signalling molecule that modulates the development and maintenance of the Central Nervous System (CNS) (Oliveira *et al*., 2018). The Shh signalling pathway further induces the differentiation of these progenitors into NSCs by promoting self-renewal and

proliferation (Liebelt *et al.*, 2016). The differentiation of neuroectodermal progenitors to NSCs is confirmed by the presence of gene markers such as Nanog and Paired-box Protein 6 (Su *et al.*, 2018). Once NSCs are formed, the reactivation of the TGF-β pathway induces the proliferation of these NSCs, thus sustaining neurogenesis. Rather than proliferation, the Wnt signalling pathway further promotes the differentiation of NSCs, determining cell specification (Navarro Quiroz *et al.*, 2018).

Different studies have shown how MSCs are able to differentiate into neural cell types either by using induction agents which are added to the culturing media. Neuronal inducing agents include RA, brain-derived neurotrophic factor (BDNF), and phorbol esters, as well as vasoactive intestinal peptide, graphene oxide (GO), silver nanoparticles (AgNP), and GO-AgNP nanocomposites (Abdal Dayem *et al.*, 2018); or the use of conditioned media from co-cultured neural cells such as neurons, oligodendrocytes, and Schwann cells (Takeda and Xu, 2015). In their study, Abdal Dayem *et al*. compare parameters for cells which were

treated with the RA neural inducing agent to AgNP-treated cells. AgNP have several beneficial properties but may also result in cytotoxicity (Xu *et al*., 2013). Abdal Dayem *et al*. report no cytotoxicity in the initial stages of neural induction and conclude that the higher reactive oxygen species generation enhances the expression of neuronal differentiation genes which subsequently results in neurite growth. On the other hand, as a result of the AgNP-treatment, they also report a downregulation of the expression of the genes encoding the antioxidant enzymes which may damage the neural cells. In this study MSCs have been made to transdifferentiate into cells of the neuronal cell lineage by adding conditioned medium obtained from the culturing of SH-SY5Y. The SH-SY5Y are human neuroblastoma-derived cells used in research as *in vitro* models for neural function and differentiation. After treating the MSCs with the spent medium the resultant fold change for both CD and neural markers seen between the treated and untreated cells was statistically significant when tested with Mann-Whitney U. P value $<0.05$ thus accepting

the alternative hypothesis that there is a difference between the two cells types.

#### 1.3.2.1. Neural Progression and Characterisation

Neuroepithelial cells are neural progenitors that constantly self-renew and produce post-mitotic cells (Yamashita, 2013) which pass through multiple stages to finally become mature neurons (Wang *et al.*, 2014). Once neurons mature they lose their stemness properties and are able to receive, process and transfer information throughout the CNS (Kole, Annis and Deshmukh, 2013). Neural stage markers (Table 1.2) are expressed by cells that are formed during neurogenesis which have been committed to the neuron cell linage and these help distinguish between cells which have a neural phenotype from other brain cell types (Tanapat, 2016).

| | Neural Cell Type | | | |
|---|---|---|---|---|
| | **Neuroepithelial cells** | **Intermediate Progenitors** | **Immature Neurons** | **Mature Neurons** |
| **Neural Marker** | NES<br>SOX2<br>Notch1<br>HES1/3<br>E-Cadherin<br>Occludin<br>SOX10 | TBR2<br>MASH1 | ND1<br>TUBB3<br>Doublecortin<br>TBR1<br>Stathmin1 | MAP2<br>NEU<br>Synaptophysin<br>160kDa Neurofilament<br>medium 200kDa Neurofilament<br>heavy<br>PSD95 |

**Table 1.2.: Neural Markers indicating the stage of neural differentiation**
Legend: NES – Nestin, ND1 – NeuroD1, TBR2 - T-box brain protein 2, MAP2 - Microtubule-associated protein *2,* SOX2 - Sex determining region Y-Box 2, TUBB3 - Beta III Tubulin, MASH-1 - mammalian achaete-scute homolog-1, NEU - neuronal-specific nuclear protein 1, Hes1/3 – Hairy and enhancer of split 1/3, SOX10 - Sex determining region Y-Box 10, TBR1 - T-box brain protein 1 and PSD95 – Postsynaptic density protein 95.

### 1.3.3. MicroRNAs

First discovered in *Caenorhabditis elegans* (Lee, Feinbaum and Ambros, 1993), miRNAs are a family of small, non-coding single stranded RNAs of approximately 22 nucleotides in length that bind to the complementary sequences in the 3’ untranslated regions of their messenger RNA (mRNA) targets (De Antonellis *et al.*, 2014). Once bound, these miRNAs become targets for degradation and negatively regulate protein expression (Elramah, Landry and Favereaux, 2014). This regulation is achieved by repressing

translation and/or decreasing transcript stability (Ristori *et al.*, 2015), causing the mRNA to degrade and consequently affect cell proliferation, differentiation, apoptosis or other biological processes (Mahmoudi and Cairns, 2017).

MiRNAs regulate the majority of protein coding genes and apart from acting as translation inhibitors, they are also directly related to the development and progression of many cancers (Manier *et al*., 2017). Holistically, neurogensis involves the self-renewal and fate specification of NSCs, the migration and maturation of young neurons and the functional integration of new neurons into the neural cavity. By base pairing with the target mRNA and subsequent regulation of the target gene expression, miRNAs are directly involved in all the phases of neurogenesis (Winter, 2015). During this process, miRNAs are themselves regulated by transcription factors such as TLX and epigenic factors such as MeCP2 and MBD1 (Shi *et al*., 2010).

#### 1.3.3.1. Nomenclature of microRNAs

The miRNA naming system follows the miRBase repository guidelines (Ambros *et al.*, 2003; Meyers *et al.*, 2008) in the form of a three-letter species abbreviation, followed by the letters mir/miR and finally a qualifier number. The three letter species abbreviation represents the species of the miRNA being referred to, for example: 'hsa' is for *Homo sapiens*, while 'mmu' is for *Mus musculus*. The subsequent use of 'mir' refers to the primary or precursor form of the miRNA, whereas 'miR' refers exclusively to the mature form. The number assigned to each miRNA is a unique identifier and is assigned in sequential order. Furthermore, the identifier number may be appended by a dash-number, letter, or the suffix 5p or 3p. The dash-number refers to two miRNAs with identical mature sequences transcribed from different locations within the genome. The letter indicates that the two miRNAs are related to each other, i.e. their mature sequences are very similar. The suffix 5p or 3p refers to the mature miRNA formed from the 5' arm of the hairpin loop, for example: *Homo sapiens* (Hsa) miR-7-3p

refers to the mature miRNA formed from the 3' arm of the hairpin loop (Bernardo *et al.*, 2012).

#### 1.3.3.2. Mechanism of action of microRNAs

Translation inhibition is a four-step process (Oliveto *et al*., 2017). In the first stage, the primary transcript folds on itself to form a stem-loop structure, which is then cropped, forming hairpins known as precursor miRNA (pre-miRNA). Cropping is performed by the microprocessor formed by the combination of the RNase enzyme Drosha and the cofactor DiGeorge syndrome chromosomal region 8. These hairpins are shuttled to the cytoplasm by Exportin 5 where the pre-miRNA is cleaved by Dicer, an RNase III enzyme in the cytoplasm. Dicing creates the "Guide Strand" and the "Passenger Strand" and these are then loaded on the Argonaut protein after which the "Passenger Strand" is destroyed. In the final step, the "Guide Strand" together with the Argonaut form the RNA Interference Silencing Complex and this complex then binds to the target mRNA to promote gene silencing and thus represses translation (Buhagiar and Ayers, 2015).

#### 1.3.3.3. The role of microRNAs in the regulation of neurogenesis

The function of miRNAs in the nervous system is to promote axonal development, modulate synaptic activity and support regeneration of peripheral nerve tissues (Lai and Breakefield, 2012).

The CNS expresses large amounts of miRNAs, which in addition to miRNA sequences and their targets not being well defined limits the current knowledge on miRNA regulation during neurogenesis. However a deeper insight is now possible as specific neural cell types may be derived from human pluripotent stem cells (Stappert, Roese-Koerner and Brüstle, 2015). MiRNAs modulate post-mitotic neural cell proliferation during the development of the CNS, inducing a balance between proliferation and differentiation of neural progenitors (Ristori *et al.*, 2015). In their study Ristori *et al*. show that during development of the hind-brain miR-107 controls *DICER* expression by targeting another miRNA (miR-9) which controls neurogenesis. Lowering the expression of miR-107 will increase the levels of miR-9

which affects *DICER* and results in an increase of both proliferating progenitors and postmitotic neurons. Table 1.3 lists the miRNAs involved in neurogenesis regulation.

| miRNA | Target | Expression | Role | Source |
|---|---|---|---|---|
| miR-9 | Hes1 Stathmin REST | + | Downregulates Neural stem cell differentiation | Tan *et al.*, 2012; Delaloy *et al.*, 2010; Packer *et al.*, 2008 |
| miR-29a | REST | - | Promotes Neural differentiation | Duan *et al.*, 2014 |
| miR-124 | PTP1B<br>SCP1 dlx-2 Jagged-1 SOX9 | -<br>+ | Promotes Neural differentiation<br>Promotes Proliferation of neuronal precursors | Visvanathan *et al.*, 2007; Cheng *et al.*, 2009 |
| miR-125 | SCNBA EPHB2 KCNQ2 FLNA SYN2 NEFM | + | Promotes Neural differentiation | Le *et al.*, 2009 |
| miR-200 family | SOX2 E2F3 | - | Promotes differentiation into neurons | Peng *et al.*, 2012 |
| miR-107 | Dicer | - | Promotes Neurogenesis | Ristori *et al.*, 2015 |
| miR-381 | Hes1 | + | Promotes Neural Stem Cell Proliferation and Differentiation | Shi *et al.*, 2015 |
| miR-765 | Hes1 | + | Promotes Neural stem cell proliferation and differentiation | Li *et al.*, 2016 |
| miR-106b~25 cluster | TGFβ insulin/IGF- FoxO | + | Promotes Neural Stem/Progenitor Cell Proliferation and Neuronal Differentiation | Brett *et al.*, 2011 |
| Let-7 family | HNF4A | - | Promotes Neuroblast proliferation and self-renewal | Hennchen *et al.*, 2015; Koh *et al.*, 2010 |
| miR-34a | MYCN | + | Promotes Proliferation | Mollinari *et al.*, 2015 |
| miR-184 | AKT2 | - | Inhibits neuroblastoma cell survival | Foley *et al.*, 2010 |
| miR-302/367 | Fibrobasts | + | Reprogram cells into neurons | Zhou *et al.*, 2015 |
| miR-181a/125b | TGFβ Nestin | + | Promotion of the generation of TH-positive neuron | Stappert, Roese-Koerner and Brüstle, 2015 |

**Table 1.3: miRNA involvement in neuronal development**

Legend: Hes1 – Hairy and Enhancer of Split 1, REST - RE-1 silencing transcription factor, PTP1B - polypyrimidine tract-binding protein 1, SCP1 - Small C-terminal domain phosphatase 1, dlx-2 - distal-less homebox 2, SOX9 - sex determining region Y-box 9, SCNBA - Sodium channel protein type 1 subunit alpha, EPHB2 – Ephrin type-B receptor 2, KCNQ2 – Potassium Voltaged-Gated Channel Subfamily Q Member 2, FLNA – Filmin Alpha, SYN2 – Synapsin II, NEFM – Neurofilament medium polypeptide, SOX2 - sex determining region Y-box 2, E2F3 – E2F Transcription Factor 3, TGFβ - transforming growth factor-beta, IGF- insulin-like growth factor 1, FOXO - Forkhead transcription factor family O, HNF4A – Hepatocyte nuclear factor 4 alpha, AKT2 - v-akt murine thymoma viral oncogene homolog 2, Th – Tyrosine hydroxylase, (+) - upregulation of miRNA expression, (-) - downregulation of miRNA expression.

#### 1.3.3.4. MicroRNA modulation of stem cell commitment

MiRNAs have been shown to interact with different signalling pathways. They influence the expression of various transcripts, creating regulatory feedback loops that affect multiple functions within the cell. This subsequently results in cell fate modulation of NSCs and their progeny (Garg *et al*., 2013). Over the years, the role played by miRNAs in stem cell fate determination and differentiation has gained considerable interest and importance and has become more recognised. Ongoing research has led to discoveries to new miRNA/stem cell related functions, enabling the development of new miRNA-based therapies in regenerative medicine. It is a well-known fact that cells can be reprogrammed using miRNAs. However further elucidation is required on whether miRNAs alone can actually induce reprogramming or whether they act to improve the efficiency of reprogramming core transcription factors such as OCT4 and SOX2 (Eguchi and Kuboki, 2016).

Another key aspect to understanding this modulation is by identifying the roles of circulating miRNAs and how these

may be put to good use as part of miRNA therapeutic applications. This form of treatment may only be made possible by developing techniques that mimic and deliver stable exosomal miRNAs which would then be able to control the proliferation and differentiation of stem cells, such as in the basics of tissue regeneration (Yao, 2016).

### 1.3.4. MicroRNAs involved in stem cell to neuroblast to mature neuron differentiation

Neuroblasts or neural precursors are cells which have been already committed to developing into neuronal cells. These precursors may undergo three distinct dividing stages. The first stage is that of symmetrical division. This process occurs during the early stages of neural development during which the neuroblast divides yielding two identical cells. Midway through neural development, the cells undergo asymmetrical division. In this stage, the cell divides to produce one precursor cell and another cell that is a transit amplifying cell (Matsuzaki and Shitamukai, 2015). This phase allows the formation of neurons while still having precursors available to produce other neurons and/or glia at

a later stage. In the final stage, precursors will differentiate into either neurons or glia, ending neurogenesis and gliogenesis respectively (Hudish and Appel, 2014).

Once stem cells are directed towards the neural lineage, a complex network regulates the proliferation, differentiation and distribution of neuronal progenitors. Examples of this network include the interaction of miR-134 and miR-184, which have both been associated with neural progenitor maintenance and proliferation (Bian, Xu and Sun, 2013), and miR-124 and miR-9, which promote neuronal differentiation (Åkerblom and Jakobsson, 2014; Coolen, Katz and Bally-Cuif, 2013). MiR-124 and miR-9 target several components of the Notch signalling pathway, responsible for the regulation of neuronal development and neural progenitor proliferation (Stappert, Roese-Koerner and Brüstle, 2015). BMP/TGFβ signalling induces the transition of stem cells towards the neural lineage and this pathway is inhibited by miR-125a/b and miR-135b, while miR-302/367 stimulate the signalling and stop neural induction (Boissart *et al.*, 2012).

#### 1.3.4.1. Rationale for the selection of microRNAs

This study investigated the role of three miRNAs - miR-107, miR-124 and miR-381 – in relation to how these can direct the differentiation of MSCs to neural like cells.

MiR-107 is specifically expressed in the brain (Wang *et al.*, 2014) and acts as a negative regulator of *Dicer* which implies that this miRNA plays a major role in the regulation of Dicer-dependent physiological processes such as neurogenesis (Ristori *et al.*, 2015). Its overexpression causes a decrease in *Dicer* gene expression, thus stabilising *Dicer* mRNA and increasing the number of neuronal progenitors (Ristori *et al.*, 2015).

MiR-124 is a highly expressed tissue-specific miRNA of the nervous system (Ludwig *et al.*, 2016). In order to maintain the neural state, miR-124 downregulates the expression of non-neural mRNAs by repressing the expression of non-neural transcripts and thus directing the gene expression profile towards the neural state (Xue *et al.*, 2016). A target of miR-124 is polypyrimidine tract-binding protein 1 (PTP1B)

mRNA, a repressor of neuron-specific pre-mRNA splicing, that activates the neuronal gene expression.

MiR-381 targets *HES1*, a gene highly expressed in the CNS, which plays a crucial role in the maintenance of NSCs during the development of the embryonic brain. Down-regulation of *HES1* causes NSCs to differentiate into mature neurons (Shi *et al*., 2015). Knockdown of the *HES1* gene upregulates the neural differentiation factor MASH-1, increasing neuronal differentiation (Shi *et al.*, 2015).

## 1.4. Rationale and Aims

It is widely agreed that miRNAs are responsible for neural induction, differentiation and fate specification and thus, have potential in the development of next generation therapeutic approaches for numerous health conditions. The identification of putative miRNAs responsible for neural development will further elucidate the mechanisms of action involved in both the physiological and pathological processes of the CNS.

The rationale for the use of miRNAs to transdifferentiate MSCs to neural-like cells arose from the possibility of targeting protein expression by transiently inhibiting mRNA translation by miRNAs, as an alternative to permanent gene modification such as in the case of CRISPR. Being a transient process, the cells being differentiated should not retain any permanent mark of the process.

The aim of this research is to investigate the role of miRNAs in MSCs commitment to a neuroblast and/or mature neuron cell lineage and to determine whether individual miRNAs can induce MSCs to become neuroblasts or undergo further neuronal differentiation for potential therapeutic applications.

To establish this, MSCs were isolated from Wharton's Jelly and characterised by trilineage differentiation. The MSCs were then treated with the conditioned medium of cultured SH-SY5Y cells, which induced a neuronal-like differentiation of the MSCs. These induced neural-like cells were further treated with RA to produce cells which are at a later stage of

maturation. All three cell types were then characterised using a series of CD and neural markers to obtain an indication of the neuronal stage of the different cells. Finally, cells were transfected with three miRNA antagonists and the change in expression was determined for the corresponding miRNA target genes and a panel of neural markers.

# Chapter 2
# Materials and Methods

## 2.1. Ethical Approval

Ethical approval for collection of cords for the culturing of MSCs was granted by the University of Malta Research Ethics Committee. A copy of this approval and the consent forms used can be found in Appendix I.

## 2.2. Experimental Design

The number of cords utilised in this project and how each was utilised can be viewed in Table 2.1. Since the quantity of MSCs cultured was extremely limited, every effort has been made to test these cells for at least one characterisation attribute as per ISCT recommendation. In brief, once the cord was processed and MSCs cultured, these cells were characterised by trilineage differentiation. Simultaneously, cells were conditioned with spent medium from cultured SH-SY5Y cells and subsequently, these cells were treated with RA. Hereafter these two cell types were referred to as Conditioned Cells (CCs) and RA-treated CCs (RA-CCs), respectively. After RNA was extracted from the three cell types, Real Time Polymerase Chain Reaction (RT-qPCR) was performed to determine which CD and neural

markers were expressed by these cells. Transfection of miRNA antagonist (siRNA) was then performed on all three cell types. RNA was once again extracted and tested for the expression of the miRNA gene targets and a selection of neural markers.

| Cord Number | 1 | 2 | 3 | 4 | 5 | 6 | 7 | 8 | 9 | 10 | 11 | 12 | 13 |
|---|---|---|---|---|---|---|---|---|---|---|---|---|---|
| Successfully cultured (MSCs) | | | | | | | | | | | | | |
| Differentiated with Conditoned Medium (CCs) | | | | | | | | | | | | | |
| CCs treated with RA | | | | | | | | | | | | | |
| Tri-lineage differentiation of MSCs - Osteo | | | | | | | | | | | | | |
| Tri-lineage differentiation of MSCs - Adipose | | | | | | | | | | | | | |
| Tri-lineage differentiation of MSCs - Chondro | | | | | | | | | | | | | |
| MSCs for CD and neural markers RT-qPCR | | | | | | | | | | | | | |
| CCs for CD and neural markers RT-qPCR | | | | | | | | | | | | | |
| CC -RA CD and neural markers RT-qPCR | | | | | | | | | | | | | |
| MSCs used for transfection of siRNA | | | | | | | | | | | | | |
| CCs used for transfection of siRNA | | | | | | | | | | | | | |
| CC-RA used for transfection of siRNA | | | | | | | | | | | | | |
| MSCs transfection neural markers | | | | | | | | | | | | | |
| CCs transfection neural markers | | | | | | | | | | | | | |
| CC -RA transfection neural markers | | | | | | | | | | | | | |
| MSCs transfection siRNA targets RT-qPCR | | | | | | | | | | | | | |
| CCs transfection siRNA targets RT-qPCR | | | | | | | | | | | | | |
| CC-RA transfection siRNA Targets RT-qPCR | | | | | | | | | | | | | |
| MSCs/Cord discarded | | | | | | | | | | | | | |
| CCs discarded | | | | | | | | | | | | | |

**Table 2.1: Experimental Layout**

Table representing the number of cord samples processed in this project and how the derived cells were utilised. Legend: MSCs – Mesenchymal Stem Cells, CCs – Conditioned Cells, CC- RA – Retinoic Acid treated CCs, RT-qPCR – Real Time Polymerase Chain Reaction, siRNA – microRNA antagonist.

## 2.3. Cell Culturing

2.3.1.Medium for cell culturing

Dulbecco's Modified Eagle Medium: Nutrient Mixture F-12 (DMEM/F-12) (Sigma-Aldrich Cat: D5523) was used as cell culture medium. Under aseptic conditions using a Class II safety cabinet (SafeFAST Elite, Faster S.r.l.), the medium was reconstituted using distilled water prepared by the distillation of tap water using the Aquatron automatic water still A8000 (Cole-Parmer, UK) and sodium bicarbonate (Sigma-Aldrich Cat No: S5761) followed by filtering using a 0.2µm filter (Thermofisher Scientific, Cat No: 564-0020). The stock medium was stored at 4$^{o}$C.

Prior to use, the medium was supplemented with 20% cryo poor plasma (CPP) (obtained from the National Blood Transfusion Services Malta). A 1% penicillin/streptomycin (P/S) solution, consisting of 10,000 units penicillin and 10 mg streptomycin per mL in 0.9% sodium chloride (Sigma-Aldrich Cat No: P0781), was then added to the medium. The addition of human plasma provided xeno-free (animal-derived) nutrients with the added benefit of preventing stem

cells from being programmed at an early stage. The CPP procedure was adapted from Muraglia *et al*. (2017). To produce the CPP under aseptic conditions, the plasma bag was supplemented with calcium chloride ($CaCl_2$) (Anatar Cat No: 10241) (2 mg/ml), mixed gently, transferred to a Transfer Bag and incubated at 37°C for a minimum of 3 hours. The addition of $CaCl_2$ and heat induced coagulation and precipitated residual factors present in the plasma. Uncoagulated plasma was then decanted into 50ml falcon tubes and stored at -20°C. When required the plasma was thawed at 37°C and centrifuged at 1000 XG for 10 minutes. The P/S was added to the medium to prevent bacterial contamination of the cell cultures by either gram-positive or gram-negative bacteria. Any unused complete medium was kept refrigerated at $4^{o}$C.

### 2.3.2. Fibrin clots

The practice of using sera with unknown animal-derived factors such as Foetal Bovine Serum (FBS) is being phased out, especially where research models for therapeutic applications are being developed (Baron, 2016). Cell lines in

culture require high levels of serum. However, animal derived sera are not standardised and present high variability of the many substances they contain both between lots and brands. This variation could greatly influence the research results and make these inconsistent (Zammit, Farrugia and Baron, 2019). In this study, FBS was substituted with human plasma obtained from healthy blood donors whose blood was collected aseptically and processed using the closed system quadruple bag blood processing system as described above in Section 2.3.1.

Plasma contains clotting factors, which are triggered by calcium into initiating the coagulation cascade resulting in haemostasis. One of the chemical components of the DMEM/F12 formulation is calcium. To prevent the coagulation of the media, the plasma was treated with $CaCl_2$. This removed most of the coagulation factors from the plasma and most of the residual cryoprecipitate was removed at a later stage by centrifugation. However, on different occasions, when medium was added to the cultures, fibrin clots would still form.

Since the composition of the plasma used is not standardised, the amount of coagulation factors present may vary from donor to donor. This makes it rather difficult to precipitate all factors, and fibrin clots may develop in the presence of excessive calcium, such as in the case during chondrogenic differentiation of MSCs, where a gel like matrix was formed allowing the differentiated chondrocytes to take on a 3D-like structure.

During culturing of the MSCs, when the Wharton's Jelly was incubated with the medium, sometimes this would coagulate due to residual traces of plasma present in the cord itself. Even though care was taken to clean the cord properly by the washing stages, if the cord is not bled properly at the collection stage, some Wharton's Jelly would end up becoming blood stained, ultimately causing the formation of a fibrin clot when the medium is added. When formed, this clot was easily removed on the subsequent medium changes and by the time MSCs started to appear in culture, fibrin clots were no longer forming.

In both cases, the gel-like substance produced by the coagulated medium was easily removed, since once the fibrin clot is removed the remaining gel converts back to a liquid. The disadvantage of this method is that any cells trapped in the fibrin clot would be lost. To prevent such losses, cells undergoing chondrogenic differentiation had minimum medium changes, especially towards the end of the 21 day differentiation period.

### 2.3.3. Culturing of Human Mesenchymal Stem Cells

Primary cell cultures are those cultures which are grown directly from donor tissue. Such cultures are different from cell lines because they are not immortalised or transformed by oncogenes. This means they have a finite lifespan of a few months. Cells for culturing were obtained from tissue by tissue maceration.

#### 2.3.3.1. Collection of cord sample

Donors were recruited from the Obstetrics and Gynaecology Ward, Mater Dei Hospital, Triq Dun Karm, L-Imsida, Malta.

The pregnant donors were informed of the ethically approved study and informed consent was obtained. Not too long after birth, a piece of the umbilical cord of around 5 to 10cm was cut off close to the placenta, entirely bled and, to preserve stem cell viability, stored by complete submersion in phosphate buffer saline (PBS) (Sigma-Aldrich, Cat: P3813) at a temperature of 2–8$^{o}$C. The sample was processed within 24 hours because the cells would not be healthy after 24-hours at 4$^{o}$C in PBS without glucose. As a prophylaxis to prevent contamination, 1% P/S was added to the storage PBS solution.

#### 2.3.3.2. Isolation and culturing of human mesenchymal stem cells

This isolation method follows the Points of Good Practice for the Sampling of Cords and Culturing of Mesenchymal Stem Cells by Zammit and Baron (2017). The transport PBS solution was discarded, and the cord was washed vigorously with 70% ethanol for 1 minute. This step helped prevent contamination by any foreign matter present on the surface of the cord, however a longer exposure to ethanol would

lead to loss of cell viability. The ethanol was then removed, and the sample washed three times for 1 minute each with cold PBS. The PBS removed any remaining traces of alcohol and debris from the surface of the cord. Once the cord had been cleaned, the epithelial and vascular tissues were removed, and the Wharton's Jelly extracted. The jelly was then cut into small pieces and transferred to a 12-well plate and a T25 flask. The tissue was then allowed to rest for 10 minutes to allow better adherence. Finally, enough complete medium to cover the base of the well/flask was added and these were then incubated at 37$^{o}$C with 5% $CO_2$ in a humidified environment.

Half the medium was replaced every 3 days. This allowed replenishing of nutrients and removal of debris while retaining some of the circulating growth factors released by the tissue itself. Once cells started to grow and colonies formed, the tissue pieces together with the spent medium were removed. Once the desired confluence (minimum of 50% confluence) was achieved the cells were detached with

2ml 2mM Ethylenediaminetetraacetic acid disodium salt dihydrate (EDTA) (Sigma-Aldrich, Cat: E5134).

### 2.3.4. Culturing of conditioned Mesenchymal Stem Cells

Conditioned medium consists of a variety of biomolecules, including miRNAs released by the cells into the culture medium during growth. These secreted biomolecules may play a role in processes such as cell growth, differentiation, invasion and angiogenesis by regulating cell-to-cell and cell-to-extracellular matrix interactions.

#### 2.3.4.1. Preparation of SH-SY5Y cells spent medium

For this project, the Neuroblastoma cell line SH-SY5Y was donated by Dr Duncan Ayers from the Centre for Molecular Medicine and Biobanking, University of Malta. The frozen SH-SY5Y cells were thawed, transferred to a sterile 15ml falcon tube containing 4ml complete DMEM (using human plasma) and centrifuged at 250 XG for 10 minutes. The supernatant was then discarded, and the cell pellet was suspended in 3ml complete DMEM (using human plasma). The suspension obtained was transferred to a sterile flask and cultured as per Section 2.3.3.2. After 2 days, the spent

medium was discarded so that dead cells, traces of animal-derived products from prior cryo-storage culturing and any remnant dimethyl sulfoxide (DMSO) in which the cells had been frozen were all removed. Fresh complete medium (3ml) was added and the flasks were re-incubated. After 3 days the medium was collected, centrifuged at 500 XG for 15 minutes at $4^{o}$C, transferred to a sterile falcon tube and refrigerated if not required. To maintain a stock of fresh spent medium readily available, the SH-SY5Y cultures were split with the aid of 2ml 2mM EDTA (Sigma-Aldrich, Cat: E5134) in PBS and these were seeded in a T25 flask at a density of 1 x$10^{6}$cells/mL and re-incubated to maintain a stock of fresh conditioned medium. Any surplus SH-SY5Y cells were frozen in 5% DMSO (Sigma-Aldrich Cat: 276855-2L) and 95% CCP at -$80^{o}$C.

2.3.4.2. Conditioning of Mesenchymal Stem Cells

To direct MSCs to become neural like cells, the MSCs were incubated with a ratio mixture of 1:1 of complete medium and conditioned medium obtained from the SH-SY5Y cells in culture. For optimal results, the conditioned medium should

be not more than 3 – 4 days old. Since the conditioned medium is an in-house prepared medium, no additional preservatives were added, so a prolonged storage will deteriorate the substance which are inducing the differentiation of the MSCs. Cells were then cultured as per section 2.3.3.2. Within 24 hours, over 70% of MSCs had started to differentiate. The medium was changed every 3 days or as necessary and, once confluent, CCs were detached with 2ml 2mM EDTA (Sigma-Aldrich, Cat: E5134) in PBS and frozen in a solution of 5% DMSO and 95% CCP at -80$^{o}$C.

2.3.4.3. Culturing of neural-like cells

The protocol for producing mature neural-like cells was adapted from Shipley *et al.* 2016. CCs were seeded in a 12-well plate at a density of 1x10$^{5}$ cells. Culture medium per well was prepared by using 960µl DMEM/F-12, 26µl CPP, 10µL P/S, 1µl N2 supplement (Thermofisher Scientific Gibco® Cat: 17502048 – composition: human transferrin (10000mg/l), insulin recombinant full chain (500mg/l), progesterone (0.63mg/l), putrescine (16611mg/l) and

selenite (0.52mg/l)), and 1µl RA. Cells were then incubated at 37°C with 5% $CO_2$ in a humidified environment. The medium was changed every 3 to 4 days. Within three weeks of RA treatment cells developed neuritic projections. Hereafter these cells were referred to as CC-RA.

## 2.4. MSC functional identification

To verify the multipotency of the cultured MSCs, these were treated for tri-lineage differentiation using the Human Mesenchymal Stem Cell Functional Identification Kit (R&D Systems, Cat No.: SC006).

Once the MSCs in culture reached an adequate degree of confluence (approximately 40%), culturing medium was replaced by oestogenic, adipogenic or chondrorogenic differentiation medium. The oestogeneic and adipogenic differentiation media were prepared using StemXVivo Oesteogenic/Adipogenic Base Media (R&D Systems, Cat No.: CCM007), 1% P/S and osteogenic or adipogenic supplement at a 1:20 dilution. Chondrogenic medium consisted of

DMEM/F12, 1% P/S, 1% ITS supplement and 1% chondrogenic supplement.

Differentiation medium was changed every 4 -5 days. Cells were then incubated at 37$^{o}$C with 5% $CO_2$ in a humidified environment. After 21 days, osteocytes were stained using the von Kossa staining method to determine the formation of calcification matrix within the cells; adipocytes were stained with Oil-Red-O for detection the lipid vacuoles; chondrocytes were stained with Alcian Blue for identifying the presence of glycosaminoglycans, which compose the extracellular matrix of cartilage. Prior to staining, all wells were gently washed with a volume of 500µl PBS after which cells were fixed in 500µl Tokuda-Baron Fixative (TB Fix) for 15 minutes (Tokuda *et al*., 2018). Following fixation, the wells were washed twice using 500µl PBS.

### 2.4.1. Von Kossa staining

Cells were stained with 500µl 1% silver nitrate (Sigma-Aldrich, Cat No.: 209139) solution (1g in 100ml distilled water) and incubated under ultraviolet light (60-watt lamp)

for 20 minutes. Following incubation, wells were washed three times with 500µl distilled water. Cells were treated for 5 minutes with 500µl 5% sodium thiosulfate (Sigma-Aldrich, Cat No.: 1603121000) (5g in 100ml distilled water). This was added to remove any residual un-reacted silver and washed again three times with distilled water. Cells were stained with 1% Nuclear Fast Red Solution (0.1g nuclear fast red (Sigma-Aldrich, Cat No.: 6409-77-4), 5g aluminium sulfate (Sigma-Aldrich, Cat No.:7784-31-8) in 100ml distilled water) for 5 minutes and rinsed again using distilled water. A volume of 500µl distilled water was added to the wells and microscopically viewed for calcium deposits that would have stained black or brown-black (depending on the strength of the UV light).

### 2.4.2. Oil-red-O staining

A stock concentration of 3% oil-red-o staining was prepared by diluting 0.30g Oil Red-O powder (Sigma-Aldrich, Cat No.: OD625) in 100ml 2-propanol at 99%. Prior to staining, a working solution was freshly prepared by diluting the 3% Oil Red-O in distilled water in a ratio of 6:4 and filtered using a

0.2µm filter. Cells were stained with 500µl of the diluted Oil Red-O. After 15 minutes of staining, the Oil Red-O was removed, and wells washed gently in 500µl distilled water. Finally, wells were topped with a fresh volume of 500µl distilled water and checked microscopically for the presence of red lipid vacuoles.

### 2.4.3. Alcian Blue staining

Cells were stained for 30 minutes using 500µl Alcian Blue solution (100mg Alcian Blue (Sigma-Aldrich, Cat No.: A5268) in 60 ml ethanol and 40 ml acetic acid) previously diluted in distilled water in a ratio of 1:3. The wells were then washed gently in 500µl distilled water. Finally, wells were topped with 500µl distilled water and checked microscopically for the presence of glycosaminoglycans.

## 2.5. RNA extraction and cDNA synthesis

RNA extracted from MSCs, CCs, and RA-CCs followed by complementary DNA (cDNA) synthesis was used to determine the respective gene expression by RT-PCR.

### 2.5.1. mRNA extraction

MRNA was extracted and purified from MSCs, CCs and RA-CCs using the SV Total RNA Isolation System (Promega Cat No.: Z3100). RNA extraction is a well-established procedure and to efficiently purify RNA, this extraction kit employs the selective binding properties of a silica-based membrane with the speed of microspin technology. Once purified, the single-stranded RNA is converted into cDNA by using the enzyme reverse transcriptase.

#### 2.5.1.1. Cell lysate preparation

The cells were dislodged using 2mM EDTA in PBS, neutralised with complete DMEM and centrifuged at 250 XG for 5 minutes. The supernatant was discarded, and the cell pellet was re-suspended in 1ml PBS. The cells were centrifuged once again at 250 XG for 5 minutes and the supernatant was discarded. A volume of 175µl of RNA Lysis Buffer were added to the washed cells, paying attention to disperse the pellet, and then vortexed to ensure proper mixing. The mixture was then passed 4-5 times through a 20-gauge needle to shear the genomic DNA and transferred

to a 1.5ml microcentrifuge tube. To the tube, 350µl of RNA Dilution Buffer were added and thoroughly mixed by inverting 3-4 times before placing in a 70°C heat block for 3 minutes, followed by centrifugation at 14000 XG for 10 minutes at a temperature of 20°C.

2.5.1.2. mRNA extraction procedure

The clear lysate obtained after centrifugation was transferred to a fresh microcentrifuge tube, 200µl 95% ethanol were added and mixed 3–4 times by pipetting. The mixture was transferred to a spin column and centrifuged at 14000XG at 22°C for 1 minute. The liquid in the collection tube was discarded and 600µl of RNA wash were added and then centrifuged 14000XG at 22°C for a further 1 minute. After discarding the liquid in the collection tube, 250µl of RNA Wash Buffer were added to the column and centrifuged at high speed for 2 minutes. The spin basket was transferred to a fresh 1.5ml microcentrifuge tube and elution was performed by adding 100µl nuclease-free water and centrifuging at 13000xG at 22°C for 1 minute. The purified RNA was quantified by spectrophotometry and

stored at -70°C. Kit instructions may be viewed in Appendix II.

2.5.1.3. Determination of mRNA concentration

Purity and homogeneity of the sample are important factors when performing molecular analysis. Nucleic acids are purified with the help of commercially available kits that allow for the separation of most cellular components. However, proteins or other organic component residues may still be present in the eluate. To ensure minimum contamination of the sample, it is essential to verify its purity by photometric measurements. The ratios of the absorbance values at the wavelengths 230nm, 260nm and 280nm provide a clear picture of the purity of a nucleic acid sample. A pure sample is quantified as having an absorbance of ≥2.0 at A260/A230 and an absorbance of 1.8 - 2.1 at a wavelength of A260/A280.

RNA concentration was determined using the Eppendorf BioPhotometer (Eppendorf®, Germany) by measuring the

absorbance of a 1:5 (total volume 100µl) diluted extract at 260 nm (A260).

#### 2.5.1.4. mRNA cDNA synthesis

DNA can be synthesised from an RNA template by a procedure known as reverse transcription (RT), which produces cDNA. This procedure uses an RNA template and a short primer complementary to the 3’ end of the RNA to initiate the first cDNA strand that is in turn amplified by PCR.

cDNA synthesis was performed using the GoScript™ Reverse Transcriptase system (Promega Corporation, Cat No.: A5000). The kit consists of a reverse transcriptase and an optimised set of reagents for efficient synthesis of first-strand cDNA in preparation for PCR amplification. The kit is designed to convert up to 5µg of total RNA or up to 500ng of poly(A) RNA into first-strand cDNA.

2.5.1.4.1. mRNA cDNA synthesis procedure

The RNA/primer mixture was prepared as per Table 2.2. Every time cDNA was prepared a total of 5µg experimental RNA was used per reaction. Each tube was securely closed and incubated in a preheated 70°C heating block for 5 minutes, after which they were immediately placed on ice for a minimum of 5 minutes. To collect the condensate and maintain the original volume, the mixture was then centrifuged for 10 seconds and kept on ice until the RT mix was prepared as per Table 2.3. A volume of 15µl of the RT reaction mix was transferred to each reaction tube on ice and 5µl of RNA and primer mix added to obtain a final reaction volume of 20µl per tube. Synthesis was performed as per Table 2.4.

| **Component** | **Volume** |
|---|---|
| Experimental RNA (5µg/reaction) | 4µl |
| Primer [Random Primer (0.5µg/reaction) or gene-specific primer (10pmol/reaction) | 1µl |
| Nuclease-Free Water | 0µl |
| Final volume | 5µl |

**Table 2.2: RNA and Primer mixture**

| Component | Volume |
|---|---|
| Nuclease-Free Water (to a final volume of 15µl) | 5.8µl |
| GoScript™ 5X Reaction Buffer | 4.0µl |
| $MgCl_2$ (final concentration 1.5mM) | 1.2µl |
| PCR Nucleotide Mix (final concentration 0.5mM each dNTP) | 1.0µl |
| Recombinant RNasin® Ribonuclease Inhibitor | 2.0µl |
| GoScript™ Reverse Transcriptase | 1.0µl |
| Final volume | 15.0µl |

**Table 2.3: Reverse transcription mix**

| Phase | Temperature | Duration |
|---|---|---|
| Denaturation | 95°C | 5 minutes |
| Annealing | 55°C | 60 minutes |
| Extension | 70°C | 15 minutes |

**Table 2.4: cDNA synthesis reaction temperatures and duration**

## 2.6. Polymerase Chain Reaction

### 2.6.1. Real Time Quantitative Polymerase Chain Reaction

RT-qPCR is used to detect, characterise and quantify RNA. The RT-qPCR follows standard PCR protocols in the sense that first the RNA must be reverse transcribed into cDNA and then amplified by repeating cycles of denaturation, annealing and elongation. However, since fluorescent labelling is used during sample preparation, it is possible to monitor the data live as the reaction progresses.

### 2.6.2. House-keeping Gene

To balance out sample-to-sample variation in RT-qPCR efficiency and sample quantification errors, gene quantification analysis entails that qPCR data be normalised against a reference gene (endogenous control) (Bustin, 2002). To select the most suitable house-keeping gene for an experiment, a series of such genes needs to be analysed using the same experimental set-up which would then be used to analyse the samples. The gene which would have shown the least expression variation between the different experimental conditions would then be selected. In this study, glyceraldehyde-3-phosphate dehydrogenase (GAPDH) was chosen as the house-keeping reference gene, based on a study conducted by Willems *et al*., (2006). In their study, Willems *et al*. tested the stability of ten reference genes during neural differentiation of embryonic stem cells. GAPDH ranked as the 3$^{rd}$ housekeeping gene according to the normalisation tools geNorm and Normfinder.

### 2.6.3. Primers

A crucial step when setting up a RT-qPCR is that of designing and using the correct primers, since this can significantly impact the quality and reliability of the results. Primers are, on average, composed of 20 base pairs and have a melting point between 55°C and 65°C. To prevent the amplification of contaminating genomic DNA, the primer must span an exon junction. Ideally the 3' end of the primer should contain a C or G residue, as both T and A tend to bind in a non-specific way and to ensure maximum product stability the GC content should be approximately 50-60%.

#### 2.6.3.1. Primer Design

The primary transcript variant of the human gene of interest was retrieved from the GenBank sequence repository genome browser. The first and last 100 bases of each exon were noted. A shortlist of sequence pairs of 20bp, one before and one after an intron, up to 250bp apart in the transcribed mRNA were selected. These sequences where selected based on a number of parameters: the 3' end should contain C or G residues (CG clamp), melting

temperature of each primer should be 50-60$^{o}$C and within 5$^{o}$C of each other, the GC content should be 40-60%, the sequence should contain no nucleotide repeats, and should not form secondary structures or primer dimers. To confirm their specificity in the human genome, the selected sequences where run through nucleotide BLAST (National Center for Biotechnology Information) and the result should have given a single gene output (possibly showing multiple variants).

Table 2.5 lists the forward and reverse sequences of the primers used throughout this project. These where synthesised by and purchased from Integrated DNA Technologies.

| Primer | Forward | Reverse |
|---|---|---|
| SOX2 | CAAGATGCACAACTCGGAGA | GGGCAGCGTGTACTTATCCT |
| OCT4 | AGTGAGAGGCAACCTGGAGA | GGAGACCCAGCAGCCTCAAA |
| TUBB3 | GGAGATCGTGCACATCCAG | TCGAGGCACGTACTTGTGAG |
| GAPDH | GAAGGTGAAGGTCGGAGTCA | GAAGATGGTGATGGGATTTC |
| NES | TCCTGGAGGCTGAGAACTCC | CTGGCCAAGGTAGGGGTACG |
| ND1 | TAAATTGAGACGCATGAAGG | GGTGGTGGGTTGGGATAAGC |
| MASH1 | GAACTGATGCGCTGCAAACG | CATGCTCGTCCAGCAGCTGC |
| NEU | TGTACACACCAGCACAGACC | CGAACATTTGCCGCAAGTCG |
| MAP2 | ATACAGGGAGGATGAAGAGG | GGAGAAGGAGGCAGATTAGC |
| DICER | CTTTCTTTGGACTGCCATGG | GTTGACCAAGAACACCGTCC |
| HES1 | CCGGATAAACCAAAGACAGC | GGTGCTTCACTGTCATTTCC |
| PTP1B | CTTGTGTCACTAACGGACCG | CTTCAGCATCAGGAGGTTGG |
| CD34 | TGAAGCCTAGCCTGTCAC | CGCACAGCTGGAGGTCTTAT |
| CD45 | GTGTTTCATCAGTACAGACG | GTTGTGGTTGAAATGACAGC |
| CD73 | ATGGTGTGGAAGGACTGATC | CCTCACTTTCTGAGCGATG |
| CD90 | TGCTCTTTGGCACTGTGG | AGAGGGAGAGCAGGAGCAG |
| CD105 | GGGGTCAACACCACAGAG | CAGGACCCTCAGGATGTG |

**Table 2.5: List of Primers**

The forward and reverse (5' $\rightarrow$ 3') primers designed for all gene markers, miRNAs and miRNA target genes.

Legend: SOX2 - SRY (sex determining region Y)-box 2, OCT4 - Octamer-binding transcription factor 4, TUBB3 - $\beta$-III-Tubulin, GAPDH - glyceraldehyde-3-phosphate dehydrogenase, NES – Nestin, ND1 – NeuroD1, MAP2 - Microtubule-associated protein 2, MASH-1 - mammalian achaete scute homolog-1, NEU - neuronal-specific nuclear protein 1 and HES1 – Hairy and enhancer of split 1, CD – Cluster of Differentiation

#### 2.6.3.2. Primer preparation

Primers in a lyophilised state were obtained from Integrated DNA Technologies and were reconstituted by adding the amount of sterile nuclease-free water indicated in the data analysis sheet, thus obtaining a concentration of 100pmoles/µl. The tubes were flicked for 15 times and vortexed for 1 minute to obtain a homogeneous solution. Stock primers were stored at -20$^{o}$C. Low concentration working solutions were prepared by diluting with sterile nuclease-free water to obtain a 10µM concentration for PCR. Aliquots were stored at a temperature of -20°C.

### 2.6.4. RT-qPCR procedure

The reaction set-up was prepared as per Table 2.6 by thawing and mixing together 2xQuantiTect SYBR Green PCR Master Mix, primers and RNase-free water. These were mixed well and 9µL were dispensed into the PCR tubes to which 1µL of the cDNA template was added. The tubes were placed in the Rotor-Gene Q (Qiagen, Netherlands) which was programmed as per Table 2.7.

| Component | Volume per reaction |
|---|---|
| 2xQuantiTect SYBR Green PCR Master Mix | 5.0µL |
| Forward Primer | 0.5µL |
| Reverse Primer | 0.5µL |
| cDNA | 1.0µL |
| RNase-free water | 3.0µL |
| Total reaction volume | 10.0µL |

**Table 2.6: RT-qPCR reaction volumes**
Legend: RT-qPCR - Real Time Quantitative Polymerase Chain Reaction

| Step | Time | Temperature | Ramp rate |
|---|---|---|---|
| PCR initial heat activation | 15 min | 95°C | 20°C/s |
| Denaturation | 15 secs | 94°C | 20°C/s |
| Annealing | 30 secs | 50°C | 20°C/s |
| Extension | 30 secs | 72°C | 2°C/s |

**Table 2.7: RT-qPCR set-up**
Legend: RT-qPCR - Real Time Quantitative Polymerase Chain Reaction

#### 2.6.4.1. Interpretation of RT-qPCR data

During qPCR, fluorescence accumulates over a period of 40 cycles. The resultant amplification curve is composed of four different phases: the linear ground, early exponential, log-linear and plateau. The quantification cycle (Cq) determining the threshold should be set at the beginning of the log-linear phase (Caraguel *et al*., 2011).

Absence or presence of the marker of interest is determined in relation to the Cq value obtained for the Non-Template Control (NTC). The NTC was performed using the same qPCR technique previously described with the difference that

no cDNA was added to the mixture (replaced by nuclease-free water). The primers used for the NTC were for GAPDH thus the Cq value obtained for the NTC should be considered as a background reaction. Based on this, all markers whose Cq values resulted higher than the NTC or within a difference of less than 1 of a Cq were considered as to be negative/absent and not expressed by the cells.

Cq values were normalised against GAPDH providing the delta-Cq ($\Delta$Cq) value. This was calculated using the following formula:

$\Delta$Cq = Cq Gene of Interest – Cq House Keeping Gene

The difference in gene expression, the delta-delta Cq ($\Delta\Delta$Cq), was established using the previously calculated $\Delta$Cq. Calculation was performed as follows:

$\Delta\Delta$Cq = - (Cq of Treated Cells - Cq of Untreated Cells)

To calculate the difference in the gene expression between MSCs and CCs, MSCs were taken to be the untreated cells, while CCs were considered to be the treated cells. With

regards to the change that occurred between the CCs and CC-RA cells, CCs were considered the untreated cells while the CC-RAs were considered the treated ones. In the case of the transfection results, the siRNA transfected cells were the treated cells, while the untreated cells were those transfected using the negative control (scramble siRNA).

## 2.7. Transfection

Transfection is the process of artificially introducing nucleic acids, DNA or RNA, into cells by utilising means other than viral infection. The insertion of DNA into a cell enables the expression or production of proteins using the machinery of the cells themselves, whereas insertion of complementary RNA into a cell is used to down-regulate the production of a specific protein by interfering with translation.

For this project the three cell types were each transfected with miRNA antagonists.

### 2.7.1. Transfection reagent

The transfection reagent used was the FluoMag Transfection Reagent by OZ Biosciences (Cat No.: FN10100). The FluoMag transfection reagent used for this experiment contains fluorescent-labelled magnetic beads thus allowing the visualisation of these nanoparticles *in vitro*. Once the vector aggregates to the nanoparticles, the magnetic particles are then concentrated onto the cells by an external magnetic field. The cellular uptake of the nanoparticles is accomplished by endocytosis and pinocytosis and can be visually seen by fluorescent microscopy.

### 2.7.2. Antagomirs and negative controls

Antagomirs are oligonucleotides that inhibit the action of the endogenous miRNAs. Once an antagomir binds to miRNA it forms a double stranded structure which is recognised and digested by DICER. Negative controls play a very important role when performing research based on miRNA since they are used to create a baseline for mRNA knockdown efficiency. Table 2.8 summaries the antagonists used for transfection. The negative control used was

MISSION® Synthetic microRNA Inhibitor (Sigma-Aldrich, Cat No.: NCSTUD001).

| Antagomirs | | | |
|---|---|---|---|
| **Name** | **Sequence** | **Code** | **Supplier** |
| siR-107 | GAAGCCCGACAAGCGC | 75334453 | Integrated |
| siR-124 | ACAGAGAGCGCCCGAA | 75334451 | DNA |
| siR-381 | GGCACACCGCGGCCA | 75334452 | Technologies |

**Table 2.8: Antagomirs used for transfection**
Legend: siR – MicroRNA antagonists

### 2.7.3.Transfection Procedure

Cells were seeded in a 12-well plate at a density of $1x10^5$. A volume of 1ml complete medium was added to each well and the plate was incubated overnight at $37^oC$ with 5% $CO_2$ in a humidified environment thus allowing cells to reattach to the bottom of the wells. The following day, for each well due to be transfected, an Eppendorf tube was labelled with the antagomir and a mixture of plain DMEM F12, antagomir and transfection reagent were added as per Table 2.9. The tubes were mixed well and incubated at room temperature for 15 minutes.

| Component | Volume per well |
|---|---|
| Plain DMEM F12 | 50µl |
| Antagomir/Negative control | 10µl |
| Transfection Reagent | 2µl |
| Total volume | 62µl |

**Table 2.9: Volumes required for transfection**
Legend: DMEM F12 - Dulbecco's Modified Eagle Medium: Nutrient Mixture F-12.

Once the incubation time elapsed, the plate was labelled according to which antagomir would be transfected where and the medium removed from the wells. A volume of 938µl complete medium was added to the Eppendorf tube, mixed well by pipetting up and down and transferred to the corresponding labelled well. Once the desired transfections were pipetted, the plate was placed on the magnet and incubated at 37$^{o}$C with 5% $CO_2$ in a humidified environment for 48 hours. After the 48-hour incubation period, the wells were washed twice with 500µl of PBS. Wells were then topped up with 500µl of PBS and viewed under the fluorescent microscope to confirm transfection efficiency was satisfactory the RNA was extracted, converted to cDNA and tested with RT-qPCR for neural markers and target gene markers for their respective miRNA.

## 2.8. Green Fluorescent Protein

### 2.8.1. Bacterial transformation and plating

The competent DH5α*E. coli* bacteria had been previously prepared and these where made available by the Department of Clinical Pharmacology, University of Malta. These were stored in aliquots of 100µL. An aliquot of these competent cells was put on ice to thaw. Once thawed, 50µL of these cells were added to 50ng of Green Fluorescent Protein (GFP) plasmid DNA (Lonza, Cat No.: VDC-1040) in a total volume of 5µL. The mix was kept on ice for 5 minutes. The tube was placed on a heating block (Eppendorf, Germany) at 42$^{o}$C for 90 seconds and afterwards immediately placed on ice for 5 minutes. A volume of 300µL Luria Broth (LB) (Sigma-Aldrich Cat No: L3522-250G) containing no antibiotics was added to the tube and incubated in a water bath (Memmert, Belgium) at 37$^{o}$C for 45 minutes. A volume of 350µL of bacterial culture was used to inoculate an LB plate containing ampicillin (Sigma-Aldrich Cat No: A5354). This was spread using a sterile disposable loop. The plate was left to stand at RT for 10 minutes and

then incubated (Helmer Scientific, USA), upside-down overnight at 37°C.

### 2.8.2. Plasmid extraction

Plasmid extraction was performed using the AccuPrep® Plasmid Mini Extraction Kit (Bioneer, Cat No: K-3030-1). The kit instructions may be found in Appendix II. A falcon tube containing 5ml LB medium supplemented with ampicillin (Sigma-Aldrich Cat No: 10835242001) was inoculated with one colony transformed with GFP as described in Section 2.8.1. The concentration of ampicillin used was 1µg/ml of LB. The culture was placed in a shaking incubator (New Brunswick Scientific, USA) at 250rpm and incubated overnight at 37°C. The following day, the bacterial was pelleted by centrifugation (Eppendorf, Germany) at 3000rpm for 15 minutes. The pellet was resuspended in 250µL Resuspension Buffer and transferred to an Eppendorf tube. A volume of 250µL Lysis Buffer was added and the tube was inverted gently 6 times, after which 350µL Neutralisation Buffer were added. The tube was again inverted gently for 6 times and centrifuged at 14000rpm for

1 minute. The supernatant was transferred to a spin-column assembly and centrifuged for another 1 minute at 14,000rpm. The flowthrough was discarded and 700µL Wash Buffer were added. The tube was centrifuged again for 1 minute at 14,000rpm. The flowthrough was discarded once more and the tube was centrifuged for 1 minute at 14,000rpm. The spin-column was transferred to a clean 1.5ml tube, 100µL Elution Buffer were added and the set-up was incubated at room temperature for 2 minutes. After this incubation, the tube was centrifuged for 1 minute at 14,000rpm. The plasmid concentration was measured by a spectrophotometer (Eppendorf, Germany) using a dilution of 2 in 100 (2µL plasmid in 98µL distilled water). The plasmid size and integrity were confirmed by gel electrophoresis.

### 2.8.3. Gel electrophoresis

The gel was prepared by dissolving 0.5g of agarose (Sigma-Aldrich Cat No: A9539) in 50mL 1x Tris-acetate-EDTA (TAE) buffer (Sigma-Aldrich Cat No: T8280) (10x TAE Buffer 40 mM Tris, 20mM acetate, 2mM EDTA; pH 8.1). The mixture was heated in a microwave until all the agarose had

dissolved, after which 1µL of ethidium bromide (Sigma-Aldrich Cat No: E1510) was added (1µL for every 50mL of 1x TAE buffer). The ethidium bromide enabled the visualisation of nucleic acid fragments in the gel under UV light. The agarose mixture was poured into the mould and a well comb was fixed in place. Once the gel had solidified, the comb was removed and the mould together with the gel was placed in the electrophoresis tank. The tank was filled with 1x TAE buffer until the gel was completely submerged. A 1000bp molecular ladder (BioRad, Cat: 170-8204) was loaded into the first lane of the gel and 10µL of the plasmid was loaded in a separate well. The electrophoresis tank was closed, and the power supply was set to a voltage of 50V with a current of 200 mA for 40 minutes. Once electrophoresis was complete, the gel was removed from the electrophoresis tank and viewed on a transilluminator (Ultra-Violet Products Ltd**.**, UK) to visualise the bands of plasmid products. The size of the DNA bands obtained was calculated by comparing their migration distances with that of the known molecular weight marker.

### 2.8.4. Transfecting Green Fluorescent Protein

GFP was transfected as per Section 2.7. Reaction volumes may be viewed at Table 2.10.

| Component | Volume per well |
|---|---|
| Plain DMEM F12 | 50µl |
| GFP (7µg) | 10µl |
| Transfection Reagent | 2µl |
| Total volume | 62µl |

**Table 2.10: Volumes required for GFP transfection**

Legend: DMEM F12 - Dulbecco's Modified Eagle Medium: Nutrient Mixture F-12, GFP –Green Fluorescent Protein

## 2.9. Statistical Analysis

Statistics were analysed using the IBM SPSS Statistics version 24. Data may be viewed in Annex IV.

### 2.9.1. Neurite length analysis

Neurite growth post RA treatment was assessed using ImageJ as indicated by Pemberton *et al* (2018). The data was checked for being normally distributed using the Sharpio-Wilk test. Normal distribution of the data was defined as $P>0.05$. Once this was established, the difference in neurite length between RA treated and untreated cells was determined by T-Test analysis. The null hypothesis

implicated that there was no significant difference between the neurite lengths seen in treated and untreated cells and is accepted if $P>0.05$. The alternative hypothesis states that there is a significant difference between the neurite length of treated and untreated cells and is accepted if $P<0.05$.

### 2.9.2. RT-qPCR analysis

RT-qPCR data was analysed using the Mann-Whitney U test. Due to the small sample size outliers could not be eliminated, thus the data was considered not to be normally distributed. The null hypothesis was that there was no difference in the gene express measured during RT-qPCR analysis between treated and untreated cells. The alternative hypothesis stated that there is a difference in the gene expression of treated and untreated cells. The null hypothesis is accepted if the result falls above the desired significance threshold, $P<0.05$.

# Chapter 3

# Results

## 3.1. Cell Culture

### 3.1.1. Isolation of Mesenchymal Stem Cells

Primary cell culture depends on various factors including, but not limited to, the quality of the source from which these cells are derived and their ability to expand. For this study, 13 cord-lengths were sampled (as detailed in Table 2.1) and MSCs were successfully cultured from 12 of these samples. Cells grew out from the cultured Wharton's Jelly approximate three to four weeks after processing (Figure 3.1A) and gradually took on a spindle-shaped phenotype. On appearance of these spindle-shaped cells and cluster of cells, the Wharton's Jelly pieces were removed to allow expansion of the cell population (Figure 3.1B). The maximum confluency obtained was between 50 – 60% within 30to 40days of culture (Figure 3.1C). In some instances, the 50-60% confluence was achieved after 60 days. However, when cell clusters were not formed, the cells showed signs of senescence, becoming large and flat followed by cytotoxin release which initiated apoptotic signalling in the cells(Haines, Juhasz and Tosaki, 2013).

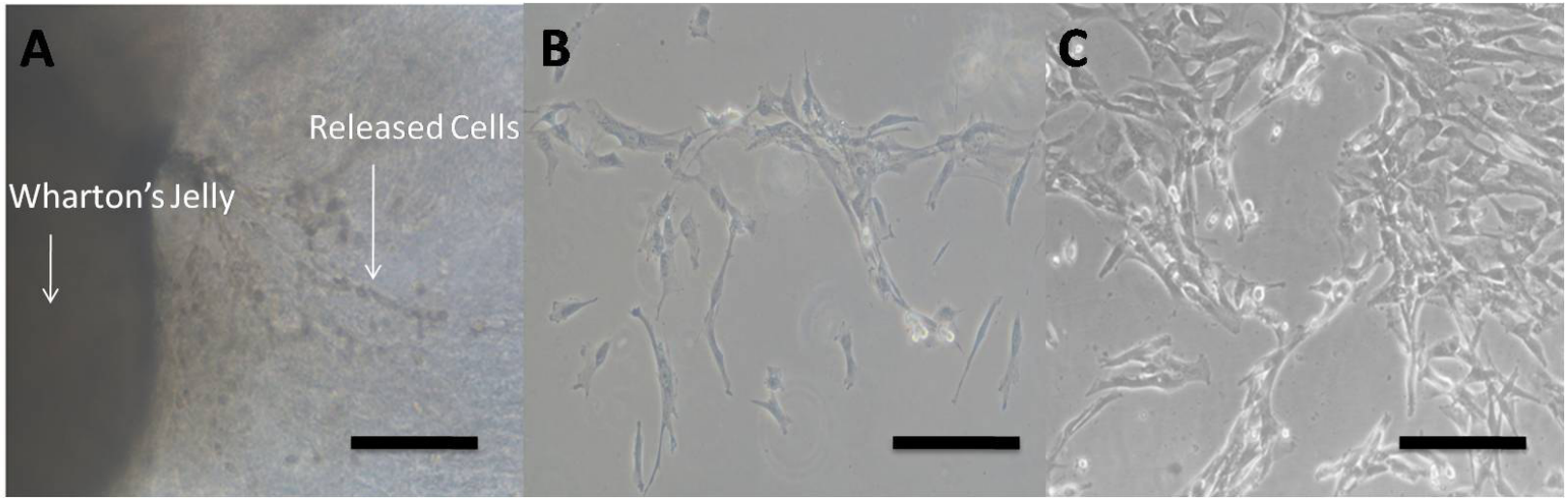


**Figure3.1: Isolation of Mesenchymal Stem Cells from Cord Samples**

Mesencyhmal Stem Cells (MSCs) were cultured from Cords 1, 3, 4, 5, 6, 7, 8, 9, 10, 11, 12 and 13. The above figure is a representation of how MSCs were observed in culture. Once extracted from the cord, Wharton's Jelly was placed in a 12-well treated cell culture plate and cultured using xeno-free medium. The Wharton's Jelly started to release spindle shaped cells (A) by the third week of incubation. Once cells started to form clusters (B), the tissue was removed from the plate. A confluence of 50% - 60% was obtained within a minimum of 40-days of culturing. Once confluent, the cells derived where used in experiments to determine trilineage differentiation, differentiation to neural-like cells (via exposure to spent medium), characterisation by CD and neural markers and transfection with miRNA antagonist. Scale bar represents 20µm.

Legend: MSCs – Mesenchymal Stem Cells, CD – Cluster of differentiation, miRNA - microRNA

### 3.1.2. Mesenchymal Stem Cell Trilineage differentiation

One of the major characteristic that defines an MSC is its ability to differentiate into osteocytes, adipocytes and chondrocytes. The trilineage differentiation capability of the cultured MSCs was confirmed by standard induction protocols, and illustrative examples of differentiation are shown in Figures 3.2 – 3.4.

The MSCs used for osteogenic differentiation were obtained from Cords 1, 3 and 5; adipocytes were differentiated from Cords 1, 4 and 5; and chondrocytes were derived from Cords 7, 8 and 9.To undergo this differentiation, MSCs were cultured in the induction medium for 21 days. Osteogenic MSC differentiation was confirmed by von Kossa staining - a calcium stain. Positivity for this differentiation was confirmed by the presence of a brownish-black to a deep black staining of the matrix mineralisation (Figures 3.2A – C).

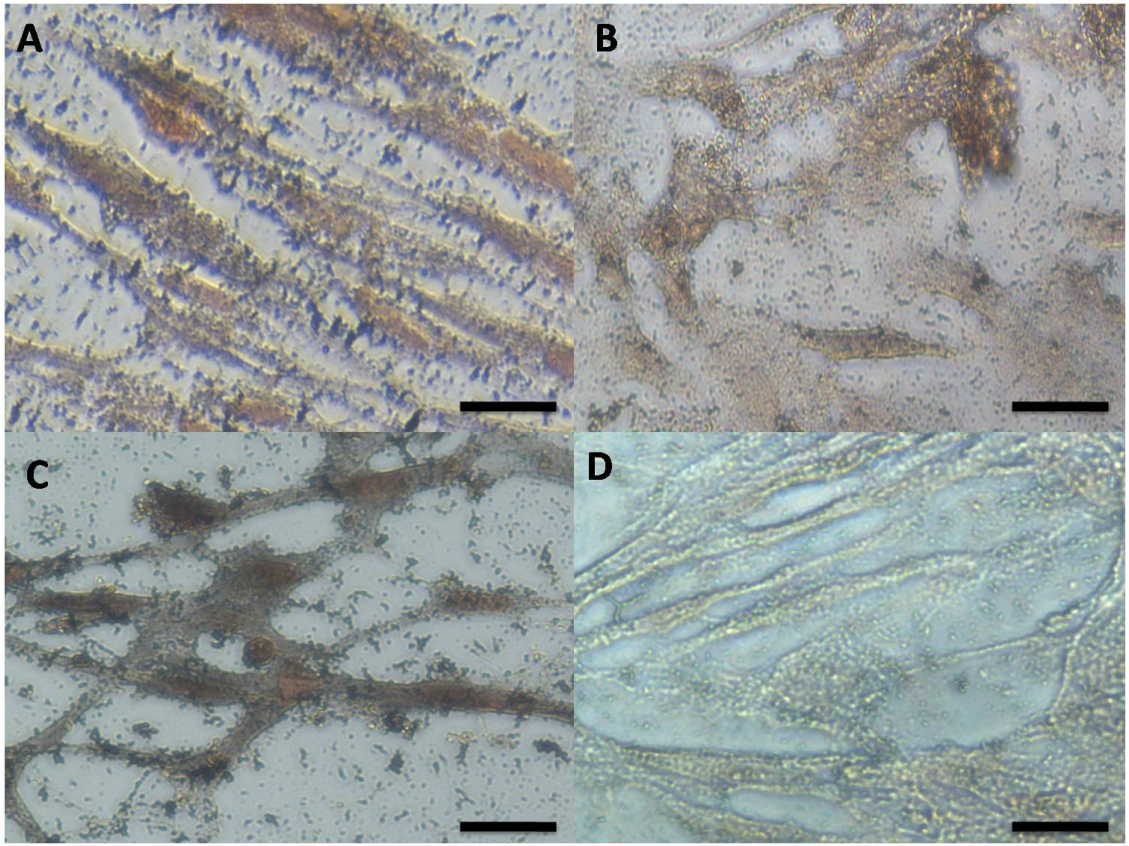


**Figure 3.2: Osteogenic differentiation**

Mesenchymal Stem Cells (MSCs) cultured from Wharton's Jelly extracted from Cord 1 (A), Cord 3 (B) and Cord 5 (C) were made to differentiate into osteocytes by means of an induction medium. Cells were cultured for 21-days in osteogenic induction medium, fixed in TB-Fix and then stained using the von Kossa staining method to detect the calcium deposits. MSC to osteogenic differentiation resulted in a light brown to blackish stain of the cells producing calcium. Figure D is a negative control and represents how undifferentiated MSCs look after von-Kossa staining is carried out, confirming that the brown-blackish stained cells are indeed due to these cells becoming calcium producing osteocytes. Scale bar represents 20µm.

Legend: MSCs – Mesenchymal Stem Cells, TB-Fix – Tokuda-Baron fixative

Culturing of MSCs under adipogenic conditions induced the formation and accumulation of lipid-rich vacuoles within the cell cytoplasm which were visualised by staining red after exposure to the adipogenic stain Oil Red O (Figures 3.3A – C).

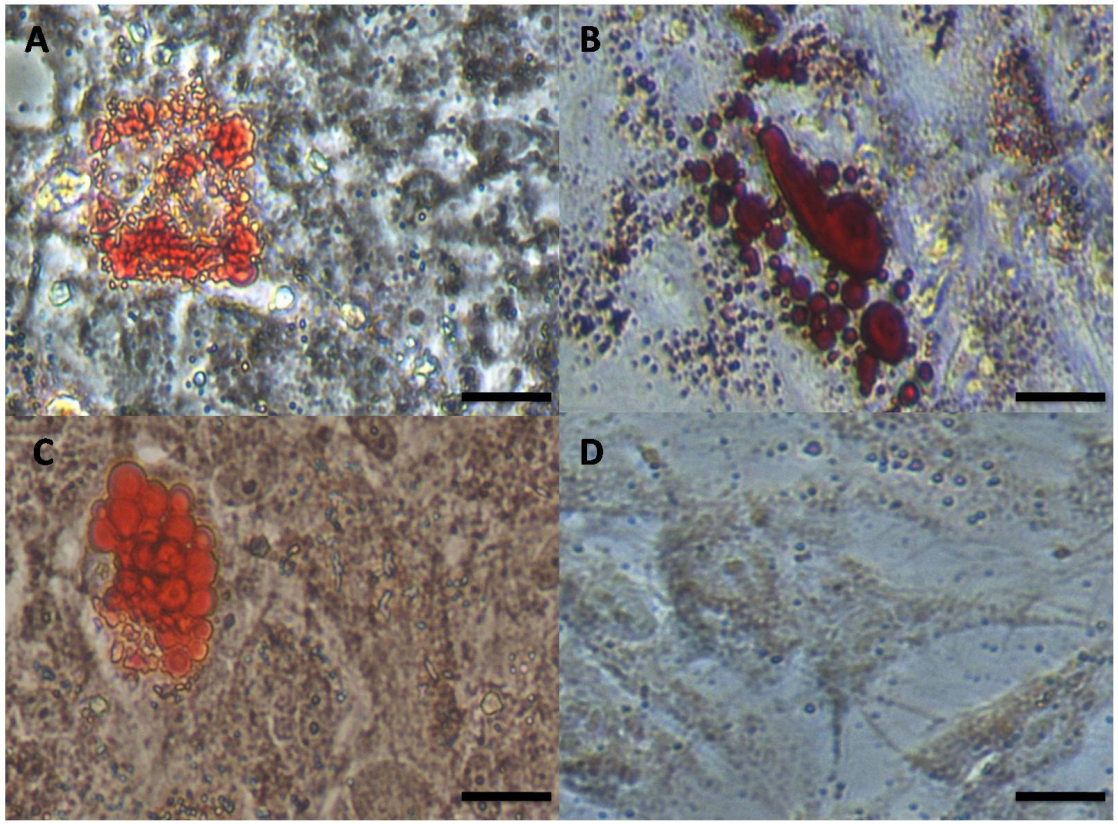


**Figure 3.3: Adipogenic differentiation**

Mesenchymal Stem Cells (MSCs) cultured from Wharton's Jelly extracted from Cord 1 (A), Cord 4 (B) and Cord 5 (C) were made to differentiate into adipocytes by means of an induction medium. Cells were cultured for 21-days in adipogenic induction medium. Cells were then fixed in TB-Fix (A, C and D) and 4%PFA (B) prior to staining. MSC to adipogenic differentiation was confirmed by Oil-Red-O staining. This stain is specific for lipid vacuoles which are *per se* stained red. Figure D is a negative control and represents how undifferentiated MSCs look when stained with the Oil-Red-O, confirming that the red stained vacuoles are indeed a result of MSCs differentiating in adipocytes. Scale bar represents 20µm.

Legend: MSCs – Mesenchymal Stem Cells, TB-Fix – Tokuda-Baron fixative

Chondrogenic differentiation was determined by the presence of glycosaminoglycan which was detected by staining of the cartilage extracellular matrix with Alcian Blue (Figures 3.4A – C).

To confirm the validity of the staining procedures, MSCs which were not treated for the trilineage differentiation were also stained using the same protocols. In all three instances, no characteristic traits associated with the positive staining seen in the differentiated cells were observed in these negative controls (Figures 3.2D, 3.3D and 3.4D).

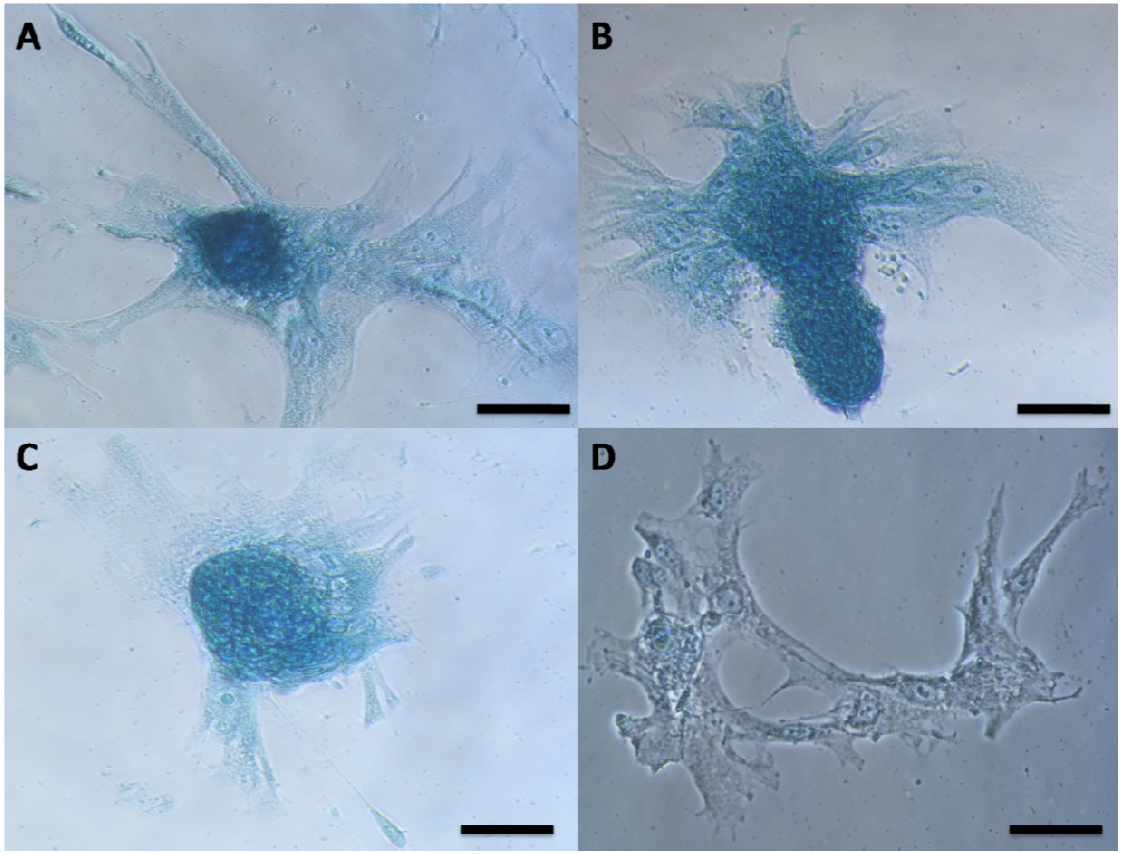


**Figure 3.4: Chondrogenic differentiation**

Mesenchymal Stem Cells (MSCs) cultured from Wharton's Jelly extracted from Cord 7 (A), Cord 8 (B) and Cord 9 (C) were made to differentiate into chondrocytes by means of an induction medium. Cells were 3D cultured in fibrin clots and chondrogenic induction medium for 21-days. Cells were then fixed in TB-Fix prior to staining with Alcian Blue. MSC to chondrogenic differentiation was confirmed by staining of the glycosoaminoglycans secreted into the extracellular matrix. Figure D is a negative control and represents how undifferentiated MSCs look when stained with the Alcian Blue, confirming that the blue stained 3D cell formation is indeed a result of MSCs differentiating into chondrocytes. Scale bar represents 20µm.

Legend: MSCs – Mesenchymal Stem Cells, TB-Fix – Tokuda-Baron fixative

Although all MSCs were exposed to the differentiation agents for the same period of time, it should be noted that MSCs were induced at different ages. The uniqueness of the source from which the cells were cultured has a great impact on the growth and proliferation of each cell population. A rapid proliferation of MSCs caused cell clusters to overlap and form fingerprint-like sheets; when a slow proliferation was obtained, the clusters were not compacted and individual cells were distinguishable. For example, in osteogenic differentiation, cells from Cord 3 grew in sheets making uniform staining of each cell difficult(Figure 3.2.B) as opposed to the cells stained from Cord1 (Figure 3.2A). Cells from Cord 5 started to show typical senescent characteristics by the time differentiation induction was concluded (Figure 3.2C). Estimating the number of MSCs that differentiated was problematic since in the case of osteotocytes, even if morphological changes were not apparent, these cells still produced calcium. This indicates that although they did not reach the point where a morphological change was induced MSCs had still begun to differentiate. Adipogenic differentiation was characterised by

the formation of lipid droplets, which may be easily removed during the washing stages of the staining procedure. This makes the actual number of droplets which were initially present very difficult to estimate. The chondrogenic-induced MSCs grew into a 3D-like structure making it impossible to determine how many cells were effectively present in the structure itself. It should also be noted that the difference in morphology of cells from Cord 4 (Figure 3.3B) was because cells were fixed in 4% paraformaldehyde. In view of the effect this fixative had on the cells, all subsequent preparations were fixed using TB-Fix.

## 3.2. Neuronal differentiation of cultured Mesenchymal Stem Cells

### 3.2.1. Conditioned Cells

The spent medium from culturing of SH-SY5Y cells was used as a condition media to induce MSCs to differentiate into neuron-like cells. The spent medium was only collected from flasks whose cells were confluent to maximise the collection of biomolecules. Preparation of the spent medium and storage may be found in section 2.3.4.1. To prevent MSCs

from differentiating due to cell contact, the spent medium was centrifuged to remove dead cells and other debris before use. The MSCs isolated from Cords 5, 6, 7, 8, 9, and 13 were induced to differentiate by adding the conditioned medium at a ratio of 1:1. The CCs used for this study were from cultures 5, 6 and 13. CCs from cultures 7, 8, and 9 had to be discarded due to contamination. On addition of the spent medium, the treated MSCs differentiated into neural-like cells within 24-hours (Figure 3.5A). By the third day, except for MSCs showing senescence, all remaining cells had differentiated (Figure 3.5B) and a confluence of 80 – 90% was achieved within the next thirty days (Figure 3.5C). MSCs which were not treated with the spent medium did not acquire the characteristic star shaped morphology of neural-like cells.

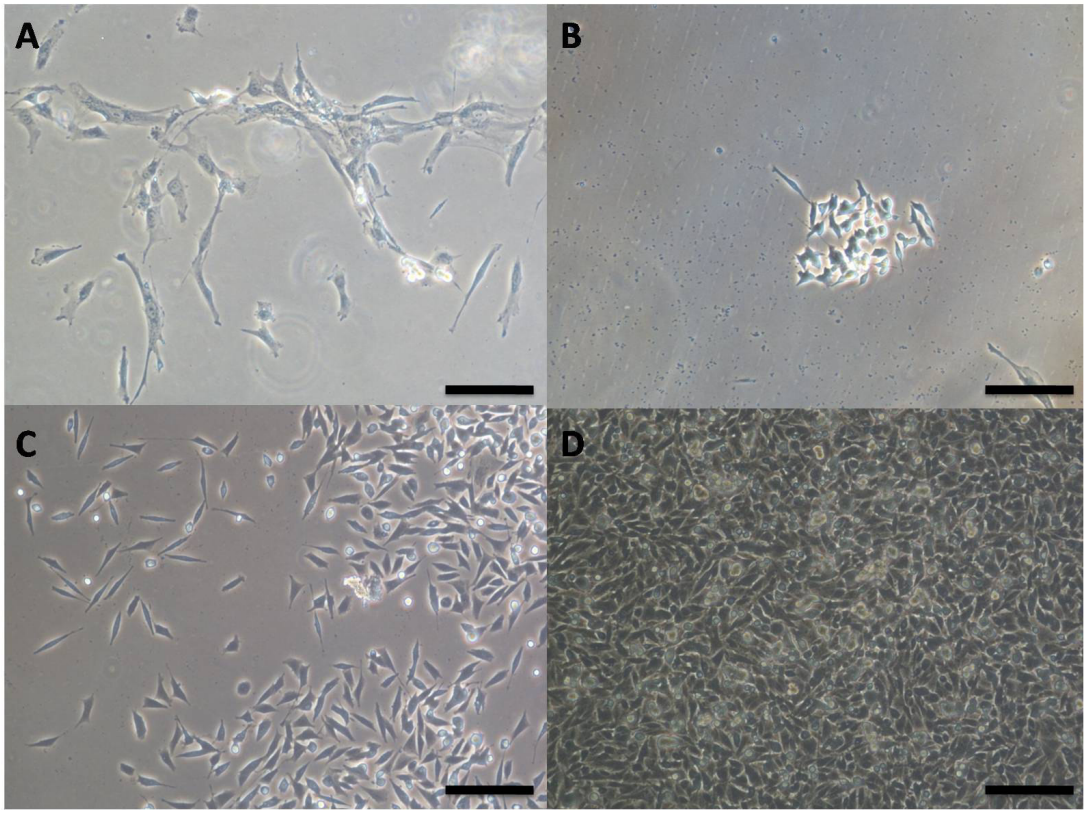


**Figure 3.5: Conditioning of Mesenchymal Stem Cells to Neural-like cells**

Mesencyhmal Stem Cells (MSCs) cultured from Cords 5, 6 and 13 were treated with the spent medium obtained from culturing of SH-SY5Y - the *in vitro* model used for neural function and differentiation experiments (at a ratio of 1:1), which induced cells to differentiate into neural-like cells. The figure above represents the transition of MSCs to neural-like cells as seen during this experiment. MSCs (A) started to differentiate within 24-hrs (B) of the addition of the spent medium and were fully differentiated within 72-hrs. Cells were left to proliferate (C) until confluence was reached (D) in approximately 3-weeks. Once confluence was achieved, cells were passaged and used for additional experiments (CD and neural marker characterisation, Retinoic Acid treatment and transfection of miRNA antagonist). Scale bar represents 20µm.

Legend: MSCs – Mesenchymal Stem Cells, CD – Cluster of differentiation, miRNA - microRNA

### 3.2.2. Conditioned Cells treated with Retinoic Acid

CCs were treated with RA to encourage the neuronal differentiation of these cells towards a more mature stage. For this study, the CCs treated with RA were cultures from Cords 5, 6 and 13. Morphological differences were visible between the RA-treated and untreated cells. Untreated cells have a large, flat, epithelial-like morphology with numerous short projections extending outward (Figure 3.6A and 3.6C), while RA-treated CCs develop several neural-like projections that connect to surrounding cells forming a neuron-like network (Figure 3.6B and 3.6C). These morphological changes were observed in approximately 80 – 90% of the treated cells within a maximum of three weeks of starting the RA treatment. Prolonging RA treatment for longer than three weeks caused the development of fibroblast-like cells. Retinoid signalling may promote the growth of endoderm, adipocytes, fibroblast-like cells or neural tissue (Soprano, Teets and Soprano, 2007). Neural fate differentiation depends on the ability of RA to reduce the FGF/Extracellular Receptor Kinase signalling which is responsible for self-renewal (Stavridis, Collins and Storey, 2010).

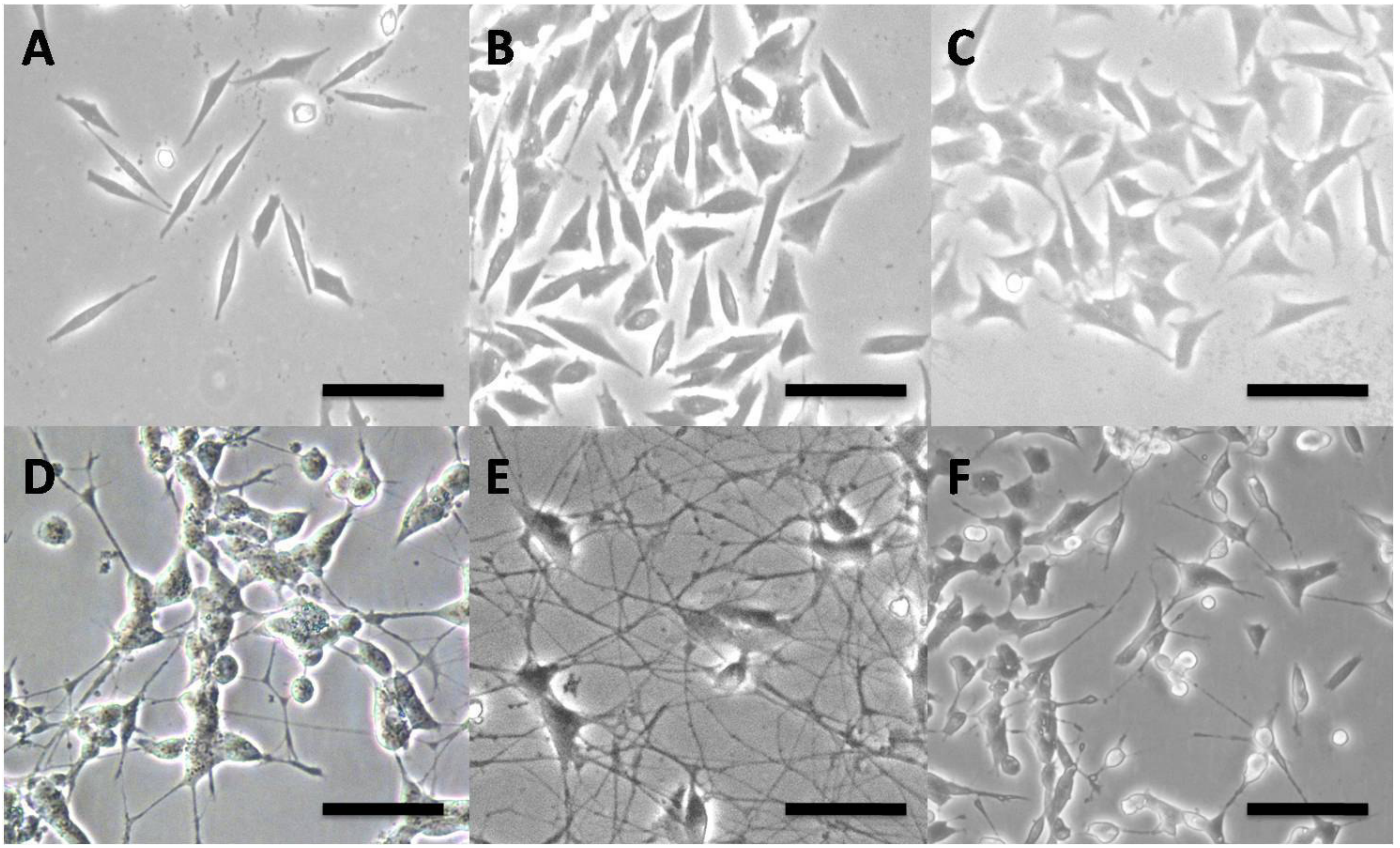


**Figure 3.6: Morphological appearance of Conditioned cells with and without Retinoic Acid treatment.**
Conditioned Cells (CCs) derived from Mesenchymal Stem Cells cultured from Cord 5 (A), Cord 6 (B) and Cord 13 (C) were seeded in a 12-well treated cell culture plate at a density of $1x10^4$ cells/ml and cultured in medium supplemented with cryo poor plasma CCP and treated with 0.2% Retinoic Acid (RA) for 15-days. RA treatment caused the Conditioned Cells to elongate and develop dendrites (from Cord 5, Cord 6 and Cord 13 CCs as seen in D, E and F respectively) thus assuming the phenotypic characteristic of neuron-like cells. Once confluence was achieved the total RNA of cells was extracted to be used in experiments for CD and neural marker characterisation and transfection of miRNA antagonist. Scale bar represents 20µm.
Legend: CC – Conditioned Cells, RA- Retinoic Acid, CD – cluster of differentiation, miRNA – microRNA

### 3.2.2.1. Comparing neurite growth between Conditioned Cells and Retinoic Acid Treated Conditioned Cells

The neurite projections of CCs and CC-RAs were measured using ImageJ. A total of 25 cells have been measured and results may be viewed in Table 3.1. An average neurite length of 3.8μm was observed in CCs while CC-RA presented neurite lengths of 15.1μm. Statistical analysis (seen in Annex IV) determined this difference to be significant.

| Cell | Neurite length | |
|---|---|---|
| | CCs | CC-RAs |
| 1 | 4.39 | 18.00 |
| 2 | 4.67 | 16.75 |
| 3 | 5.24 | 16.60 |
| 4 | 5.53 | 12.20 |
| 5 | 4.19 | 10.89 |
| 6 | 4.40 | 16.65 |
| 7 | 4.34 | 18.38 |
| 8 | 0.96 | 25.27 |
| 9 | 6.04 | 13.29 |
| 10 | 5.81 | 13.10 |
| 11 | 3.82 | 17.30 |
| 12 | 4.30 | 14.74 |
| 13 | 1.41 | 15.39 |
| 14 | 1.99 | 12.60 |
| 15 | 3.24 | 11.85 |
| 16 | 4.84 | 19.16 |
| 17 | 2.55 | 11.57 |
| 18 | 2.97 | 17.34 |
| 19 | 4.46 | 11.37 |
| 20 | 6.30 | 8.76 |
| 21 | 1.41 | 17.57 |
| 22 | 1.45 | 10.42 |
| 23 | 3.36 | 14.10 |
| 24 | 2.91 | 14.58 |
| 25 | 5.14 | 19.08 |

**Table 3.1: Neurite Length**
The neurite length in CCs and CC-RAs was measured using Image J. CCs presented an average length of 3.8 μm while CC-RA cells had an average neurite length of 15.1μm. Statistical analysis showed this difference to be significant ($P<0.05$).
Legend: CCs – Conditioned Cells, CC-RAs – Retinoic Acid treated CCs

## 3.3. Characterisation by cluster of differentiation cell surface markers

MSCs, CCs and CC-RA cells were evaluated via RT-qPCR for the recommended ISCT CD markers for the characterisation of Wharton's Jelly-derived MSCs. These included CD73, CD90, CD105, CD34 and CD45. The samples used to perform this characterisation were cells cultured and differentiated from Cords 5, 6 and 13. The average Cq of each CD marker is shown in Table 3.2 and the raw data is available in Appendix III. CD90 and CD105 were detected during the early cycles of the RT-qPCR for all the three cell types. In MSCs, CD73 was detected during the final cycles of the RT-qPCR and both CD 34 and CD45 were beyond the $40^{th}$ cycle and so not detected by the system, while in CCs and CC-RAs, expression of CD73, CD34 and CD45 registered values very close to the $40^{th}$ cycle.

| Cell Type | Sample | CD73 | CD90 | CD105 | CD34 | CD45 |
|---|---|---|---|---|---|---|
| MSC | Cord 5 | 31.65 | 24.43 | 26.11 | 39.85 | 40.00 |
| | Cord 6 | 33.80 | 27.62 | 28.63 | 40.00 | 40.00 |
| | Cord 13 | 32.82 | 26.97 | 31.36 | 40.00 | 40.00 |
| CC | Cord 5 | 38.95 | 22.07 | 24.00 | 31.82 | 40.00 |
| | Cord 6 | 32.98 | 20.27 | 23.67 | 32.87 | 34.62 |
| | Cord 13 | 40.00 | 24.60 | 25.64 | 33.76 | 40.00 |
| CC-RA | Cord 5 | 35.69 | 27.01 | 26.19 | 38.59 | 40.00 |
| | Cord 6 | 40.00 | 29.43 | 29.69 | 40.00 | 40.00 |
| | Cord 13 | 40.00 | 27.43 | 26.20 | 35.83 | 40.00 |

**Table3.2: Characterisation by CD Markers**

The RNA extracted from the cultured MSCs, CC and CC-RA cells was analysed by RT-qPCR for the expression of a panel of CD markers. The table shows the average cycling quantification (Cq) values detected during the analysis. The Cq is detected when the sample reaction surpasses that of pre-assigned threshold. The maximum Cq value reading is 40.00. When a sample Cq reaches this value, the expression which is being sought is said to be absent (value is inversely proportion to the expression). The average Cq for the expression of CD73 is seen to decrease in both CC and CC-RA cells. CD34 and CD45 expression are relatively close to the 40.00 limit for all the three cell types. On the other hand, CD 90 and CD105 were detected during much early cycles of the RT-qPCR run.

CD – Cluster of differentiation, MSC – Mesenchymal Stem Cells, CC – Conditioned Cells, CC-RA – Retinoic Acid treated CC, Cq – cycle quantification, RT-qPCR – Real Time quantification polymerase chain reaction

Figures 3.7 and 3.8 show the average fold change of these CD markers expressed by CC and CC-RA cells when these are compared to MSCs and CCs respectively. Graphs are plotted with the fold change on the y-axis and the CD of interest on the x-axis. The baseline (1.00) for comparing MSCs and CCs were the MSCs. When comparing CC and CC-RAs the baseline (starting point) was the CD expression in CCs. This means that in the case of Figure 3.7, the bars are showing whether the fold changed in CCs increased or decreased in respect to CD expression of the MSCs. In Figure 3.7A, CD73 in CCs was not detected and therefore the fold change decreased from 1.00 to 0.00. CD90 was also decreased by a fold change of 0.20, while as per Figure 3.7B, CD105 had a fold change increase of 1964.57. It was not possible to calculate the fold change of CD34 and CD45 because these where not expressed.

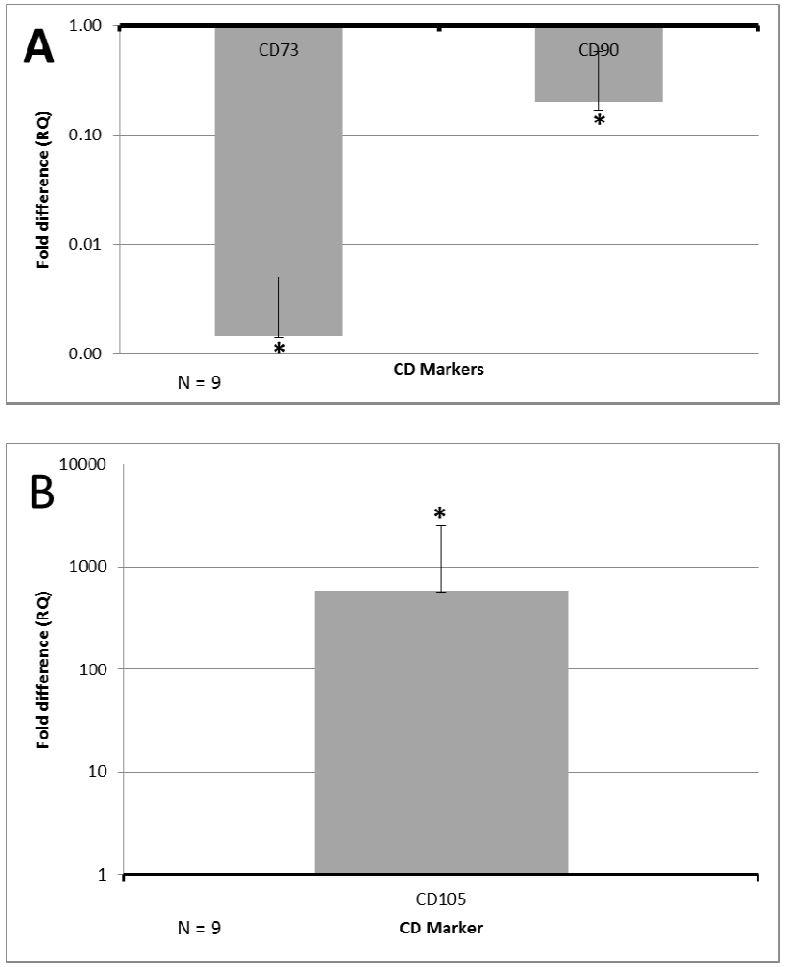


**Figure 3.7: Fold change in CD marker RNA expression from Mesencymal Stem Cells to Conditioned Cells**

The figure illustrates the average fold change difference between the CD markers detected in MSCs and CCs during RT-qPCR analysis. The starting point of this calculated fold change was the MSCs, and which was considered to be the baseline (1.00). Thus a fold-change difference of less than 1.00 represents a decrease in expression, while a fold change greater than 1.00 shows an increase in marker expression. When comparing CD markers expressed by MSCs and CCs, the fold difference for CD73 (A) was 0.00, CD90 (A) resulted in a 0.20 fold difference and CD105 (B) had a fold difference of 5.76. CD34 and CD45 were not expressed by MSCs and CCs. N represents the number of technical replicates. Error bars represent the $RQ_{min}$ and $RQ_{max}$. The * denotes a significance in the fold difference between the cell types ($P<0.05$).

Legend: MSCs – Mesenchymal Stem Cells, CCs - Conditioned Cells, CD - Cluster of differentiation, RT-qPCR – Real Time quantification polymerase chain reaction

Similarly, in Figure 3.8, graphs are representing the Fold change in expression in CC-RA with respect to CCs. In Figure 3.9, both CD90 and CD105 have a fold change decrease of 4.2 and 0.79 respectively. It was not possible to calculate the fold change of CD34 and CD45 in the three cell types because these where not expressed. The same hold for CD73 in CC and CC-RA cells.

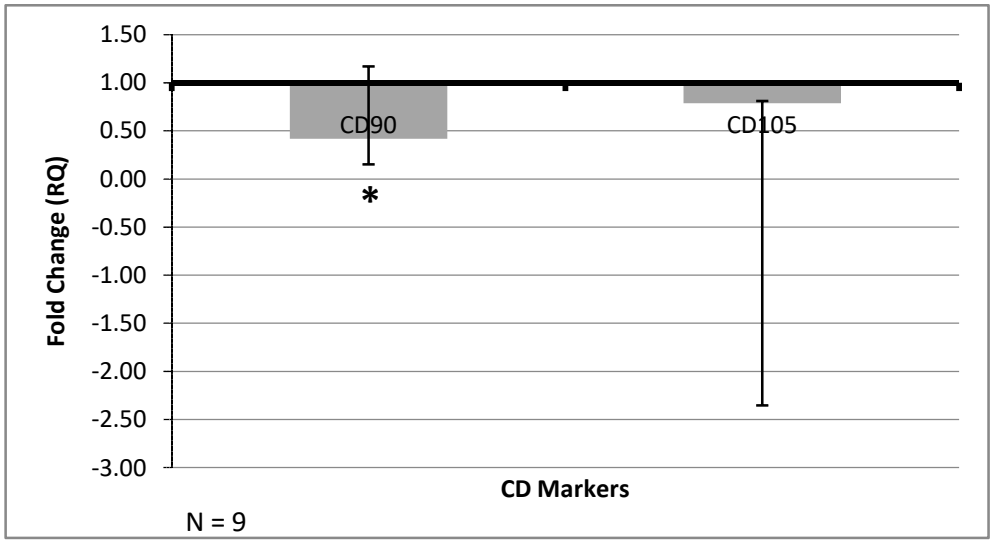


**Figure 3.8: Fold change in Neural Marker RNA expression from Conditioned Cells to Retinoic Acid-treated Conditioned Cells.**
The figure illustrates the average fold change difference between the CD markers detected in CCs and CC-RA cells during RT-qPCR analysis. The starting point of this calculated fold change was the CCs, which was considered to be the baseline (1.00). Thus, a fold-change difference of less than 1.00 represents a decrease in expression, concurrently a fold change greater than 1.00 shows an increase in marker expression. When comparing CD markers expressed by the CCs and CC-RA cells, the fold difference for CD90 was 0.42 while CD105 had a fold difference of 0.79. CD73, CD34 and CD45 were not expressed by CCs and CC-RA. N represents the number of technical replicates. Error bars represent the $RQ_{min}$ and $RQ_{max}$. The * denotes a significance in the fold difference between the cell types ($P<0.05$).
Legend: CC - Conditioned Cells, CC-RA – Retinoic Acid treated CC, CD-Cluster of differentiation, RT-qPCR – Real Time quantification polymerase chain reaction

## 3.4. Cell Characterisation by Neural Markers

Neural lineage markers are expressed by cells that are formed during neurogenesis and help distinguish between cells which have a neural phenotype and other brain cell types (Tanapat, 2016). In the absence of specific differentiating agents MSCs can express neural markers, which in turn confirms their predisposition to differentiate into cells of non-mesengenic lineages such as neurons (Fazeli *et al*., 2015).

MSCs, CCs and CC-RA cells were evaluated via RT-qPCR for RNA expression of neuronal markers determining a specific neural stage: neuroepithelial (NES and SOX2), intermediate progenitors (MASH1), immature (TUBB3 and ND1) and mature (MAP2 and NEU). Again, the samples tested were cells cultured from Cords 5, 6 and 13. Testing for the neuronal stage of the cell type has confirmed that MSCs can transdifferentiate into neural-like cells upon addition of neuroblastoma-spent medium, thus becoming CCs. This cell type was further differentiated towards maturity upon

treatment with RA, ultimately resulting in the development of CC-RA cells.

OCT4 is not a neural marker but was included in this panel to monitor the loss of stemness during the transition from MSCs to neural-like cells. OCT4 is usually still expressed at lower levels by the developing neural cells since it promotes neuroectoderm formation. Eventually this marker is drastically reduced to a point where it is no longer expressed by fully mature neural cells (Lee *et al*., 2010).

Table 3.3 shows the average neural marker Cq values obtained by RT-qPCR analysis and the raw data is shown in Appendix III. With the exception of MAP2 and NEU, all the neural markers (and OCT4) tested in the MSCs registered signals during the early cycles of the RT-qPCR analysis. CC and CC-RA cells follow a similar pattern, meaning that neural markers and OCT4 where again detected during the early cycles. MAP2 and NEU were also detected in CC and CC-RA cells except for marker NEU in the cells isolated from cord5.

| Cell Type | Sample | NES | SOX2 | OCT4 | TUBB3 | MASH1 | ND1 | MAP2 | NEUN |
|---|---|---|---|---|---|---|---|---|---|
| MSC | Cord 5 | 30.00 | 25.84 | 24.53 | 27.16 | 21.58 | 25.87 | 39.36 | 39.76 |
| | Cord 6 | 30.40 | 26.62 | 24.81 | 29.91 | 24.68 | 26.66 | 38.43 | 40.00 |
| | Cord 13 | 34.06 | 32.57 | 31.24 | 33.16 | 30.09 | 32.81 | 40.00 | 40.00 |
| CC | Cord 5 | 21.30 | 26.58 | 29.05 | 18.78 | 21.41 | 25.51 | 21.17 | 30.28 |
| | Cord 6 | 16.60 | 24.96 | 27.34 | 15.68 | 17.68 | 20.73 | 17.42 | 28.20 |
| | Cord 13 | 20.41 | 24.43 | 23.69 | 19.99 | 22.70 | 24.72 | 20.56 | 28.85 |
| CC-RA | Cord 5 | 26.23 | 28.45 | 27.96 | 24.38 | 24.05 | 27.15 | 25.11 | 40.00 |
| | Cord 6 | 25.80 | 31.52 | 27.42 | 25.29 | 25.10 | 28.33 | 25.05 | 33.45 |
| | Cord 13 | 26.40 | 19.98 | 18.23 | 26.02 | 18.57 | 18.89 | 25.86 | 35.86 |

**Table 3.3: Neuronal Markers RNA expression**

The table shows the average neuronal marker expression cycle quantification (Cq) data obtained from the RT-qPCR analysis of the RNA extracted from MSCs, CCs and CC-RA cells. The Cq is detected when the sample reaction surpasses that of pre-assigned threshold. The maximum Cq value reading is 40.00. When a sample Cq reaches this value, the expression which is being sought is said to be absent (value is inversely proportion to the expression). In MSCs both MAP2 and NEU are on the threshold limit (40.00) indicating that no reaction was registered during the RT-qPCR analysis. The same is observed in NEU for CC-RA cells isolated from Cord 5. The remaining markers where all detected during the early cycles of the analysis.

Legend: MSCs – Mesenchymal Stem Cells, CCs – Conditioned Cells, CC-RAs – Retinoic Acid treated CCs, Cq – cycle quantification, RT-qPCR – Real Time quantification polymerase chain reaction, NES – Nestin, SOX2 - Sex determining region Y-Box 2, OCT4 - Octamer-binding transcription factor 4, MASH1 - Mammalian achaete-scute homolog-1, TUBB3 - Beta III Tubulin, ND1 – NeuroD1, MAP2 - Microtubule-associatedprotein, NEU - Neuronal-specific nuclear protein 1

Figures 3.9 and 3.10 show the fold changes of these markers. Graphs were plotted using the same criteria described in Section 3.3, i.e. the expression of MSCs was taken as the starting point (1.00) when comparing fold change between MSCs and CCs. On the other hand, CCs were the baseline for the difference between CCs and CC-RA cells. Any fold differences of less or higher than 1.00 were shown respectively as a decrease and increase.

Figure 3.9A-B, shows an increase in the fold change of NES (22.74), TUBB3 (24.35). MAP2 (9757.90) and NEU (24.59) and a fold change decrease in SOX2 (0.15), OCT4 (0.08) MASH1 (0.16) and ND1 (0.17).

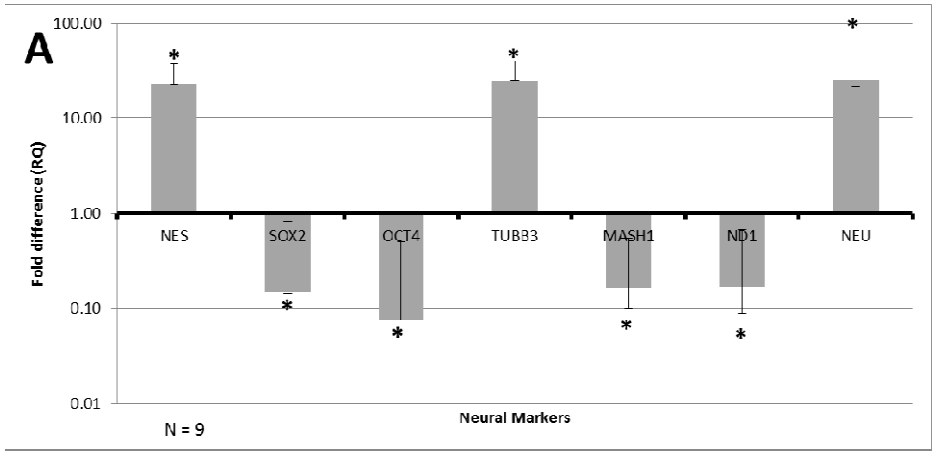


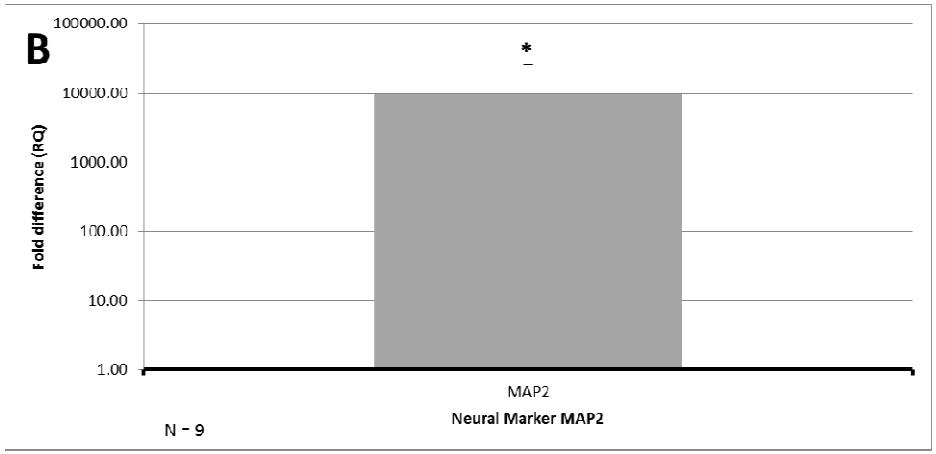


**Figure 3.9: Fold change in Neural Marker RNA expression from MSCs and CCs.**

The figure illustrates the average fold change difference between the neural markers detected in CCs and CC-RA cells during RT-qPCR analysis. The starting point of this calculated fold change was the MSCs, and which was considered to be the baseline (1.00). A fold-change difference of 0.00 represents no expression, so the smaller the Fold-difference the greater is the loss of the expression present in CCs. When comparing the neural markers expressed by MSCs and CCs, the fold differences were as follows: NES 22.74, SOX2 0.26, OCT4 0.15, TUBB3 8.28, MASH1 0.11, ND1 0.16, MAP2 97.58 and NEU 23.43. Important to note is the decrease of the stemness markers SOX2 and OCT4, and an increase of neural markers NES, TUBB3, MAP2 and NEU. N represents the number of technical replicates. Error bars represent the $RQ_{min}$ and $RQ_{max}$. The * denotes a significance in the fold difference between the cell types ($P<0.05$).
Legend: MSCs – Mesenchymal Stem Cells, CCs – Conditioned Cells, RT-qPCR – Real Time quantification polymerase chain reaction, NES – Nestin, SOX2 - Sex determining region Y-Box 2, OCT4 - Octamer-binding transcription factor 4, MASH1 - Mammalian achaete-scute homolog-1, TUBB3 - Beta III Tubulin, ND1 – NeuroD1, MAP2 - Microtubule-associatedprotein, NEU - Neuronal-specific nuclear protein 1

When comparing CC and CC-RA in Figure 3.10, NES (0.33), TUBB3 (0.24) and MAP2 (0.82) all had a fold change which was less than the 1.00 baseline. The same figure reports the values for SOX2 (69.81), OCT4 (173.85), MASH1 (14.51), ND1 (11.39) and NEU (2.57) as being over the 1.00 mark.

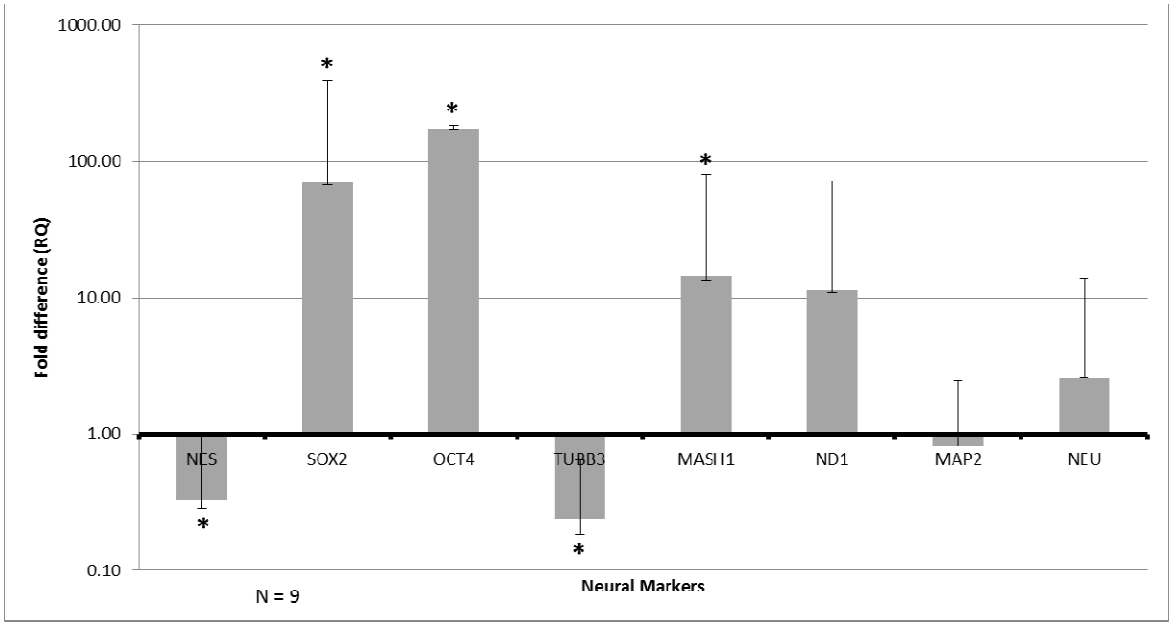


**Figure 3.10: Fold change in Neural Marker RNA expression from between CCs and CC-RA Cells**

The figure illustrates the average fold change difference between the neural markers detected in CCs and CC-RA cells during RT-qPCR analysis. The starting point of this calculated fold change was the CCs, and which was considered to be the baseline (1.00). A fold-change difference of 0.00 represents no expression, so the smaller the fold-difference the greater is the loss of the expression present in CCs. When comparing the neural markers expressed by MSCs and CCs, the fold differences were as follows: NES 0.33, SOX2 69.81, OCT4 173.85, TUBB3 0.24, MASH1 14.51, ND1 11.39, MAP2 0.82 and NEU 2.57. The elevated fold change seen in MAP2 is because this neural marker was not expressed by MSCs. Of note is the decrease in NES and TUBB3 and the increase of MASH1, ND1 and NEU, which signifies the shift of these neuron-like cells to a more mature neuronal stage. N represents the number of technical replicates. Error bars represent the $RQ_{min}$ and $RQ_{max}$. The * denotes a significance in the fold difference between the cell types ($P<0.05$).

Legend: CC – Conditioned Cells, CC-RA – Retinoic Acid treated CC, RT-qPCR – Real Time quantification polymerase chain reaction, NES – Nestin, SOX2 - Sex determining region Y-Box 2, OCT4 - Octamer-binding transcription factor 4, MASH1 - Mammalian achaete-scute homolog-1, TUBB3 - Beta III Tubulin, ND1 – NeuroD1, MAP2 - *Microtubule-associatedprotein,* NEU - Neuronal-specific nuclear protein 1

## 3.5. Transfection of microRNA antagonists

MiRNAs are known to regulate the differentiation of both MSCs and neural cells. However, little is known regarding whether individual miRNAs can induce this change. In this study, antagonists to miR-107, miR-124 and miR-381 have been tested to verify if these miRNAs may indeed cause MSCs to differentiate into neuroblasts. Furthermore, the same antagonists have been tested to elucidate whetherthese miRNAs may encourage these cells to differentiation further on towards becoming mature neurons.

### 3.5.1. Transfection Efficiency

Transfection efficiency is limited by several factors which include the health and viability of the cells, the number of passages, the degree of confluence and the transfection method used. In this study tranfection of CCs was done after 7 days from the 2$^{nd}$ passage, and CC-RA cells were transfected on the 21$^{st}$ day of the RA-treatment.

Primary cultures are difficult to maintain as these have both a limited growth potential and life-span. The MSCs used for transfection were cultured from Cords 9 and 11, and CCs and RA-CC cells were from cultures 5, 6 and 13. MSCs were transfected on the 22$^{nd}$ day from when the first cells were isolated. On the 20$^{th}$ day, MSCs were seeded in 12-wellplatesat a density of 1x10$^{4}$cells/ml. The recovery rate of MSCs was expected to be much lower than that of CCs and CC-RA cells since upon dissociation cells may initiate apoptosis signalling (Deng *et al*., 2017). MSC transfection was performed within two days of seeding to minimise such losses. To prevent the same thing happening to the CC-RA cells, these were seeded as CCs, treated with RA directly in the 12-well plate and transfected after 21 days Similarly CCs were transfected after 21 days from when these were transformed from the MSCs using the conditioned medium. Uptake of the transfection reagent (fluorescent labelled beads) by the cells was confirmed by fluorescent microscopy (Figures 3.11– 3.18).

After treating cells with the transfection reagent for 48-hours, they were washed in PBS to remove any unbound microparticles and viewed microscopically using x200 magnification. Brightfield microscopy (Figure 3.11– 3.18 images A – D) shows that all cells maintained both membrane architecture and structure integrity. When observing the same fields at the same magnification using a red fluorescence filter (Figure 3.11– 3.18images F – I), it is possible to view the bound nanoparticles which appear as fluorescent specks. Merging of both brightfield and fluorescent images (Figure 3.11– 3.18images K – N), gives an approximation of the number of cells which absorbed and incorporated the transfection reagent. To ensure that the fluorescence was caused by the transfection reagent,untransfected cells were also viewed under the same conditions (Figure 3.11– 3.18images E, J and O). No fluorescence was seen when viewed using the red filter, which is evidence that the fluorescent specks seen in the transfected cells were indeed the consequence of the magnetic fluorescent microparticles. The overall transfection efficiency characterised by the uptake of the microparticles

showed that most cells did indeed incorporate the magnetic beads. However, this efficiency only indicates how many microparticles have been incorporated into the cells. It is not possible to know the exact amount of miRNA antagonist that actual aggregated to the beads and how much of this was taken up by the cell itself. The efficiency of these microparticles was confirmed by transfection of GFP and the results are illustrated in Figure 3.19. CCs and CC-RA cells used for the GFP transfection were both from Cord 6. This result confirms that transfection of GFP was successful, thus since the miRNA antagonists are smaller in length, it is reasonable to conclude that these too were able to aggregate to the microparticles and be subsequently taken up by the cells.

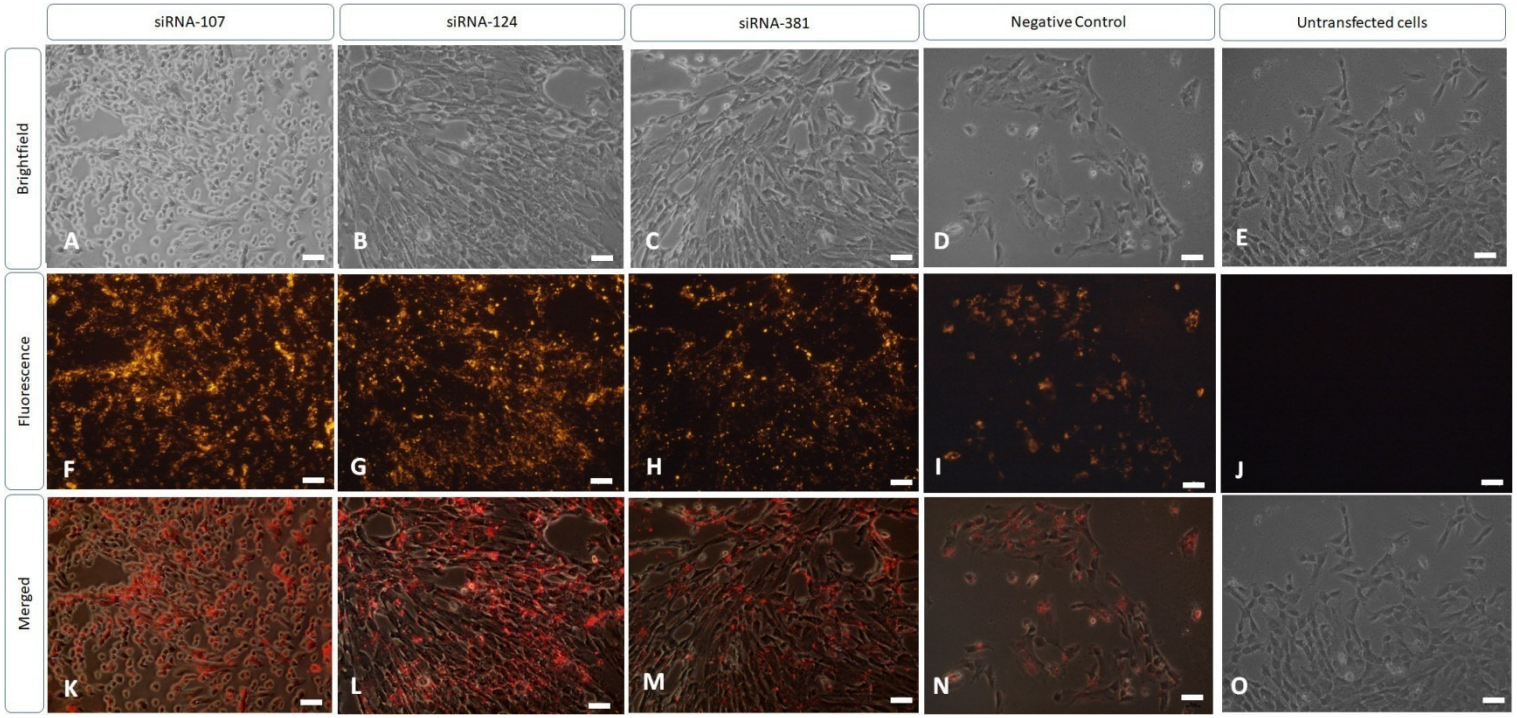


**Figure 3.11: Transfection of Cord 9 Mesenchymal Stem Cells**

miRNA antagonists were transfected into Cord 5 MSCs using magnetic florescent nanoparticles upholding the xeno-free set-up adopted throughout the whole experiment. Cells were transfected for 48-hrs and washed in PBS to remove any nanoparticles which had not been incorporated in the cells. Brightfield images (A – E) show that the membrane architecture and structure of the cells were intact after the uptake of the nanoparticles. Once on the cells, the nanoparticles were incorporated in the cell by endocytosis and the attached miRNA antagonist was uptaken via pinocytosis. Incorporation of the nanoparticles is represented by the fluorescent images (F-J) and the merged images (K-O) show the position of the nanoparticles in relation to the cell. The negative control represents the cells transfected with the MISSION® Synthetic microRNA Inhibitor. Scale bar represents 20µm.

Legend: MSCs – Mesenchymal Stem Cells

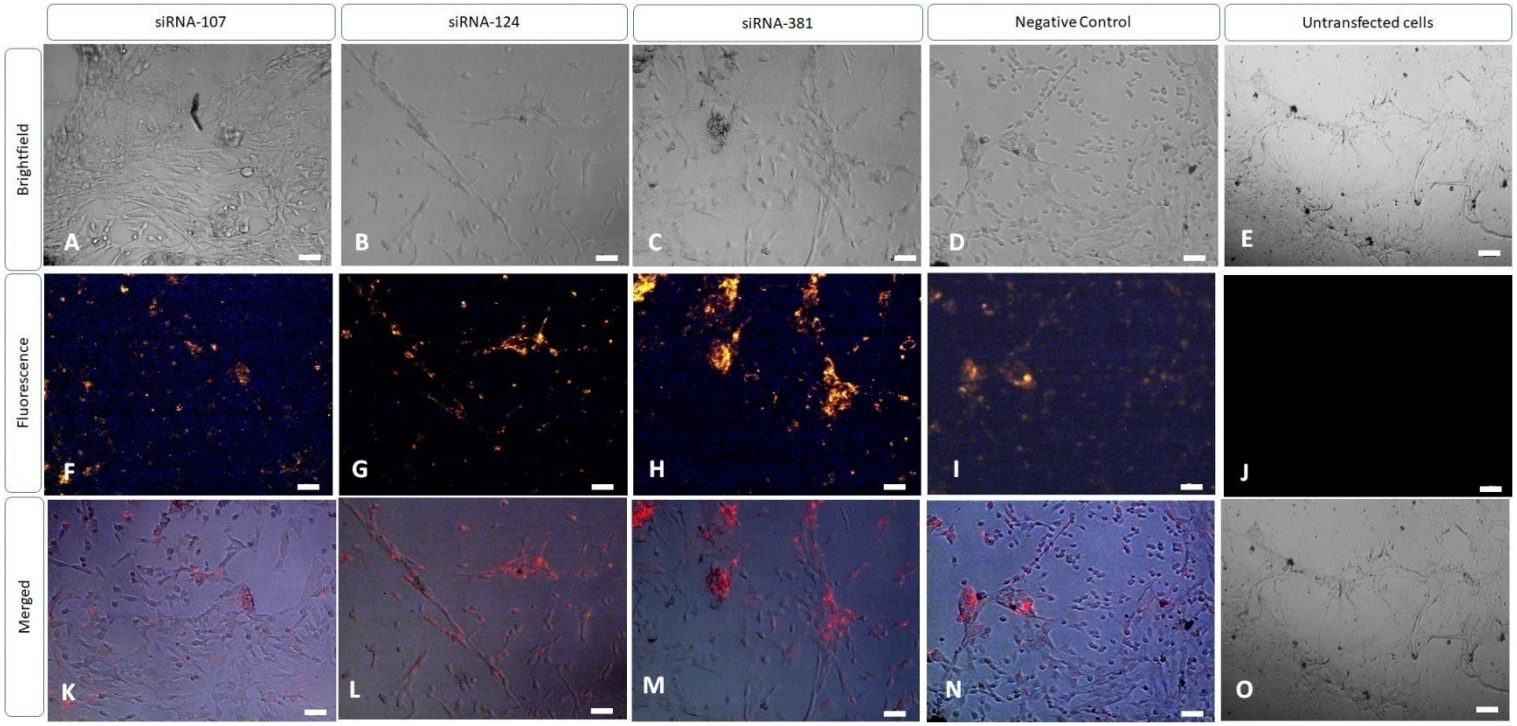


**Figure 3.12: Transfection of Cord 11 Mesenchymal Stem Cells**

miRNA antagonists were transfected into Cord 11 MSCs using magnetic florescent nanoparticles upholding the xeno-free set-up adopted throughout the whole experiment. Cells were transfected for 48-hrs and washed in PBS to remove any nanoparticles which had not been incorporated in the cells. Brightfield images (A – E) show that the membrane architecture and structure of the cells were intact after the uptake of the nanoparticles. Once on the cells, the nanoparticles were incorporated in the cell by endocytosis and the attached miRNA antagonist was uptaken via pinocytosis. Incorporation of the nanoparticles is represented by the fluorescent images (F-J) and the merged images (K-O) show the position of the nanoparticles in relation to the cell. The negative control represents the cells transfected with the MISSION® Synthetic microRNA Inhibitor. Scale bar represents 20μm.

Legend: MSCs – Mesenchymal Stem Cells

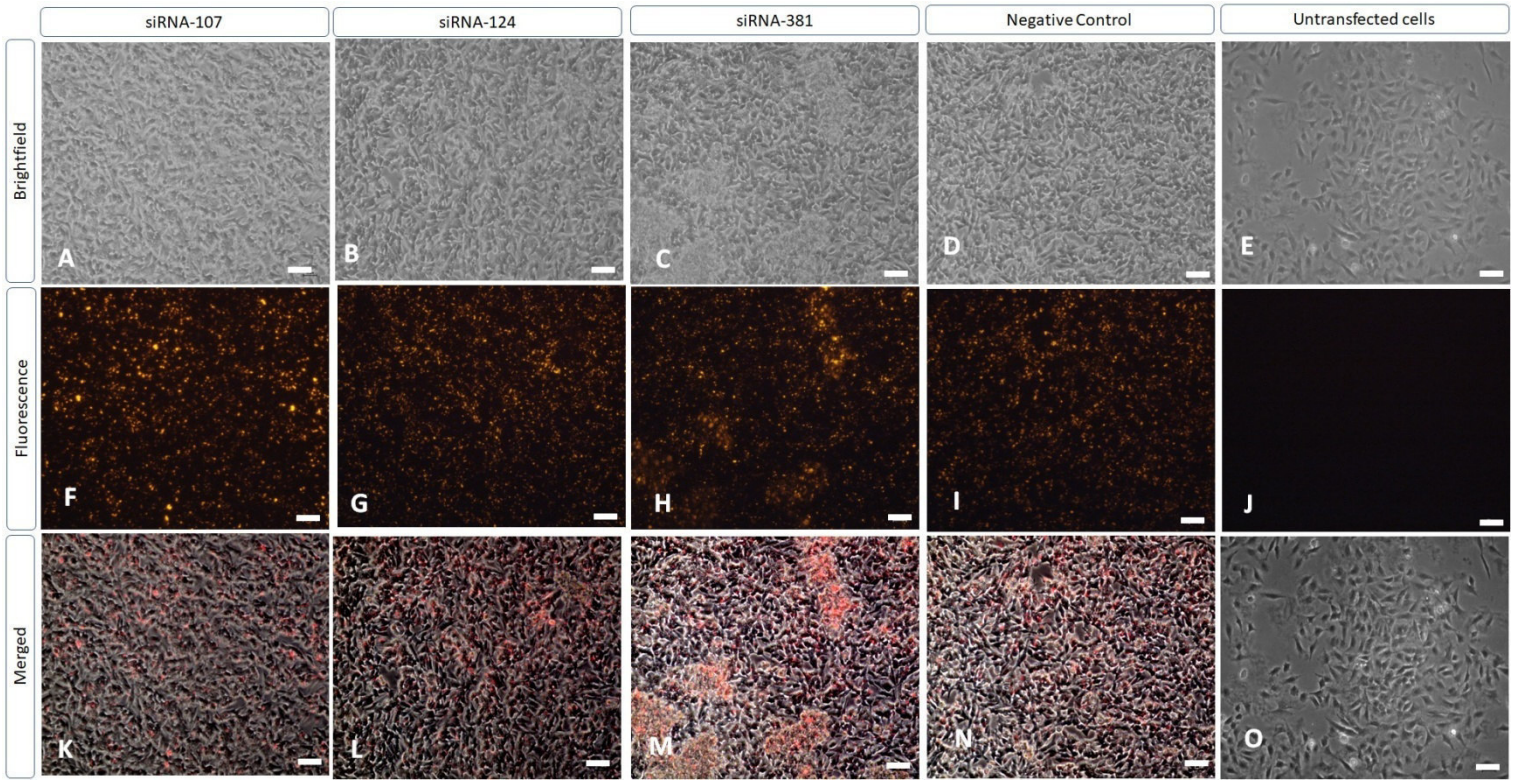


**Figure 3.13: Transfection of Cord 5 Conditioned Cells**

miRNA antagonists were transfected into Cord 5 CCs using magnetic florescent nanoparticles upholding the xeno-free set-up adopted throughout the whole experiment. Cells were transfected for 48-hrs and washed in PBS to remove any nanoparticles which had not been incorporated in the cells. Brightfield images (A – E) show that the membrane architecture and structure of the cells were intact after the uptake of the nanoparticles. Once on the cells, the nanoparticles were incorporated in the cell by endocytosis and the attached miRNA antagonist was uptaken via pinocytosis. Incorporation of the nanoparticles is represented by the fluorescent images (F-J) and the merged images (K-O) show the position of the nanoparticles in relation to the cell. The negative control represents the cells transfected with the MISSION® Synthetic microRNA Inhibitor. Scale bar represents 20µm.

Legend: CCs – Conditioned Cells

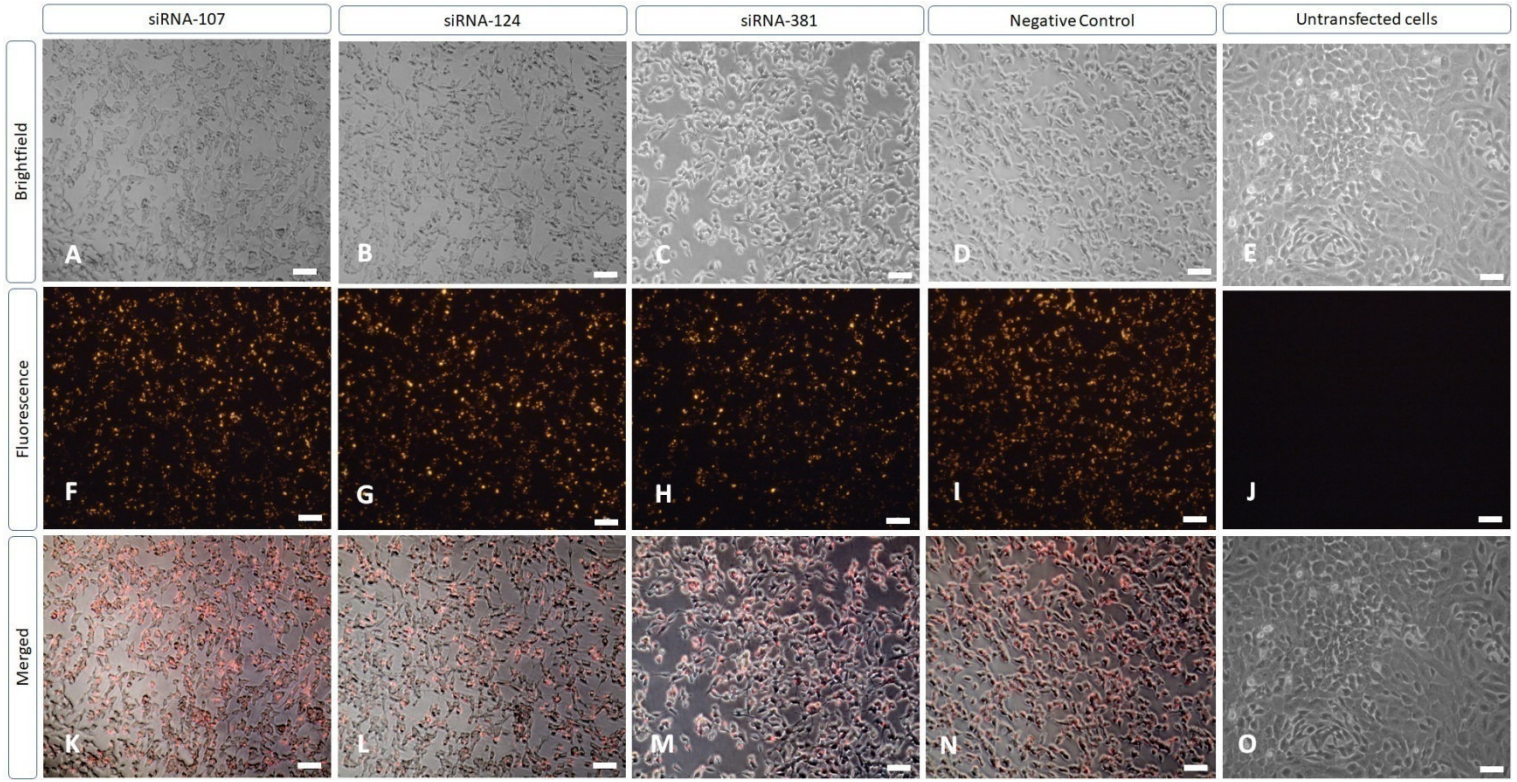


**Figure3.14: Transfection of Cord 6 Conditioned Cells**

miRNA antagonists were transfected into Cord 6 CCs using magnetic florescent nanoparticles upholding the xeno-free set-up adopted throughout the whole experiment. Cells were transfected for 48-hrs and washed in PBS to remove any nanoparticles which had not been incorporated in the cells. Brightfield images (A – E) show that the membrane architecture and structure of the cells were intact after the uptake of the nanoparticles. Once on the cells, the nanoparticles were incorporated in the cell by endocytosis and the attached miRNA antagonist was uptaken via pinocytosis. Incorporation of the nanoparticles is represented by the fluorescent images (F-J) and the merged images (K-O) show the position of the nanoparticles in relation to the cell. The negative control represents the cells transfected with the MISSION® Synthetic microRNA Inhibitor. Scale bar represents 20µm.

Legend: CCs – Conditioned Cells

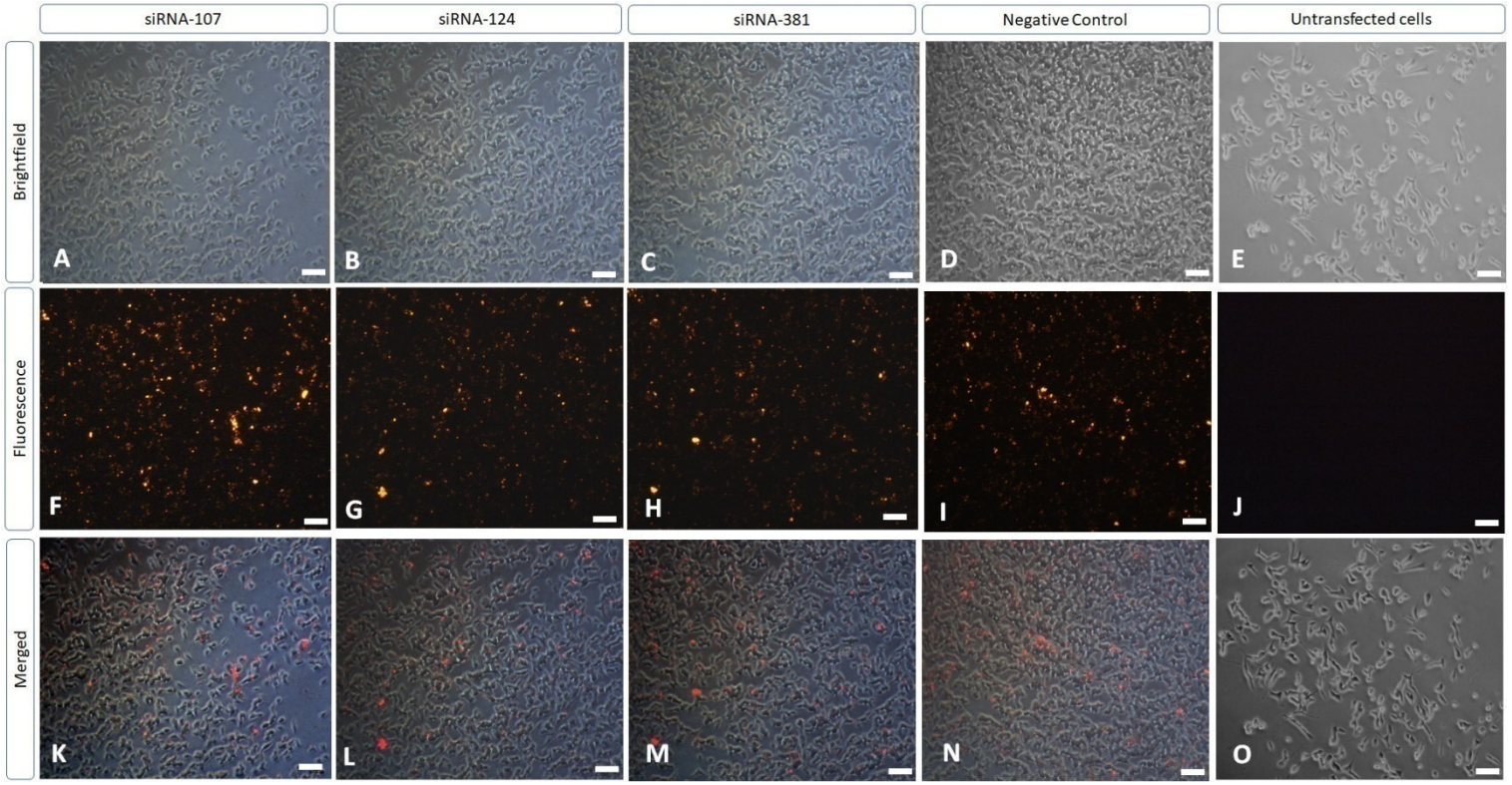


**Figure 3.15: Transfection of Cord 13 Conditioned Cells**

miRNA antagonists were transfected into Cord 13 CCs using magnetic florescent nanoparticles upholding the xeno-free set-up adopted throughout the whole experiment. Cells were transfected for 48-hrs and washed in PBS to remove any nanoparticles which had not been incorporated in the cells. Brightfield images (A – E) show that the membrane architecture and structure of the cells were intact after the uptake of the nanoparticles. Once on the cells, the nanoparticles were incorporated in the cell by endocytosis and the attached miRNA antagonist was uptaken via pinocytosis. Incorporation of the nanoparticles is represented by the fluorescent images (F-J) and the merged images (K-O) show the position of the nanoparticles in relation to the cell. The negative control represents the cells transfected with the MISSION® Synthetic microRNA Inhibitor. Scale bar represents 20μm.

Legend: CCs – Conditioned Cells

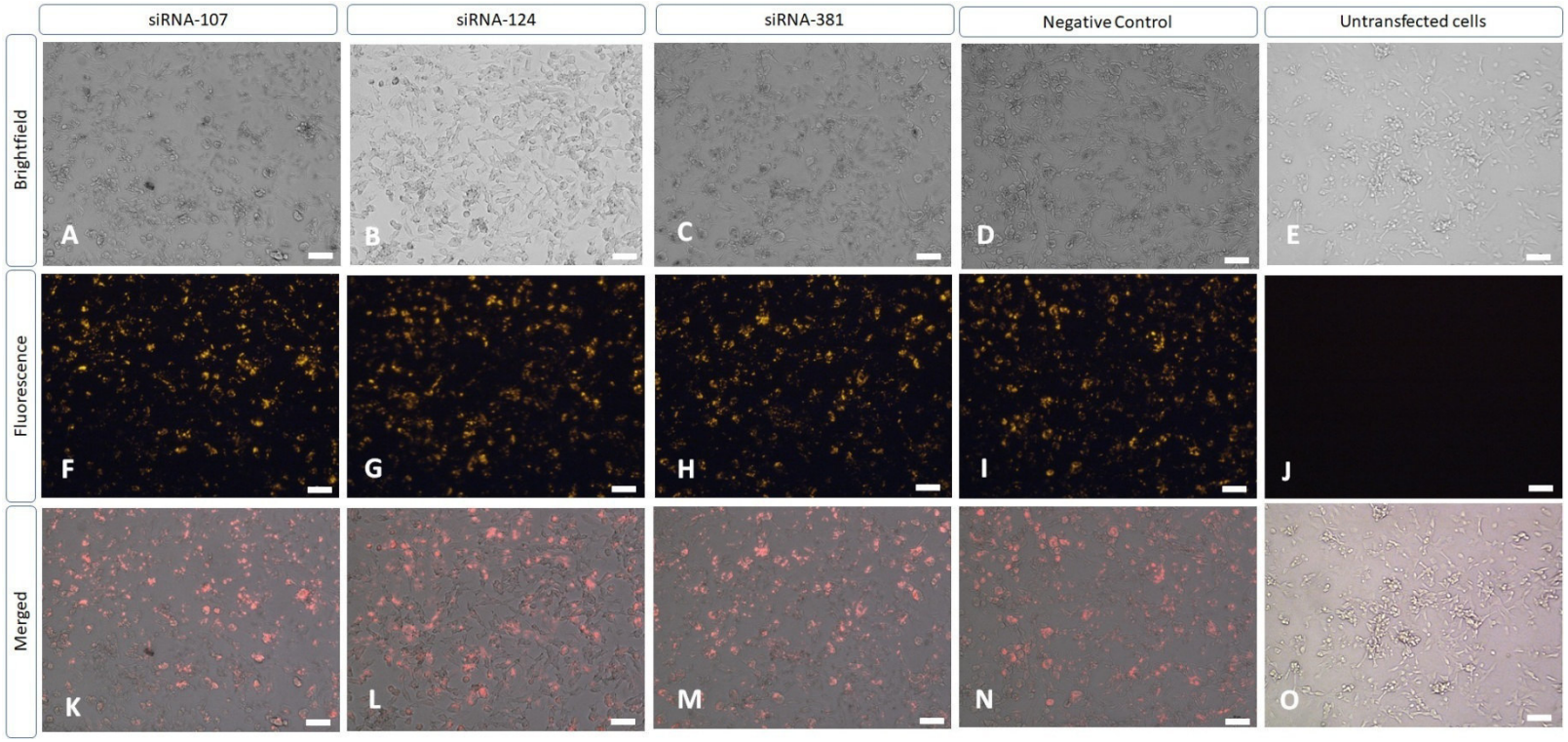


**Figure 3.16: Transfection of Cord 5 Retinoic Acid treated Conditioned Cells**

miRNA antagonists were transfected into Cord 6 CC-RA cells using magnetic florescent nanoparticles upholding the xeno-free set-up adopted throughout the whole experiment. Cells were transfected for 48-hrs and washed in PBS to remove any nanoparticles which had not been incorporated in the cells. Brightfield images (A – E) show that the membrane architecture and structure of the cells were intact after the uptake of the nanoparticles. Once on the cells, the nanoparticles were incorporated in the cell by endocytosis and the attached miRNA antagonist was uptaken via pinocytosis. Incorporation of the nanoparticles is represented by the fluorescent images (F-J) and the merged images (K-O) show the position of the nanoparticles in relation to the cell. The negative control represents the cells transfected with the MISSION® Synthetic microRNA Inhibitor. Scale bar represents 20µm.

Legend: CC-RA – Retinoic Acid treated Conditioned Cells

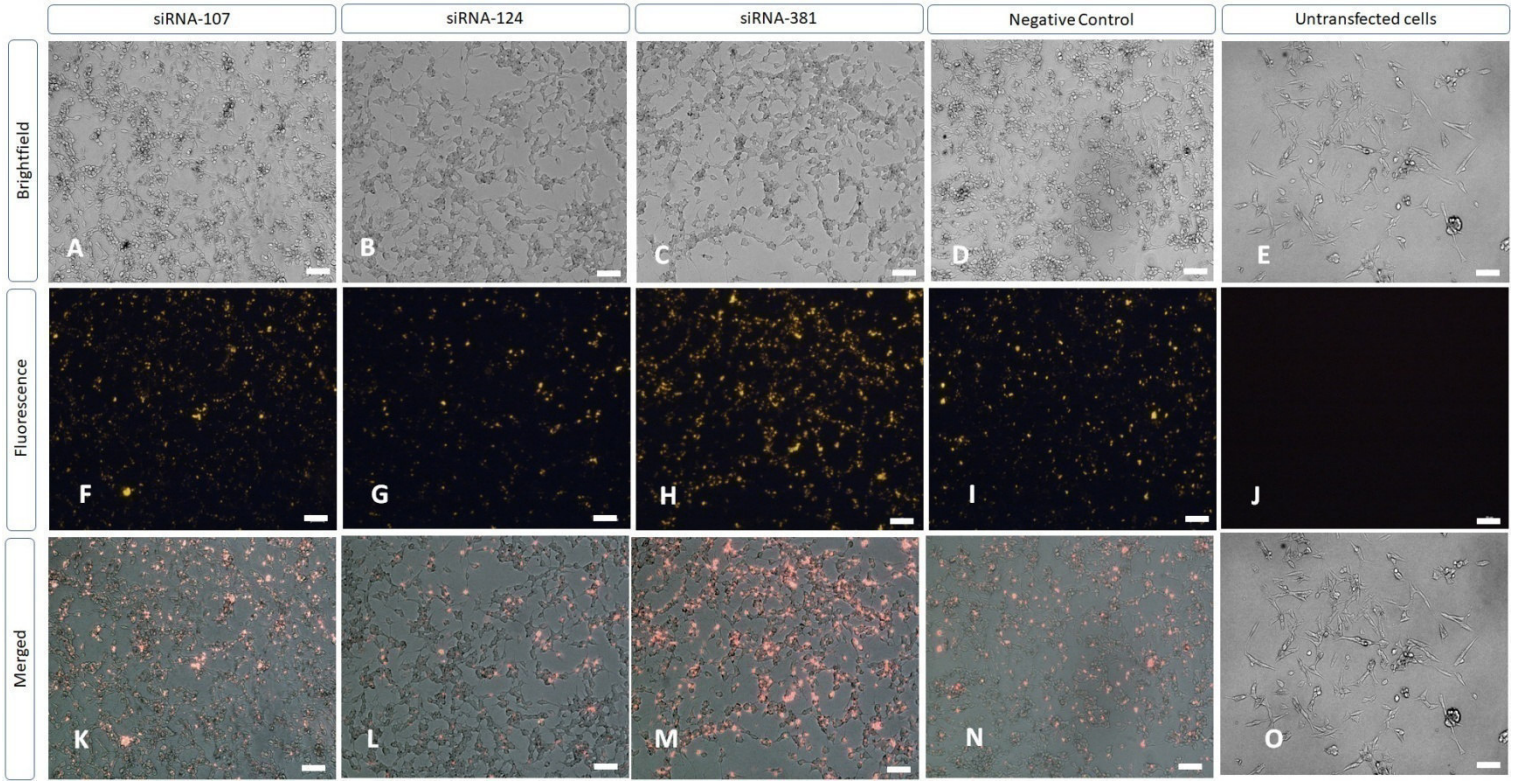


**Figure 3.17: Transfection of Cord 6 Retinoic Acid treated Conditioned Cells**

miRNA antagonists were transfected into Cord 6 CC-RA cells using magnetic florescent nanoparticles upholding the xeno-free set-up adopted throughout the whole experiment. Cells were transfected for 48-hrs and washed in PBS to remove any nanoparticles which had not been incorporated in the cells. Brightfield images (A – E) show that the membrane architecture and structure of the cells were intact after the uptake of the nanoparticles. Once on the cells, the nanoparticles were incorporated in the cell by endocytosis and the attached miRNA antagonist was uptaken via pinocytosis. Incorporation of the nanoparticles is represented by the fluorescent images (F-J) and the merged images (K-O) show the position of the nanoparticles in relation to the cell. The negative control represents the cells transfected with the MISSION® Synthetic microRNA Inhibitor. Scale bar represents 20µm.

Legend: CC-RA – Retinoic Acid treated Conditioned Cells

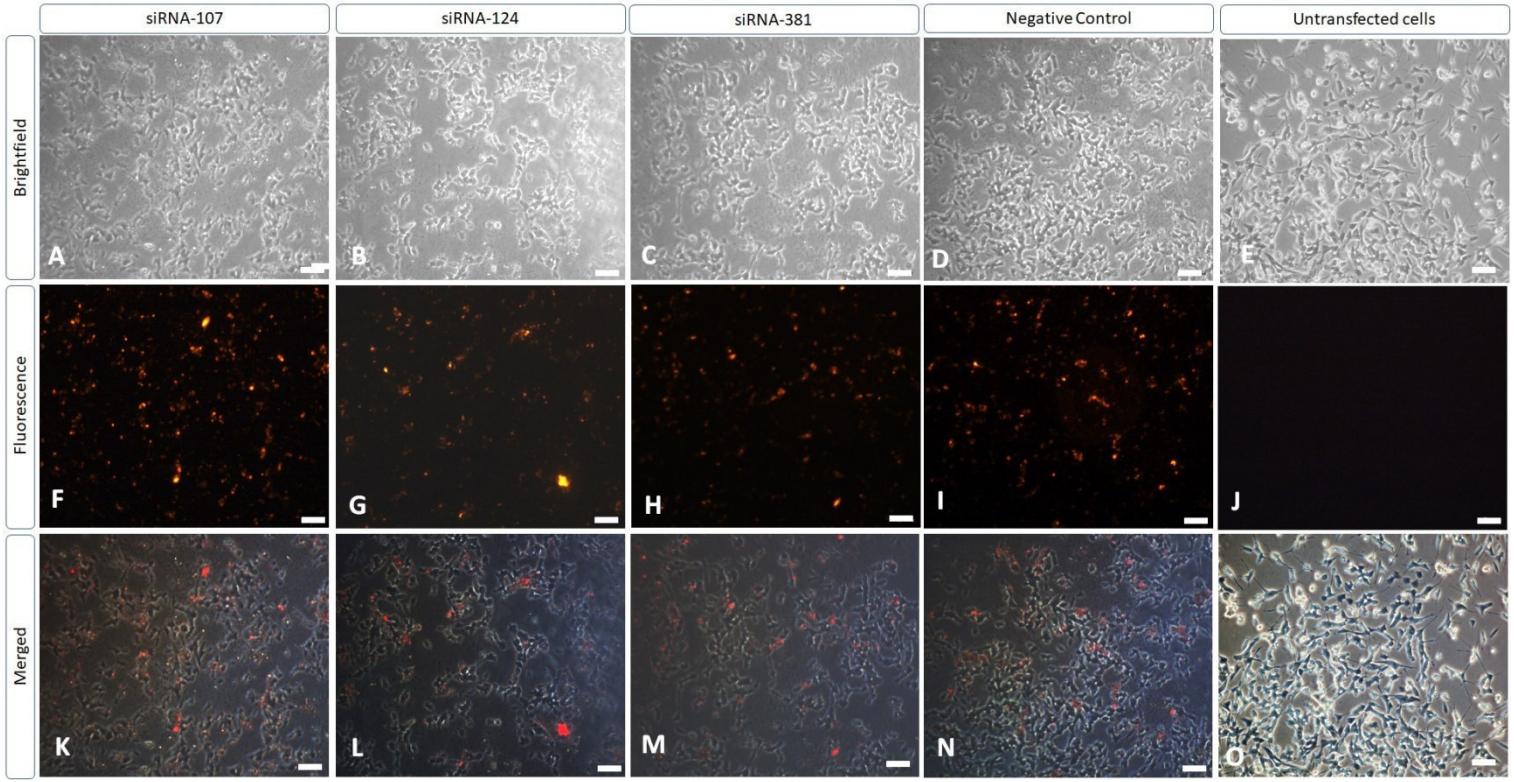


**Figure 3.18: Transfection of Cord 13 Retinoic Acid treated Conditioned Cells**

miRNA antagonists were transfected into Cord 13 CC-RA cells using magnetic florescent nanoparticles upholding the xeno-free set-up adopted throughout the whole experiment. Cells were transfected for 48-hrs and washed in PBS to remove any nanoparticles which had not been incorporated in the cells. Brightfield images (A – E) show that the membrane architecture and structure of the cells were intact after the uptake of the nanoparticles. Once on the cells, the nanoparticles were incorporated in the cell by endocytosis and the attached miRNA antagonist was uptaken via pinocytosis. Incorporation of the nanoparticles is represented by the fluorescent images (F-J) and the merged images (K-O) show the position of the nanoparticles in relation to the cell. The negative control represents the cells transfected with the MISSION® Synthetic microRNA Inhibitor. Scale bar represents 20µm.

CC-RA – Retinoic Acid treated Conditioned Cells

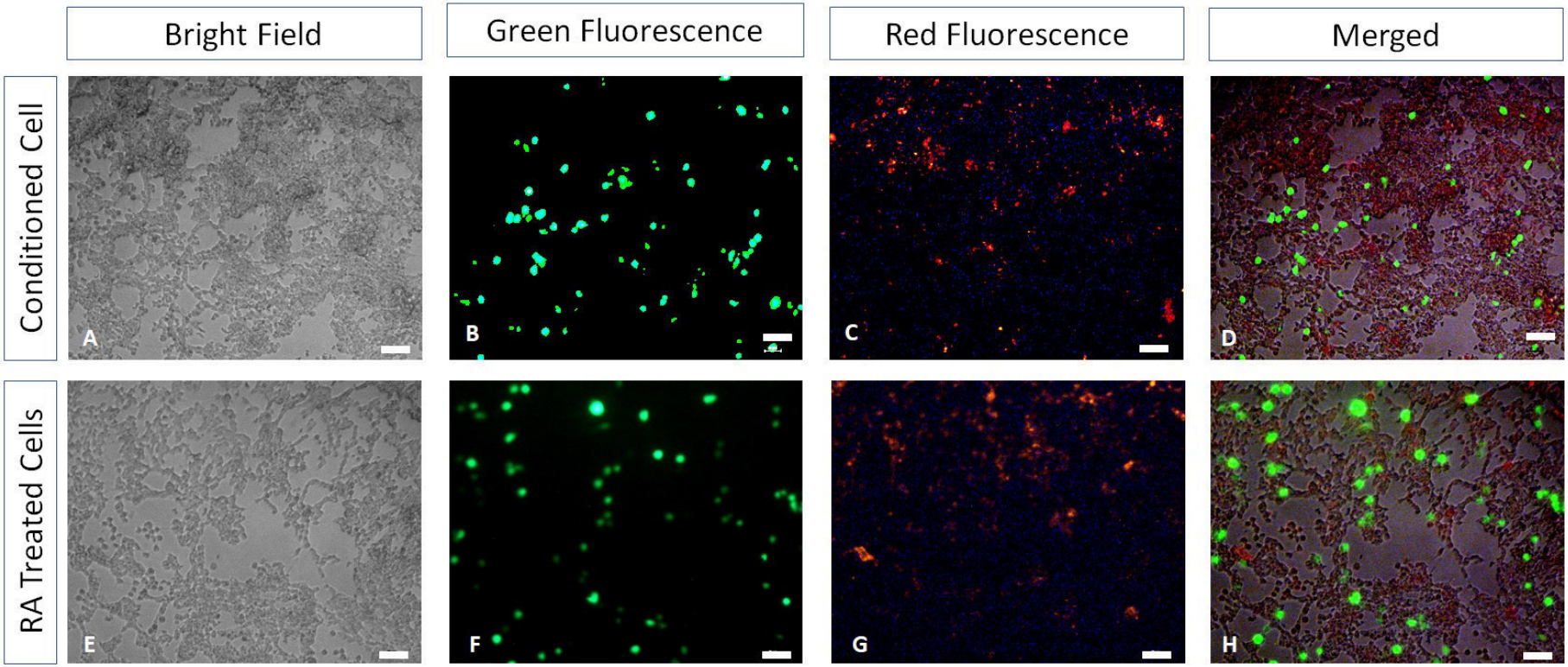


**Figure3.19: Transfection of Green Fluorescent Protein**

Green Fluoresent Protein (GFP) was transfected into CCs and CC-RA cells to further confirm the efficiency of the transfection employing the fluorescent nanoparticles. Again, bright field images (A and E) confirm the membrane architecture and structure of the cells were intact after transfection. The green fluorescence images (B and F) indicate that GFP was transfected into the cells, while the red fluorescent images (C and G) show the incorporation of the nanoparticles in the cell. The merged images (G and H) identify the GFP transfected cells in relation to the incorporated nanoparticles and the other cells. Scale bar represents 20μm.

Legend: GFP – Green Fluorescent Protein, CCs - Conditioned cells, CC-RA – Retinoic Acid treated CC

### 3.5.2. The effect of microRNA antagonist transfection on target genes

Shown in Table 3.4 are the Cq values registered during the RT-qPCR analysis for the three targets genes expressed by MSCs, CCs and CC-RA cells post transfection of siR-107 (target *DICER*), siR-124 (target *PTP1B*) and siR-381 (target *HES1*). Included in the table are the Cq values obtained when measuring the target gene expression in the cells transfected with the negative control, i.e. the cells transfected with the MISSION® Synthetic microRNA Inhibitor. The target gene expression in MSCs post siRNA (and control) transfection register Cq values during the final cycles of the RT-qPCR. Cord 9 *HES1* and Cord 11 *DICER* having a Cq value of 40.00, meaning that no RNA for these two genes was detected. A similar pattern may be seen with CCs. However, in this case RNA for *PTP1B* Cq values were detected during the early cycles. For this target, Cq values ranged from 25.57 – 26.38 in the siRNA transfected cells and from 27.96 – 28.97 in the cells transfected with the MISSION® Synthetic microRNA Inhibitor. With regards to the expression of these target genes found in CC-RA cells,

Cq values for *DICER* ranged from 27.25 – 30.01, *PTP1B* was detected between 25.90 – 31.91 and *HES1* values where between 25.60 – 29.63. Raw data may be viewed in Appendix III.

| Cell Type | Sample | DICER | PTP1B | HES1 | DICER NEG CTL | PTP1B NEG CTL | HES1 NEG CTL |
|---|---|---|---|---|---|---|---|
| MSC | Cord 9 | 32.61 | 32.94 | 40.00 | 34.90 | 34.45 | 33.49 |
| | Cord 11 | 40.00 | 31.46 | 31.30 | 34.43 | 30.37 | 32.49 |
| CC | Cord 5 | 30.13 | 26.38 | 36.58 | 34.24 | 28.97 | 38.58 |
| | Cord 6 | 32.31 | 26.39 | 33.82 | 31.89 | 28.26 | 32.03 |
| | Cord 13 | 32.14 | 25.57 | 30.15 | 32.43 | 27.96 | 29.37 |
| CC-RA | Cord 5 | 28.45 | 31.91 | 25.60 | 29.02 | 23.43 | 28.03 |
| | Cord 6 | 30.01 | 26.76 | 29.63 | 28.60 | 22.82 | 27.54 |
| | Cord 13 | 27.32 | 25.90 | 26.56 | 27.25 | 23.33 | 27.33 |

**Table 3.4: Gene Target RNA expression.**

The table shows the average cycle quantification (Cq) which represent the time taken for the qPCR set-up to detect the signal emitted during amplification. Cultured cells where transfected with miRNA antagonist for 48-hrs after which total RNA was extracted and analysed using RT-qPCR to detect the expression of their respective targets. The targets were as follows: DICER for transfection of siR-107, PTP1B for siR-124 and HES1 for siR-381. Except for HES1 and DICER in MSCs respectively from Cord 9 and Cord 11, all other targets registered a Cq value. Cq values are inverse to the amount of target nucleic acid, meaning that lower Cq values (typically below 29 cycles) indicate high amounts of target sequence while higher Cq values (above 38 cycles) mean a lower amount of target nucleic acid. With the exception of the two results whose Cq was 40.00, all other targets registered a Cq results which ranged between 22.82 and 38.58. The negative control is the MISSION® Synthetic microRNA Inhibitor.

Legend: MSCs – Mesenchymal Stem Cells, CCs – Conditioned Cells, CC-RAs – Retinoic Acid treated CCs, NEG CTL – Negative miRNA antagonist control, NTC – Non template control, HES1 – Hairy and enhancer of split 1, PTP1B - Protein-tyrosine phosphatase 1B, Cq – cycle quantification, RT-qPCR – Real Time quantification polymerase chain reaction

*DICER* plays an important regulatory role in several biological functions. The *DICER1* gene produces a protein which regulates the RNA expression of other genes and is responsible for the formation of miRNAs. Due to its various regulatory effect on gene RNA expression, *DICER* is also associated with cell growth, proliferation and differentiation (U.S. Department of Health & Human Services, 2019). *DICER* is regulated by miR-107, where a decreased RNA expression of this miRNA increases *DICER*, promoting neurogenesis (Ristori *et al.*, 2015).

Like other members of the Hairy and Enhancer of Split proteins, *HES1* is responsible for several physiological processes including cellular differentiation, cell cycle arrest, apoptosis and self-renewal (Liu, Dai and Du, 2015). The presence of miR-381 increases the RNA expression of HES1 (Shi *et al.*, 2015).

MiR-124 regulates the progression of neural differentiation. The RNA expression of the mRNA binding protein*PTP1B*, a global regulator of pre-mRNA splicing, is down-regulated by

miR-124(Neo *et al*., 2014). One of the roles of *PTP1B* is to prevent the early onset of neural progenitors (Linares *et al.*, 2015).This means that in the presence of themR-124 antagonist, the *PTP1B* gene RNA expression should increase and prevent neural differentiation.

Figure 3.20 A - C show the average fold change in gene target expression obtained after transfecting the three cell types with the siRNAs for MSCs (A), CCs (B) and CC-RA (C). The baseline (1.00) is based on the Cq values registered during the RT-qPCR analysis of the cells transfected with the MISSION® Synthetic microRNA Inhibitor, that is the Negative control is the starting point of the fold change. Results show that post transfection the fold change in MSCs was 8.25 for *DICER*, 0.03 for *PTP1B* and 1.14 in *HES1*. In CCs the fold change seen in DICER was 12.22, in *PTP1B* 5.13 and *HES1* 1.81. Finally, the calculated fold change in CC-RA cells was 5.93 for *DICER*, 0.08 for *PTP1B* and 1.55 for *HES1*.

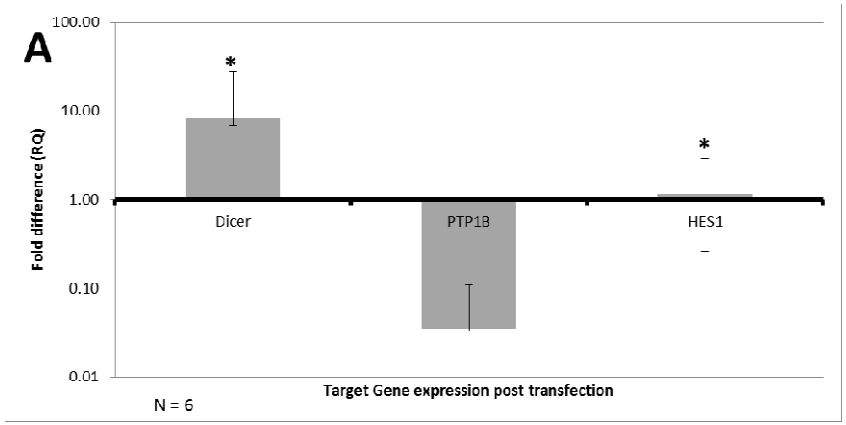


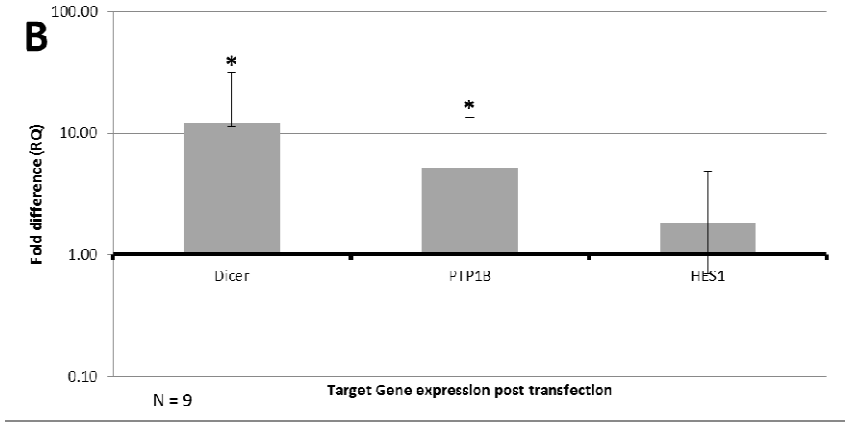


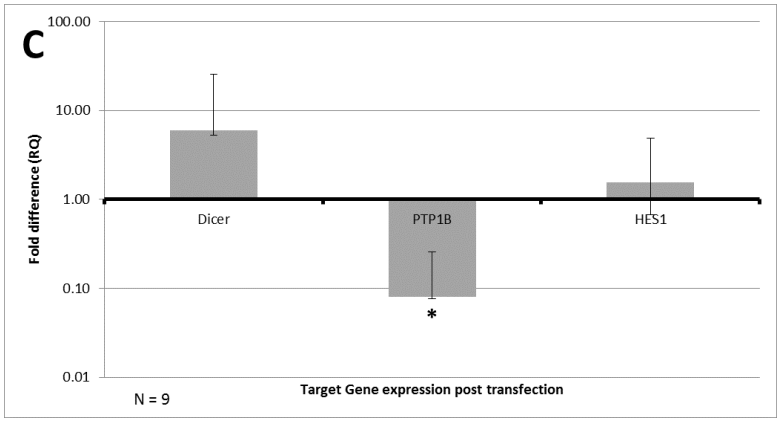


**Figure 3.20: Fold change in Target Gene expression post miRNA antagonist transfection**

The above barchart shows the average fold change difference between the miRNA target gene expressed post-transfection of miRNA antagonists by MSCs (A), CCs (B) and CC-RAs (C) cells during RT-qPCR analysis. The starting point of this calculated fold change was the Negative Transfection Control (MISSION® Synthetic microRNA Inhibitor), and which was considered to be the baseline (1.00). A fold-change difference of 0.00 represents no expression, so the smaller the fold-difference, the greater is the loss of the expression of these markers in the cells. The fold difference in MSCs was *DICER* 8.25, *PTP1B* 0.03 and *HES1* 1.14. In CC cells *DICER* had a fold difference of 12.22, *PTP1B* 5.13 and *HES1* 1.81. The fold difference observed for CC-RA in *DICER* was 5.93, *PTP1P* 0.08 and *HES1* 1.55. N represents the number of technical replicates. Error bars represent the $RQ_{min}$ and $RQ_{max}$. The * denotes a significance in the fold difference between the cell types ($P<0.05$).

Legend: MSCs – Mesenchymal Stem Cells, CCs – Conditioned Cells, CC-RA – Retinoic Acid treated CCs, RT-qPCR – Real Time quantification polymerase chain reaction, Hairy and enhancer of split 1, PTP1B - Protein-tyrosine phosphatase 1B, miRNA - microRNA

### 3.5.3. Neural marker RNA expression post-transfection with microRNA antagonists

The changes in the RNA expression of neural markers NES, TUBB3, ND1, MAP2 and NEU were assessed post-transfection of the miRNA antagonists. These markers were selected from the previous panel since: NES is the primary marker for neural epithelial cells and should reflect the transdifferentiation of the MSCs and further maturation of the neural cells; TUBB3 is the marker which is most likely to show the change during the transition from MSCs to neural-like cells; ND1 was the only marker used in the previous panel which represents the intermediate neural progenitor stage; Both MAP2 and NEU are late neural markers and would confirm whether the CCs and CC-RA cells had proceeded to a more mature stage.

RT-qPCR data for the expression of these markers has been summarised in Table 3.5 (raw Data in Appendix III).

**A: NES**

| Cell Type | Sample | si107 | si124 | si381 | NEG CTL |
|---|---|---|---|---|---|
| MSC | Cord 9 | 36.60 | 34.54 | 40.00 | 34.26 |
| | Cord 11 | 40.00 | 33.27 | 40.00 | 33.86 |
| CC | Cord 5 | 30.95 | 28.81 | 29.14 | 30.24 |
| | Cord 6 | 32.49 | 30.34 | 29.68 | 31.02 |
| | Cord 13 | 32.23 | 30.60 | 29.81 | 30.75 |
| CC-RA | Cord 5 | 29.05 | 27.82 | 24.01 | 26.23 |
| | Cord 6 | 39.55 | 28.83 | 26.81 | 25.88 |
| | Cord 13 | 25.75 | 26.82 | 26.95 | 26.40 |

**B: TUBB3**

| Cell Type | Sample | si107 | si124 | si381 | NEG CTL |
|---|---|---|---|---|---|
| MSC | Cord 9 | 32.11 | 32.82 | 31.16 | 34.34 |
| | Cord 11 | 35.36 | 31.64 | 29.08 | 32.96 |
| CC | Cord 5 | 28.73 | 27.14 | 27.04 | 28.14 |
| | Cord 6 | 28.51 | 28.34 | 28.20 | 28.76 |
| | Cord 13 | 32.61 | 31.64 | 29.08 | 32.86 |
| CC-RA | Cord 5 | 26.94 | 27.07 | 22.60 | 24.38 |
| | Cord 6 | 31.86 | 32.98 | 25.94 | 25.29 |
| | Cord 13 | 26.38 | 34.86 | 24.89 | 26.02 |

**C: ND1**

| Cell Type | Sample | si107 | si124 | si381 | NEG CTL |
|---|---|---|---|---|---|
| MSC | Cord 9 | 26.75 | 29.15 | 27.89 | 29.18 |
| | Cord 11 | 19.30 | 19.46 | 19.34 | 18.89 |
| CC | Cord 5 | 28.40 | 25.62 | 30.48 | 26.83 |
| | Cord 6 | 28.58 | 30.51 | 30.54 | 30.08 |
| | Cord 13 | 40.00 | 35.43 | 40.00 | 36.36 |
| CC-RA | Cord 5 | 28.07 | 35.33 | 25.73 | 27.15 |
| | Cord 6 | 29.41 | 23.94 | 27.45 | 28.33 |
| | Cord 13 | 18.94 | 18.46 | 19.17 | 18.89 |

**D: MAP2**

| Cell Type | Sample | si107 | si124 | si381 | NEG CTL |
|---|---|---|---|---|---|
| MSC | Cord 9 | 39.83 | 40.00 | 39.26 | 39.96 |
| | Cord 11 | 40.00 | 40.00 | 40.00 | 40.00 |
| CC | Cord 5 | 29.82 | 26.98 | 28.03 | 29.52 |
| | Cord 6 | 29.93 | 29.05 | 29.04 | 29.80 |
| | Cord 13 | 36.42 | 32.49 | 34.18 | 31.66 |
| CC-RA | Cord 5 | 28.32 | 26.68 | 23.64 | 25.11 |
| | Cord 6 | 38.04 | 33.04 | 25.73 | 25.05 |
| | Cord 13 | 26.02 | 30.96 | 25.31 | 25.86 |

**E: NEU**

| Cell Type | Sample | si107 | si124 | si381 | NEG CTL |
|---|---|---|---|---|---|
| MSC | Cord 9 | 40.00 | 40.00 | 40.00 | 39.80 |
| | Cord 11 | 40.00 | 40.00 | 40.00 | 40.00 |
| CC | Cord 5 | 40.00 | 40.00 | 40.00 | 40.00 |
| | Cord 6 | 40.00 | 40.00 | 40.00 | 30.10 |
| | Cord 13 | 30.50 | 32.48 | 30.49 | 30.94 |
| CC-RA | Cord 5 | 40.00 | 40.00 | 40.00 | 40.00 |
| | Cord 6 | 40.00 | 36.32 | 40.00 | 33.60 |
| | Cord 13 | 34.25 | 35.46 | 35.54 | 35.09 |

**Table 3.5: Neural markers RNA Expression post miRNA antagonist transfection.**

The table shows the average neural marker expression cycle quantification (Cq) data obtained from the RT-qPCR analysis of MSCs, CCs and CC-RA cells after these where tranasfected with siRNAs. The Cq is detected when the sample reaction surpasses that of pre-assigned threshold. The maximum Cq value reading is 40.00. When a sample Cq reaches this value, the expression which is being sought absent (value is inversely proportion to the expression). A panel of neural markers was tested post transfection of miRNA antagonist siR-107, siR-124 and siR-381. The average cycling quantification (Cq) of these markers ranged from 25.75 – 34.86 for NES (A), 22.60 – 34.86 for TUBB3 (B), 18.46 - 40.00 for ND1 (C), 23.64 - 40.00 for MAP2(D) and 30.10 - 40.00 for NEU (E). The negative control is the MISSION® Synthetic microRNA Inhibitor.

Legend: MSCs – Mesenchymal Stem Cells, CCs – Conditioned Cells, CC-RAs – Retinoic Acid treated CCs, NEG CTL – Negative miRNA antagonist control si – miRNA antagonist, NES – Nestin, TUBB3 –Beta III Tubulin, ND1 – Neuro D1, MAP2 – Microtubule-associated protein, NEU – Neuronal-specific nuclear protein

As seen in Table 3.5A, NES expression in MSCs was detected during the late cycles of the RT-qPCR analsysis with Cq values ranging from 33.27 – 40.00. To note that even RNA extracted from the cells transfected with the negative control were detected relatively late (Cq values of 3426 and 33.86). Except for the cells transfect with the siR-381, CCs follow a similar pattern to that of MSCs with Cq values of over 30.00. Transfection of siR-381 resulted with the expression of NES being signaled just below the $30^{th}$ cycle. Transfections for CC-RA cells showed NES expressed at an early stage of the RT-qPCR. Except for CC-RA cells extracted from Cord 6 transfected with siR-107 (which had a Cq value of 39.55) all other transfected cells had Cq values ranging between 24.01 and 29.05.

TUBB3 (as seen in Table 3.5B) was also expressed by the three cell types. Cq values for MSCs ranged were on the higher end of the RT-qPCR cycles with Cq values 29.08 – 35.36. Both CCs and CC-RA cells had TUBB 3 detected at an earlier stage with Cq values ranging between 27.04 – 32.86 for CCs and between 24.38 – 34.86 for CC-RAs.

Table 3.5C show the Cq values for the three cell types when tested for the expression of ND1 post transfection of siRNA. Both MSCs and CC-RA registered the expression of ND1 during the first phases of the RT-qPCR analysis with Cq values ranging from 18.89 – 29.18 in MSCs and from 18.46 – 35.33 in CC-RA. CCs showed ND1 expression at a later cycling period (Cq values ranging from 25.62 – 36.36), with Cord 5 transfection of siR-107 and siR-381 not expressing ND1 (Cq value of 40.00).

Expression of MAP2 (Table 3.5D) signalling was not registered within MSCs (Cq values where 40.00 or within less than 1Cq of this threshold). In contract both CC and CC-RA cells were able to express MAP2 after transfection of the siRNAs. CCs were able to express MAP2 at with a Cq value between 26.98 – 36.42. Post transfection CC-RA MAP2 was detected at Cq values ranging from 23.64 – 33.04. CC-RA Cord 6 transfected with siR-107 expressed MAP2 at a very late stage during RT-qPCR analysis (Cq value 38.04).

Table 3.5E shows that NEU expression was not detected neither in MSCs post transfection nor in the cells transfected with the MISSION® Synthetic microRNA Inhibitor. This was also seen in CC and CC-RA cells isolated from Cord 5. Testing CCs obtained from Cord 6 shows that while NEU expression was registered in the negative control transfection (Cq 30.10), no expression was seen post siRNA transfection (Cq value 40.00). This was not the case with CCs from Cord 13 whose NES expression was relatively detected during the same cycling period (Cq value between 30.49 – 32.48). A similar result to that of Cord 13 CCs was observed with CC-RA cells from the same cord. All Cq values from the siR-transfection and negative control where within approximately 1Cq from each other (values ranged from 34.25 -35.4). Expression of NES in CC-RA cells from Cord 6 was seen in both the negative control (Cq 33.60) and post siR-124 transfection (Cq 36.32) but not post transfection of siR-107 and siR-381 (Cq 40.00).

Figure 3.21 - 3.25 shows the average fold difference in neural marker expression post siRNA transfection. Once

again, the fold change was calculated against the negative control Cq values.

Figure 3.21 groups the fold change seen in NES for the three cell types. Here, MSC (A) resulted as having a fold change of 0.03, 0.12 and 0.02 respectively for transfection of siR-107, siR-124 and siR-381; CCs (B) had a fold change of 0.66 with siR-107, 0.40 with siR-124 and 1.32 with siR-381; The fold change seen in CC-RAs (C) was 0.87 for siR-107, 0.27 for siR-124 and 1.01 for siR-381.

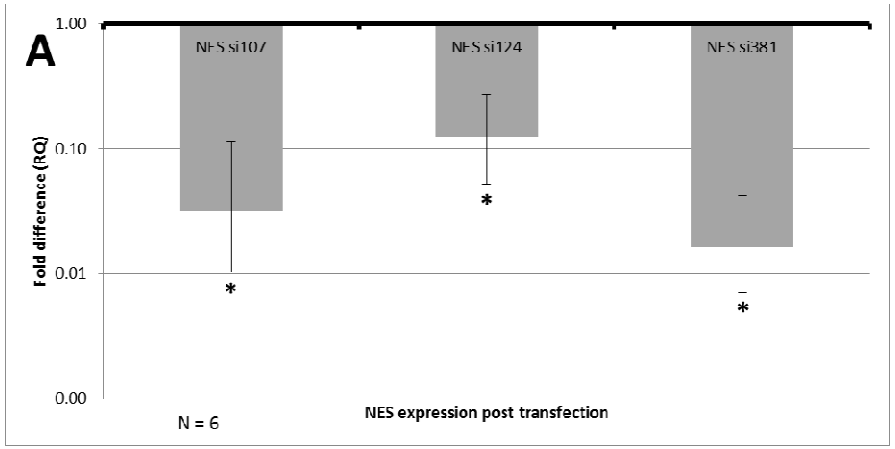


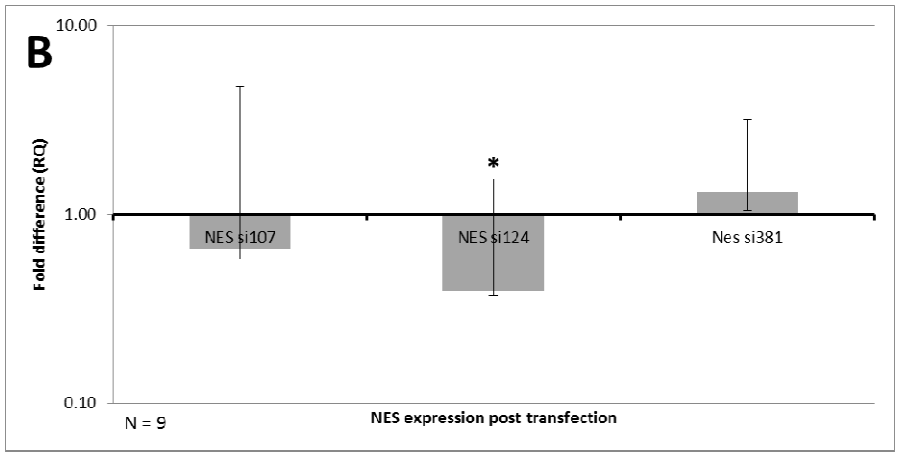


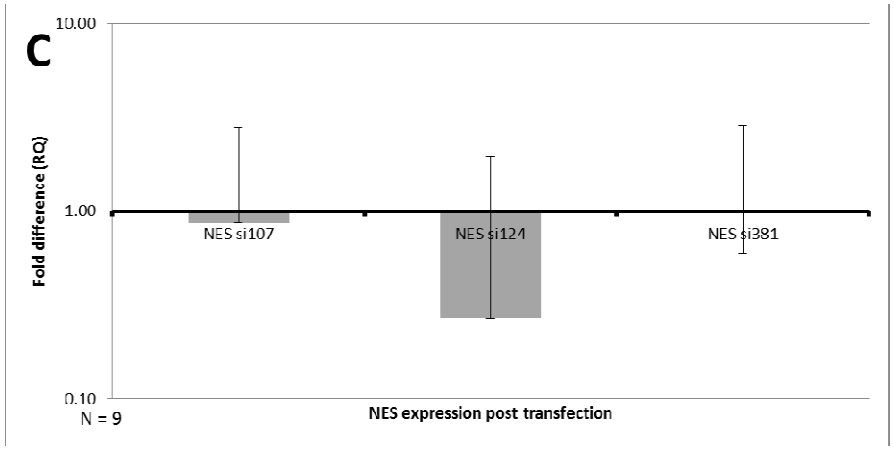


**Figure 3.21: NES RNA expression post miRNA antagonists transfection**

The figure represents the average fold change difference between the NES expressed post transfection of miRNA antagonists by MSCs (A), CCs (B) and CC-RAs (C) cells during RT-qPCR analysis. The starting point of this calculated fold change was the Negative Transfection Control (MISSION® Synthetic microRNA Inhibitor), which was considered to be the baseline (1.00). A fold-change difference of 0.00 represents no expression, so the smaller the Fold-difference the greater is the loss of the expression of NES in the cells. Transfection of siR-107 produced a fold difference of in MSC of 0.03, 0.66 in CCs and 0.87 in CC-RA cells; siR-124 transfection fold difference was 0.12 in MSCs, 0.40 in CCs and 0.27 in CC-RAs and fold difference for transfection of siR-381 resulted as 0.87 in MSCs, 0.27 in CCs and 1.01 in CC-RA cells. N represents the number of technical replicates. Error bars represent the $RQ_{min}$ and $RQ_{max}$. The * denotes a significance in the fold difference between the cell types ($P<0.05$).

Legend: MSCs – Mesenchymal Stem Cells, CCs – Conditioned Cells, CC-RAs – Retinoic Acid treated CCs, RT-qPCR – Real Time quantification polymerase chain reaction, NES – Nestin, miRNA – microRNA

The fold change for the expression of TUBB3 is shown in Figure 3.22. The MSCs show a fold change of 0.59 for siR-107, 0.34 for siR-124 and 14.09 for siR-381. The fold change in CCs was 2.61 with siR-107, 0.54 with siR-124 and 4.43 with siR-381. The change seen in CC-RA (C) was 0.77, 0.00 and 1.53 respectively for siR-107, siR-124 and siR-381.

h

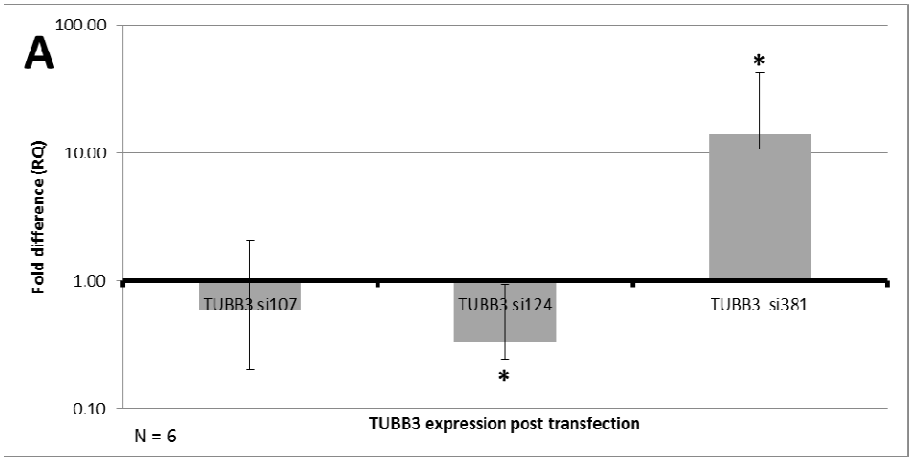


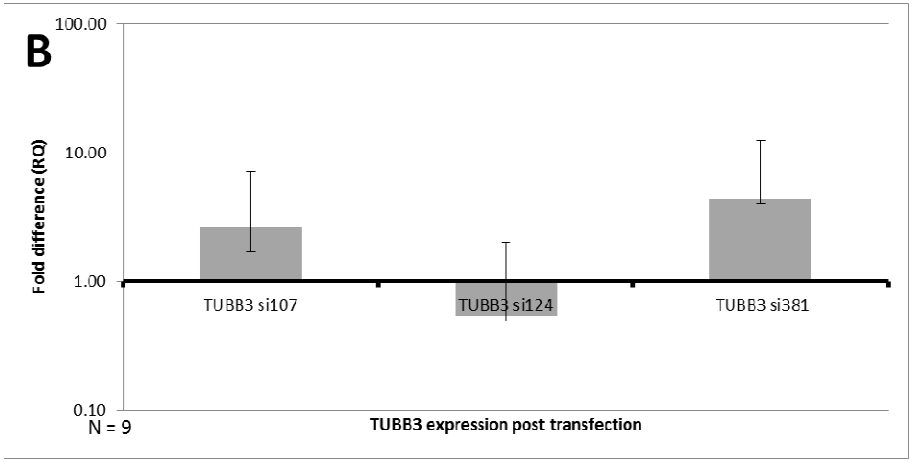


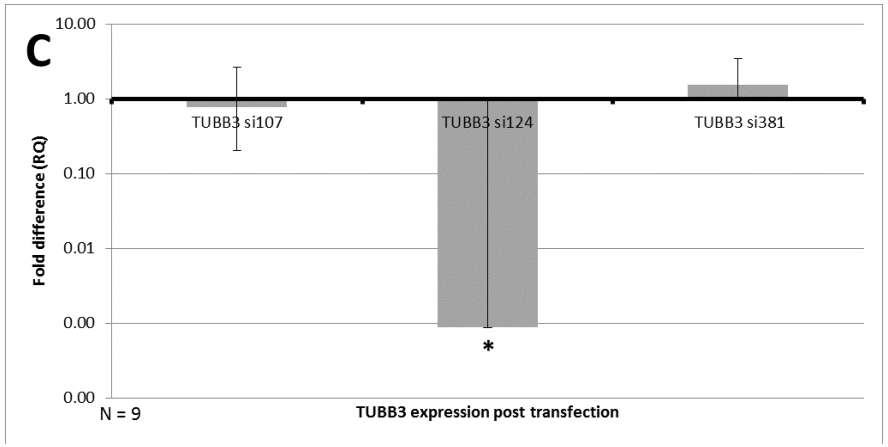


**Figure 3.22: TUBB3 RNA expression post miRNA antagonists transfection**

The figure represents the average fold change difference between the TUBB3 expressed post transfection of miRNA antagonists by MSCs (A), CCs (B) and CC-RAs (C) cells during RT-qPCR analysis. The starting point of this calculated fold change was the Negative Transfection Control (MISSION® Synthetic microRNA Inhibitor), which was considered to be the baseline (1.00). A fold-change difference of 0.00 represents no expression, so the smaller the fold-difference the greater is the loss of the expression of TUBB3 in the cells. Transfection of siR-107 produced a fold difference of 0.59 in MSCs, 2.61 in CCs and 0.77 in CC-RA cells; siR-124 transfection fold difference was 0.34 in MSCs, 0.54 in CCs and 0.00 in CC-RAs and fold difference for transfection of siR-381 resulted as 14.09 in MSCs, 4.43 in CCs and 1.53 in CC-RA cells. N represents the number of technical replicates. Error bars represent the $RQ_{min}$ and $RQ_{max}$. The * denotes a significance in the fold difference between the cell types ($P<0.05$).

Legend: MSCs – Mesenchymal Stem Cells, CCs – Conditioned Cells, CC-RAs – Retinoic Acid treated CCs, RT-qPCR – Real Time quantification polymerase chain reaction, TUBB3 - Beta III Tubulin, miRNA – microRNA

Figure 3.23 shows the fold change in the expression of ND1. MSCs (A) had a fold change of 0.61 after transfection of siR-107, 0.52 after siR-124 and 0.57 after siR381. Following transfection the fold change seen in CCs (B) was 0.34 for siR-107, 0.43 for siR-124 and 0.44 for siR-381. The fold change for CC-RA (C) cells was 1.48 with siR-107, 1.39 with siR-124 and 1.05 with siR-381.

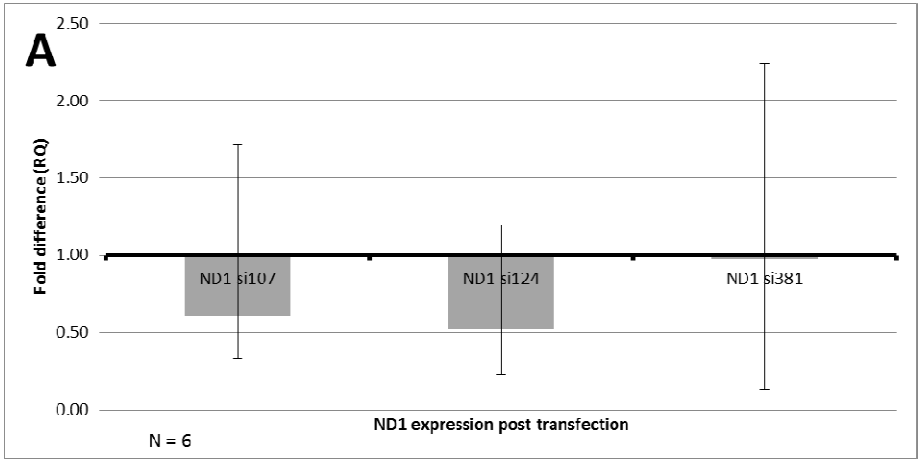


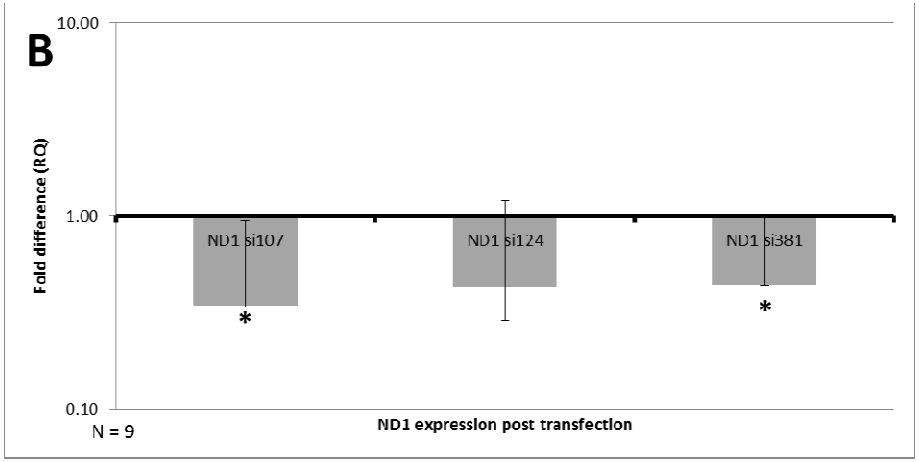


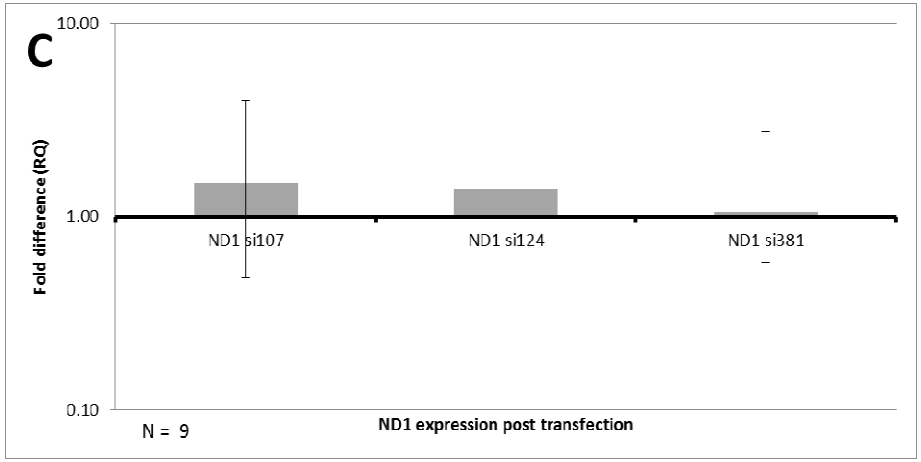


**Figure 3.23: ND1 RNA expression post miRNA antagonists transfection**

The figure represents the average fold change difference between the ND1 expressed post transfection of miRNA antagonists by MSCs (A), CCs (B) and CC-RAs (C) cells during RT-qPCR analysis. The starting point of this calculated fold change was the Negative Transfection Control (MISSION® Synthetic microRNA Inhibitor), which was considered to be the baseline (1.00). A fold-change difference of 0.00 represents no expression, so the smaller the Fold-difference the greater is the loss of the expression of ND1 in the cells. Transfection of siR-107 produced a fold difference of 0.61 in MSCs, of 0.34 in CCs and 1.48 in CC-RA cells; siR-124 transfection fold difference was 0.52 in MSCs, 0.43 in CCs and 1.39 in CC-RAs and fold difference for transfection of siR-381 resulted as 0.97 in MSCs, 0.44 in CCs and 1.05 in CC-RA cells. N represents the number of technical replicates. Error bars represent the $RQ_{min}$ and $RQ_{max}$. The * denotes a significance in the fold difference between the cell types ($P<0.05$).

Legend: MSCs – Mesenchymal Stem Cells, CCs – Conditioned Cells, CC-RAs – Retinoic Acid treated CC, RT-qPCR – Real Time quantification polymerase chain reaction, ND1 – NeuroD1, miRNA - microRNA

Figure 3.24 represents the fold change in MAP2. MAP2 was not expressed by MSCs. The fold change seen in CCs (A) was 1.75, 0.60 and 1.08 respectively for transfection of siR-107, siR-124 and siR-381. CC-RA (B) cells resulted as having a fold change of 0.55 with siR-107, 0.01 with siR-124 and 1.30 with siR-381.

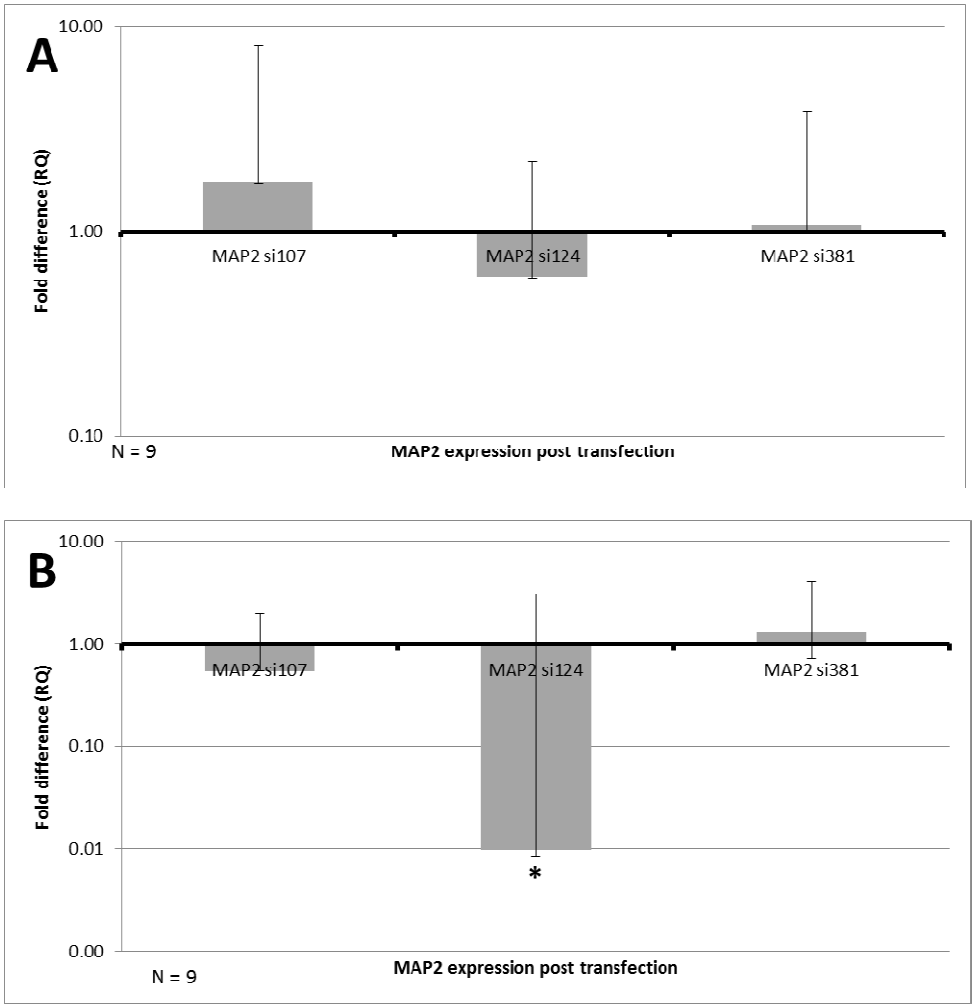


**Figure3.24: MAP2 expression post miRNA antagonists transfection**

The figure represents the average fold change difference between MAP2 expressed post transfection of miRNA antagonists by CCs (A) and CC-RAs (B) cells during RT-qPCR analysis. The starting point of this calculated fold change was the Negative Transfection Control, (MISSION® Synthetic microRNA Inhibitor), which was considered to be the baseline (1.00). A fold-change difference of 0.00 represents no expression, so the smaller the Fold-difference the greater is the loss of the expression of MAP2 in the cells. Transfection of siR-107 produced a fold difference of 1.75 in CCs and 0.55 in CC-RA cells; siR-124 transfection fold difference was 0.60 in CCs and 0.01 in CC-RAs and fold difference for transfection of siR-381 resulted as 1.08 in CCs and 1.30 in CC-RA cells. MSCs did not express MAP2. N represents the number of technical replicates. Error bars represent the $RQ_{min}$ and $RQ_{max}$. The * denotes a significance in the fold difference between the cell types ($P<0.05$).

Legend: MSCs – Mesenchymal Stem Cells, CCs – Conditioned Cells, CC-RAs – Retinoic Acid treated CCs, RT-qPCR – Real Time quantification polymerase chain reaction, MAP2 - Microtubule-associatedprotein, miRNA - microRNA

Fold change for NEU expression post transfection is summarised in Figure 3.25. MSCs did not express NEU so the fold change could not be calculated. In CCs (A) there is a fold change of 0.87 post transfection of siR-107, of 0.01 post siR-124 and of 0.38 post siR-381. CC-RA (B) cells showed a fold change of 1.74 with siR-107, 0.26 with siR-124 and 0.42 with siR-381.

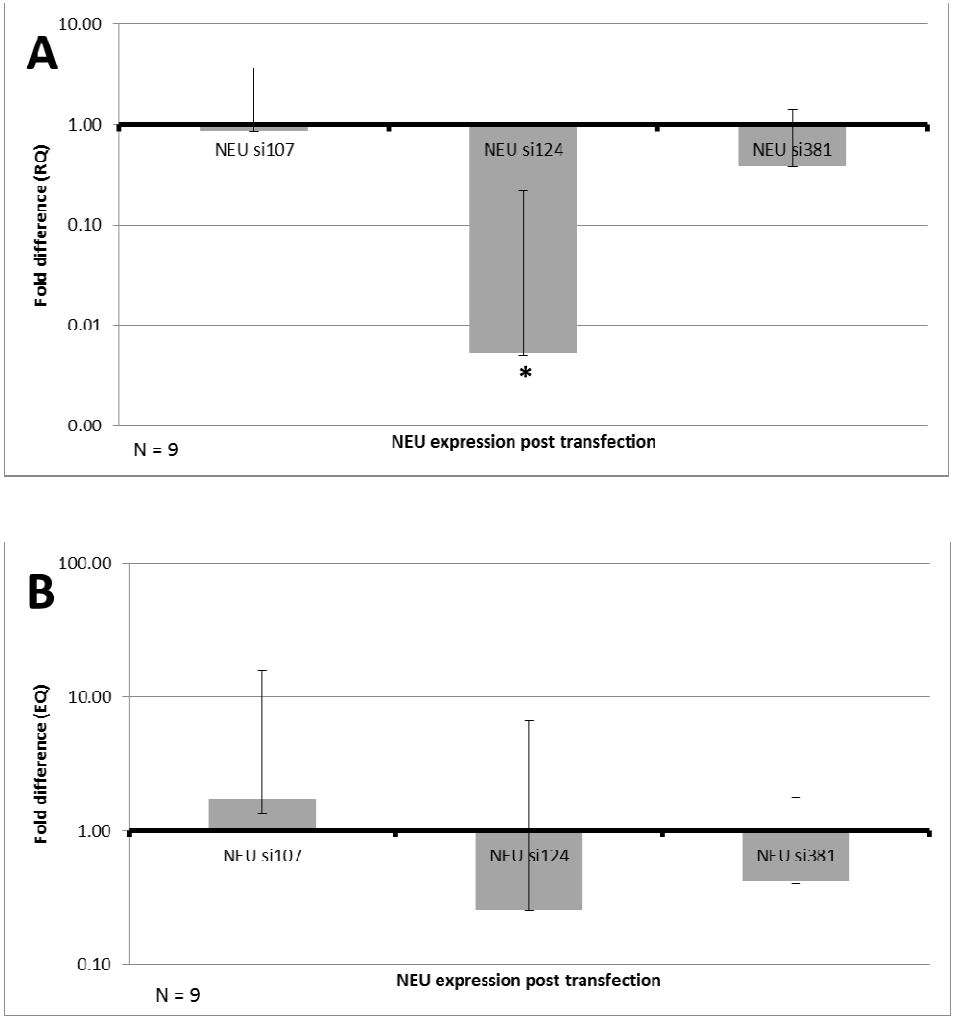


**Figure 3.25: NEU expression post miRNA antagonists transfection**

The figure represents the average fold change difference between NEU expressed post transfection of miRNA antagonists by CCs (A) and CC-RAs (B) cells during RT-qPCR analysis. The starting point of this calculated fold change was the Negative Transfection Control (MISSION® Synthetic microRNA Inhibitor), which was considered to be the baseline (1.00). A fold-change difference of 0.00 represents no expression, so the smaller the Fold-difference the greater is the loss of the expression of NEU in the cells. Transfection of siR-107 produced a fold dfference of 0.10 in MSCs, of 0.87 in CCs and 1.74 in CC-RA cells; siR-124 transfection fold difference was 0.15 in MSCs, 0.01in CCs and 0.26 in CC-RA sand fold difference for transfection of siR-381 resulted as 0.57 in MSCs, 0.38 in CCs and 0.42 in CC-RA cells. MSCs did not express NEU. N represents the number of technical replicates. Error bars represent the $RQ_{min}$ and $RQ_{max}$. The * denotes a significance in the fold difference between the cell types ($P<0.05$).

Legend: MSCs – Mesenchymal Stem Cells, CCs – Conditioned Cells, CC-RAs – Retinoic Acid treated CCs, RT-qPCR – Real Time quantification polymerase chain reaction, NEU - Neuronal-specific nuclear protein 1, miRNA - microRNA

# Chapter 4
# Discussion

## 4.1. Project development

In this project a selection of miRNAs which are known to be involved in neuronal development were considered as a means to induce transdifferentiation of MSCs towards becoming neural like cells and if possible to mature these further along the neuronal cell lineage. To obtain neural-like cells, MSCs were conditioned with spent medium of the SH-SY5Y. No miRNA work was done on the SH-SY5Y; these cells were only cultured to obtain their spent medium. Soon after MSCs where treated with the spent medium, the MSCs differentiated into neural-like cells which were referred to as CCs. The CCs were further treated with RA to cause these to develop further. These matured cells where called CC-RA. At this stage of the project, 3 cells types at different stages of differentiation had been generated. The MSCs were the initial stage, the CCs were the second stage, where cells were in the primary phases of neruogenesis, and the CC-RAs were the third stage, which were neural-like cells at a more advance neuronal stage. Both CD and neuronal markers helped characterise the shift in protein expression from MSCs to CCs to CC-RAs. Once these cells were

transfected with the siRNAs, the target gene expression for each miRNA was analysed to see whether the transfection had had any effect on neurogenesis. Following this, the 3 cells types were retested for a selection of neural markers which are characteristic of the different neuronal stages. This was done to see whether the siRNAs had any effect on the neural expression, which would have indicated the transition of the MSCs to a neural cell lineage.

MSCs are known to differentiate into neural cells and over the past thirty years, MSCs have been extensively researched for neuronal applications due to their unique properties, i.e. their multipotentiality and ease of isolation (Fellows *et al*., 2016), together with the possibility to expand and manipulate these cells *in vitro* (Takeda and Xu, 2015). Regeneration of nervous tissue has always been problematic due to one major factor: mature neural cells do not proliferate or differentiate. MSCs are not limited by this but are however limited by the number of population doublings, depending on the age of the patient and culture conditions (Turinetto, Vitale and Giachino, 2016). Direct

reprogramming of the cells results in their transdifferentiation into ectodermal cells. During tissue repair MSCs regulate the microenvironment via there immunomodulatory effect. The release of cytokines and other molecules, such as growth factors which include EGF , keratinocyte growth factor, vascular endothelial growth factor-ɑlpha, TGF, macrophage inflammatory protein and insulin-like growth factor-1 (IGF-1) (Lin and Du, 2018), helps to restore the damaged cells, and also stimulate the immune response for removal of necrotic tissue (Ayala-Cuellar *et al*., 2019). At this stage, circulating MSCs may start to differentiate, replacing the cells (Squillaro, Peluso and Galderisi, 2016). This differentiation ability was shown in a study where BM derived MSCs were able to differentiate into functional pancreatic β cell phenotypes (Chen, Jiang and Yang, 2004). This was later confirmed by Chao *et al*. (2008) who showed that MSCs transdifferentiate into islet-like clusters which express both insulin and glucagon.

The brain is the leading organ regulating the body. However, regeneration of neural tissue is not possible,

which makes any type of brain damage permanent, thus potentially causing a decrease in quality of life. The regeneration ability of the brain is strongly restricted to a substantial functional restoration and unlike other organs such as skin and liver, it is not able to regrow any structural loss (Yao, Mu and Gage, 2012). The transdifferentiation of MSCs to cells of the neuronal lineage has further expanded the potential therapeutic applications of these stem cells. Several clinical trials have employed MSCs in the neuro-regenerative field, including treatment of traumatic brain injury, Parkinson's Disease, Multiple Sclerosis, Ischaemic Stroke and Amyotrophic Lateral Sclerosis (Roszek and Czarnecka, 2014). Such trials have confirmed MSCs are indeed capable of restoring nervous system functionality. A property of MSCs seen during stem cell therapy is their ability to migrate to the site of injury and restore function (De Becker and Riet, 2016). Once the MSCs migrate to the neurological lesions, they initiate repair by releasing a group of neurotrophins and subsequently differentiate into the neural cell lineage (Jahromi *et al*., 2017). Apart from cell-cell signalling and physically replacing the damaged cells by

differentiating, there are other ways in which MSCs may restore cell function and tissue repair. MSC paracrine activity involves the secretion of different proteins such as neurotrophic factors and cytokines. It also comprises microvesicles and exsomes which contain genetic material, and are transferred to other cells. Growth factors such as VEGF, nerve growth factor and IGF-1 are also major components of the MSC secretome (Martins *et al*., 2017).

## 4.2. Mesenchymal Stem Cells isolated from Wharton's Jelly maintain multipotency

The trilineage differentiation was performed on the cells extracted from three biological replicates. However, due to the limited number of cells isolated from the cords, a full trilineage differentiation was not performed on each cohort. This confirmed that the technique used for MSC isolation was appropriate and that these cells maintained their stemness characteristics. The trilineage differentiation results were confirmed by staining the differentiated MSCs with specific histological stains i.e. von Kossa for the calcification matrix found in osteocytes, Oil-Red-O for

staining of the lipid vacuoles which are produced by the metabolism of adipocytes and Alcian Blue for glycosaminoglycans present in chondrocytes. To confirm that the positive staining was due to the MSC differentiation induction procedure, undifferentiated MSCs were also stained and these did not show any positive reactivity. Nowadays, other markers such as osteopontin and osteocalcin in the case of osteogenic differentiation are also being considered (Shen *et al*., 2019).

Throughout this study, experimental procedures were limited by the amount of MSCs isolated, thus it was not possible to undertake every test on all cord samples. To confirm the MSC extraction and culturing techniques had been successful, the trilineage differentiation of MSCs was spread over a cohort of 7 cord samples. These cells were induced to differentiate into osteocytes, adipocytes and chondrocytes. To adhere with the ISCT recommendations as much as possible, MSCs cultured from each cord were confirmed to be MSCs by having these cells differentiate into

at least one of the tri-lineage differentiation cell type and/or characterised by the CD markers guideline.

## 4.3. Mesenchymal Stem Cells can differentiate into neural-like cells

The *in vitro* transdifferentaition of MSCs into neural-like cells can be achieved by culturing MSCs in the presence of cerebrospinal fluid (Otify *et al*., 2014) and neural inducer agents (Rafieemeh, Kheirandish and Soleimani, 2016) including angiogenic factor bFGF (Mohammad *et al*., 2015) and Cardiotrophin-1, a cytokine from the Interlukin-6 family that induces the growth or cardiac myocytes and neural tissue development (Peng *et al*., 2017). Other studies have shown that MSCs cocultured in the presence of other cells (e.g. myoblasts) where able to differentiate into cardiac muscle (Witt *et al*., 2017) and addition of cerebrospinal fluid induced MSCs to transdifferentiate into neural cells (Ge *et al*., 2015). After transdifferentiation, these cells developed into multipolar and bipolar neuronal progenitor cells mixed with oligodendrocyte progenitor cells and neural elongated-like stem cells. In addition immunohistochemistry for glial

fibrillary acidic protein and cytological stains for Nissel bodies, neurites and glycogen confirmed this morphological change. The SH-SY5Y cell line is widely used as an *in vitro* model for neural experiments. To obtain accurate results these cells should be differentiated to a mature stage. Shipley *et al*. (2016) showed that it is possible to bring about the maturation of SH-SY5Y by the addition of RA. They demonstrated that when treated with RA, the SH-SY5Y developed extensive and elongated neuritic projections and were positive for neural markers MAP2 and neurofilament H. In addition to the methods which induce MSC differentiation mentioned previously, commercial kits that induce such differentiation might also be considered a form industrial spent medium. In this study, the transdifferentiation of MSCs to the neuronal cell lineage was induced *in vitro* by the addition of spent medium obtained from the culturing of the neuroblastomic cell line SH-SY5Y and these induced cells were further differentiated by RA treatment. On treating MSCs with the spent medium, the cells changed structure and assumed a star-shaped morphology followed by the generation of neuritic projections with RA treatment.

However to fully determine whether or not MSCs have indeed transdifferentiated into neurons these cells need to be further characterised as shown in previous studies. Furthermore to fully confirm the transdifferentiation these neural-like cells should be able to transmit electricity.

The RNA expression for a panel of CD markers was tested before and after neural differentiation. The cultured MSCs were positive for CD73, CD90 and CD105, and negative for CD34 and CD45 which is in accordance with the ISCT guidelines for the identification of MSCs. However, some studies have shown that although MSCs were both plastic-adherent and positive for trilineage differentiation, testing of the recommended CD markers resulted in a positive expression of CD34 and CD45 (Okolicsanyi *et al*., 2015). Apart from the markers tested in this project, other CD markers have been associated with the identification of MSCs, such as CD44, CD29 and CD10 (a table listing these CD markers may be viewed at Table 1.1). The CD markers used for characterisation are not exclusive for MSC profiling but are also expressed by non-stem cells. For example,

CD44 is a CD marker used to characterise MSCs derived from adipose tissue (Ullah, Subbarao and Rho, 2015) and is also widely expressed on cancer cells (Wang *et al.*, 2018). When identifying and categorising MSCs, the source of the tissue and method of isolation and expansion should be considered in conjunction with other characteristics such as stemness properties (ability to self-renew), lineage differentiation and expression of transcription factors (such as OCT4, NANOG, and SOX2) (Okolicsanyi *et al.*, 2015).

In this study, the RNA expression level of CD markers of the three cell types tested (MSCs, CCs and CC-RAs) varied between samples isolated from different cords (so-called biological replicates). Each RT-qPCR analysis was performed in triplicates. The results obtained helped exclude any experimental errors for that particular set-up, meaning that any variation seen between the biological replicates was indeed due to a biological variation. This difference in expression level between biological samples was highlighted because RNA expression analysis was performed, and the observed variations may not have been detected if CD

marker characterisation had been performed by a qualitative technique such as immunocytochemical staining. A similar outcome would be seen if CD markers were analysed using a cell sorting technique which identifies a cell based on the presence of a surface marker. Similarly, to immunocytochemistry, cell sorting is more a qualitative approach and only classifies the presence of the markers tested as being present or not. The quantitative data which is obtained from such analysis is based on the number of cells which express the marker of interest and not at what intensity this is expressed.

### 4.4. Mesenchymal Stem cells express neural markers

Neuroepithelial cells are neural progenitors and are constantly self-renewing and producing post-mitotic cells that become immature neurons (Zhang and Jiao, 2015). NES and SOX2 are both early neural progenitor markers and where found to be present (but were expressed at different levels) in all three cells types (MSCs, CCs and CC-RAs). In undifferentiated MSCs, NES is still expressed and a degree of this expression is maintained even when these undergo

differentiation e.g. to osteocytes (Wong, Ghassemi and Yellowley, 2014). The fold change increase in NES expression seen in the CCs compared to MSCs indicates that MSCs are being differentiated into neural-like cells. When comparing CC-RAs and CCs, the decrease in NES fold change shows CC-RA cells are at a more mature neuronal stage. Since SOX2 acts both as a stemness marker and as an early neural marker (Heo *et al.*, 2016), using this marker helps characterise the stemness of the MSCs and also monitors the differentiation of MSCs to CCs to CC-RAs. Comparing CCs and MSCs, an decreased fold change in SOX2 expression was obtained in CCs indicating loss of stemness, while the fold increase seen between the CC-RA and CC cell types may suggest an increase in the shift towards neural-like cells, since SOX2 is important for the regulation of NSCs proliferation (Shimozaki, 2014). Intermediate progenitors undergo mitosis to produce neurons (Wang *et al.*, 2014) and MASH1 is a transcription factor essential for neural differentiation (Peng *et al.*, 2015). As with SOX2, MASH1 presented a fold decrease in CCs when compared to MSCs and a fold increase when CC-RA

were compared to CCs. Driving the immature neural stage are the transcription factors ND1 and TUBB3. ND1 transforms non-neuronal ectodermal cells into fully differentiated neurons (Navarro Quiroz *et al*., 2018), while TUBB3 is expressed by neurons at the early stages of morphological differentiation (Kovacs, Szabo and Pirity, 2016). The fold change decrease in ND1 but increase in TUBB3 expression between CCs and MSCs is a clear indicator that once conditioned with the spent medium, MSCs are being induced to become neuron-like cells. Subsequent treatment with RA prompted the CCs into further differentiation, as suggested by the fold decrease in TUBB3 and increase in ND1. This neural stage transition was indeed confirmed by MAP2 and NEU. These two markers were not detected in MSCs but were expressed by CCs, thus the increase fold-change expression. The lack of expression of these two neural markers is expected in MSCs, since these markers denote an advanced neuronal stage of development. It is unclear why both CC and CC-RA cells of Cord 5 did not express NEU. To exclude a technical error, the sample was retested alongside SH-SY5Y cells (which are

known to express NEU) and expression of NEU in SH-SY5Y was confirmed but was still absent in Cord 5 cells. In CC-RA cells a fold change increase was seen in NEU and a fold decrease resulted in MAP2 showing that CC-RAs are more mature than CCs.

As with the case of the CD marker analyses, neural expression analysis using RT-qPCR has demonstrated that the biological replicates have different levels of neural RNA expression. In terms of differentiation, the time span from when the cord is prepared and MSCs are isolated up until the moment they are conditioned with the spent medium is critical. Despite being processed and maintained in the exact same conditions and keeping passages to a minimum, cells from different cord samples may have retained a different proliferation and differentiation potential. Furthermore, MSCs are known to express neuronal associated proteins and under stress cell structure may resemble that obtained during neural development. Croft and Przyborski (2006) suggest that this morphological change is mainly caused by cellular shrinkage as a result of

F-Actin disruption and changes in gene transcription brought about by inhibition of PKC signalling. Thus, changes in cell morphology and molecular expression do not provide a reliable indicator of neural differentiation and other properties such as synapse formation, neuronal polarity and electrophysiology should be considered for confirming neuronal development.

## 4.5. MicroRNAs may induce transdifferentiation of Mesenchymal Stem Cells

In this study 3 miRNAs (miR-107, miR-124 and miR-381) were investigated to determine whether these alone were capable of (i) inducing the transdifferentiation of MSCs into neural cells and (ii) differentiating CCs and CC-RA cells further along the neural cell lineage. To confirm if these miRNAs can indeed induce MSCs to differentiate, each miRNA was tested for its corresponding target gene. *DICER*, which is crucial for the biogenesis of small regulatory RNAs and acts as a regulator of other cellular processes (Song and Rossi, 2017), was the gene used to monitor the transfection of miR-107. *PTP1B* which promotes neural

programming of stem cells (Matulka *et al*., 2013) was selected as the target for miR-124 and *HES1* which regulates NSC proliferation and differentiation is targeted by miR-381(Shi *et al*., 2015). The fold change in expression of the target genes of these 3 miRNAs (*DICER*, *PTP1B* and *HES1*) was analysed by RT-qPCR to determine the effect of transfection of siRNA 107, 124 and 381. *DICER* and *PTP1B* are negatively regulated in the presence of miR-107 and miR-124 respectively, meaning that a decrease in these miRNAs will cause an increase of the target gene expression. By up-regulating these genes, neurogenesis and neural differentiation is inhibited. *HES1* is upregulated in the presence of miR-381, inhibiting NSC proliferation and differentiation. On transfecting the antagonist of these miRNAs, it was expected that a net increase in both *DICER* and *PTP1B* and a net decrease in *HES1* would be observed.

There are numerous methods to transfect cells which can be based on either using a physical or chemical approach that may or not include viral vectors. In this study a physical non-viral approach was considered because (i) the

experimental design was xeno-free so no viruses/plasmids were used and (ii) chemical transfection would expose the cell to additional stress since these agents reduce the negative charge of the nucleic acids.

Some of the results obtained in relation to the change in expression of the target genes were not as expected. This might have been caused by the transfection method used. When these gene targets were analysed post-transfection of their respective miRNA antagonist, no expression change was observed in most samples. The reason for such results is either that transfection was not as efficient as expected or the antagonist also targeting other genes, which are not involved in neuronal differentiation. This is known as the off-target effect, which arises when an introduced RNA has a base sequence that can interact with multiple genes reducing their expression. Alternatively, there may have been over-expression of the target gene itself, induced by the mechanism of cell survival upon encountering the respective antagonist. Regarding the results which showed either an increase or decrease in target genes expression in

the opposite direction of what was expected, it is reasonable to assume that either there was no uptake of the siRNA by the cell or that the miRNA is involved in processes which act both for and against neural differentiation. From the overall results observed, only the *HES1* gene in MSCs and the *DICER* gene in CCs and CC-RA cells were in accordance with the function of the siRNA.

## 4.6. Neural markers may also be affected by microRNAs

A panel of neural markers was analysed for the presence of a net change in expression post-transfection with miRNA antagonists. These comprised NES - representing the neuroepithelial stage; TUBB3 and ND1 - for the detection of immature neurons and, MAP2 and NEU - for the detection of mature neurons.

*DICER* is a regulator of neurogenesis and although studies have shown that it does not directly affect NES expression (Pons-Espinal *et al*., 2017), it is possible that a reduction in *DICER* expression would eventually influence the levels of

NES and TUBB3 because of a drop in the number of NSCs being produced. Since *DICER* is fundamental for the optimal progression of neurogenesis, and is also a requirement for the proliferation, viability, migration and differentiation of neural cells, its decrease would directly cause a reduction in ND1 (Davis, Mor and Ashery-Padan, 2011). Expression of the neural markers MAP2 and NEU is in turn reduced in the presence of elevated *DICER* levels (McLoughlin *et al*., 2012)as this favours NSC production.

Transfection of siR-107 did upregulate DICER in CC and CC-RA cells but not in MSCs. However, a general net decrease in NES expression was observed in all the three cell types, suggesting a decrease in the number of NSCs. in MSCs, expression of ND1 and TUBB3 were decreased post-transfection with the antagonist. An increase in expression of TUBB3 was observed in CCs, however expression of ND1 decreased in these cells. For CC-RA cells, ND1 expression increased and TUBB3 decreased. The lack of net change in expression observed in some of the different biological replicates of CC and CC-RA cells may be due to inefficient

transfection of these cells. In some of the biological replicates a net decrease in NES expression was effectively observed, indicating that neurogenesis was reduced in these samples. The decrease in NES neuronal markers expressed by these cell types overall shows that miR-107 may have the potential of transdifferentiating MSCs into neuronal cells and push neurons towards a more mature stage. Using a zebra fish model, Risatori *et al*. (2015) demonstrated that neural progenitors are enriched with miR-107 leading to a decrease in neurogenesis and brain development. In their study, the question of whether expression of miR-107 regulated *DICER* during neurogenesis was addressed. Mimics were directly injected in the embryos and brain development was monitored. The increase in miR-107 caused the loss of the midbrain-hindbrain boundary and inhibition of miR-107 caused an increase in expression of neural progenitors and neural differentiation.

miR-124 is implicated in neurogenesis, although both its function and mechanism in this system are still not clear and need to be further analysed (Jiao *et al*., 2017). The

impact of *PBTP1* on expression of neural markers is still poorly defined, nevertheless investigations show that the presence of miR-124 enhances the expression of neuronal markers NES (Jiao *et al.*, 2017), TUBB3 (Wei *et al*., 2018), MAP2 (Zou *et al*., 2014) and NEU (Saraiva *et al*., 2018), whilst down-regulating ND1 (Sun *et al*., 2015).

In contrast to the decreased levels of *PTP1B* expression seen post-transfection of the miR-124 antagonist a change in neural marker expression was still seen. Once again, the lack of a net expression change in some of the samples may be the result of a lower transfection efficiency. Out of the three siRNAs tested, siR-124 was the one which caused the greatest change in expression in the neural markers in CC-RA cells. To a lesser degree, siR-124 also caused changes in the neural expression of CCs, indicating that cells in the early stages of neural maturation are also affected by miR-124. In a study conducted by Jiao *et al*. (2017), NSCs were cultured from rat embryos and transfected with miR-124 mimics. An MTT assay showed a significant increase in the number of NSCs which was confirmed by an increase in NES

expression. The study supports the findings of this project since transfection of siR-124 resulted in a decrease of NES expression.

*HES1* is a downstream regulator of the Notch signalling pathway, which in turn is responsible for stem cell neural fate determination (Perron *et al*., 2018). Over-expression of *HES1* directly increases expression of NES and TUBB3 due to this gene being a promoter of NSC proliferation and differentiation (Shi *et al.*, 2015). Similarly, expression of both neural markers would decrease with a lowering of *HES1* expression. ND1 is a downstream marker of *HES1* meaning that a suppression of *HES1* expression would maintain neural cells in an undifferentiated state (Liu, Dai and Du, 2015) and the inverse correlation between HES1 and MAP2 induces mature neural differentiation upon a decrease in *HES1* expression (Fiaschetti *et al*., 2014). Shi *et al*. (2015) used rat embryos to isolate NSCs and subsequently transfect them with miR-381 mimics. RT-qPCR analysis confirmed the upregulation of NES and TUBB3 and Western Blot confirmed *HES1* as a target for miR-381.

In the current study, expression of *HES 1* was increased post-transfection with siR-381 in the CCs and CC-RA cell types in contrast to downregulation observed in MSCs. However, there was no change in expression of most of the neural markers in CCs and CC-RA cells following transfection with the miR-381 antagonist. Furthermore, an increase in TUBB3 expression in CCs was observed, indicating that there was no or little uptake of miR-381 by these cells. With regards to MSCs, the expression of NES decreased, TUBB3 increased and no change was seen for ND1. These results suggest that either miR-381 does not transdifferentiate MSCs or cause neurons to move further down the neuronal pathway or transfection was inefficient.

Transfection is a multi-factorial process that depends on the cellular binding and internalisation of the complex as well as subsequent release and uptake. The health of the cell, metabolic activity and proliferation rate are also critical factors which contribute to a successful transfection. The cell type also affects the transfection outcome. For instance,

primary cells such as MSCs and immature progenitors lack cell surface receptors that trigger receptor-complex interactions and internalisation, have a lower proliferation rate and often lack the ability to bind to transfection complexes. The age of the culture and degree of confluence are other factors which determine the efficiency of a transfection protocol. Since cells that are proliferating are more likely to take up foreign nucleic acids, it is important that prior to transfection, cells are not fully confluent or in a stationary growth phase. In addition, low confluence of cells may result in inadequate yields of RNA for expression analysis. Transfection efficiency is reduced in cells which have been repeatedly passaged, particularly cells which are entering senescence and hence, in this study the number of passages was kept to a minimum. In this study, both age and proliferation were a major limitation when transfecting MSCs. Reaching a point where cells were confluent enough to obtain a minimum usable RNA concentration took time and, in some cases, MSCs may have entered cellular senescence, thus making transfection more difficult.

MiRNAs regulate multiple gene targets and in turn, specific miRNAs can also become targets of other miRNAs. As a result of such multi-level regulation, an overall net change is not always achievable. The transfected miRNA antagonist may be influencing a range of target genes other than the one under investigation.

## 4.7. Knowledge Contribution

### 4.7.1. Contributing to the Professional Biomedical Practice

Standard good laboratory practice provides the guidelines of which basic precautions should be followed to ensure that experiments are conducted in the most appropriate way to obtain reliable results. Although certain practices, such as the use of protective clothing and the thorough cleaning of work areas are well-established, other methods require further optimisation to achieve the desired outcome.

In this project, MSCs were isolated from Wharton's Jelly. The number of cells extracted was somewhat limited. This indicates that an alternative approach for isolating these cells, such as using a full enzyme digest technique, where

the Wharton's Jelly would be treated with Collagenase II for several hours and processed further to extract the single cells, needs to be considered. Even though the extracted cells were few, the degree of contamination observed during culturing was around 10%, which is as one would expect. All laboratories experience contamination at one stage or another, and this is normally due to bacteria, fungi or yeast infections. The contaminations seen in this study were more likely to have been a consequence of some contaminated dissection utensils rather than a repercussion of contaminated cord lengths, based on the fact that contamination of cell culture was experienced by all the researchers working in the laboratory at the same time. The method devised to preserve the cord lengths by using PBS and P/S was one of the steps taken to prevent such contamination, as the P/S present would have already started acting on any contaminants present on the epithelia of the cord lengths. Although using DMEM-F12 might have helped preserve the cells, the glucose in the medium would also have sustained bacterial growth. Washing the cord lengths with 70% ethanol was another step taken to remove

any persistent contaminates; however this had the drawback that an exposure longer than 1 minute resulted in no cell growth. The subsequent washing with PBS was intended to remove any alcohol traces and additional debris present on the cord epithelia.

Another factor which contributed to successful MSC culturing was the correct bleeding of the cord lengths during sampling. Improper bleeding led to Wharton's Jelly becoming heavily blood stained. In such cases the red blood cells would be a persistent presence during culturing, causing debris to settle at the bottom of the plate and thus not allowing the plastic-adherent cells to grow. Washing the Wharton's Jelly with an erythrocyte lysing buffer may solve the issue, however insight is required on whether the MSCs would be affected by this additional washing step or not. Another alternative to consider is the addition of heparin to the transport medium. This would prevent the blood from clotting in the veins and arteries of the cord lengths. However, such an outcome would depend on the actual length of the cord, whether delayed clamping of the cord at

birth was practiced and the possibility that the transport medium would not have completely permeated the inside of the cord length.

MSCs are known to undergo early differentiaton when cultured using animal-derived products. A step taken for the prevention of early differentiation was providinga xeno-free setup by substituting FBS for human derived plasma. Although it might be more practical opting for commercial serum-free medium, such products are still not properly defined, with numerous components not being disclosed due to product protection. While it is true that plasma constituents may vary from person to person, the fact that this is derived from healthy blood donors intended for transfusion, to support the treatment of several conditions implies that the quality of the plasma falls within rigorous standard requirements, which *per se*means that its constituents are well-defined. However, there is aneed for additional optimisation to completely deplete the plasma from its clotting factors, so as to prevent undesired coagulation from occurring. This would cause subsequent

loss of MSCs that would have become embedded in the resultant fibrin cloth.

It is widely accepted that MSCs necessitate characterisation in order to be called as such. Trilineage differentiation and CD markers are what the ISCT suggests as the gold standard for characterising MSCs. However, both methods are not exclusive of this cell type. Perivascular cells which are being regarded as MSC precursors may also undergo trilineage differentiation and have many CD markers in common with MSCs. On the other hand, the overlap in CD markers present across the various cell types makes their use very limited. Ideally a broader spectrum of CD markers should be considered in conjunction with other markers (such as stemness markers) that are intended to demonstrate the multipotency potential of these cells.

Another modification which was adopted in this project is the use of TB-Fix during the fixative stage of the trilineage characterisation. Most papers suggest the use of 4% PFA; however when used in this project, this concentration of PFA

showed unfavourable results, as cells lost structure and definition. TB-Fix proved to be much more tolerated where stem cells were involved.

When considering performing qPCR experiments, testing a series of house-keeping genes for a specific cell type would further provide consistent and robust data. Ideally for every marker tested an NTC should be performed in conjunction with every run. This is meant to eliminate any background reactions which might be interfering with that specific marker. When observing NTC values note should be taken of the overall Cq values. These should remain consistent throughout and have a maximum variation of 1Cq between replicates. In this project, the variance seen in NTC values may indicate a degree of contamination which may have influenced the results of such experiments. If contamination is suspected, it is suggested to start by changing the components of the set-up one at a time. The first step would be ensuring that the working space has been cleaned with RNAse Zap and that all consumables are sterile. This would eliminate any residual RNA present. Following this,

the next step would be changing the nuclease free water, since water contamination is very common. If contamination is still suspected to be present there is no alternative left other than to change all the reagents.

Becoming proficient in a technique or mastering a skill is just the start. It is learning to view things from a different perspective that ensures a continuous improvement in standard practices.

### 4.7.2. Future investigations of miRNA transdifferentiation

Further research on the regulation of activity of the selected miRNAs would help elucidate their impact on MSCs transdifferentiation. Transfection of miRNA mimics – agents that imitate the action of miRNAs - would confirm the up or down-regulation of target gene expression by over-expression of the selected miRNAs. The size and structure of miRNA mimics and siRNA antagonists are identical so transfection efficiency should be similar i.e. any technical limitation for siRNAs will be encountered for mimics as well (Wang, 2011). Functionally however, mimics and siRNA

antagonists are not just equal and opposite. While they are expected to target the same genes, they are generally designed to bind specifically to one target gene so the off-target effects will be different between miRNAs mimics and siRNA antagonists for any given target. This means that an effect may be observed with only the miRNA mimics or the siRNA antagonists, particularly for miRNAs that target opposing genes within a pathway. Neuronal development can be visualised as a number of troughs representing the cellular stages from stem cells to fully differentiated neurons and peaks representing the differentiation steps. These cellular stages are namely neurogenesis, followed by the formation of distinct cell populations, differentiation and outgrowth of axons and dendrites. During this development not all cells progress through these stages at the same time thus resulting in a mixed population of neuronal cells. In order for cells to progress to the next stage of neuronal differentiation, a number of genes have to be expressed at the correct levels, at the same time, so as to overcome a specific threshold (thus envisioned as a peak) and enter the next cellular phase (envisioned as a trough). Since the

regulatory processes of neuronal development are very complex each stage can be envisioned as a very long trough, with cells within a population having progressed to different degrees along a particular stage. During this transition the chromatin of a cell is not stable and as a result of this instability, the overall gene expression within a specific cell might be closer to the biological threshold of the previous stage than the next stage. This makes differentiating all the cells within a population towards one specific stage of neuronal development extremely difficult. Furthermore, tipping the balance towards de-differentiation might be easier for a certain cell population than towards differentiation further down the neuronal lineage.

A microarray for global transcription and global miRNA expression then confirm the effect of up regulation or downregulation of miRNAs on the target genes. Furthermore, it would also indicate which miRNAs are present, thus helping in selecting and short-listing miRNAs for additional functional assay experiments.

Using additional stemness markers to SOX2 and OCT4 would better support the characterisation of MSCs, eliminating the need of using CD markers that have limitations due to their lack of specificity. Other stemness markers to be considered include NANOG and Glial fibrillary acidic protein. Concurrently, additional neural markers would help categorise further the neural stage of the differentiated cells and the effect the miRNAs may have on their development.

In this study, spent medium has played an important part in the differentiation of MSCs into cells of the neuronal lineage. There are undoubtedly components that are being released by the SH-SY5Y in culture that induce MSCs to differentiate. Identifying the components present in the conditioned medium may help to characterise more completely what factors are initiating and directing the differentiation of the MSCs. Once a number of these substances are identified, further testing would be required to verify if these can boost miRNA modulation.

## 4.8. Conclusion

Utilisation of MSCs is simple and safe with their plasticity in regenerative medicine making this therapeutic approach both suitable and efficient. Such an approach would reduce the need for donor tissue in transplantation, ultimately reducing drastically the complications associated with this procedure. In addition, treatment of a disease at an early stage with MSCs would reduce the need for life-long treatment (Martin-Rendon and Gyöngyösi, 2017).

The aim of this project was to identify putative miRNAs that cause MSCs to differentiate into neural precursors and/or cells of mature neuronal cell lineage. Being able to direct the differentiation of MSCs to become NSCs or further down the neuronal cell lineage, presents potential therapeutic applications. Transfection with the selected inhibitors showed that MSCs do react to the presence of miR-107 and miR-124 antagonists (NES was downregulated thus a reduction in neurogenesis). However, due to the marginal changes observed these miRNAs are not sufficient to induce such a change on their own. CCs were more susceptible to

miRNAs 107 and 124 as observed by the upregulation of the targets *DICER* and *PTP1B* showing potential to further differentiate intermediate neural progenitors and immature neuron cell types.

MiRNAs are crucial elements involved in the mechanisms of cell cycle, proliferation, differentiation, apoptosis, and metabolism. They are responsible for neural induction, neuronal differentiation and fate specification and thus have begun to develop into a next generation therapeutic approach for many conditions. Stem cells have a well-established role in therapeutic approaches and, by combining putative miRNAs responsible for the neural development with stem cells, it could be possible to further elucidate the mechanisms of action involved in both the physiological and pathological processes of the CNS.

# References

Ab Kadir, R., Zainal Ariffin, S. H., Megat Abdul Wahab, R., Kermani, S. and Senafi, S. (2012) Characterization of mononucleated human peripheral blood cells, *TheScientificWorldJournal*, **2012**, p. 843843.

Abdal Dayem, A., Lee, S. B., Choi, H. Y. and Cho, S.-G. (2018) Silver Nanoparticles: Two-Faced Neuronal Differentiation-Inducing Material in Neuroblastoma (SH-SY5Y) Cells, *International Journal of Molecular Sciences*, **19**(5), [online] Available from: https://www.ncbi.nlm.nih.gov/pmc/articles/PMC5983825/ (Accessed 19 March 2019).

Åkerblom, M. and Jakobsson, J. (2014) MicroRNAs as Neuronal Fate Determinants, *The Neuroscientist: A Review Journal Bringing Neurobiology, Neurology and Psychiatry*, **20**(3), pp. 235–242.

Allouba, M. H., ElGuindy, A. M., Krishnamoorthy, N., Yacoub, M. H. and Aguib, Y. E. (2015) NaNog: A pluripotency homeobox (master) molecule, *Global Cardiology Science & Practice*, **2015**(3), [online] Available from: https://www.ncbi.nlm.nih.gov/pmc/articles/PMC4625207/ (Accessed 23 October 2019).

Ambros, V., Bartel, B., Bartel, D. P., Burge, C. B., Carrington, J. C., Chen, X., Dreyfuss, G., Eddy, S. R., Griffiths-Jones, S., Marshall, M., Matzke, M., Ruvkun, G. and Tuschl, T. (2003) A uniform system for microRNA annotation, *RNA (New York, N.Y.)*, **9**(3), pp. 277–279.

Avolio, E., Caputo, M. and Madeddu, P. (2015) Stem cell therapy and tissue engineering for correction of congenital heart disease, *Frontiers in Cell and Developmental Biology*, **3**, p. 39.

Ayala-Cuellar, A. P., Kang, J.-H., Jeung, E.-B. and Choi, K.-C. (2019) Roles of Mesenchymal Stem Cells in Tissue Regeneration and Immunomodulation, *Biomolecules & Therapeutics*, **27**(1), pp. 25–33.

Baglioni, S., Francalanci, M., Squecco, R., Lombardi, A., Cantini, G., Angeli, R., Gelmini, S., Guasti, D., Benvenuti, S., Annunziato, F., Bani, D., Liotta, F., Francini, F., Perigli, G., Serio, M. and Luconi, M. (2009) Characterization of human adult stem-cell populations isolated from visceral and subcutaneous adipose tissue, *FASEB journal: official publication of the Federation of American Societies for Experimental Biology*, **23**(10), pp. 3494–3505.

Baron, B. (2016) Biochemical Formulation of Chemically-Defined and Non-Xenogeneic Culture Media for Research and Clinical Applications of Human Stem Cells, [online] Available from: www.austinpublishinggroup.com/ebook.

Barry, F. P. and Murphy, J. M. (2004) Mesenchymal stem cells: clinical applications and biological characterization, *The International Journal of Biochemistry & Cell Biology*, **36**(4), pp. 568–584.

Bartsch, G., Yoo, J. J., De Coppi, P., Siddiqui, M. M., Schuch, G., Pohl, H. G., Fuhr, J., Perin, L., Soker, S. and Atala, A. (2005) Propagation, expansion, and multilineage differentiation of human somatic stem cells from dermal progenitors, *Stem Cells and Development*, **14**(3), pp. 337–348.

Barzilay, R., Ben-Zur, T., Bulvik, S., Melamed, E. and Offen, D. (2009) Lentiviral delivery of LMX1a enhances dopaminergic phenotype in differentiated human bone marrow mesenchymal stem cells, *Stem Cells and Development*, **18**(4), pp. 591–601.

Berebichez-Fridman, R. and Montero-Olvera, P. R. (2018) Sources and Clinical Applications of Mesenchymal Stem Cells: State-of-the-art review, *Sultan Qaboos University Medical Journal*, **18**(3), pp. e264–e277.

Bernardo, B. C., Charchar, F. J., Lin, R. C. Y. and McMullen, J. R. (2012) A microRNA guide for clinicians and basic scientists: background and experimental techniques, *Heart, Lung & Circulation*, **21**(3), pp. 131–142.

Bian, S., Xu, T. and Sun, T. (2013) Tuning the cell fate of neurons and glia by microRNAs, *Current Opinion in Neurobiology*, **23**(6), pp. 928–934.

Bloom, A. B. and Zaman, M. H. (2014) Influence of the microenvironment on cell fate determination and migration, *Physiological Genomics*, **46**(9), pp. 309–314.

Boissart, C., Nissan, X., Giraud-Triboult, K., Peschanski, M. and Benchoua, A. (2012) miR-125 potentiates early neural specification of human embryonic stem cells, *Development (Cambridge, England)*, **139**(7), pp. 1247–1257.

Brett, J. O., Renault, V. M., Rafalski, V. A., Webb, A. E. and Brunet, A. (2011) The microRNA cluster miR-106b~25 regulates adult neural stem/progenitor cell proliferation and neuronal differentiation, *Aging*, **3**(2), pp. 108–124.

Bricard, G., Cadassou, O., Cassagnes, L.-E., Cros-Perrial, E., Payen-Gay, L., Puy, J.-Y., Lefebvre-Tournier, I., Tozzi, M. G., Dumontet, C. and Jordheim, L. P. (2017) The cytosolic 5'-nucleotidase cN-II lowers the adaptability to glucose deprivation in human breast cancer cells, *Oncotarget*, **8**(40), pp. 67380–67393.

Buhagiar, A. and Ayers, D. (2015) Chemoresistance, Cancer Stem Cells, and miRNA Influences: The Case for Neuroblastoma, *Analytical Cellular Pathology (Amsterdam)*, **2015**, [online] Available from: http://www.ncbi.nlm.nih.gov/pmc/articles/PMC4516851/ (Accessed 18 June 2017).

Buisseret, L., Pommey, S., Allard, B., Garaud, S., Bergeron, M., Cousineau, I., Ameye, L., Bareche, Y., Paesmans, M., Crown, J. P. A., Di Leo, A., Loi, S., Piccart-Gebhart, M., Willard-Gallo, K., Sotiriou, C. and Stagg, J. (2018) Clinical significance of CD73 in triple-negative breast cancer: multiplex analysis of a phase III clinical trial, *Annals of Oncology*, **29**(4), pp. 1056–1062.

Bustin, S. A. (2002) Quantification of mRNA using real-time reverse transcription PCR (RT-PCR): trends and problems, *Journal of Molecular Endocrinology*, **29**(1), pp. 23–39.

Cai, J., Li, W., Su, H., Qin, D., Yang, J., Zhu, F., Xu, J., He, W., Guo, X., Labuda, K., Peterbauer, A., Wolbank, S., Zhong, M., Li, Z., Wu, W., So, K.-F., Redl, H., Zeng, L., Esteban, M. A. and Pei, D. (2010) Generation of human induced pluripotent stem cells from umbilical cord matrix and amniotic membrane mesenchymal cells, *The Journal of Biological Chemistry*, **285**(15), pp. 11227–11234.

Caplan, A. I. (2017) Mesenchymal Stem Cells: Time to Change the Name!, *Stem Cells Translational Medicine*, **6**(6), pp. 1445–1451.

Caraguel, C. G. B., Stryhn, H., Gagné, N., Dohoo, I. R. and Hammell, K. L. (2011) Selection of a cutoff value for real-time polymerase chain reaction results to fit a diagnostic purpose: analytical and epidemiologic approaches, *Journal of Veterinary Diagnostic Investigation: Official Publication of the American Association of Veterinary Laboratory Diagnosticians, Inc*, **23**(1), pp. 2–15.

Chambers, S. M., Qi, Y., Mica, Y., Lee, G., Zhang, X.-J., Niu, L., Bilsland, J., Cao, L., Stevens, E., Whiting, P., Shi, S.-H. and Studer, L. (2012) Combined small-molecule inhibition accelerates developmental timing and converts human pluripotent stem cells into nociceptors, *Nature Biotechnology*, **30**(7), pp. 715–720.

Chao, K. C., Chao, K. F., Fu, Y. S. and Liu, S. H. (2008) Islet-like clusters derived from mesenchymal stem cells in Wharton's Jelly of the human umbilical cord for transplantation to control type 1 diabetes, *PloS One*, **3**(1), p. e1451.

Chen, L.-B., Jiang, X.-B. and Yang, L. (2004) Differentiation of rat marrow mesenchymal stem cells into pancreatic islet beta-cells, *World Journal of Gastroenterology*, **10**(20), pp. 3016–3020.

Chen, Q., Shou, P., Zheng, C., Jiang, M., Cao, G., Yang, Q., Cao, J., Xie, N., Velletri, T., Zhang, X., Xu, C., Zhang, L., Yang, H., Hou, J., Wang, Y. and Shi, Y. (2016a) Fate decision of mesenchymal stem cells: adipocytes or osteoblasts?, *Cell Death and Differentiation*, **23**(7), pp. 1128–1139.

Cheng, H., Zheng, Z. and Cheng, T. (2020) New paradigms on hematopoietic stem cell differentiation, *Protein & Cell*, **11**(1), pp. 34–44.

Cheng, L.-C., Pastrana, E., Tavazoie, M. and Doetsch, F. (2009) miR-124 regulates adult neurogenesis in the subventricular zone stem cell niche, *Nature Neuroscience*, **12**(4), pp. 399–408.

Cho, J., D'Antuono, M., Glicksman, M., Wang, J. and Jonklaas, J. (2018) A review of clinical trials: mesenchymal stem cell transplant therapy in type 1 and type 2 diabetes mellitus, *American Journal of Stem Cells*, **7**(4), pp. 82–93.

Coolen, M., Katz, S. and Bally-Cuif, L. (2013) miR-9: a versatile regulator of neurogenesis, *Frontiers in Cellular Neuroscience*, **7**, p. 220.

Cortés-Medina, L. V., Pasantes-Morales, H., Aguilera-Castrejon, A., Picones, A., Lara-Figueroa, C. O., Luis, E., Montesinos, J. J., Cortés-Morales, V. A., De la Rosa Ruiz, M. P., Hernández-Estévez, E., Bonifaz, L. C., Alvarez-Perez, M. A. and Ramos-Mandujano, G. (2019) Neuronal Transdifferentiation Potential of Human Mesenchymal Stem Cells from Neonatal and Adult Sources by a Small Molecule Cocktail, *Stem Cells International*, **2019**, p. 7627148.

Croft, A. P. and Przyborski, S. A. (2006) Formation of neurons by non-neural adult stem cells: potential mechanism implicates an artifact of growth in culture, *Stem Cells (Dayton, Ohio)*, **24**(8), pp. 1841–1851.

Dasgupta, B. and Seibel, W. (2018) Compound C/Dorsomorphin: Its Use and Misuse as an AMPK Inhibitor, *Methods in Molecular Biology (Clifton, N.J.)*, **1732**, pp. 195–202.

Datta, I., Mishra, S., Mohanty, L., Pulikkot, S. and Joshi, P. G. (2011) Neuronal plasticity of human Wharton's jelly mesenchymal stromal cells to the dopaminergic cell type compared with human bone marrow mesenchymal stromal cells, *Cytotherapy*, **13**(8), pp. 918–932.

Davies, O. G., Cooper, P. R., Shelton, R. M., Smith, A. J. and Scheven, B. A. (2015) Isolation of adipose and bone marrow mesenchymal stem cells using CD29 and CD90 modifies their capacity for osteogenic and adipogenic differentiation, *Journal of Tissue Engineering*, **6**, p. 2041731415592356.

Davis, N., Mor, E. and Ashery-Padan, R. (2011) Roles for Dicer1 in the patterning and differentiation of the optic cup neuroepithelium, *Development (Cambridge, England)*, **138**(1), pp. 127–138.

Dawson, H. D. and Lunney, J. K. (2018) Porcine cluster of differentiation (CD) markers 2018 update, *Research in Veterinary Science*, **118**, pp. 199–246.

De Antonellis, P., Carotenuto, M., Vandenbussche, J., De Vita, G., Ferrucci, V., Medaglia, C., Boffa, I., Galiero, A., Di Somma, S., Magliulo, D., Aiese, N., Alonzi, A., Spano, D., Liguori, L., Chiarolla, C., Verrico, A., Schulte, J. H., Mestdagh, P., Vandesompele, J., Gevaert, K. and Zollo, M. (2014) Early targets of miR-34a in neuroblastoma, *Molecular & cellular proteomics: MCP*, **13**(8), pp. 2114–2131.

De Becker, A. and Riet, I. V. (2016) Homing and migration of mesenchymal stromal cells: How to improve the efficacy of cell therapy?, *World Journal of Stem Cells*, **8**(3), pp. 73–87.

Delaloy, C., Liu, L., Lee, J.-A., Su, H., Shen, F., Yang, G.-Y., Young, W. L., Ivey, K. N. and Gao, F.-B. (2010) MicroRNA-9 coordinates proliferation and migration of human embryonic stem cell-derived neural progenitors, *Cell Stem Cell*, **6**(4), pp. 323–335.

Deng, B., Jiang, H., Zeng, K., Liang, Y., Wu, Y. and Yang, Y. (2017) Removal from adherent culture contributes to apoptosis in human bone marrow mesenchymal stem cells, *Molecular Medicine Reports*, **15**(6), pp. 3499–3506.

Dominici, M., Le Blanc, K., Mueller, I., Slaper-Cortenbach, I., Marini, F., Krause, D., Deans, R., Keating, A., Prockop, D. and Horwitz, E. (2006) Minimal criteria for defining multipotent mesenchymal stromal cells. The International Society for Cellular Therapy position statement, *Cytotherapy*, **8**(4), pp. 315–317.

Dorey, K. and Amaya, E. (2010) FGF signalling: diverse roles during early vertebrate embryogenesis, *Development (Cambridge, England)*, **137**(22), pp. 3731–3742.

Duan, P., Sun, S., Li, B., Huang, C., Xu, Y., Han, X., Xing, Y. and Yan, W. (2014) miR-29a modulates neuronal differentiation through targeting REST in mesenchymal stem cells, *PloS One*, **9**(5), p. e97684.

Eguchi, T. and Kuboki, T. (2016) Cellular Reprogramming Using Defined Factors and MicroRNAs, *Stem Cells International*, **2016**, p. 7530942.

Elramah, S., Landry, M. and Favereaux, A. (2014) MicroRNAs regulate neuronal plasticity and are involved in pain mechanisms, *Frontiers in Cellular Neuroscience*, **8**, p. 31.

Engel, P., Boumsell, L., Balderas, R., Bensussan, A., Gattei, V., Horejsi, V., Jin, B.-Q., Malavasi, F., Mortari, F., Schwartz-Albiez, R., Stockinger, H., van Zelm, M. C., Zola, H. and Clark, G. (2015) CD Nomenclature 2015: Human Leukocyte Differentiation Antigen Workshops as a Driving Force in Immunology, *Journal of Immunology (Baltimore, Md.: 1950)*, **195**(10), pp. 4555–4563.

Fazeli, Z., Ghaderian, S. M. H., Rajabibazl, M., Salami, S., Vazifeh Shiran, N. and Omrani, M. D. (2015) Expression Pattern of Neuronal Markers in PB-MSCs Treated by Growth Factors Noggin, bFGF and EGF, *International Journal of Molecular and Cellular Medicine*, **4**(4), pp. 209–217.

Fellows, C. R., Matta, C., Zakany, R., Khan, I. M. and Mobasheri, A. (2016) Adipose, Bone Marrow and Synovial Joint-Derived Mesenchymal Stem Cells for Cartilage Repair, *Frontiers in Genetics*, **7**, p. 213.

Feng, L., Cook, B., Tsai, S.-Y., Zhou, T., LaFlamme, B., Evans, T. and Chen, S. (2016) Discovery of a Small-Molecule BMP Sensitizer for Human Embryonic Stem Cell Differentiation, *Cell Reports*, **15**(9), pp. 2063–2075.

Fiaschetti, G., Abela, L., Nonoguchi, N., Dubuc, A. M., Remke, M., Boro, A., Grunder, E., Siler, U., Ohgaki, H., Taylor, M. D., Baumgartner, M., Shalaby, T. and Grotzer, M. A. (2014) Epigenetic silencing of miRNA-9 is associated with HES1 oncogenic activity and poor prognosis of medulloblastoma, *British Journal of Cancer*, **110**(3), pp. 636–647.

Foley, N. H., Bray, I. M., Tivnan, A., Bryan, K., Murphy, D. M., Buckley, P. G., Ryan, J., O'Meara, A., O'Sullivan, M. and Stallings, R. L. (2010) MicroRNA-184 inhibits neuroblastoma cell survival through targeting the serine/threonine kinase AKT2, *Molecular Cancer*, **9**, p. 83.

Garg, N., Po, A., Miele, E., Campese, A. F., Begalli, F., Silvano, M., Infante, P., Capalbo, C., De Smaele, E., Canettieri, G., Di Marcotullio, L., Screpanti, I., Ferretti, E. and Gulino, A. (2013) microRNA-17-92 cluster is a direct Nanog target and controls neural stem cell through Trp53inp1, *The EMBO Journal*, **32**(21), pp. 2819–2832.

Ge, W., Ren, C., Duan, X., Geng, D., Zhang, C., Liu, X., Chen, H., Wan, M. and Geng, R. (2015) Differentiation of mesenchymal stem cells into neural stem cells using cerebrospinal fluid, *Cell Biochemistry and Biophysics*, **71**(1), pp. 449–455.

Gronthos, S., Franklin, D. M., Leddy, H. A., Robey, P. G., Storms, R. W. and Gimble, J. M. (2001) Surface protein characterization of human adipose tissue-derived stromal cells, *Journal of Cellular Physiology*, **189**(1), pp. 54–63.

Gronthos, S., Graves, S. E., Ohta, S. and Simmons, P. J. (1994) The STRO-1+ fraction of adult human bone marrow contains the osteogenic precursors, *Blood*, **84**(12), pp. 4164–4173.

Haines, D. D., Juhasz, B. and Tosaki, A. (2013) Management of multicellular senescence and oxidative stress, *Journal of Cellular and Molecular Medicine*, **17**(8), pp. 936–957.

Hämmerle, B., Yañez, Y., Palanca, S., Cañete, A., Burks, D. J., Castel, V. and Font de Mora, J. (2013) Targeting neuroblastoma stem cells with retinoic acid and proteasome inhibitor, *PloS One*, **8**(10), p. e76761.

Healy, M. E., Bergin, R., Mahon, B. P. and English, K. (2015) Mesenchymal stromal cells protect against caspase 3-mediated apoptosis of CD19(+) peripheral B cells through contact-dependent upregulation of VEGF, *Stem Cells and Development*, **24**(20), pp. 2391–2402.

Hennchen, M., Stubbusch, J., Abarchan-El Makhfi, I., Kramer, M., Deller, T., Pierre-Eugene, C., Janoueix-Lerosey, I., Delattre, O., Ernsberger, U., Schulte, J. B. and Rohrer, H. (2015) Lin28B and Let-7 in the Control of Sympathetic Neurogenesis and Neuroblastoma Development, *The Journal of Neuroscience: The Official Journal of the Society for Neuroscience*, **35**(50), pp. 16531–16544.

Heo, J. S., Choi, Y., Kim, H.-S. and Kim, H. O. (2016) Comparison of molecular profiles of human mesenchymal stem cells derived from bone marrow, umbilical cord blood, placenta and adipose tissue, *International Journal of Molecular Medicine*, **37**(1), pp. 115–125.

Hoogduijn, M. J. and Dor, F. J. M. F. (2013) Mesenchymal stem cells: are we ready for clinical application in transplantation and tissue regeneration?, *Frontiers in Immunology*, **4**, p. 144.

Hou, T., Xu, J., Wu, X., Xie, Z., Luo, F., Zhang, Z. and Zeng, L. (2009) Umbilical cord Wharton's Jelly: a new potential cell source of mesenchymal stromal cells for bone tissue engineering, *Tissue Engineering. Part A*, **15**(9), pp. 2325–2334.

Huang, G. T.-J., Gronthos, S. and Shi, S. (2009) Mesenchymal stem cells derived from dental tissues vs. those from other sources: their biology and role in regenerative medicine, *Journal of Dental Research*, **88**(9), pp. 792–806.

Huang, J., Zhao, L., Xing, L. and Chen, D. (2010) MicroRNA-204 regulates Runx2 protein expression and mesenchymal progenitor cell differentiation, *Stem Cells (Dayton, Ohio)*, **28**(2), pp. 357–364.

Hudish, L. I. and Appel, B. (2014) microRNA regulation of neural precursor self-renewal and differentiation, *Neurogenesis*, **1**(1), [online] Available from: https://www.ncbi.nlm.nih.gov/pmc/articles/PMC4973589/ (Accessed 3 October 2017).

In 't Anker, P. S., Scherjon, S. A., Kleijburg-van der Keur, C., Noort, W. A., Claas, F. H. J., Willemze, R., Fibbe, W. E. and Kanhai, H. H. H. (2003) Amniotic fluid as a novel source of mesenchymal stem cells for therapeutic transplantation, *Blood*, **102**(4), pp. 1548–1549.

Jahromi, I. R., Mehrabani, D., Mohammadi, A., Seno, M. M. G., Dianatpour, M., Zare, S. and Tamadon, A. (2017) Emergence of signs of neural cells after exposure of bone marrow-derived mesenchymal stem cells to fetal brain extract, *Iranian Journal of Basic Medical Sciences*, **20**(3), pp. 301–307.

Ji, S. T., Kim, H., Yun, J., Chung, J. S. and Kwon, S.-M. (2017) Promising Therapeutic Strategies for Mesenchymal Stem Cell-Based Cardiovascular Regeneration: From Cell Priming to Tissue Engineering, *Stem Cells International*, **2017**, p. 3945403.

Jiang, M., Gao, T., Liu, Yuansheng, Cao, X., Li, Y., Li, J., Liu, Yuanjiao and Piao, J. (2019) CD14 dictates differential activation of mesenchymal stromal cells through AKT, NF-κB and P38 signals, *Bioscience Reports*, **39**(7).

Jiao, F., Wang, J., Dong, Z.-L., Wu, M.-J., Zhao, T.-B., Li, D.-D. and Wang, X. (2012) Human mesenchymal stem cells derived from limb bud can differentiate into all three embryonic germ layers lineages, *Cellular Reprogramming*, **14**(4), pp. 324–333.

Jiao, S., Liu, Y., Yao, Y. and Teng, J. (2017) miR-124 promotes proliferation and differentiation of neuronal stem cells through inactivating Notch pathway, *Cell & Bioscience*, **7**, p. 68.

Kadar, K., Kiraly, M., Porcsalmy, B., Molnar, B., Racz, G. Z., Blazsek, J., Kallo, K., Szabo, E. L., Gera, I., Gerber, G. and Varga, G. (2009) Differentiation potential of stem cells from human dental origin - promise for tissue engineering, *Journal of Physiology and Pharmacology: An Official Journal of the Polish Physiological Society*, **60 Suppl 7**, pp. 167–175.

Kariminekoo, S., Movassaghpour, A., Rahimzadeh, A., Talebi, M., Shamsasenjan, K. and Akbarzadeh, A. (2016) Implications of mesenchymal stem cells in regenerative medicine, *Artificial Cells, Nanomedicine, and Biotechnology*, **44**(3), pp. 749–757.

Kasai, H., Inoue, K., Imamura, K., Yuvienco, C., Montclare, J. K. and Yamano, S. (2019) Efficient siRNA delivery and gene silencing using a lipopolypeptide hybrid vector mediated by a caveolae-mediated and temperature-dependent endocytic pathway, *Journal of Nanobiotechnology*, **17**(1), p. 11.

Kasprzak, A. and Adamek, A. (2018) Role of Endoglin (CD105) in the Progression of Hepatocellular Carcinoma and Anti-Angiogenic Therapy, *International Journal of Molecular Sciences*, **19**(12), [online] Available from: https://www.ncbi.nlm.nih.gov/pmc/articles/PMC6321450/ (Accessed 23 September 2019).

Katarzyna Roszek and Joanna Czarnecka (2014) Perspectives of Mesenchymal Stem Cell-Based Neuroregeneration, *Neuroregeneration. J Stem Cells Res, Rev & Rep*, **1**(3).

Kessaris, N., Pringle, N. and Richardson, W. D. (2008) Specification of CNS glia from neural stem cells in the embryonic neuroepithelium, *Philosophical Transactions of the Royal Society of London. Series B, Biological Sciences*, **363**(1489), pp. 71–85.

Kisselbach, L., Merges, M., Bossie, A. and Boyd, A. (2009) CD90 Expression on human primary cells and elimination of contaminating fibroblasts from cell cultures, *Cytotechnology*, **59**(1), pp. 31–44.

Kita, K., Gauglitz, G. G., Phan, T. T., Herndon, D. N. and Jeschke, M. G. (2010) Isolation and characterization of mesenchymal stem cells from the sub-amniotic human umbilical cord lining membrane, *Stem Cells and Development*, **19**(4), pp. 491–502.

Koh, W., Sheng, C. T., Tan, B., Lee, Q. Y., Kuznetsov, V., Kiang, L. S. and Tanavde, V. (2010) Analysis of deep sequencing microRNA expression profile from human embryonic stem cells derived mesenchymal stem cells reveals possible role of let-7 microRNA family in downstream targeting of hepatic nuclear factor 4 alpha, *BMC genomics*, **11 Suppl 1**, p. S6.

Kole, A. J., Annis, R. P. and Deshmukh, M. (2013) Mature neurons: equipped for survival, *Cell Death & Disease*, **4**(6), p. e689.

Kovacs, G., Szabo, V. and Pirity, M. K. (2016) Absence of Rybp Compromises Neural Differentiation of Embryonic Stem Cells, *Stem Cells International*, **2016**, p. 4034620.

Kuznetsov, S. A., Krebsbach, P. H., Satomura, K., Kerr, J., Riminucci, M., Benayahu, D. and Robey, P. G. (1997) Single-colony derived strains of human marrow stromal fibroblasts form bone after transplantation in vivo, *Journal of Bone and Mineral Research: The Official Journal of the American Society for Bone and Mineral Research*, **12**(9), pp. 1335–1347.

Lai, C. P.-K. and Breakefield, X. O. (2012) Role of exosomes/microvesicles in the nervous system and use in emerging therapies, *Frontiers in Physiology*, **3**, p. 228.

Le, M. T. N., Xie, H., Zhou, B., Chia, P. H., Rizk, P., Um, M., Udolph, G., Yang, H., Lim, B. and Lodish, H. F. (2009) MicroRNA-125b promotes neuronal differentiation in human cells by repressing multiple targets, *Molecular and Cellular Biology*, **29**(19), pp. 5290–5305.

Lee, J., Abdeen, A. A. and Kilian, K. A. (2014) Rewiring mesenchymal stem cell lineage specification by switching the biophysical microenvironment, *Scientific Reports*, **4**, p. 5188.

Lee, R. C., Feinbaum, R. L. and Ambros, V. (1993) The C. elegans heterochronic gene lin-4 encodes small RNAs with antisense complementarity to lin-14, *Cell*, **75**(5), pp. 843–854.

Lee, S.-H., Jeyapalan, J. N., Appleby, V., Mohamed Noor, D. A., Sottile, V. and Scotting, P. J. (2010) Dynamic methylation and expression of Oct4 in early neural stem cells, *Journal of Anatomy*, **217**(3), pp. 203–213.

Li, S., Zhao, W., Xu, Q., Yu, Y. and Yin, C. (2016) MicroRNA-765 regulates neural stem cell proliferation and differentiation by modulating Hes1 expression, *American Journal of Translational Research*, **8**(7), pp. 3115–3123.

Li, W.-C., Yu, W.-Y., Quinlan, J. M., Burke, Z. D. and Tosh, D. (2005) The molecular basis of transdifferentiation, *Journal of Cellular and Molecular Medicine*, **9**(3), pp. 569–582.

Liebelt, B. D., Shingu, T., Zhou, X., Ren, J., Shin, S. A. and Hu, J. (2016) Glioma Stem Cells: Signaling, Microenvironment, and Therapy, *Stem Cells International*, **2016**, p. 7849890.

Lin, L. and Du, L. (2018) The role of secreted factors in stem cells-mediated immune regulation, *Cellular Immunology*, **326**, pp. 24–32.

Linares, A. J., Lin, C.-H., Damianov, A., Adams, K. L., Novitch, B. G. and Black, D. L. (2015) The splicing regulator PTBP1 controls the activity of the transcription factor Pbx1 during neuronal differentiation, *eLife*, **4**, p. e09268.

Liu, Z.-H., Dai, X.-M. and Du, B. (2015) Hes1: a key role in stemness, metastasis and multidrug resistance, *Cancer Biology & Therapy*, **16**(3), pp. 353–359.

Ludwig, N., Leidinger, P., Becker, K., Backes, C., Fehlmann, T., Pallasch, C., Rheinheimer, S., Meder, B., Stähler, C., Meese, E. and Keller, A. (2016) Distribution of miRNA expression across human tissues, *Nucleic Acids Research*, **44**(8), pp. 3865–3877.

Lv, F.-J., Tuan, R. S., Cheung, K. M. C. and Leung, V. Y. L. (2014) Concise review: the surface markers and identity of human mesenchymal stem cells, *Stem Cells (Dayton, Ohio)*, **32**(6), pp. 1408–1419.

Madhu, V., Dighe, A. S., Cui, Q. and Deal, D. N. (2016) Dual Inhibition of Activin/Nodal/TGF-β and BMP Signaling Pathways by SB431542 and Dorsomorphin Induces Neuronal Differentiation of Human Adipose Derived Stem Cells, *Stem Cells International*, **2016**, p. 1035374.

Mahmoudi, E. and Cairns, M. J. (2017) MiR-137: an important player in neural development and neoplastic transformation, *Molecular Psychiatry*, **22**(1), pp. 44–55.

Maleki, M., Ghanbarvand, F., Reza Behvarz, M., Ejtemaei, M. and Ghadirkhomi, E. (2014) Comparison of mesenchymal stem cell markers in multiple human adult stem cells, *International Journal of Stem Cells*, **7**(2), pp. 118–126.

Mamidi, M. K., Nathan, K. G., Singh, G., Thrichelvam, S. T., Mohd Yusof, N. A. N., Fakharuzi, N. A., Zakaria, Z., Bhonde, R., Das, A. K. and Majumdar, A. S. (2012) Comparative cellular and molecular analyses of pooled bone marrow multipotent mesenchymal stromal cells during continuous passaging and after successive cryopreservation, *Journal of Cellular Biochemistry*, **113**(10), pp. 3153–3164.

Manier, S., Liu, C.-J., Avet-Loiseau, H., Park, J., Shi, J., Campigotto, F., Salem, K. Z., Huynh, D., Glavey, S. V., Rivotto, B., Sacco, A., Roccaro, A. M., Bouyssou, J., Minvielle, S., Moreau, P., Facon, T., Leleu, X., Weller, E., Trippa, L. and Ghobrial, I. M. (2017) Prognostic role of circulating exosomal miRNAs in multiple myeloma, *Blood*, **129**(17), pp. 2429–2436.

Martin-Rendon, E. and Gyöngyösi, M. (2017) Mesenchymal stromal cell therapy as treatment for ischemic heart failure: the MSC-HF study, *Cardiovascular Diagnosis and Therapy*, **7**(Suppl 2), pp. S69–S72.

Martins, L. F., Costa, R. O., Pedro, J. R., Aguiar, P., Serra, S. C., Teixeira, F. G., Sousa, N., Salgado, A. J. and Almeida, R. D. (2017) Mesenchymal stem cells secretome-induced axonal outgrowth is mediated by BDNF, *Scientific Reports*, **7**, [online] Available from: https://www.ncbi.nlm.nih.gov/pmc/articles/PMC5482809/ (Accessed 7 April 2020).

Maslova, O. O. (2012) Current view of mesenchymal stem cells biology (brief review), *Biopolymers and Cell*, **28**(3), pp. 190–198.

Matsuzaki, F. and Shitamukai, A. (2015) Cell Division Modes and Cleavage Planes of Neural Progenitors during Mammalian Cortical Development, *Cold Spring Harbor Perspectives in Biology*, **7**(9), p. a015719.

Matulka, K., Lin, H.-H., Hříbková, H., Uwanogho, D., Dvořák, P. and Sun, Y.-M. (2013) PTP1B is an effector of activin signaling and regulates neural specification of embryonic stem cells, *Cell Stem Cell*, **13**(6), pp. 706–719.

McLoughlin, H. S., Fineberg, S. K., Ghosh, L. L., Tecedor, L. and Davidson, B. L. (2012) Dicer is required for proliferation, viability, migration and differentiation in corticoneurogenesis, *Neuroscience*, **223**, pp. 285–295.

Meyers, B. C., Axtell, M. J., Bartel, B., Bartel, D. P., Baulcombe, D., Bowman, J. L., Cao, X., Carrington, J. C., Chen, X., Green, P. J., Griffiths-Jones, S., Jacobsen, S. E., Mallory, A. C., Martienssen, R. A., Poethig, R. S., Qi, Y., Vaucheret, H., Voinnet, O., Watanabe, Y., Weigel, D. and Zhu, J.-K. (2008) Criteria for annotation of plant MicroRNAs, *The Plant Cell*, **20**(12), pp. 3186–3190.

Michelis, K. C., Nomura-Kitabayashi, A., Lecce, L., Franzén, O., Koplev, S., Xu, Y., Santini, M. P., D'Escamard, V., Lee, J. T. L., Fuster, V., Hajjar, R., Reddy, R. C., Chikwe, J., Stelzer, P., Filsoufi, F., Stewart, A., Anyanwu, A., Björkegren, J. L. M. and Kovacic, J. C. (2018) CD90 Identifies Adventitial Mesenchymal Progenitor Cells in Adult Human Medium- and Large-Sized Arteries, *Stem Cell Reports*, **11**(1), pp. 242–257.

Mishra, L., Derynck, R. and Mishra, B. (2005) Transforming growth factor-beta signaling in stem cells and cancer, *Science (New York, N.Y.)*, **310**(5745), pp. 68–71.

Moerman, E. J., Teng, K., Lipschitz, D. A. and Lecka-Czernik, B. (2004) Aging activates adipogenic and suppresses osteogenic programs in mesenchymal marrow stroma/stem cells: the role of PPAR-gamma2 transcription factor and TGF-beta/BMP signaling pathways, *Aging Cell*, **3**(6), pp. 379–389.

Mohammad, M., Yaseen, N., Al-Joubory, A., Abdullah, R., Mahmood, N., Ahmed, A. A. and Al-Shammari, A. (2015) Production of Neural Progenitors from Bone Marrow Mesenchymal Stem Cells, *Stem Cell Discovery*, **6**(1), pp. 1–12.

Mollinari, C., Racaniello, M., Berry, A., Pieri, M., de Stefano, M. C., Cardinale, A., Zona, C., Cirulli, F., Garaci, E. and Merlo, D. (2015) miR-34a regulates cell proliferation, morphology and function of newborn neurons resulting in improved behavioural outcomes, *Cell Death & Disease*, **6**, p. e1622.

Mollinari, C., Zhao, J., Lupacchini, L., Garaci, E., Merlo, D. and Pei, G. (2018) Transdifferentiation: a new promise for neurodegenerative diseases, *Cell Death & Disease*, **9**(8), p. 830.

Monguió-Tortajada, M., Roura, S., Gálvez-Montón, C., Franquesa, M., Bayes-Genis, A. and Borràs, F. E. (2017) Mesenchymal Stem Cells Induce Expression of CD73 in Human Monocytes In Vitro and in a Swine Model of Myocardial Infarction In Vivo, *Frontiers in Immunology*, **8**, p. 1577.

Moraes, D. A., Sibov, T. T., Pavon, L. F., Alvim, P. Q., Bonadio, R. S., Da Silva, J. R., Pic-Taylor, A., Toledo, O. A., Marti, L. C., Azevedo, R. B. and Oliveira, D. M. (2016) A reduction in CD90 (THY-1) expression results in increased differentiation of mesenchymal stromal cells, *Stem Cell Research & Therapy*, **7**(1), p. 97.

Moretti, P., Hatlapatka, T., Marten, D., Lavrentieva, A., Majore, I., Hass, R. and Kasper, C. (2010) Mesenchymal stromal cells derived from human umbilical cord tissues: primitive cells with potential for clinical and tissue engineering applications, *Advances in Biochemical Engineering/Biotechnology*, **123**, pp. 29–54.

Morito, T., Muneta, T., Hara, K., Ju, Y.-J., Mochizuki, T., Makino, H., Umezawa, A. and Sekiya, I. (2008) Synovial fluid-derived mesenchymal stem cells increase after intra-articular ligament injury in humans, *Rheumatology (Oxford, England)*, **47**(8), pp. 1137–1143.

Mukonoweshuro, B., Brown, C. J., Fisher, J. and Ingham, E. (2014) Immunogenicity of undifferentiated and differentiated allogeneic mouse mesenchymal stem cells, *Journal of Tissue Engineering*, **5**, p. 2041731414534255.

Muraglia, A., Nguyen, V. T., Nardini, M., Mogni, M., Coviello, D., Dozin, B., Strada, P., Baldelli, I., Formica, M., Cancedda, R. and Mastrogiacomo, M. (2017) Culture Medium Supplements Derived from Human Platelet and Plasma: Cell Commitment and Proliferation Support, *Frontiers in Bioengineering and Biotechnology*, **5**, [online] Available from: https://www.ncbi.nlm.nih.gov/pmc/articles/PMC5702080/ (Accessed 26 June 2018).

Naghdi, M., Tiraihi, T., Namin, S. A. M. and Arabkheradmand, J. (2009) Transdifferentiation of bone marrow stromal cells into cholinergic neuronal phenotype: a potential source for cell therapy in spinal cord injury, *Cytotherapy*, **11**(2), pp. 137–152.

Nassiri, F., Cusimano, M. D., Scheithauer, B. W., Rotondo, F., Fazio, A., Yousef, G. M., Syro, L. V., Kovacs, K. and Lloyd, R. V. (2011) Endoglin (CD105): a review of its role in angiogenesis and tumor diagnosis, progression and therapy, *Anticancer Research*, **31**(6), pp. 2283–2290.

Navarro Quiroz, E., Navarro Quiroz, R., Ahmad, M., Gomez Escorcia, L., Villarreal, J. L., Fernandez Ponce, C. and Aroca Martinez, G. (2018) Cell Signaling in Neuronal Stem Cells, *Cells*, **7**(7).

Neo, W. H., Yap, K., Lee, S. H., Looi, L. S., Khandelia, P., Neo, S. X., Makeyev, E. V. and Su, I. -hsin (2014) MicroRNA miR-124 controls the choice between neuronal and astrocyte differentiation by fine-tuning Ezh2 expression, *The Journal of Biological Chemistry*, **289**(30), pp. 20788–20801.

Okolicsanyi, R. K., Camilleri, E. T., Oikari, L. E., Yu, C., Cool, S. M., van Wijnen, A. J., Griffiths, L. R. and Haupt, L. M. (2015) Human Mesenchymal Stem Cells Retain Multilineage Differentiation Capacity Including Neural Marker Expression after Extended In Vitro Expansion, *PloS One*, **10**(9), p. e0137255.

Oliveira, L. de M., Teixeira, F. M. E. and Sato, M. N. (2018) Impact of Retinoic Acid on Immune Cells and Inflammatory Diseases, *Mediators of Inflammation*, **2018**, p. 3067126.

Oliveto, S., Mancino, M., Manfrini, N. and Biffo, S. (2017) Role of microRNAs in translation regulation and cancer, *World Journal of Biological Chemistry*, **8**(1), pp. 45–56.

Otify, D. Y., Youssef, E., Nagy, N. B., Marei, M. K. and Youssif, M. I. (2014) Transdifferentiation of Bone Marrow Mesenchymal Stem Cells into Neural Cells via Cerebrospinal Fluid, *Biomedicine and Biotechnology*, **2**(4), pp. 66–79.

Otsuru, S., Hofmann, T. J., Olson, T. S., Dominici, M. and Horwitz, E. M. (2013) Improved isolation and expansion of bone marrow mesenchymal stromal cells using a novel marrow filter device, *Cytotherapy*, **15**(2), pp. 146–153.

Packer, A. N., Xing, Y., Harper, S. Q., Jones, L. and Davidson, B. L. (2008) The bifunctional microRNA miR-9/miR-9* regulates REST and CoREST and is downregulated in Huntington's disease, *The Journal of Neuroscience: The Official Journal of the Society for Neuroscience*, **28**(53), pp. 14341–14346.

Park, S. B., Seo, K. W., So, A. Y., Seo, M. S., Yu, K. R., Kang, S. K. and Kang, K. S. (2012) SOX2 has a crucial role in the lineage determination and proliferation of mesenchymal stem cells through Dickkopf-1 and c-MYC, *Cell Death and Differentiation*, **19**(3), pp. 534–545.

Pemberton, K., Mersman, B. and Xu, F. (2018) Using ImageJ to Assess Neurite Outgrowth in Mammalian Cell Cultures: Research Data Quantification Exercises in Undergraduate Neuroscience Lab, *Journal of undergraduate neuroscience education: JUNE: a publication of FUN, Faculty for Undergraduate Neuroscience*, **16**(2), pp. A186–A194.

Pendleton, C., Li, Q., Chesler, D. A., Yuan, K., Guerrero-Cazares, H. and Quinones-Hinojosa, A. (2013) Mesenchymal stem cells derived from adipose tissue vs bone marrow: in vitro comparison of their tropism towards gliomas, *PloS One*, **8**(3), p. e58198.

Peng, C., Li, N., Ng, Y.-K., Zhang, J., Meier, F., Theis, F. J., Merkenschlager, M., Chen, W., Wurst, W. and Prakash, N. (2012) A unilateral negative feedback loop between miR-200 microRNAs and Sox2/E2F3 controls neural progenitor cell-cycle exit and differentiation, *The Journal of Neuroscience: The Official Journal of the Society for Neuroscience*, **32**(38), pp. 13292–13308.

Peng, H., Ke, X.-X., Hu, R., Yang, L., Cui, H. and Wei, Y. (2015) Essential role of GATA3 in regulation of differentiation and cell proliferation in SK-N-SH neuroblastoma cells, *Molecular Medicine Reports*, **11**(2), pp. 881–886.

Peng, L., Shu, X., Lang, C. and Yu, X. (2017) Cardiotrophin-1 stimulates the neural differentiation of human umbilical cord blood-derived mesenchymal stem cells and survival of differentiated cells through PI3K/Akt-dependent signaling pathways, *Cytotechnology*, **69**(6), pp. 933–941.

Perron, A., Nishikawa, Y., Iwata, J., Shimojo, H., Takaya, J., Kobayashi, K., Imayoshi, I., Mbenza, N. M., Takenoya, M., Kageyama, R., Kodama, Y. and Uesugi, M. (2018) Small-molecule screening yields a compound that inhibits the cancer-associated transcription factor Hes1 via the PHB2 chaperone, *The Journal of Biological Chemistry*, **293**(21), pp. 8285–8294.

Perron, M. and Saragovi, H. U. (2018) Inhibition of CD45 Phosphatase Activity Induces Cell Cycle Arrest and Apoptosis of CD45+ Lymphoid Tumors Ex Vivo and In Vivo, *Molecular Pharmacology*, **93**(6), pp. 575–580.

Pittenger, M. F., Mackay, A. M., Beck, S. C., Jaiswal, R. K., Douglas, R., Mosca, J. D., Moorman, M. A., Simonetti, D. W., Craig, S. and Marshak, D. R. (1999) Multilineage potential of adult human mesenchymal stem cells, *Science (New York, N.Y.)*, **284**(5411), pp. 143–147.

Pons-Espinal, M., de Luca, E., Marzi, M. J., Beckervordersandforth, R., Armirotti, A., Nicassio, F., Fabel, K., Kempermann, G. and De Pietri Tonelli, D. (2017) Synergic Functions of miRNAs Determine Neuronal Fate of Adult Neural Stem Cells, *Stem Cell Reports*, **8**(4), pp. 1046–1061.

Rafieemeh, H., Kheirandish, M. and Soleimani, M. (2016) Neural Differentiation of Human Umbilical Cord Blood-derived Mesenchymal Stem Cells, *Avicenna Journal of Medical Biochemistry*, **4**(1), pp. 5–29066.

Raynaud, C. M., Maleki, M., Lis, R., Ahmed, B., Al-Azwani, I., Malek, J., Safadi, F. F. and Rafii, A. (2012) Comprehensive characterization of mesenchymal stem cells from human placenta and fetal membrane and their response to osteoactivin stimulation, *Stem Cells International*, **2012**, p. 658356.

Riekstina, U., Muceniece, R., Cakstina, I., Muiznieks, I. and Ancans, J. (2008) Characterization of human skin-derived mesenchymal stem cell proliferation rate in different growth conditions, *Cytotechnology*, **58**(3), pp. 153–162.

Ristori, E., Lopez-Ramirez, M. A., Narayanan, A., Hill-Teran, G., Moro, A., Calvo, C.-F., Thomas, J.-L. and Nicoli, S. (2015a) A Dicer-miR-107 Interaction Regulates Biogenesis of Specific miRNAs Crucial for Neurogenesis, *Developmental Cell*, **32**(5), pp. 546–560.

Rosenthal, N. and Badylak, S. (2016) Regenerative medicine: today's discoveries informing the future of medical practice, *NPJ Regenerative medicine*, **1**, p. 16007.

Rotter, N., Oder, J., Schlenke, P., Lindner, U., Böhrnsen, F., Kramer, J., Rohwedel, J., Huss, R., Brandau, S., Wollenberg, B. and Lang, S. (2008) Isolation and characterization of adult stem cells from human salivary glands, *Stem Cells and Development*, **17**(3), pp. 509–518.

Sacchetti, B., Funari, A., Remoli, C., Giannicola, G., Kogler, G., Liedtke, S., Cossu, G., Serafini, M., Sampaolesi, M., Tagliafico, E., Tenedini, E., Saggio, I., Robey, P. G., Riminucci, M. and Bianco, P. (2016) No Identical 'Mesenchymal Stem Cells' at Different Times and Sites: Human Committed Progenitors of Distinct Origin and Differentiation Potential Are Incorporated as Adventitial Cells in Microvessels, *Stem Cell Reports*, **6**(6), pp. 897–913.

Saraiva, C., Talhada, D., Rai, A., Ferreira, R., Ferreira, L., Bernardino, L. and Ruscher, K. (2018) MicroRNA-124-loaded nanoparticles increase survival and neuronal differentiation of neural stem cells in vitro but do not contribute to stroke outcome in vivo, *PloS One*, **13**(3), p. e0193609.

Sauzay, C., Voutetakis, K., Chatziioannou, A., Chevet, E. and Avril, T. (2019) CD90/Thy-1, a Cancer-Associated Cell Surface Signaling Molecule, *Frontiers in Cell and Developmental Biology*, **7**, [online] Available from: https://www.ncbi.nlm.nih.gov/pmc/articles/PMC6497726/ (Accessed 23 September 2019).

Schüring, A. N., Schulte, N., Kelsch, R., Röpke, A., Kiesel, L. and Götte, M. (2011) Characterization of endometrial mesenchymal stem-like cells obtained by endometrial biopsy during routine diagnostics, *Fertility and Sterility*, **95**(1), pp. 423–426.

Secunda, R., Vennila, R., Mohanashankar, A. M., Rajasundari, M., Jeswanth, S. and Surendran, R. (2015) Isolation, expansion and characterisation of mesenchymal stem cells from human bone marrow, adipose tissue, umbilical cord blood and matrix: a comparative study, *Cytotechnology*, **67**(5), pp. 793–807.

Seifrtová, M., Havelek, R., Cmielová, J., Jiroutová, A., Soukup, T., Brůčková, L., Mokrý, J., English, D. and Rezáčová, M. (2012) The response of human ectomesenchymal dental pulp stem cells to cisplatin treatment, *International Endodontic Journal*, **45**(5), pp. 401–412.

Shen, C., Yang, C., Xu, S. and Zhao, H. (2019) Comparison of osteogenic differentiation capacity in mesenchymal stem cells derived from human amniotic membrane (AM), umbilical cord (UC), chorionic membrane (CM), and decidua (DC), *Cell & Bioscience*, **9**, [online] Available from: https://www.ncbi.nlm.nih.gov/pmc/articles/PMC6371545/ (Accessed 12 November 2019).

Shenoy, A. and Blelloch, R. H. (2014) Regulation of microRNA function in somatic stem cell proliferation and differentiation, *Nature Reviews. Molecular Cell Biology*, **15**(9), pp. 565–576.

Shi, X., Yan, C., Liu, B., Yang, C., Nie, X., Wang, X., Zheng, J., Wang, Y. and Zhu, Y. (2015) miR-381 Regulates Neural Stem Cell Proliferation and Differentiation via Regulating Hes1 Expression, *PloS One*, **10**(10), p. e0138973.

Shi, Y., Zhao, X., Hsieh, J., Wichterle, H., Impey, S., Banerjee, S., Neveu, P. and Kosik, K. S. (2010) MicroRNA regulation of neural stem cells and neurogenesis, *The Journal of Neuroscience: The Official Journal of the Society for Neuroscience*, **30**(45), pp. 14931–14936.

Shimozaki, K. (2014) Sox2 transcription network acts as a molecular switch to regulate properties of neural stem cells, *World Journal of Stem Cells*, **6**(4), pp. 485–490.

Shipley, M. M., Mangold, C. A. and Szpara, M. L. (2016) Differentiation of the SH-SY5Y Human Neuroblastoma Cell Line, *Journal of Visualized Experiments: JoVE*, (108), p. 53193.

Sidney, L. E., Branch, M. J., Dunphy, S. E., Dua, H. S. and Hopkinson, A. (2014a) Concise review: evidence for CD34 as a common marker for diverse progenitors, *Stem Cells (Dayton, Ohio)*, **32**(6), pp. 1380–1389.

Sigurjonsson, O. E., Perreault, M.-C., Egeland, T. and Glover, J. C. (2005) Adult human hematopoietic stem cells produce neurons efficiently in the regenerating chicken embryo spinal cord, *Proceedings of the National Academy of Sciences of the United States of America*, **102**(14), pp. 5227–5232.

Singh, V. K., Saini, A., Kalsan, M., Kumar, N. and Chandra, R. (2016) Describing the Stem Cell Potency: The Various Methods of Functional Assessment and In silico Diagnostics, *Frontiers in Cell and Developmental Biology*, **4**, p. 134.

Sisakhtnezhad, S. and Matin, M. M. (2012) Transdifferentiation: a cell and molecular reprogramming process, *Cell and Tissue Research*, **348**(3), pp. 379–396.

Solnica-Krezel, L. and Sepich, D. S. (2012) Gastrulation: making and shaping germ layers, *Annual Review of Cell and Developmental Biology*, **28**, pp. 687–717

Song, M.-S. and Rossi, J. J. (2017) Molecular mechanisms of Dicer: endonuclease and enzymatic activity, *The Biochemical Journal*, **474**(10), pp. 1603–1618.

Soprano, D. R., Teets, B. W. and Soprano, K. J. (2007) Role of retinoic acid in the differentiation of embryonal carcinoma and embryonic stem cells, *Vitamins and Hormones*, **75**, pp. 69–95.

Soysa, S. N. and Alles, A. N. (2018) Sources of Mesenchymal Stromal Cells: An Overview, *American Journal of Pharmacolog*, **1**(1), p. 1007.

Squillaro, T., Peluso, G. and Galderisi, U. (2016) Clinical Trials With Mesenchymal Stem Cells: An Update, *Cell Transplantation*, **25**(5), pp. 829–848.

Stappert, L., Roese-Koerner, B. and Brüstle, O. (2015) The role of microRNAs in human neural stem cells, neuronal differentiation and subtype specification, *Cell and Tissue Research*, **359**, pp. 47–64.

Stavridis, M. P., Collins, B. J. and Storey, K. G. (2010) Retinoic acid orchestrates fibroblast growth factor signalling to drive embryonic stem cell differentiation, *Development (Cambridge, England)*, **137**(6), pp. 881–890.

Su, Z., Zhang, Y., Liao, B., Zhong, X., Chen, X., Wang, H., Guo, Y., Shan, Y., Wang, L. and Pan, G. (2018) Antagonism between the transcription factors NANOG and OTX2 specifies rostral or caudal cell fate during neural patterning transition, *The Journal of Biological Chemistry*, **293**(12), pp. 4445–4455.

Sun, Y., Luo, Z.-M., Guo, X.-M., Su, D.-F. and Liu, X. (2015) An updated role of microRNA-124 in central nervous system disorders: a review, *Frontiers in Cellular Neuroscience*, **9**, p. 193.

Taïhi, I., Nassif, A., Isaac, J., Fournier, B. P. and Ferré, F. (2019) Head to Knee: Cranial Neural Crest-Derived Cells as Promising Candidates for Human Cartilage Repair, *Stem Cells International*, **2019**, p. 9310318.

Takeda, Y. S. and Xu, Q. (2015) Neuronal Differentiation of Human Mesenchymal Stem Cells Using Exosomes Derived from Differentiating Neuronal Cells, *PloS One*, **10**(8), p. e0135111.

Takeda, Y. S. and Xu, Q. (2015) Neuronal Differentiation of Human Mesenchymal Stem Cells Using Exosomes Derived from Differentiating Neuronal Cells, *PloS One*, **10**(8), p. e0135111.

Tan, S.-L., Ohtsuka, T., González, A. and Kageyama, R. (2012) MicroRNA9 regulates neural stem cell differentiation by controlling Hes1 expression dynamics in the developing brain, *Genes to Cells: Devoted to Molecular & Cellular Mechanisms*, **17**(12), pp. 952–961.

Tanapat, P. (2016) Neuronal Cell Markers, *Materials and Methods*, [online] Available from: /method/Neuronal-Cell-Markers.html (Accessed 24 February 2018).

Tang, D.-Q., Wang, Q., Burkhardt, B. R., Litherland, S. A., Atkinson, M. A. and Yang, L.-J. (2012) In vitro generation of functional insulin-producing cells from human bone marrow-derived stem cells, but long-term culture running risk of malignant transformation, *American Journal of Stem Cells*, **1**(2), pp. 114–127.

Taran, R., Mamidi, M. K., Singh, G., Dutta, S., Parhar, I. S., John, J. P., Bhonde, R., Pal, R. and Das, A. K. (2014) In vitro and in vivo neurogenic potential of mesenchymal stem cells isolated from different sources, *Journal of Biosciences*, **39**(1), pp. 157–169.

Tokuda, K., Baron, B., Kuramitsu, Y., Kitagawa, T., Tokuda, N., Morishige, N., Kobayashi, M., Kimura, K., Nakamura, K. and Sonoda, K.-H. (2018) Optimization of fixative solution for retinal morphology: a comparison with Davidson's fixative and other fixation solutions, *Japanese Journal of Ophthalmology*, **62**(4), pp. 481–490.

Tsai, M.-S., Lee, J.-L., Chang, Y.-J. and Hwang, S.-M. (2004) Isolation of human multipotent mesenchymal stem cells from second-trimester amniotic fluid using a novel two-stage culture protocol, *Human Reproduction (Oxford, England)*, **19**(6), pp. 1450–1456.

Turinetto, V., Vitale, E. and Giachino, C. (2016) Senescence in Human Mesenchymal Stem Cells: Functional Changes and Implications in Stem Cell-Based Therapy, *International Journal of Molecular Sciences*, **17**(7).

U.S. Department of Health & Human Services (2019) DICER1 gene, *Genetics Home Reference*, [online] Available from: https://ghr.nlm.nih.gov/gene/DICER1 (Accessed 8 June 2019).

Ullah, I., Subbarao, R. B. and Rho, G. J. (2015) Human mesenchymal stem cells - current trends and future prospective, *Bioscience Reports*, **35**(2), [online] Available from: https://www.ncbi.nlm.nih.gov/pmc/articles/PMC4413017/ (Accessed 21 February 2018).

Ullah, I., Subbarao, Raghavendra Baregundi and Rho, G. J. (2015) Human mesenchymal stem cells - current trends and future prospective, *Bioscience Reports*, **35**(2).

Visvanathan, J., Lee, S., Lee, B., Lee, J. W. and Lee, S.-K. (2007) The microRNA miR-124 antagonizes the anti-neural REST/SCP1 pathway during embryonic CNS development, *Genes & Development*, **21**(7), pp. 744–749.

Wagner, W., Wein, F., Seckinger, A., Frankhauser, M., Wirkner, U., Krause, U., Blake, J., Schwager, C., Eckstein, V., Ansorge, W. and Ho, A. D. (2005) Comparative characteristics of mesenchymal stem cells from human bone marrow, adipose tissue, and umbilical cord blood, *Experimental Hematology*, **33**(11), pp. 1402–1416.

Wang, L., Zuo, X., Xie, K. and Wei, D. (2018) The Role of CD44 and Cancer Stem Cells, *Methods in Molecular Biology (Clifton, N.J.)*, **1692**, pp. 31–42.

Wang, M., Yuan, Q. and Xie, L. (2018) Mesenchymal Stem Cell-Based Immunomodulation: Properties and Clinical Application, *Stem Cells International*, **2018**, p. 3057624.

Wang, W.-X., Danaher, R. J., Miller, C. S., Berger, J. R., Nubia, V. G., Wilfred, B. S., Neltner, J. H., Norris, C. M. and Nelson, P. T. (2014) Expression of miR-15/107 family microRNAs in human tissues and cultured rat brain cells, *Genomics, Proteomics & Bioinformatics*, **12**(1), pp. 19–30.

Wang, Y.-C., Yang, J. S., Johnston, R., Ren, Q., Lee, Y.-J., Luan, H., Brody, T., Odenwald, W. F. and Lee, T. (2014) Drosophila intermediate neural progenitors produce lineage-dependent related series of diverse neurons, *Development (Cambridge, England)*, **141**(2), pp. 253–258.

Wang, Z. (2011) The guideline of the design and validation of MiRNA mimics, *Methods in Molecular Biology (Clifton, N.J.)*, **676**, pp. 211–223.

Ward, M. R., Abadeh, A. and Connelly, K. A. (2018) Concise Review: Rational Use of Mesenchymal Stem Cells in the Treatment of Ischemic Heart Disease, *Stem Cells Translational Medicine*, **7**(7), pp. 543–550.

Wei, C., Ren, L., Li, K. and Lu, Z. (2018) The regulation of survival and differentiation of neural stem cells by miR-124 via modulating PAX3, *Neuroscience Letters*, **683**, pp. 19–26.

West, M. D., Nasonkin, I., Larocca, D., Chapman, K. B., Binette, F. and Sternberg, H. (2016) Adult Versus Pluripotent Stem Cell-Derived Mesenchymal Stem Cells: The Need for More Precise Nomenclature, *Current Stem Cell Reports*, **2**, pp. 299–303.

Willems, E., Mateizel, I., Kemp, C., Cauffman, G., Sermon, K. and Leyns, L. (2006) Selection of reference genes in mouse embryos and in differentiating human and mouse ES cells, *The International Journal of Developmental Biology*, **50**(7), pp. 627–635.

Winter, J. (2015) MicroRNAs of the miR379-410 cluster: New players in embryonic neurogenesis and regulators of neuronal function, *Neurogenesis (Austin, Tex.)*, **2**(1), p. e1004970.

Witt, R., Weigand, A., Boos, A. M., Cai, A., Dippold, D., Boccaccini, A. R., Schubert, D. W., Hardt, M., Lange, C., Arkudas, A., Horch, R. E. and Beier, J. P. (2017) Mesenchymal stem cells and myoblast differentiation under HGF and IGF-1 stimulation for 3D skeletal muscle tissue engineering, *BMC cell biology*, **18**(1), p. 15.

Wong, A., Ghassemi, E. and Yellowley, C. E. (2014) Nestin expression in mesenchymal stromal cells: regulation by hypoxia and osteogenesis, *BMC Veterinary Research*, **10**, p. 173.

Wu, N., Doorenbos, M. and Chen, D. F. (2016) Induced Pluripotent Stem Cells: Development in the Ophthalmologic Field, *Stem Cells International*, **2016**, p. 2361763.

Xu, F., Piett, C., Farkas, S., Qazzaz, M. and Syed, N. I. (2013) Silver nanoparticles (AgNPs) cause degeneration of cytoskeleton and disrupt synaptic machinery of cultured cortical neurons, *Molecular Brain*, **6**, p. 29.

Xue, Q., Yu, C., Wang, Y., Liu, L., Zhang, K., Fang, C., Liu, F., Bian, G., Song, B., Yang, A., Ju, G. and Wang, J. (2016) miR-9 and miR-124 synergistically affect regulation of dendritic branching via the AKT/GSK3β pathway by targeting Rap2a, *Scientific Reports*, **6**, p. 26781.

Yamashita, M. (2013) From neuroepithelial cells to neurons: changes in the physiological properties of neuroepithelial stem cells, *Archives of Biochemistry and Biophysics*, **534**(1–2), pp. 64–70.

Yao, J., Mu, Y. and Gage, F. H. (2012) Neural stem cells: mechanisms and modeling, *Protein & Cell*, **3**(4), pp. 251–261.

Yao, S. (2016) MicroRNA biogenesis and their functions in regulating stem cell potency and differentiation, *Biological Procedures Online*, **18**, p. 8.

Yu, H. H., Featherston, T., Tan, S. T., Chibnall, A. M., Brasch, H. D., Davis, P. F. and Itinteang, T. (2016) Characterization of Cancer Stem Cells in Moderately Differentiated Buccal Mucosal Squamous Cell Carcinoma, *Frontiers in Surgery*, **3**, p. 46.

Zammit, V. and Baron, B. (2017) Points of Good Practice for the Sampling of Cords and Culturing of Mesenchymal Stem Cells, [online] Available from: https://www.um.edu.mt/library/oar/handle/123456789/19643 (Accessed 17 June 2018).

Zammit, V., Farrugia, M. and Baron, B. (2019) Redirection of transfusion waste and by-products for xeno-free research applications, *J Clin Transl Res*, **5**(2).

Zeineddine, D., Hammoud, A. A., Mortada, M. and Boeuf, H. (2014) The Oct4 protein: more than a magic stemness marker, *American Journal of Stem Cells*, **3**(2), pp. 74–82.

Zhang, D. and Kilian, K. A. (2013) The effect of mesenchymal stem cell shape on the maintenance of multipotency, *Biomaterials*, **34**(16), pp. 3962–3969.

Zhang, J. and Jiao, J. (2015) Molecular Biomarkers for Embryonic and Adult Neural Stem Cell and Neurogenesis, *BioMed Research International*, **2015**, p. 727542.

Zhang, Q., Xiang, W., Yi, D.-Y., Xue, B.-Z., Wen, W.-W., Abdelmaksoud, A., Xiong, N.-X., Jiang, X.-B., Zhao, H.-Y. and Fu, P. (2018) Current status and potential challenges of mesenchymal stem cell-based therapy for malignant gliomas, *Stem Cell Research & Therapy*, **9**(1), p. 228.

Zhang, X., Hirai, M., Cantero, S., Ciubotariu, R., Dobrila, L., Hirsh, A., Igura, K., Satoh, H., Yokomi, I., Nishimura, T., Yamaguchi, S., Yoshimura, K., Rubinstein, P. and Takahashi, T. A. (2011) Isolation and characterization of mesenchymal stem cells from human umbilical cord blood: reevaluation of critical factors for successful isolation and high ability to proliferate and differentiate to chondrocytes as compared to mesenchymal stem cells from bone marrow and adipose tissue, *Journal of Cellular Biochemistry*, **112**(4), pp. 1206–1218.

Zheng, M., Wiraja, C., Yeo, D. C., Chang, H., Lio, D. C. S., Shi, W., Pu, K., Paller, A. S. and Xu, C. (2018) Oligonucleotide Molecular Sprinkler for Intracellular Detection and Spontaneous Regulation of mRNA for Theranostics of Scar Fibroblasts, *Small (Weinheim an Der Bergstrasse, Germany)*, **14**(49), p. e1802546.

Zhou, C., Gu, H., Fan, R., Wang, B. and Lou, J. (2015) MicroRNA 302/367 Cluster Effectively Facilitates Direct Reprogramming from Human Fibroblasts into Functional Neurons, *Stem Cells and Development*, **24**(23), pp. 2746–2755.

Zhou, Y., Chen, H., Li, H. and Wu, Y. (2017) 3D culture increases pluripotent gene expression in mesenchymal stem cells through relaxation of cytoskeleton tension, *Journal of Cellular and Molecular Medicine*, **21**(6), pp. 1073–1084.

Zou, D., Chen, Y., Han, Y., Lv, C. and Tu, G. (2014) Overexpression of microRNA-124 promotes the neuronal differentiation of bone marrow-derived mesenchymal stem cells, *Neural Regeneration Research*, **9**(12), pp. 1241–1248.

# Appendix I
# Ethical Approval

L-UNIVERSITÀ TA' MALTA

Msida – Malta
Skola Medika
Sptar Mater Dei

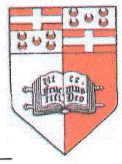

UNIVERSITY OF MALTA

Msida – Malta
Medical School
Mater Dei Hospital

Ref No: **90/2016**

Tuesday 7th February 2017

Ms. Vanessa Zammit
[redacted]

Dear Ms. Vanessa Zammit,

Please refer to your application submitted to the Research Ethics Committee in connection with your research entitled:

**miRNa influences in mesenchymal stem cell commitment to neuroblast lineage development**

The University Research Ethics Committee granted ethical approval for the above mentioned protocol.

Yours sincerely,

[redacted]

Chairman
Research Ethics Committee

***Email:*** umms@um.edu.mt • ***Web:*** http://www.um.edu.mt/ms

**CONSENT FORM**

I am over eighteen (18) year of age.

I have been asked to participate in a research study entitled:

**microRNA influences in mesenchymal stem cell commitment to neuroblast lineage development**

I am being asked to donate a cord sample for mesenchymal stem cell culturing in order to identify microRNAs which may induce neuroblast development.

I am also aware that cultured cells from the donated cord may also be used in other ethically approved related studies.

***Samples will be collected anonymously and any unused material will be destroyed.***

The purpose and details of the study have been explained to me by _____ and any difficulties which I raised have been adequately clarified.

I give my consent to Ms. Vanessa Zammit [redacted] and her delegate to take the necessary sample, and also acknowledge that Ms. Vanessa Zammit will retain sole ownership over cultivated cells.

I am not being selected on the basis of any medical implications or genetics predisposition related to this study but purely for research purposes. I understand that the results of this study may be used for medical or scientific purposes and that the results achieved from this study in which I am participating may be reported or published: however, I shall not be personally identified in any way, either individually or collectively.

I am under no obligation to participate in this study and am doing so voluntarily.

I may withdraw from the study at any time, without giving any reason.

I am not receiving any remuneration for participating in this study.

I relinquish all rights to any intellectual property that may arise from this or any other related work.

In case of queries during the study I may contact: **Ms. Vanessa Zammit** on mobile number: [redacted]

_____ _____

Signature of participant Signature of researcher

_____ _____

Name of participant *(in block letters)*: Name of researcher *(in block letters)*

_____ _____

I.D. No. I.D. No.

_____

Date

**FORMOLA TA' KUNSENS**

Jiena għalaqt tmintax (18)-il sena.

Talbuni biex niehu sehem fi studju ta' riċerka bl-isem ta':

**L-influwenzi tal-microRNA fuq iċ-ċelloli staminali mesenkimali sabiex dawn jevolvu u jsiru ċelluli neuroblast.**

Jiena mitluba nagħti kampjun tal-kurdun għat-tkabbir ta' ċelloli staminali mesenkimali sabiex jistaw jiġu identifikati microRNAs li jistgħu jikkaġunaw l-iżvilupp ta' neuroblast.

Jiena konxja li ċ-ċelluli li huma mkabbra mill-kurdun jistgħu jintużaw ukoll fi studji oħra relatati u etikament approvati.

***Il-kampjuni se jinġabru b'mod anonimu u kwalunkwe materjal mhux użat se jinqered.***

L-għan u d-dettalji tal-istudju ġew spjegati lili minn _____ u ġew mwieġba u iċċarati l-mistoqsijiet u d-diffikultajiet kollha tiegħi.

Jiena nagħti l-kunsens tiegħi lil Ms Vanessa Zammit [redacted] u d-delegati tagħha sabiex tieħu l-kampjun meħtieġ, u wkoll nirrikonoxxi lil Ms Vanessa Zammit bħala unika sid ta dawn taċ-ċelloli.

Jiena minix niġi magħżula minħabba xi implikazzjoni medika jew predispożizzjoni ġenetika relatata ma dan l-istudju imma purament għal raġunijiet ta' riċerka. Nifhem li r-riżultati ta' dan l-istudju jistgħu jintużaw għal għanijiet mediċi jew xjentifiċi, u li r-riżultati miksuba minn dan l-istudju li fih jiena parteċipanti jistgħu jiġu rrapportati jew ippubblikati: madankollu, minix se kunu identifikata personalment bl-ebda mod, la individwalment u lanqas kollettivament.

Jien m'għandi ebda obbligu biex nipparteċipa f'dan l-istudju u qeda nagħmel dan b'mod volontarju.

Jiena nista nirtira mill-istudju fi kwalunkwe ħin, mingħajr ma nagħti ebda raġuni.

Jien mhux qed nirċievi ebda remunerazzjoni għall-parteċipazzjoni f'dan l-istudju.

Jien nirrinunzja d-drittijiet kollha għal kwalunkwe proprjetà intellettwali li jistgħu johorgu minn dan jew xi xogħol ieħor relatat.

F'każ ta' mistoqsijiet nista' nikkuntattja lil **Ms. Vanessa Zammit** fuq in-numru: [redacted]

| | |
|---|---|
| _____ | _____ |
| Firma tal-parteċipant | Firma tar-riċerkatur |
| _____ | _____ |
| Isem tal-parteċipant (b'ittri kbar) | Isem tar-riċerkatur (b'ittri kbar): |
| _____ | _____ |
| Numru ta' l- identita | Numru ta' l- identita |

_____

Data

# Annex II

# Kit inserts

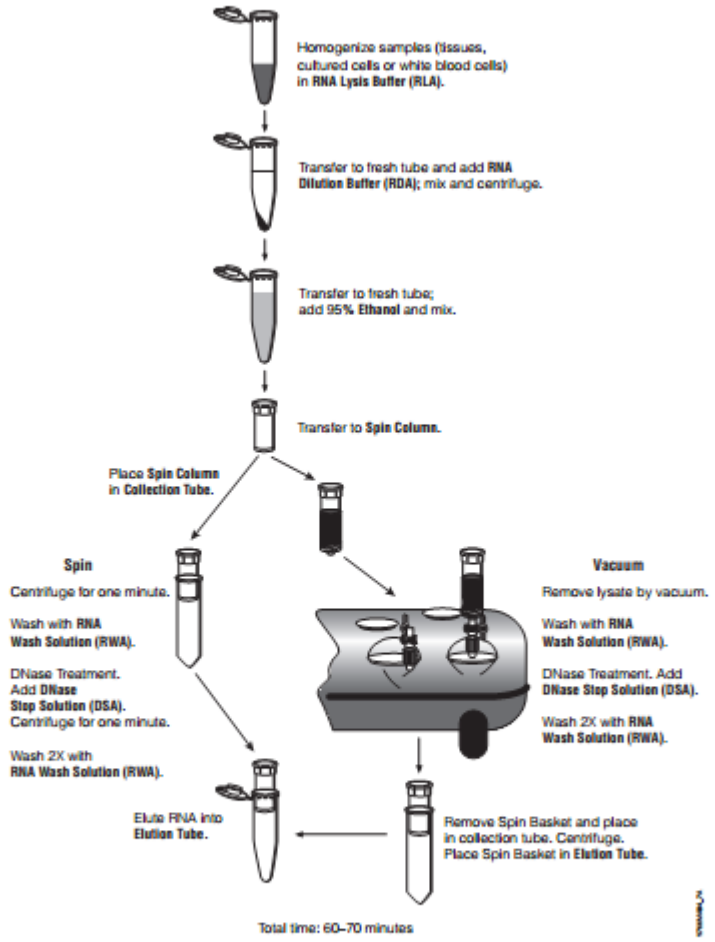


**Figure 1. Schematic representation of the SV Total RNA Isolation System.** For information on the protocol, please read Section 4 and Sections 8.A–D.

BIONEER

Innovation · Value · Discovery

One page protocol

# *AccuPrep*® Plasmid Mini Extraction Kit (K-3030, K-3030-1)

## Ⅰ Before You Begin

1) Did you add RNase A powder to PA1 Buffer and completely dissolve it? After adding RNase A, PA1 Buffer should be stored at 4℃.
2) Did you add the correct amount of absolute ethanol to PB Buffer?
3) Before starting extraction process, heat the EA Buffer at 56 - 60℃.

## Ⅱ Experimental Protocol

1) Pick up a single colony from fresh cultured LB (Luria-Bertani) agar plate (contains antibiotics) or your established media and inoculate the cell into the 1 - 5 ml of fresh LB liquid media or your established media at 37℃ with shaking for 12 - 16 hours.
   Do not overgrowth *E.coli* cell. It will decrease the productivity because of the cell death and inefficient lysis.
   For high copy number plasmid DNA : 1 ~ 5 ml of *E.coli* cells
   For low copy number plasmid DNA : 1 ~ 10 ml of *E.coli* cells
2) Collect the *E.coli* cells by centrifugation at 8,000 rpm for 2 min or 3,000 rpm for 5 min. And completely remove of the media by pipetting.
3) Add 250 µl of PA1 Buffer to the collected cells and completely resuspend by vortexing or pipetting.
4) Add 250 µl of P2 Buffer and mix by inverting the tube 3 - 4 times gently. (Caution) Avoid vortex! Vortexing may cause shearing of genomic DNA. It is important to invert gently
5) Add 350 µl of PA3 Buffer and immediately mix by inverting the tube 3 - 4 times, gently.
   (Caution) Again, be cautions not to shear genomic DNA. Genomic DNA and cell debris will form an insoluble complex.
6) Centrifuge the tube at 13,000 rpm, 4℃ for 10 min in a microcentrifuge. After centrifugation, white protein aggregate will appear at the bottom of the tube.
   (Option) If your centrifuge is not enough to get a cleared lysate, please centrifuge again.
7) Add 100 µl of BST Solution to the Binding column tube (fit in a collection tube) and centrifuge for 30 sec at 13,000 rpm.
8) Discard the solution from the collection tube and reuse the collection tube.
9) Transfer the cleared lysate to the Binding column (fit in a collection tube) and centrifuge at 13,000 rpm for 1 min. Pour off the flow-through and re-assemble the Binding column with the collection tube.
10) (Option) Add 500 µl of PB Buffer and wait for 5 min and centrifuge at 13,000 rpm for 1 min. Discard the solution from the collection tube and reuse the collection tube.
    This step is required if you are using an endA+ strains which has a high endonuclease activity. BL21, CJ236, HB101, JM83, JM 101, JM110,

BIONEER
Innovation + Value + Discovery

One page protocol

## *AccuPrep*® Plasmid Mini Extraction Kit (K-3030, K-3030-1)

LE392, NM series strains, PR series strains, Q358, PR1, TB1, TG1, Y10 series strains, BMH71-18 and ES1301 are endA+ strains, thus they produce highly active endonucleases that can degrade plasmids. Denaturation step is not required for the DH5α, XL1-Blue, BJS183, DH1, DH20, DH21, JM103, JM105, JM106, JM107, JM108, JM109, MM294, SK1590, SK1592, SK2267, SRB and XLO strains.

11) Add 700 µl of W2 Buffer to the Binding column and centrifuge at 13,000 rpm for 1 min. Pour off the flow-through and re-assemble the Binding column with the collection tube.

12) Centrifuge once more at 13,000 rpm for 5 min to remove ethanol completely.

13) Transfer the Binding column to a1.5 ml tube (not provided).

14) Add 50 - 100 µl of EA Buffer to the Binding column, and wait for at least 1 min.
(Option) If you want to get a more concentrated solution of plasmid, a smaller volume is appropriate, but total yield may be reduced. If the plasmid is low copy or larger than 10 kb, the yield of plasmid may not be sufficient. Pre-warmed (about 60 ℃) EA Buffer will improve efficiency of elution.

15) Elute the plasmid DNA by centrifugation at 13,000 rpm for 1 min.
(Option) If you want more quantity, elute the sample twice.

※ For more information, please visit www.Bioneer.com for a full manual.

# Appendix III
# Raw Data

**CD Markers**

| | Cord 5 | NTC | CqCD73 | CqCD90 | CqCD105 | CqCD34 | CqCD45 | CqGAPDH | ΔCq CD73 | Δq CD90 | ΔCq CD105 | ΔCq CD34 | ΔCq CD45 |
|---|---|---|---|---|---|---|---|---|---|---|---|---|---|
| MSC | Run1 | 34.60 | 31.59 | 24.34 | 26.91 | 40.00 | 40.00 | 20.76 | 10.83 | 3.58 | 23.33 | 19.24 | 19.24 |
| | Run2 | 35.18 | 31.75 | 24.31 | 25.58 | 40.00 | 40.00 | 20.91 | 10.84 | 3.40 | 22.18 | 19.09 | 19.09 |
| | Run3 | 33.65 | 31.61 | 24.64 | 25.85 | 39.55 | 40.00 | 20.97 | 10.64 | 3.67 | 22.18 | 18.58 | 19.03 |

| | Cord 6 | NTC | CqCD73 | CqCD90 | CqCD105 | CqCD34 | CqCD45 | CqGAPDH | ΔCq CD73 | ΔCq CD90 | ΔCq CD105 | ΔCq CD34 | ΔCq CD45 |
|---|---|---|---|---|---|---|---|---|---|---|---|---|---|
| MSC | Run1 | 40.00 | 33.36 | 27.39 | 28.78 | 40.00 | 40.00 | 24.23 | 9.13 | 3.16 | 25.62 | 15.77 | 15.77 |
| | Run2 | 40.00 | 33.61 | 27.79 | 28.48 | 40.00 | 40.00 | 24.18 | 9.43 | 3.61 | 24.87 | 15.82 | 15.82 |
| | Run3 | 39.13 | 34.42 | 27.67 | 28.64 | 40.00 | 40.00 | 23.90 | 10.52 | 3.77 | 24.87 | 16.10 | 16.10 |

| | Cord 13 | NTC | CqCD73 | CqCD90 | CqCD105 | CqCD34 | CqCD45 | CqGAPDH | ΔCq CD73 | ΔCq CD90 | ΔCq CD105 | ΔCq CD34 | ΔCq CD45 |
|---|---|---|---|---|---|---|---|---|---|---|---|---|---|
| MSC | Run1 | 34.33 | 32.43 | 26.60 | 31.10 | 40.00 | 40.00 | 25.72 | 6.71 | 0.88 | 30.22 | 14.28 | 14.28 |
| | Run2 | 34.67 | 33.46 | 27.37 | 31.48 | 40.00 | 40.00 | 26.27 | 7.19 | 1.10 | 30.38 | 13.73 | 13.73 |
| | Run3 | 34.58 | 32.57 | 26.93 | 31.50 | 40.00 | 40.00 | 26.18 | 6.39 | 0.75 | 30.75 | 13.82 | 13.82 |

| | Cord 5 | NTC | CqCD73 | CqCD90 | CqCD105 | CqCD34 | CqCD45 | CqGAPDH | ΔCq CD73 | ΔCq CD90 | ΔCq CD105 | ΔCq CD34 | ΔCq CD45 |
|---|---|---|---|---|---|---|---|---|---|---|---|---|---|
| CC | Run1 | 34.76 | 39.30 | 22.05 | 23.96 | 31.18 | 40.00 | 16.28 | 23.02 | 5.77 | 18.19 | 14.90 | 23.72 |
| | Run2 | 34.51 | 39.08 | 21.98 | 23.97 | 32.23 | 40.00 | 16.36 | 22.72 | 5.62 | 18.35 | 15.87 | 23.64 |
| | Run3 | 35.73 | 38.48 | 22.18 | 24.07 | 32.06 | 40.00 | 16.23 | 22.25 | 5.95 | 18.12 | 15.83 | 23.77 |

| | Cord 6 | NTC | CqCD73 | CqCD90 | CqCD105 | CqCD34 | CqCD45 | CqGAPDH | ΔCq CD73 | ΔCq CD90 | ΔCq CD105 | ΔCq CD34 | ΔCq CD45 |
|---|---|---|---|---|---|---|---|---|---|---|---|---|---|
| CC | Run1 | 32.36 | 33.02 | 20.16 | 23.55 | 33.45 | 34.30 | 15.26 | 17.76 | 4.90 | 18.65 | 18.19 | 19.04 |
| | Run2 | 33.23 | 32.74 | 20.22 | 23.54 | 33.79 | 34.20 | 15.20 | 17.54 | 5.02 | 18.52 | 18.59 | 19.00 |
| | Run3 | 32.81 | 33.18 | 20.42 | 23.91 | 33.38 | 35.36 | 15.27 | 17.91 | 5.15 | 18.76 | 18.11 | 20.09 |

| | Cord 13 | NTC | CqCD73 | CqCD90 | CqCD105 | CqCD34 | CqCD45 | CqGAPDH | ΔCq CD73 | ΔCq CD90 | ΔCq CD105 | ΔCq CD34 | ΔCq CD45 |
|---|---|---|---|---|---|---|---|---|---|---|---|---|---|
| CC | Run1 | 33.11 | 40.00 | 24.30 | 25.82 | 33.79 | 40.00 | 18.69 | 21.31 | 5.61 | 20.21 | 15.10 | 21.31 |
| | Run2 | 33.62 | 40.00 | 24.82 | 22.49 | 34.13 | 40.00 | 18.77 | 21.23 | 6.05 | 19.44 | 15.36 | 21.23 |
| | Run3 | 32.81 | 40.00 | 24.67 | 25.61 | 33.36 | 40.00 | 18.96 | 21.04 | 5.71 | 19.90 | 14.40 | 21.04 |

| | Cord 5 | NTC | CqCD73 | CqCD90 | CqCD105 | CqCD34 | CqCD45 | CqGAPDH | dCq CD73 | dCq CD90 | dCq CD105 | dCq CD34 | dCq CD45 |
|---|---|---|---|---|---|---|---|---|---|---|---|---|---|
| CC-RA | Run1 | 31.98 | 35.33 | 26.98 | 26.36 | 38.94 | 40.00 | 19.70 | 15.63 | 7.28 | 19.08 | 19.24 | 20.30 |
| | Run2 | 31.61 | 35.22 | 27.08 | 25.94 | 38.07 | 40.00 | 19.73 | 15.49 | 7.35 | 18.59 | 18.34 | 20.27 |
| | Run3 | 31.08 | 36.52 | 26.96 | 26.27 | 38.76 | 40.00 | 19.71 | 16.81 | 7.25 | 19.02 | 19.05 | 20.29 |

| | Cord 6 | NTC | CqCD73 | CqCD90 | CqCD105 | CqCD34 | CqCD45 | CqGAPDH | ΔCq CD73 | ΔCq CD90 | ΔCq CD105 | ΔCq CD34 | ΔCq CD45 |
|---|---|---|---|---|---|---|---|---|---|---|---|---|---|
| CC-RA | Run1 | 40.00 | 40.00 | 29.05 | 30.18 | 40.00 | 40.00 | 22.86 | 17.14 | 6.19 | 23.99 | 17.14 | 17.14 |
| | Run2 | 40.00 | 40.00 | 29.73 | 29.25 | 40.00 | 40.00 | 22.84 | 17.16 | 6.89 | 22.36 | 17.16 | 17.16 |
| | Run3 | 39.86 | 40.00 | 29.51 | 29.63 | 40.00 | 40.00 | 23.12 | 16.88 | 6.39 | 23.24 | 16.88 | 16.88 |

| | Cord 13 | NTC | CqCD73 | CqCD90 | CqCD105 | CqCD34 | CqCD45 | CqGAPDH | ΔCq CD73 | ΔCq CD90 | ΔCq CD105 | ΔCq CD34 | ΔCq CD45 |
|---|---|---|---|---|---|---|---|---|---|---|---|---|---|
| CC-RA | Run1 | 34.42 | 40.00 | 27.95 | 26.09 | 35.69 | 40.00 | 20.42 | 19.58 | 7.53 | 18.56 | 15.27 | 19.58 |
| | Run2 | 34.42 | 40.00 | 27.18 | 26.34 | 35.47 | 40.00 | 20.72 | 19.28 | 6.46 | 19.88 | 14.75 | 19.28 |
| | Run3 | 34.53 | 40.00 | 27.15 | 26.18 | 36.32 | 40.00 | 20.67 | 19.33 | 6.48 | 19.70 | 15.65 | 19.33 |

| | From MSCs to CC | | | | | From CC to CC-RA | | | | |
|---|---|---|---|---|---|---|---|---|---|---|
| Cord 5 | ΔΔCq CD73 | ΔΔCq CD90 | ΔΔCq CD105 | ΔΔCq CD34 | ΔΔCq CD45 | ΔΔCq CD73 | ΔΔCq CD90 | ΔΔCq CD105 | ΔΔCq CD34 | ΔΔCq CD45 |
| Run 1 | -12.19 | -2.19 | 5.14 | 4.34 | -4.48 | 7.39 | -1.51 | -0.89 | -4.34 | 3.42 |
| Run 2 | -11.88 | -2.22 | 3.83 | 3.22 | -4.55 | 7.23 | -1.73 | -0.24 | -2.47 | 3.37 |
| Run 3 | -11.61 | -2.28 | 4.06 | 2.75 | -4.74 | 5.44 | -1.3 | -0.9 | -3.22 | 3.48 |

| | From MSCs to CC | | | | | From CC to CC-RA | | | | |
|---|---|---|---|---|---|---|---|---|---|---|
| Cord 6 | ΔΔCq CD73 | ΔΔCq CD90 | ΔΔCq CD105 | ΔΔCq CD34 | ΔΔCq CD45 | ΔΔCq CD73 | ΔΔCq CD90 | ΔΔCq CD105 | ΔΔCq CD34 | ΔΔCq CD45 |
| Run 1 | -8.63 | -1.74 | 6.97 | -2.42 | -3.27 | 0.62 | -1.29 | -5.34 | 1.05 | 1.9 |
| Run 2 | -8.11 | -1.41 | 6.35 | -2.77 | -3.18 | 0.38 | -1.87 | -3.84 | 1.43 | 1.84 |
| Run 3 | -7.39 | -1.38 | 6.11 | -2.01 | -3.99 | 1.03 | -1.24 | -4.48 | 1.23 | 3.21 |

| | From MSCs to CC | | | | | From CC to CC-RA | | | | |
|---|---|---|---|---|---|---|---|---|---|---|
| Cord 13 | ΔΔCq CD73 | ΔΔCq CD90 | ΔΔCq CD105 | ΔΔCq CD34 | ΔΔCq CD45 | ΔΔCq CD73 | ΔΔCq CD90 | ΔΔCq CD105 | ΔΔCq CD34 | ΔΔCq CD45 |
| Run 1 | -14.6 | -4.73 | 10.01 | -0.82 | -7.03 | 1.73 | -1.92 | 1.65 | -0.17 | 1.73 |
| Run 2 | -14.04 | -4.95 | 10.94 | -1.63 | -7.5 | 1.95 | -0.41 | -0.44 | 0.61 | 1.95 |
| Run 3 | -14.65 | -4.96 | 10.85 | -0.58 | -7.22 | 1.71 | -0.77 | 0.2 | -1.25 | 1.71 |

**Neural Markers Pre-Transfection**

| | Cord 5 | NTC | CqNES | CqSOX2 | CqOCT4 | CqTUBB3 | CqMASH1 | CqND1 | CqMAP2 | CqNEU | CqGAPDH |
|---|---|---|---|---|---|---|---|---|---|---|---|
| MSC | Run1 | 32.93 | 30.07 | 26.02 | 24.66 | 27.3 | 21.77 | 25.94 | 39.12 | 39.29 | 20.5 |
| | Run2 | 33.91 | 30.21 | 25.74 | 24.40 | 26.97 | 21.56 | 25.83 | 39.87 | 40.00 | 20.42 |
| | Run3 | 33.43 | 29.71 | 25.77 | 24.52 | 27.20 | 21.42 | 25.84 | 39.08 | 40.00 | 20.41 |

| | Cord 5 | ΔCq NES | ΔCq SOX2 | ΔCq OCT4 | ΔCq TUBB3 | ΔCq MASH1 | ΔCq ND1 | ΔCq MAP2 | ΔCq NEU |
|---|---|---|---|---|---|---|---|---|---|
| MSC | Run1 | 9.57 | 5.52 | 4.16 | 6.80 | 1.27 | 5.44 | 18.62 | 18.79 |
| | Run2 | 9.79 | 5.32 | 3.98 | 6.55 | 1.14 | 5.41 | 19.45 | 19.58 |
| | Run3 | 9.30 | 5.36 | 4.11 | 6.79 | 1.01 | 5.43 | 18.67 | 19.59 |

| | Cord6 | NTC | CqNES | CqSOX2 | CqOCT4 | CqTUBB3 | CqMASH1 | CqND1 | CqMAP2 | CqNEU | CqGAPDH |
|---|---|---|---|---|---|---|---|---|---|---|---|
| MSC | Run1 | 32.62 | 30.60 | 26.76 | 24.92 | 29.53 | 24.48 | 26.36 | 38.03 | 40.00 | 23.12 |
| | Run2 | 31.91 | 29.41 | 26.62 | 24.87 | 29.86 | 24.89 | 26.77 | 38.15 | 40.00 | 23.13 |
| | Run3 | 32.21 | 30.12 | 26.49 | 24.63 | 30.33 | 24.67 | 26.86 | 39.12 | 40.00 | 23.40 |

| | Cord6 | ΔCq NES | ΔCq SOX2 | ΔCq OCT4 | ΔCq TUBB3 | ΔCq MASH1 | ΔCq ND1 | ΔCq MAP2 | ΔCq NEU |
|---|---|---|---|---|---|---|---|---|---|
| MSC | Run1 | 7.48 | 3.64 | 1.80 | 6.41 | 1.36 | 3.24 | 14.91 | 16.88 |
| | Run2 | 6.28 | 3.49 | 1.74 | 6.73 | 1.76 | 3.64 | 15.02 | 16.87 |
| | Run3 | 6.72 | 3.09 | 1.23 | 6.93 | 1.27 | 3.46 | 15.72 | 16.60 |

| | Cord 13 | NTC | CqNES | CqSOX2 | CqOCT4 | CqTUBB3 | CqMASH1 | CqND1 | CqMAP2 | CqNEU | CqGAPDH |
|---|---|---|---|---|---|---|---|---|---|---|---|
| MSC | Run1 | 38.46 | 33.51 | 32.71 | 31.41 | 33.08 | 29.34 | 31.84 | 40.00 | 40.00 | 24.68 |
| | Run2 | 38.45 | 34.12 | 32.84 | 30.65 | 33.19 | 29.82 | 33.08 | 40.00 | 40.00 | 24.84 |
| | Run3 | 38.00 | 34.56 | 32.15 | 31.65 | 33.21 | 31.10 | 33.50 | 40.00 | 40.00 | 25.62 |

| | Cord 13 | ΔCq NES | ΔCq SOX2 | ΔCq OCT4 | ΔCq TUBB3 | ΔCq MASH1 | ΔCq ND1 | ΔCq MAP2 | ΔCq NEU |
|---|---|---|---|---|---|---|---|---|---|
| MSC | Run1 | 8.83 | 8.03 | 6.73 | 8.40 | 4.66 | 7.16 | 15.32 | 15.32 |
| | Run2 | 9.28 | 8.00 | 5.81 | 8.35 | 4.98 | 8.24 | 15.16 | 15.16 |
| | Run3 | 8.94 | 6.53 | 6.03 | 7.59 | 5.48 | 7.88 | 14.38 | 14.38 |

| | Cord 5 | NTC | CqNES | CqSOX2 | CqOCT4 | CqTUBB3 | CqMASH1 | CqND1 | CqMAP2 | CqNEU | CqGAPDH |
|---|---|---|---|---|---|---|---|---|---|---|---|
| CC | Run1 | 29.74 | 21.33 | 26.37 | 28.32 | 18.81 | 21.63 | 25.44 | 21.27 | 30.15 | 16.42 |
| | Run2 | 29.67 | 21.34 | 26.37 | 29.48 | 18.78 | 21.22 | 25.58 | 21.06 | 30.55 | 16.37 |
| | Run3 | 30.02 | 21.23 | 27.00 | 29.35 | 18.76 | 21.38 | 25.50 | 21.17 | 30.15 | 16.42 |

| | Cord 5 | ΔCq NES | ΔCq SOX2 | ΔCq OCT4 | ΔCq TUBB3 | ΔCq MASH1 | ΔCq ND1 | ΔCq MAP2 | ΔCq NEU |
|---|---|---|---|---|---|---|---|---|---|
| CC | Run1 | 4.91 | 9.95 | 11.90 | 2.39 | 5.21 | 9.02 | 4.85 | 13.73 |
| | Run2 | 4.97 | 10.00 | 13.11 | 2.41 | 4.85 | 9.21 | 4.69 | 14.18 |
| | Run3 | 4.81 | 10.58 | 12.93 | 2.34 | 4.96 | 9.08 | 4.75 | 13.73 |

| | Cord 6 | NTC | CqNES | CqSOX2 | CqOCT4 | CqTUBB3 | CqMASH1 | CqND1 | CqMAP2 | CqNEU | CqGAPDH |
|---|---|---|---|---|---|---|---|---|---|---|---|
| CC | Run1 | 32.26 | 16.58 | 25.20 | 27.45 | 15.32 | 17.79 | 20.76 | 17.73 | 28.42 | 14.19 |
| | Run2 | 33.36 | 16.49 | 24.98 | 27.41 | 15.82 | 17.23 | 20.69 | 17.35 | 27.93 | 14.07 |
| | Run3 | 32.53 | 16.72 | 24.71 | 27.15 | 15.89 | 18.03 | 20.73 | 17.18 | 28.24 | 14.03 |

| | Cord 6 | ΔCq NES | ΔCq SOX2 | ΔCq OCT4 | ΔCq TUBB3 | ΔCq MASH1 | ΔCq ND1 | ΔCq MAP2 | ΔCq NEU |
|---|---|---|---|---|---|---|---|---|---|
| CC | Run1 | 2.39 | 11.01 | 13.26 | 1.13 | 3.60 | 6.57 | 3.54 | 14.23 |
| | Run2 | 2.42 | 10.91 | 13.34 | 1.75 | 3.16 | 6.62 | 3.28 | 13.86 |
| | Run3 | 2.69 | 10.68 | 13.12 | 1.86 | 4.00 | 6.70 | 3.15 | 14.21 |

| | Cord 13 | NTC | CqNES | CqSOX2 | CqOCT4 | CqTUBB3 | CqMASH1 | CqND1 | CqMAP2 | CqNEU | CqGAPDH |
|---|---|---|---|---|---|---|---|---|---|---|---|
| CC | Run1 | 40.00 | 20.49 | 24.25 | 23.60 | 20.15 | 22.78 | 24.21 | 19.90 | 28.22 | 15.66 |
| | Run2 | 40.00 | 20.42 | 24.73 | 23.72 | 20.02 | 22.58 | 25.05 | 21.33 | 29.29 | 15.80 |
| | Run3 | 40.00 | 20.32 | 24.32 | 23.76 | 19.81 | 22.75 | 24.90 | 20.46 | 29.04 | 15.92 |

| | Cord 13 | ΔCq NES | ΔCq SOX2 | ΔCq OCT4 | ΔCq TUBB3 | ΔCq MASH1 | ΔCq ND1 | ΔCq MAP2 | ΔCq NEU |
|---|---|---|---|---|---|---|---|---|---|
| CC | Run1 | 4.83 | 8.59 | 7.94 | 4.49 | 7.12 | 8.55 | 4.24 | 12.56 |
| | Run2 | 4.62 | 8.93 | 7.92 | 4.22 | 6.78 | 9.25 | 5.53 | 13.49 |
| | Run3 | 4.40 | 8.40 | 7.84 | 3.89 | 6.83 | 8.98 | 4.54 | 13.12 |

| | Cord 5 | NTC | CqSOX2 | CqOCT4 | CqMASH1 | CqGAPDH | ΔCq SOX2 | ΔCq OCT4 | ΔCq MASH1 |
|---|---|---|---|---|---|---|---|---|---|
| CC-RA | Run1 | 32.98 | 28.19 | 28.04 | 24.32 | 19.70 | 8.49 | 8.34 | 4.62 |
| | Run2 | 32.61 | 28.64 | 28.11 | 23.41 | 19.73 | 8.91 | 8.38 | 3.68 |
| | Run3 | 33.08 | 28.51 | 27.73 | 24.42 | 19.71 | 8.80 | 8.02 | 4.71 |

| | Cord 5 | NTC | CqNES | CqTUBB3 | CqMAP2 | CqNEU | CqGAPDH | ΔCq NES | ΔCq TUBB3 | ΔCq MAP2 | ΔCq NEU |
|---|---|---|---|---|---|---|---|---|---|---|---|
| CC-RA | Run1 | 40.00 | 26.16 | 24.63 | 24.97 | 40.00 | 19.92 | 6.24 | 4.71 | 5.05 | 20.08 |
| | Run2 | 40.00 | 25.63 | 24.32 | 25.22 | 40.00 | 19.96 | 5.67 | 4.36 | 5.26 | 20.04 |
| | Run3 | 40.00 | 26.91 | 24.20 | 25.15 | 40.00 | 19.80 | 7.11 | 4.40 | 5.35 | 20.20 |

| | Cord 5 | NTC | CqND1 | CqGAPDH | ΔCq ND1 |
|---|---|---|---|---|---|
| CC-RA | Run1 | 40.00 | 26.96 | 17.52 | 9.44 |
| | Run2 | 40.00 | 27.56 | 17.53 | 10.03 |
| | Run3 | 40.00 | 26.93 | 17.47 | 9.46 |

| CC-RA | Cord 6 | NTC | CqSOX2 | CqOCT4 | CqMASH1 | CqGAPDH | ΔCq SOX2 | ΔCq OCT4 | ΔCq MASH1 |
|---|---|---|---|---|---|---|---|---|---|
| | Run1 | 40.00 | 32.39 | 27.41 | 24.85 | 22.86 | 9.53 | 4.55 | 1.99 |
| | Run2 | 40.00 | 30.80 | 27.64 | 25.41 | 22.84 | 7.96 | 4.80 | 2.57 |
| | Run3 | 39.86 | 31.38 | 27.21 | 25.04 | 23.12 | 8.26 | 4.09 | 1.92 |

| CC-RA | Cord 6 | NTC | CqNES | CqTUBB3 | CqMAP2 | CqNEU | CqGAPDH | ΔCq NES | ΔCq TUBB3 | ΔCq MAP2 | ΔCq NEU |
|---|---|---|---|---|---|---|---|---|---|---|---|
| | Run1 | 34.44 | 26.47 | 25.25 | 25.91 | 33.19 | 22.44 | 4.03 | 2.81 | 3.47 | 10.75 |
| | Run2 | 34.82 | 25.54 | 25.65 | 24.94 | 33.45 | 22.37 | 3.17 | 3.28 | 2.57 | 11.08 |
| | Run3 | 34.74 | 25.39 | 24.96 | 24.29 | 33.72 | 21.81 | 3.58 | 3.15 | 2.48 | 11.91 |

| CC-RA | Cord 6 | NTC | CqND1 | CqGAPDH | ΔCq ND1 |
|---|---|---|---|---|---|
| | Run1 | 40.00 | 27.76 | 21.15 | 6.61 |
| | Run2 | 40.00 | 28.70 | 21.02 | 7.68 |
| | Run3 | 40.00 | 28.52 | 21.15 | 7.37 |

| | Cord 13 | NTC | CqSOX2 | CqOCT4 | CqMASH1 | CqGAPDH | ΔCq SOX2 | ΔCq OCT4 | ΔCq MASH1 |
|---|---|---|---|---|---|---|---|---|---|
| CC-RA | Run1 | 34.42 | 20.91 | 22.19 | 21.90 | 20.42 | 0.49 | 1.77 | 1.48 |
| | Run2 | 34.42 | 21.30 | 22.31 | 21.46 | 20.72 | 0.58 | 1.59 | 0.74 |
| | Run3 | 34.53 | 21.03 | 22.18 | 21.35 | 20.67 | 0.36 | 1.51 | 0.68 |

| | Cord 13 | NTC | CqNES | CqTUBB3 | CqMAP2 | CqNEU | CqGAPDH | ΔCq NES | ΔCq TUBB3 | ΔCq MAP2 | ΔCq NEU |
|---|---|---|---|---|---|---|---|---|---|---|---|
| CC-RA | Run1 | 40.00 | 26.47 | 25.96 | 25.85 | 34.38 | 17.41 | 9.06 | 8.55 | 8.44 | 16.97 |
| | Run2 | 40.00 | 26.48 | 25.94 | 25.82 | 34.88 | 17.50 | 8.98 | 8.44 | 8.32 | 17.38 |
| | Run3 | 40.00 | 26.25 | 26.16 | 25.90 | 36.01 | 17.74 | 8.51 | 8.42 | 8.16 | 18.27 |

| | Cord 13 | NTC | CqND1 | CqGAPDH | ΔCq ND1 |
|---|---|---|---|---|---|
| CC-RA | Run1 | 40.00 | 18.93 | 15.59 | 3.34 |
| | Run2 | 40.00 | 19.01 | 15.68 | 3.33 |
| | Run3 | 40.00 | 18.73 | 15.64 | 3.09 |

| From MSCs to CC | | | | | | | | |
|---|---|---|---|---|---|---|---|---|
| Cord 5 | ΔΔCq NES | ΔΔCq SOX2 | ΔΔCq OCT4 | ΔΔCq TUBB3 | ΔΔCq MASH1 | ΔΔCq ND1 | ΔΔCq MAP2 | ΔΔCq NEU |
| Run 1 | 4.66 | -4.43 | -7.74 | 4.41 | -3.94 | -3.58 | 13.77 | 5.06 |
| Run 2 | 4.82 | -4.68 | -9.13 | 4.14 | -3.71 | -3.80 | 14.76 | 5.40 |
| Run 3 | 4.49 | -5.22 | -8.82 | 4.45 | -3.95 | -3.65 | 13.92 | 5.86 |

| From MSCs to CC | | | | | | | | |
|---|---|---|---|---|---|---|---|---|
| Cord 6 | ΔΔCq NES | ΔΔCq SOX2 | ΔΔCq OCT4 | ΔΔCq TUBB3 | ΔΔCq MASH1 | ΔΔCq ND1 | ΔΔCq MAP2 | ΔΔCq NEU |
| Run 1 | 5.09 | -7.37 | -11.46 | 5.28 | -2.24 | -3.33 | 11.37 | 2.65 |
| Run 2 | 3.86 | -7.42 | -11.6 | 4.98 | -1.4 | -2.98 | 11.74 | 3.01 |
| Run 3 | 4.03 | -7.59 | -11.89 | 5.07 | -2.73 | -3.24 | 12.57 | 2.39 |

| From MSCs to CC | | | | | | | | |
|---|---|---|---|---|---|---|---|---|
| Cord 13 | ΔΔCq NES | ΔΔCq SOX2 | ΔΔCq OCT4 | ΔΔCq TUBB3 | ΔΔCq MASH1 | ΔΔCq ND1 | ΔΔCq MAP2 | ΔΔCq NEU |
| Run 1 | 4.00 | -0.56 | -1.21 | 3.91 | -2.46 | -1.39 | 11.08 | 2.76 |
| Run 2 | 4.66 | -0.93 | -2.11 | 4.13 | -1.80 | -1.01 | 9.63 | 1.67 |
| Run 3 | 4.54 | -1.87 | -1.81 | 3.70 | -1.35 | -1.10 | 9.84 | 1.26 |

| From CC to CC-RA | | | | | | | | |
|---|---|---|---|---|---|---|---|---|
| Cord 5 | ΔΔCq NES | ΔΔCq SOX2 | ΔΔCq OCT4 | ΔΔCq TUBB3 | ΔΔCq MASH1 | ΔΔCq ND1 | ΔΔCq MAP2 | ΔΔCq NEU |
| Run 1 | -1.33 | 1.46 | 3.56 | -2.32 | 0.59 | -0.42 | -0.20 | -6.35 |
| Run 2 | -0.70 | 1.09 | 4.73 | -1.95 | 1.17 | -0.82 | -0.57 | -5.86 |
| Run 3 | -2.30 | 1.78 | 4.91 | -2.06 | 0.25 | -0.38 | -0.60 | -6.47 |

| From CC to CC-RA | | | | | | | | |
|---|---|---|---|---|---|---|---|---|
| Cord 6 | ΔΔCq NES | ΔΔCq SOX2 | ΔΔCq OCT4 | ΔΔCq TUBB3 | ΔΔCq MASH1 | ΔΔCq ND1 | ΔΔCq MAP2 | ΔΔCq NEU |
| Run 1 | -1.64 | 1.48 | 8.71 | -1.68 | 1.61 | -0.04 | 0.07 | 3.48 |
| Run 2 | -0.75 | 2.95 | 8.54 | -1.53 | 0.59 | -1.06 | 0.71 | 2.78 |
| Run 3 | -0.89 | 2.42 | 9.03 | -1.29 | 2.08 | -0.67 | 0.67 | 2.30 |

| From CC to CC-RA | | | | | | | | |
|---|---|---|---|---|---|---|---|---|
| Cord 13 | ΔΔCq NES | ΔΔCq SOX2 | ΔΔCq OCT4 | ΔΔCq TUBB3 | ΔΔCq MASH1 | ΔΔCq ND1 | ΔΔCq MAP2 | ΔΔCq NEU |
| Run 1 | -4.23 | 8.10 | 6.17 | -4.06 | 5.64 | 5.21 | -4.20 | -4.41 |
| Run 2 | -4.36 | 8.35 | 6.33 | -4.22 | 6.04 | 5.92 | -2.79 | -3.89 |
| Run 3 | -4.11 | 8.04 | 6.33 | -4.53 | 6.15 | 5.89 | -3.62 | -5.15 |

**Gene Targets**

| | Cord 9 | NTC | CqDICER | CqPTP1B | CqHES1 | CqDICER NEG CTL | CqPTP1B NEG CTL | CqHES1 NEG CTL | Cqsi107 GAPDH | Cqsi124 GAPDH | Cqsi381 GAPDH | CqsiNEG GAPDH |
|---|---|---|---|---|---|---|---|---|---|---|---|---|
| MSC | Run1 | 40.00 | 32.93 | 33.12 | 40.00 | 34.67 | 34.44 | 33.82 | 23.51 | 26.17 | 26.30 | 27.45 |
| | Run2 | 40.00 | 32.39 | 32.78 | 40.00 | 35.10 | 34.23 | 33.18 | 23.64 | 26.23 | 26.06 | 27.58 |
| | Run3 | 40.00 | 32.52 | 32.92 | 40.00 | 34.92 | 34.69 | 33.47 | 23.29 | 25.72 | 26.21 | 27.57 |

| | Cord 9 | dCqsi107 DICER | ΔCqsi124 PTP1B | ΔCqsi381 HES1 | ΔCqDICER NEG CTL | ΔCq PTP1B NEG CTL | ΔCqsi381 NEG | ΔΔCqDICER | ΔΔCqPTP1B | ΔΔCq HES1 |
|---|---|---|---|---|---|---|---|---|---|---|
| MSC | Run1 | 9.42 | 6.95 | 13.70 | 7.22 | 6.99 | 7.52 | -2.20 | 0.04 | -6.18 |
| | Run2 | 8.75 | 6.55 | 13.94 | 7.52 | 6.65 | 7.12 | -1.23 | 0.10 | -6.82 |
| | Run3 | 9.23 | 7.20 | 13.79 | 7.35 | 7.12 | 7.26 | -1.88 | -0.08 | -6.53 |

| | Cord 11 | NTC | CqDICER | CqPTP1B | CqHES1 | CqDICER NEG CTL | CqPTP1B NEG CTL | CqHES1 NEG CTL | Cqsi107 GAPDH | Cqsi124 GAPDH | Cqsi381 GAPDH | CqsiNEG GAPDH |
|---|---|---|---|---|---|---|---|---|---|---|---|---|
| MSC | Run1 | 40.00 | 40.00 | 31.86 | 32.07 | 34.41 | 30.33 | 32.89 | 31.50 | 27.57 | 22.49 | 26.83 |
| | Run2 | 40.00 | 40.00 | 31.55 | 30.71 | 35.07 | 29.56 | 32.29 | 30.53 | 27.88 | 22.42 | 26.45 |
| | Run3 | 40.00 | 40.00 | 30.98 | 31.11 | 33.80 | 31.21 | 32.29 | 30.27 | 27.69 | 22.29 | 26.25 |

| | Cord 11 | ΔCqsi107 DICER | ΔCqsi124 PTP1B | ΔCqsi381 HES1 | ΔCqDICER NEG CTL | ΔCqPTP1B NEG CTL | ΔCqsi381 NEG | ΔΔCqDICER | ΔΔCqPTP1B | ΔΔCqHES1 |
|---|---|---|---|---|---|---|---|---|---|---|
| MSC | Run1 | 8.50 | 4.29 | 9.58 | 7.58 | 2.76 | 6.06 | -0.92 | -1.53 | -3.52 |
| | Run2 | 9.47 | 3.67 | 8.29 | 8.62 | 1.68 | 5.84 | -0.85 | -1.99 | -2.45 |
| | Run3 | 9.73 | 3.29 | 8.82 | 7.55 | 3.52 | 6.04 | -2.18 | 0.23 | -2.78 |

| | Cord 5 | NTC | CqDICER | CqPTP1B | CqHES1 | CqDICER NEG CTL | CqPTP1B NEG CTL | CqHES1 NEG CTL | Cqsi107 GAPDH | Cqsi124 GAPDH | Cqsi381 GAPDH | CqsiNEG GAPDH |
|---|---|---|---|---|---|---|---|---|---|---|---|---|
| CC | Run1 | 39.58 | 29.79 | 26.02 | 36.66 | 34.03 | 28.27 | 38.31 | 25.92 | 24.01 | 24.04 | 25.90 |
| | Run2 | 40.00 | 30.28 | 26.36 | 36.50 | 34.21 | 29.07 | 38.88 | 25.95 | 24.32 | 24.16 | 25.83 |
| | Run3 | 40.00 | 30.33 | 26.77 | 36.58 | 34.48 | 29.56 | 38.54 | 26.11 | 24.09 | 24.27 | 24.90 |

| | Cord 5 | ΔCqsi107 DICER | ΔCqsi124 PTP1B | ΔCqsi381 HES1 | ΔCqDICER NEG CTL | ΔCq PTP1B NEG CTL | ΔCqsi381 NEG | ΔΔCqDICER | ΔΔCqPTP1B | ΔΔCq HES1 |
|---|---|---|---|---|---|---|---|---|---|---|
| CC | Run1 | 3.87 | 2.01 | 12.62 | 8.13 | 4.26 | 12.41 | 4.26 | 2.25 | -0.21 |
| | Run2 | 4.33 | 2.04 | 12.34 | 8.38 | 4.75 | 13.05 | 4.05 | 2.71 | 0.71 |
| | Run3 | 4.22 | 2.68 | 12.31 | 9.58 | 5.47 | 13.64 | 5.36 | 2.79 | 1.33 |

| | Cord 6 | NTC | CqDICER | CqPTP1B | CqHES1 | CqDICER NEG CTL | CqPTP1B NEG CTL | CqHES1 NEG CTL | Cqsi107 GAPDH | Cqsi124 GAPDH | Cqsi381 GAPDH | CqsiNEG GAPDH |
|---|---|---|---|---|---|---|---|---|---|---|---|---|
| CC | Run1 | 35.23 | 33.02 | 26.48 | 33.97 | 31.61 | 28.17 | 32.33 | 27.46 | 24.21 | 27.07 | 24.08 |
| | Run2 | 34.31 | 32.04 | 26.67 | 34.35 | 32.37 | 28.19 | 32.59 | 27.84 | 24.29 | 27.07 | 24.55 |
| | Run3 | 34.51 | 31.86 | 26.03 | 33.14 | 31.69 | 28.42 | 31.16 | 28.05 | 24.31 | 26.82 | 24.47 |

| | Cord 6 | ΔCqsi107 DICER | ΔCqsi124 PTP1B | ΔCqsi381 HES1 | ΔCqDICER NEG CTL | ΔCq PTP1B NEG CTL | ΔCqsi381 NEG | ΔΔCqDICER | ΔΔCqPTP1B | ΔΔCq HES1 |
|---|---|---|---|---|---|---|---|---|---|---|
| CC | Run1 | 5.56 | 2.27 | 6.90 | 7.53 | 3.96 | 8.25 | 1.97 | 1.69 | 1.35 |
| | Run2 | 4.20 | 2.38 | 7.28 | 7.82 | 3.90 | 8.04 | 3.62 | 1.52 | 0.76 |
| | Run3 | 3.81 | 1.72 | 6.32 | 7.22 | 4.11 | 6.69 | 3.41 | 2.39 | 0.37 |

| | Cord 11 | NTC | CqDICER | CqPTP1B | CqHES1 | CqDICER NEG CTL | CqPTP1B NEG CTL | CqHES1 NEG CTL | Cqsi107 GAPDH | Cqsi124 GAPDH | Cqsi381 GAPDH | CqsiNEG GAPDH |
|---|---|---|---|---|---|---|---|---|---|---|---|---|
| CC | Run1 | 36.32 | 31.70 | 25.69 | 30.42 | 32.90 | 27.70 | 29.07 | 26.82 | 24.41 | 27.96 | 25.97 |
| | Run2 | 36.74 | 32.08 | 25.29 | 29.92 | 32.10 | 28.36 | 29.89 | 26.04 | 24.79 | 27.49 | 25.84 |
| | Run3 | 35.93 | 32.65 | 25.73 | 30.12 | 32.30 | 27.81 | 29.14 | 26.26 | 24.85 | 27.03 | 25.90 |

| | Cord 11 | ΔCqsi107 DICER | ΔCqsi124 PTP1B | ΔCqsi381 HES1 | ΔCqDICER NEG CTL | ΔCq PTP1B NEG CTL | ΔCqsi381 NEG | ΔΔCqDICER | ΔΔCqPTP1B | ΔΔCq HES1 |
|---|---|---|---|---|---|---|---|---|---|---|
| CC | Run1 | 4.88 | 1.28 | 2.46 | 6.93 | 3.29 | 3.10 | 2.05 | 2.01 | 0.64 |
| | Run2 | 6.04 | 0.50 | 2.43 | 6.26 | 3.57 | 4.05 | 0.22 | 3.07 | 1.62 |
| | Run3 | 6.39 | 0.88 | 3.09 | 6.40 | 2.96 | 3.24 | 0.01 | 2.08 | 0.15 |

| | Cord 5 | NTC | CqDICER | CqPTP1B | CqHES1 | CqDICER NEG CTL | CqPTP1B NEG CTL | CqHES1 NEG CTL | Cqsi107 GAPDH | Cqsi124 GAPDH | Cqsi381 GAPDH | CqsiNEG GAPDH |
|---|---|---|---|---|---|---|---|---|---|---|---|---|
| RA-CC | Run1 | 40.00 | 28.68 | 31.80 | 25.64 | 28.55 | 23.42 | 28.02 | 20.40 | 27.71 | 17.57 | 19.82 |
| | Run2 | 40.00 | 28.27 | 32.12 | 25.44 | 29.55 | 23.45 | 27.86 | 20.52 | 27.17 | 17.67 | 20.07 |
| | Run3 | 40.00 | 28.39 | 31.80 | 25.71 | 28.95 | 23.42 | 28.22 | 20.46 | 27.99 | 17.52 | 19.88 |

| | Cord 5 | ΔCqsi107 DICER | ΔCqsi124 PTP1B | ΔCqsi381 HES1 | ΔCqDICER NEG CTL | ΔCq PTP1B NEG CTL | ΔCqsi381 NEG | ΔΔCqDICER | ΔΔCqPTP1B | ΔΔCq HES1 |
|---|---|---|---|---|---|---|---|---|---|---|
| CC-RA | Run1 | 8.28 | 4.09 | 8.07 | 8.73 | -4.29 | 8.20 | 0.45 | -8.38 | 0.13 |
| | Run2 | 7.75 | 4.95 | 7.77 | 9.48 | -3.72 | 7.79 | 1.73 | -8.67 | 0.02 |
| | Run3 | 7.93 | 3.81 | 8.19 | 9.07 | -4.57 | 8.34 | 1.14 | -8.38 | 0.15 |

| | Cord 6 | NTC | CqDICER | CqPTP1B | CqHES1 | CqDICER NEG CTL | CqPTP1B NEG CTL | CqHES1 NEG CTL | Cqsi107 GAPDH | Cqsi124 GAPDH | Cqsi381 GAPDH | CqsiNEG GAPDH |
|---|---|---|---|---|---|---|---|---|---|---|---|---|
| RA-CC | Run1 | 40.00 | 29.92 | 26.62 | 29.02 | 28.78 | 22.84 | 27.51 | 24.33 | 18.05 | 21.26 | 18.89 |
| | Run2 | 40.00 | 30.07 | 26.54 | 30.16 | 28.68 | 22.79 | 27.39 | 24.09 | 18.14 | 21.45 | 18.78 |
| | Run3 | 39.68 | 30.04 | 27.11 | 29.70 | 28.33 | 22.84 | 27.72 | 23.99 | 17.97 | 21.12 | 19.32 |

| | Cord 6 | ΔCqsi107 DICER | ΔCqsi124 PTP1B | ΔCqsi381 HES1 | ΔCqDICER NEG CTL | ΔCq PTP1B NEG CTL | ΔCqsi381 NEG | ΔΔCqDICER | ΔΔCqPTP1B | ΔΔCq HES1 |
|---|---|---|---|---|---|---|---|---|---|---|
| CC-RA | Run1 | 5.59 | 8.57 | 7.76 | 9.89 | 4.79 | 8.62 | 4.30 | -3.78 | 0.86 |
| | Run2 | 5.98 | 8.40 | 8.71 | 9.90 | 4.65 | 8.61 | 3.92 | -3.75 | -0.10 |
| | Run3 | 6.05 | 9.14 | 8.58 | 9.01 | 4.87 | 8.40 | 2.96 | -4.27 | -0.18 |

| | Cord 11 | NTC | CqDICER | CqPTP1B | CqHES1 | CqDICER NEG CTL | CqPTP1B NEG CTL | CqHES1 NEG CTL | Cqsi107 GAPDH | Cqsi124 GAPDH | Cqsi381 GAPDH | CqsiNEG GAPDH |
|---|---|---|---|---|---|---|---|---|---|---|---|---|
| RA-CC | Run1 | 40.00 | 27.07 | 25.97 | 26.39 | 26.71 | 23.27 | 27.69 | 15.77 | 15.49 | 16.02 | 15.59 |
| | Run2 | 40.00 | 27.77 | 25.84 | 26.24 | 27.02 | 23.34 | 27.12 | 15.87 | 15.79 | 16.05 | 15.68 |
| | Run3 | 40.00 | 27.12 | 25.89 | 27.06 | 28.01 | 23.39 | 27.18 | 15.93 | 15.61 | 16.00 | 15.64 |

| | Cord 11 | ΔCqsi107 DICER | ΔCqsi124 PTP1B | ΔCqsi381 HES1 | ΔCqDICER NEG CTL | ΔCq PTP1B NEG CTL | ΔCqsi381 NEG | ΔΔCqDICER | ΔΔCqPTP1B | ΔΔCq HES1 |
|---|---|---|---|---|---|---|---|---|---|---|
| CC-RA | Run1 | 11.30 | 10.48 | 10.37 | 11.12 | 7.78 | 12.10 | -0.18 | -2.70 | 1.73 |
| | Run2 | 11.90 | 10.05 | 10.19 | 11.34 | 7.55 | 11.44 | -0.56 | -2.50 | 1.25 |
| | Run3 | 11.19 | 10.28 | 11.06 | 12.37 | 7.78 | 11.54 | 1.18 | -2.50 | 0.48 |

**Neural Markers Post Transfection**

| | Cord 9 | NTC | Cqsi107 NES | Cqsi124 NES | Cqsi381 NES | CqsiNEG NES | Cqsi07 GAPDH | Cqsi124 GAPDH | Cqsi381 GAPDH | CqsiNEG GAPDH |
|---|---|---|---|---|---|---|---|---|---|---|
| MSC | Run1 | 37.72 | 36.32 | 34.88 | 40.00 | 34.12 | 23.64 | 24.41 | 26.54 | 26.92 |
| | Run2 | 36.90 | 36.99 | 34.10 | 40.00 | 34.57 | 23.66 | 24.22 | 26.04 | 27.00 |
| | Run3 | 37.16 | 36.50 | 34.63 | 40.00 | 34.09 | 24.02 | 24.55 | 26.31 | 27.18 |

| | Cord 9 | ΔCqsi107NES | ΔCqsi124 NES | ΔCqsi381 NES | ΔCqsiNEG NES | ΔΔCqsi107 NES | ΔΔCqsi124 NES | ΔΔCqsi381 NES |
|---|---|---|---|---|---|---|---|---|
| MSC | Run1 | 12.68 | 10.47 | 13.46 | 7.20 | -5.48 | -3.27 | -6.26 |
| | Run2 | 13.33 | 9.88 | 13.96 | 7.57 | -5.76 | -2.31 | -6.39 |
| | Run3 | 12.48 | 10.08 | 13.69 | 6.91 | -5.57 | -3.17 | -6.78 |

| | Cord 9 | NTC | Cqsi107 TUBB3 | Cqsi124 TUBB3 | Cqsi381 TUBB3 | CqsiNEG TUBB3 | Cqsi07 GAPDH | Cqsi124 GAPDH | Cqsi381 GAPDH | CqsiNEG GAPDH |
|---|---|---|---|---|---|---|---|---|---|---|
| MSC | Run1 | 37.72 | 32.07 | 32.91 | 30.98 | 34.69 | 23.64 | 24.41 | 26.54 | 26.92 |
| | Run2 | 36.90 | 31.92 | 32.71 | 31.37 | 34.08 | 23.66 | 24.22 | 26.04 | 27.00 |
| | Run3 | 37.16 | 32.33 | 32.85 | 31.12 | 34.25 | 24.02 | 24.55 | 26.31 | 27.18 |

| | Cord 9 | ΔCqsi107 TUBB3 | ΔCqsi124 TUBB3 | ΔCqsi381 TUBB3 | ΔCqsiNEG TUBB3 | ΔΔCqsi107 TUBB3 | ΔΔCqsi124 TUBB3 | ΔΔCqsi381 TUBB3 |
|---|---|---|---|---|---|---|---|---|
| MSC | Run1 | 8.43 | 8.50 | 4.44 | 7.77 | -0.66 | -0.73 | 3.33 |
| | Run2 | 8.26 | 8.49 | 5.33 | 7.08 | -1.18 | -1.41 | 1.75 |
| | Run3 | 8.31 | 8.30 | 4.81 | 7.07 | -1.24 | -1.23 | 2.26 |

| | Cord 9 | NTC | Cqsi107 ND1 | Cqsi124 ND1 | Cqsi381 ND1 | CqsiNEG ND1 | Cqsi07 GAPDH | Cqsi124 GAPDH | Cqsi381 GAPDH | CqsiNEG GAPDH |
|---|---|---|---|---|---|---|---|---|---|---|
| MSC | Run1 | 40.00 | 26.66 | 29.25 | 27.86 | 28.75 | 23.51 | 26.17 | 26.30 | 27.45 |
| | Run2 | 40.00 | 26.84 | 29.33 | 27.56 | 29.42 | 23.64 | 26.23 | 26.06 | 27.58 |
| | Run3 | 40.00 | 26.76 | 28.88 | 28.24 | 29.38 | 23.29 | 25.72 | 26.21 | 27.57 |

| | Cord 9 | ΔCqsi107 ND1 | ΔCqsi124 ND1 | ΔCqsi381 ND1 | ΔCqsiNEG ND1 | ΔΔCqsi107 ND1 | ΔΔCqsi124 ND1 | ΔΔCqsi381 ND1 |
|---|---|---|---|---|---|---|---|---|
| MSC | Run1 | 3.15 | 3.08 | 1.56 | 1.30 | -1.85 | -1.78 | -0.26 |
| | Run2 | 3.20 | 2.10 | 1.50 | 1.84 | -1.36 | -1.26 | 0.34 |
| | Run3 | 3.47 | 3.16 | 2.03 | 1.81 | -1.66 | -1.35 | -0.22 |

| | Cord 9 | NTC | Cqsi107 MAP2 | Cqsi124 MAP2 | Cqsi381 MAP2 | CqsiNEG MAP2 | Cqsi07 GAPDH | Cqsi124 GAPDH | Cqsi381 GAPDH | CqsiNEG GAPDH |
|---|---|---|---|---|---|---|---|---|---|---|
| MSC | Run1 | 37.72 | 40.00 | 40.00 | 37.78 | 39.89 | 23.64 | 24.41 | 26.54 | 26.92 |
| | Run2 | 36.90 | 39.49 | 40.00 | 40.00 | 40.00 | 23.66 | 24.22 | 26.04 | 27.00 |
| | Run3 | 37.16 | 40.00 | 40.00 | 40.00 | 40.00 | 24.02 | 24.55 | 26.31 | 27.18 |

| | Cord 9 | ΔCqsi107 MAP2 | ΔCqsi124 MAP2 | ΔCqsi381 MAP2 | ΔCqsiNEG MAP2 | ΔΔCqsi107 MAP2 | ΔΔCqsi124 MAP2 | ΔΔCqsi381 MAP2 |
|---|---|---|---|---|---|---|---|---|
| MSC | Run1 | 16.36 | 15.59 | 11.24 | 12.97 | -3.39 | -2.62 | 1.73 |
| | Run2 | 15.83 | 15.78 | 13.96 | 13.00 | -2.83 | -2.78 | -0.96 |
| | Run3 | 15.98 | 15.45 | 13.69 | 12.82 | -3.16 | -2.63 | -0.87 |

| | Cord 9 | NTC | Cqsi107 NEU | Cqsi124 NEU | Cqsi381 NEU | CqsiNEG NEU | Cqsi07 GAPDH | Cqsi124 GAPDH | Cqsi381 GAPDH | CqsiNEG GAPDH |
|---|---|---|---|---|---|---|---|---|---|---|
| MSC | Run1 | 37.72 | 40.00 | 40.00 | 40.00 | 39.39 | 23.64 | 24.41 | 26.54 | 26.92 |
| | Run2 | 36.90 | 40.00 | 40.00 | 40.00 | 40.00 | 23.66 | 24.22 | 26.04 | 27.00 |
| | Run3 | 37.16 | 40.00 | 40.00 | 40.00 | 40.00 | 24.02 | 24.55 | 26.31 | 27.18 |

| | Cord 9 | ΔCqsi107 NEU | ΔCqsi124 NEU | ΔCqsi381 NEU | ΔCqsiNEG NEU | ΔΔCqsi107 NEU | ΔΔCqsi124 NEU | ΔΔCqsi381 NEU |
|---|---|---|---|---|---|---|---|---|
| MSC | Run1 | 16.36 | 15.59 | 13.46 | 12.47 | -3.89 | -3.12 | -0.99 |
| | Run2 | 16.34 | 15.78 | 13.96 | 13.00 | -3.34 | -2.78 | -0.96 |
| | Run3 | 15.98 | 15.45 | 13.69 | 12.82 | -3.16 | -2.63 | -0.87 |

| | Cord 11 | NTC | Cqsi107 NES | Cqsi124 NES | Cqsi381 NES | CqsiNEG NES | Cqsi07 GAPDH | Cqsi124 GAPDH | Cqsi381 GAPDH | CqsiNEG GAPDH |
|---|---|---|---|---|---|---|---|---|---|---|
| MSC | Run1 | 40.00 | 40.00 | 32.97 | 40.00 | 33.58 | 28.76 | 23.48 | 28.06 | 27.87 |
| | Run2 | 40.00 | 40.00 | 33.50 | 40.00 | 34.02 | 29.49 | 23.78 | 27.84 | 27.12 |
| | Run3 | 40.00 | 40.00 | 33.33 | 40.00 | 33.97 | 27.91 | 23.60 | 27.95 | 27.34 |

| | Cord 11 | ΔCqsi107NES | ΔCqsi124 NES | ΔCqsi381 NES | ΔCqsiNEG NES | ΔΔCqsi107 NES | ΔΔCqsi124 NES | ΔΔCqsi381 NES |
|---|---|---|---|---|---|---|---|---|
| MSC | Run1 | 11.24 | 9.49 | 11.94 | 5.71 | -5.53 | -3.78 | -6.23 |
| | Run2 | 10.51 | 9.72 | 12.16 | 6.90 | -3.61 | -2.82 | -5.26 |
| | Run3 | 12.09 | 9.73 | 12.05 | 6.63 | -5.46 | -3.10 | -5.42 |

| | Cord 11 | NTC | Cqsi107 TUBB3 | Cqsi124 TUBB3 | Cqsi381 TUBB3 | CqsiNEG TUBB3 | Cqsi07 GAPDH | Cqsi124 GAPDH | Cqsi381 GAPDH | CqsiNEG GAPDH |
|---|---|---|---|---|---|---|---|---|---|---|
| MSC | Run1 | 40.00 | 35.84 | 31.37 | 28.88 | 32.34 | 28.76 | 23.48 | 28.06 | 27.87 |
| | Run2 | 40.00 | 35.22 | 31.57 | 29.52 | 33.43 | 29.49 | 23.78 | 27.84 | 27.12 |
| | Run3 | 40.00 | 35.03 | 31.99 | 28.85 | 33.10 | 27.91 | 23.60 | 27.95 | 27.34 |

| | Cord 11 | ΔCqsi107 TUBB3 | ΔCqsi124 TUBB3 | ΔCqsi381 TUBB3 | ΔCqsiNEG TUBB3 | ΔΔCqsi107 TUBB3 | ΔΔCqsi124 TUBB3 | ΔΔCqsi381 TUBB3 |
|---|---|---|---|---|---|---|---|---|
| MSC | Run1 | 7.08 | 7.89 | 0.82 | 4.47 | -2.61 | -3.42 | 3.65 |
| | Run2 | 5.73 | 7.79 | 1.68 | 6.31 | 0.58 | -1.48 | 4.63 |
| | Run3 | 7.12 | 8.39 | 0.90 | 5.76 | -1.36 | -2.63 | 4.86 |

| | Cord 11 | NTC | Cqsi107 ND1 | Cqsi124 ND1 | Cqsi381 ND1 | CqsiNEG ND1 | Cqsi07 GAPDH | Cqsi124 GAPDH | Cqsi381 GAPDH | CqsiNEG GAPDH |
|---|---|---|---|---|---|---|---|---|---|---|
| MSC | Run1 | 40.00 | 19.33 | 19.42 | 19.47 | 18.93 | 15.77 | 15.49 | 16.02 | 15.59 |
| | Run2 | 40.00 | 19.05 | 19.70 | 19.32 | 19.01 | 15.87 | 15.79 | 16.05 | 15.68 |
| | Run3 | 40.00 | 19.53 | 19.27 | 19.22 | 18.73 | 15.93 | 15.61 | 16.00 | 15.64 |

| | Cord 11 | ΔCqsi107 ND1 | ΔCqsi124 ND1 | ΔCqsi381 ND1 | ΔCqsiNEG ND1 | ΔΔCqsi107 ND1 | ΔΔCqsi124 ND1 | ΔΔCqsi381 ND1 |
|---|---|---|---|---|---|---|---|---|
| MSC | Run1 | 3.56 | 3.93 | 3.45 | 3.34 | -0.22 | -0.59 | -0.11 |
| | Run2 | 3.18 | 3.91 | 3.27 | 3.33 | 0.15 | -0.58 | 0.06 |
| | Run3 | 3.60 | 3.66 | 3.22 | 3.09 | -0.51 | -0.57 | -0.13 |

| | Cord 11 | NTC | Cqsi107 MAP2 | Cqsi124 MAP2 | Cqsi381 MAP2 | CqsiNEG MAP2 | Cqsi07 GAPDH | Cqsi124 GAPDH | Cqsi381 GAPDH | CqsiNEG GAPDH |
|---|---|---|---|---|---|---|---|---|---|---|
| MSC | Run1 | 40.00 | 40.00 | 40.00 | 40.00 | 40.00 | 23.64 | 24.41 | 26.54 | 26.92 |
| | Run2 | 40.00 | 40.00 | 40.00 | 40.00 | 40.00 | 23.66 | 24.22 | 26.04 | 27.00 |
| | Run3 | 40.00 | 40.00 | 40.00 | 40.00 | 40.00 | 24.02 | 24.55 | 26.31 | 27.18 |

| | Cord 11 | ΔCqsi107 MAP2 | ΔCqsi124 MAP2 | ΔCqsi381 MAP2 | ΔCqsiNEG MAP2 | ΔΔCqsi107 MAP2 | ΔΔCqsi124 MAP2 | ΔΔCqsi381 MAP2 |
|---|---|---|---|---|---|---|---|---|
| MSC | Run1 | 16.36 | 15.59 | 13.46 | 13.08 | -3.28 | -2.51 | -0.38 |
| | Run2 | 16.34 | 15.78 | 13.96 | 13.00 | -3.34 | -2.78 | -0.96 |
| | Run3 | 15.98 | 15.45 | 13.69 | 12.82 | -3.16 | -2.63 | -0.87 |

| | Cord 11 | NTC | Cqsi107 NEU | Cqsi124 NEU | Cqsi381 NEU | CqsiNEG NEU | Cqsi07 GAPDH | Cqsi124 GAPDH | Cqsi381 GAPDH | CqsiNEG GAPDH |
|---|---|---|---|---|---|---|---|---|---|---|
| MSC | Run1 | 40.00 | 40.00 | 40.00 | 40.00 | 40.00 | 23.64 | 24.41 | 26.54 | 26.92 |
| | Run2 | 40.00 | 40.00 | 40.00 | 40.00 | 40.00 | 23.66 | 24.22 | 26.04 | 27.00 |
| | Run3 | 40.00 | 40.00 | 40.00 | 40.00 | 40.00 | 24.02 | 24.55 | 26.31 | 27.18 |

| | Cord 11 | ΔCqsi107 NEU | ΔCqsi124 NEU | ΔCqsi381 NEU | ΔCqsiNEG NEU | ΔΔCqsi107 NEU | ΔΔCqsi124 NEU | ΔΔCqsi381 NEU |
|---|---|---|---|---|---|---|---|---|
| MSC | Run1 | 16.36 | 15.59 | 13.46 | 13.08 | -3.28 | -2.51 | -0.38 |
| | Run2 | 16.34 | 15.78 | 13.96 | 13.00 | -3.34 | -2.78 | -0.96 |
| | Run3 | 15.98 | 15.45 | 13.69 | 12.82 | -3.16 | -2.63 | -0.87 |

| | Cord 5 | NTC | Cqsi107 NES | Cqsi124 NES | Cqsi381 NES | CqsiNEG NES | Cqsi07 GAPDH | Cqsi124 GAPDH | Cqsi381 GAPDH | CqsiNEG GAPDH |
|---|---|---|---|---|---|---|---|---|---|---|
| CC | Run1 | 33.80 | 31.59 | 29.28 | 29.38 | 29.90 | 27.68 | 24.04 | 24.62 | 26.29 |
| | Run2 | 33.62 | 30.89 | 28.98 | 28.85 | 29.79 | 27.44 | 23.71 | 24.61 | 26.59 |
| | Run3 | 33.21 | 30.36 | 28.17 | 29.19 | 31.02 | 27.72 | 23.70 | 24.36 | 26.35 |

| | Cord 5 | ΔCqsi107NES | ΔCqsi124 NES | ΔCqsi381 NES | ΔCqsiNEG NES | ddCqsi107 NES | ddCqsi124 NES | ΔΔCqsi381 NES |
|---|---|---|---|---|---|---|---|---|
| CC | Run1 | 3.91 | 5.24 | 4.76 | 3.61 | -0.30 | -1.63 | -1.15 |
| | Run2 | 3.45 | 5.27 | 4.24 | 3.20 | -0.25 | -2.07 | -1.04 |
| | Run3 | 2.64 | 4.47 | 4.83 | 4.67 | 2.03 | 0.20 | -0.16 |

| | Cord 5 | NTC | Cqsi107 TUBB3 | Cqsi124 TUBB3 | Cqsi381 TUBB3 | CqsiNEG TUBB3 | Cqsi07 GAPDH | Cqsi124 GAPDH | Cqsi381 GAPDH | CqsiNEG GAPDH |
|---|---|---|---|---|---|---|---|---|---|---|
| CC | Run1 | 33.80 | 28.92 | 27.17 | 26.93 | 28.20 | 27.68 | 24.04 | 24.62 | 26.29 |
| | Run2 | 33.62 | 28.81 | 27.18 | 27.12 | 27.91 | 27.44 | 23.71 | 24.61 | 26.59 |
| | Run3 | 33.21 | 28.45 | 27.06 | 27.08 | 28.31 | 27.72 | 23.70 | 24.36 | 26.35 |

| | Cord 5 | ΔCqsi107 TUBB3 | ΔCqsi124 TUBB3 | ΔCqsi381 TUBB3 | ΔCqsiNEG TUBB3 | ΔΔCqsi107 TUBB3 | ΔΔCqsi124 TUBB3 | ΔΔCqsi381 TUBB3 |
|---|---|---|---|---|---|---|---|---|
| CC | Run1 | 1.24 | 3.13 | 2.31 | 1.91 | 0.67 | -1.22 | -0.40 |
| | Run2 | 1.37 | 3.47 | 2.51 | 1.32 | -0.05 | -2.15 | -1.19 |
| | Run3 | 0.73 | 3.36 | 2.72 | 1.96 | 1.23 | -1.40 | -0.76 |

| | Cord 5 | NTC | Cqsi107 ND1 | Cqsi124 ND1 | Cqsi381 ND1 | CqsiNEG ND1 | Cqsi07 GAPDH | Cqsi124 GAPDH | Cqsi381 GAPDH | CqsiNEG GAPDH |
|---|---|---|---|---|---|---|---|---|---|---|
| CC | Run1 | 31.87 | 29.10 | 26.40 | 30.61 | 28.01 | 23.11 | 21.62 | 24.59 | 24.82 |
| | Run2 | 31.97 | 27.71 | 25.87 | 30.13 | 28.21 | 22.58 | 21.91 | 24.50 | 24.61 |
| | Run3 | 31.93 | 28.38 | 24.60 | 30.70 | 24.28 | 22.63 | 21.82 | 24.70 | 26.43 |

| | Cord 5 | ΔCqsi107 ND1 | ΔCqsi124 ND1 | ΔCqsi381 ND1 | ΔCqsiNEG ND1 | ΔΔCqsi107 ND1 | ΔΔCqsi124 ND1 | ΔΔCqsi381 ND1 |
|---|---|---|---|---|---|---|---|---|
| CC | Run1 | 5.99 | 4.78 | 6.02 | 3.19 | -2.80 | -1.59 | -2.83 |
| | Run2 | 5.13 | 3.96 | 5.63 | 3.60 | -1.53 | -0.36 | -2.03 |
| | Run3 | 5.75 | 2.78 | 6.00 | -2.15 | -7.90 | -4.93 | -8.15 |

| | Cord 5 | NTC | Cqsi107 MAP2 | Cqsi124 MAP2 | Cqsi381 MAP2 | CqsiNEG MAP2 | Cqsi07 GAPDH | Cqsi124 GAPDH | Cqsi381 GAPDH | CqsiNEG GAPDH |
|---|---|---|---|---|---|---|---|---|---|---|
| CC | Run1 | 33.80 | 29.78 | 27.07 | 28.56 | 29.71 | 27.68 | 24.04 | 24.62 | 26.29 |
| | Run2 | 33.62 | 29.87 | 27.12 | 27.78 | 29.04 | 27.44 | 23.71 | 24.61 | 26.59 |
| | Run3 | 33.21 | 29.81 | 26.76 | 27.76 | 29.81 | 27.72 | 23.70 | 24.36 | 26.35 |

| | Cord 5 | ΔCqsi107 MAP2 | ΔCqsi124 MAP2 | ΔCqsi381 MAP2 | ΔCqsiNEG MAP2 | ΔΔCqsi107 MAP2 | ΔΔCqsi124 MAP2 | ΔΔCqsi381 MAP2 |
|---|---|---|---|---|---|---|---|---|
| CC | Run1 | 2.10 | 3.03 | 3.94 | 3.42 | 1.32 | 0.39 | -0.52 |
| | Run2 | 2.43 | 3.41 | 3.17 | 2.45 | 0.02 | -0.96 | -0.72 |
| | Run3 | 2.09 | 3.06 | 3.40 | 3.46 | 1.37 | 0.40 | 0.06 |

| | Cord 5 | NTC | Cqsi107 NEU | Cqsi124 NEU | Cqsi381 NEU | CqsiNEG NEU | Cqsi07 GAPDH | Cqsi124 GAPDH | Cqsi381 GAPDH | CqsiNEG GAPDH |
|---|---|---|---|---|---|---|---|---|---|---|
| CC | Run1 | 40,00 | 40.00 | 40.00 | 40.00 | 40.00 | 27.68 | 24.04 | 24.62 | 26.29 |
| | Run2 | 40.00 | 40.00 | 40.00 | 40.00 | 40.00 | 27.44 | 23.71 | 24.61 | 26.59 |
| | Run3 | 40.00 | 40.00 | 40.00 | 40.00 | 40.00 | 27.72 | 23.70 | 24.36 | 26.35 |

| | Cord 5 | ΔCqsi107 NEU | ΔCqsi124 NEU | ΔCqsi381 NEU | ΔCqsiNEG NEU | ΔΔCqsi107 NEU | ΔΔCqsi124 NEU | ΔΔCqsi381 NEU |
|---|---|---|---|---|---|---|---|---|
| CC | Run1 | 12.32 | 15.96 | 15.38 | 13.71 | 1.39 | -2.25 | -1.67 |
| | Run2 | 12.56 | 16.29 | 15.39 | 13.41 | 0.85 | -2.88 | -1.98 |
| | Run3 | 12.28 | 16.30 | 15.64 | 13.65 | 1.37 | -2.65 | -1.99 |

| | Cord 6 | NTC | Cqsi107 NES | Cqsi124 NES | Cqsi381 NES | CqsiNEG NES | Cqsi07 GAPDH | Cqsi124 GAPDH | Cqsi381 GAPDH | CqsiNEG GAPDH |
|---|---|---|---|---|---|---|---|---|---|---|
| CC | Run1 | 32.95 | 31.83 | 30.59 | 30.03 | 30.25 | 28.82 | 26.06 | 27.23 | 26.54 |
| | Run2 | 32.83 | 32.38 | 30.87 | 29.72 | 30.97 | 27.80 | 25.87 | 26.73 | 26.09 |
| | Run3 | 32.85 | 32.49 | 30.34 | 29.68 | 31.02 | 28.24 | 26.26 | 26.39 | 27.24 |

| | Cord 6 | ΔCqsi107NES | ΔCqsi124 NES | ΔCqsi381 NES | ΔCqsiNEG NES | ΔΔCqsi107 NES | ΔΔCqsi124 NES | ΔΔCqsi381 NES |
|---|---|---|---|---|---|---|---|---|
| CC | Run1 | 3.01 | 4.53 | 2.80 | 3.71 | 0.70 | -0.82 | 0.91 |
| | Run2 | 4.58 | 5.00 | 2.99 | 4.88 | 0.30 | -0.12 | 1.89 |
| | Run3 | 4.25 | 4.08 | 3.29 | 3.78 | -0.47 | -0.30 | 0.49 |

| | Cord 6 | NTC | Cqsi107 TUBB3 | Cqsi124 TUBB3 | Cqsi381 TUBB3 | CqsiNEG TUBB3 | Cqsi07 GAPDH | Cqsi124 GAPDH | Cqsi381 GAPDH | CqsiNEG GAPDH |
|---|---|---|---|---|---|---|---|---|---|---|
| CC | Run1 | 32.95 | 28.75 | 28.79 | 28.39 | 28.19 | 28.82 | 26.06 | 27.23 | 26.54 |
| | Run2 | 32.83 | 28.35 | 28.46 | 28.03 | 28.81 | 27.80 | 25.87 | 26.73 | 26.09 |
| | Run3 | 32.85 | 28.42 | 27.76 | 28.18 | 29.29 | 28.24 | 26.26 | 26.39 | 27.24 |

| | Cord 6 | ΔCqsi107 TUBB3 | ΔCqsi124 TUBB3 | ΔCqsi381 TUBB3 | ΔCqsiNEG TUBB3 | ΔΔCqsi107 TUBB3 | ΔΔCqsi124 TUBB3 | ΔΔCqsi381 TUBB3 |
|---|---|---|---|---|---|---|---|---|
| CC | Run1 | -0.07 | 2.73 | 1.16 | 1.65 | 1.72 | -1.08 | 0.49 |
| | Run2 | 0.55 | 2.59 | 1.30 | 2.72 | 2.17 | 0.13 | 1.42 |
| | Run3 | 0.18 | 1.50 | 1.79 | 2.05 | 1.87 | 0.55 | 0.26 |

| | Cord 6 | NTC | Cqsi107 ND1 | Cqsi124 ND1 | Cqsi381 ND1 | CqsiNEG ND1 | Cqsi07 GAPDH | Cqsi124 GAPDH | Cqsi381 GAPDH | CqsiNEG GAPDH |
|---|---|---|---|---|---|---|---|---|---|---|
| CC | Run1 | 31.87 | 28.08 | 30.33 | 30.64 | 30.14 | 23.16 | 25.63 | 25.17 | 26.78 |
| | Run2 | 31.97 | 28.76 | 30.09 | 30.40 | 30.57 | 23.09 | 25.71 | 24.94 | 26.80 |
| | Run3 | 31.93 | 28.91 | 31.12 | 30.57 | 29.52 | 23.08 | 25.59 | 25.06 | 26.80 |

| | Cord 6 | ΔCqsi107 ND1 | ΔCqsi124 ND1 | ΔCqsi381 ND1 | ΔCqsiNEG ND1 | ΔΔCqsi107 ND1 | ΔΔCqsi124 ND1 | ΔΔCqsi381 ND1 |
|---|---|---|---|---|---|---|---|---|
| CC | Run1 | 4.92 | 4.70 | 5.47 | 3.36 | -1.56 | -1.34 | -2.11 |
| | Run2 | 5.67 | 4.38 | 5.46 | 3.77 | -1.90 | -0.61 | -1.69 |
| | Run3 | 5.83 | 5.53 | 5.51 | 2.72 | -3.11 | -2.81 | -2.79 |

| | Cord 6 | NTC | Cqsi107 MAP2 | Cqsi124 MAP2 | Cqsi381 MAP2 | CqsiNEG MAP2 | Cqsi07 GAPDH | Cqsi124 GAPDH | Cqsi381 GAPDH | CqsiNEG GAPDH |
|---|---|---|---|---|---|---|---|---|---|---|
| CC | Run1 | 32.95 | 29.33 | 28.94 | 28.93 | 29.71 | 28.82 | 26.06 | 27.23 | 26.54 |
| | Run2 | 32.83 | 30.25 | 29.02 | 29.26 | 29.90 | 27.80 | 25.87 | 26.73 | 26.09 |
| | Run3 | 32.85 | 30.21 | 29.19 | 28.93 | 29.79 | 28.24 | 26.26 | 26.39 | 27.24 |

| | Cord 6 | ΔCqsi107 MAP2 | ΔCqsi124 MAP2 | ΔCqsi381 MAP2 | ΔCqsiNEG MAP2 | ΔΔCqsi107 MAP2 | ΔΔCqsi124 MAP2 | ΔΔCqsi381 MAP2 |
|---|---|---|---|---|---|---|---|---|
| CC | Run1 | 0.51 | 2.88 | 1.70 | 3.17 | 2.66 | 0.29 | 1.47 |
| | Run2 | 2.45 | 3.15 | 2.53 | 3.81 | 1.36 | 0.66 | 1.28 |
| | Run3 | 1.97 | 2.93 | 2.54 | 2.55 | 0.58 | -0.38 | 0.01 |

| | Cord 6 | NTC | Cqsi107 NEU | Cqsi124 NEU | Cqsi381 NEU | CqsiNEG NEU | Cqsi07 GAPDH | Cqsi124 GAPDH | Cqsi381 GAPDH | CqsiNEG GAPDH |
|---|---|---|---|---|---|---|---|---|---|---|
| CC | Run1 | 32.95 | 40.00 | 40.00 | 40.00 | 30.11 | 28.82 | 26.06 | 27.23 | 26.54 |
| | Run2 | 32.83 | 40.00 | 40.00 | 40.00 | 30.29 | 27.80 | 25.87 | 26.73 | 26.09 |
| | Run3 | 32.85 | 40.00 | 40.00 | 40.00 | 29.91 | 28.24 | 26.26 | 26.39 | 27.24 |

| | Cord 6 | ΔCqsi107 NEU | ΔCqsi124 NEU | ΔCqsi381 NEU | ΔCqsiNEG NEU | ΔΔCqsi107 NEU | ΔΔCqsi124 NEU | ΔΔCqsi381 NEU |
|---|---|---|---|---|---|---|---|---|
| CC | Run1 | 11.18 | 13.94 | 12.77 | 3.57 | -7.61 | -10.37 | -9.20 |
| | Run2 | 12.20 | 14.13 | 13.27 | 4.20 | -8.00 | -9.93 | -9.07 |
| | Run3 | 11.76 | 13.74 | 13.61 | 2.67 | -9.09 | -11.07 | -10.94 |

| | Cord 13 | NTC | Cqsi107 NES | Cqsi124 NES | Cqsi381 NES | CqsiNEG NES | Cqsi07 GAPDH | Cqsi124 GAPDH | Cqsi381 GAPDH | CqsiNEG GAPDH |
|---|---|---|---|---|---|---|---|---|---|---|
| CC | Run1 | 40.00 | 35.91 | 33.09 | 34.10 | 33.58 | 28.76 | 23.48 | 28.06 | 29.03 |
| | Run2 | 40.00 | 36.49 | 33.50 | 33.83 | 32.91 | 29.49 | 23.78 | 27.84 | 28.81 |
| | Run3 | 40.00 | 36.73 | 33.18 | 33.89 | 33.11 | 28.91 | 23.60 | 27.95 | 28.90 |

| | Cord 13 | ΔCqsi107NES | ΔCqsi124 NES | ΔCqsi381 NES | ΔCqsiNEG NES | ΔΔCqsi107 NES | ΔΔCqsi124 NES | ΔΔCqsi381 NES |
|---|---|---|---|---|---|---|---|---|
| CC | Run1 | 7.15 | 9.61 | 6.04 | 4.55 | -2.60 | -5.06 | -1.49 |
| | Run2 | 7.00 | 9.72 | 5.99 | 4.10 | -2.90 | -5.62 | -1.89 |
| | Run3 | 7.82 | 9.58 | 5.94 | 4.21 | -3.61 | -5.37 | -1.73 |

| | Cord 13 | NTC | Cqsi107 TUBB3 | Cqsi124 TUBB3 | Cqsi381 TUBB3 | CqsiNEG TUBB3 | Cqsi07 GAPDH | Cqsi124 GAPDH | Cqsi381 GAPDH | CqsiNEG GAPDH |
|---|---|---|---|---|---|---|---|---|---|---|
| CC | Run1 | 40.00 | 32.21 | 31.37 | 28.88 | 32.34 | 28.76 | 23.48 | 28.06 | 29.03 |
| | Run2 | 40.00 | 33.02 | 31.57 | 29.52 | 33.43 | 29.49 | 23.78 | 27.84 | 28.81 |
| | Run3 | 40.00 | 32.61 | 31.99 | 28.85 | 32.80 | 28.91 | 23.60 | 27.95 | 28.90 |

| | Cord 13 | ΔCqsi107 TUBB3 | ΔCqsi124 TUBB3 | ΔCqsi381 TUBB3 | ΔCqsiNEG TUBB3 | ΔΔCqsi107 TUBB3 | ΔΔCqsi124 TUBB3 | ΔΔCqsi381 TUBB3 |
|---|---|---|---|---|---|---|---|---|
| CC | Run1 | 3.45 | 7.89 | 0.82 | 3.31 | -0.14 | -4.58 | 2.49 |
| | Run2 | 3.53 | 7.79 | 1.68 | 4.62 | 1.09 | -3.17 | 2.94 |
| | Run3 | 3.70 | 8.39 | 0.90 | 3.90 | 0.20 | -4.49 | 3.00 |

| | Cord 13 | NTC | Cqsi107 ND1 | Cqsi124 ND1 | Cqsi381 ND1 | CqsiNEG ND1 | Cqsi07 GAPDH | Cqsi124 GAPDH | Cqsi381 GAPDH | CqsiNEG GAPDH |
|---|---|---|---|---|---|---|---|---|---|---|
| CC | Run1 | 39.61 | 40.00 | 35.55 | 40.00 | 36.06 | 29.01 | 25.31 | 30.17 | 27.10 |
| | Run2 | 39.67 | 40.00 | 35.04 | 40.00 | 36.68 | 29.41 | 24.80 | 29.46 | 27.12 |
| | Run3 | 40.00 | 40.00 | 35.70 | 40.00 | 36.33 | 29.84 | 24.82 | 30.41 | 26.89 |

| | Cord 13 | ΔCqsi107 ND1 | ΔCqsi124 ND1 | ΔCqsi381 ND1 | ΔCqsiNEG ND1 | ΔΔCqsi107 ND1 | ΔΔCqsi124 ND1 | ΔΔCqsi381 ND1 |
|---|---|---|---|---|---|---|---|---|
| CC | Run1 | 10.99 | 10.24 | 9.83 | 8.96 | -2.03 | -1.28 | -0.87 |
| | Run2 | 10.59 | 10.24 | 10.54 | 9.56 | -1.03 | -0.68 | -0.98 |
| | Run3 | 10.16 | 10.88 | 9.59 | 9.44 | -0.72 | -1.44 | -0.15 |

| | Cord 13 | NTC | Cqsi107 MAP2 | Cqsi124 MAP2 | Cqsi381 MAP2 | CqsiNEG MAP2 | Cqsi07 GAPDH | Cqsi124 GAPDH | Cqsi381 GAPDH | CqsiNEG GAPDH |
|---|---|---|---|---|---|---|---|---|---|---|
| CC | Run1 | 40.00 | 36.16 | 32.40 | 34.40 | 31.41 | 28.76 | 23.48 | 28.06 | 29.03 |
| | Run2 | 40.00 | 36.21 | 32.71 | 34.02 | 32.02 | 29.49 | 23.78 | 27.84 | 28.81 |
| | Run3 | 40.00 | 36.90 | 32.36 | 34.13 | 31.54 | 28.91 | 23.60 | 27.95 | 28.90 |

| | Cord 13 | ΔCqsi107 MAP2 | ΔCqsi124 MAP2 | ΔCqsi381 MAP2 | ΔCqsiNEG MAP2 | ΔΔCqsi107 MAP2 | ΔΔCqsi124 MAP2 | ΔΔCqsi381 MAP2 |
|---|---|---|---|---|---|---|---|---|
| CC | Run1 | 7.40 | 8.92 | 6.34 | 2.38 | -5.02 | -6.54 | -3.96 |
| | Run2 | 6.72 | 8.93 | 6.18 | 3.21 | -3.51 | -5.72 | -2.97 |
| | Run3 | 7.99 | 8.76 | 6.18 | 2.64 | -5.35 | -6.12 | -3.54 |

| | Cord 13 | NTC | Cqsi107 NEU | Cqsi124 NEU | Cqsi381 NEU | CqsiNEG NEU | Cqsi07 GAPDH | Cqsi124 GAPDH | Cqsi381 GAPDH | CqsiNEG GAPDH |
|---|---|---|---|---|---|---|---|---|---|---|
| CC | Run1 | 40.00 | 30.18 | 32.60 | 30.22 | 31.25 | 28.76 | 23.48 | 28.06 | 29.03 |
| | Run2 | 40.00 | 30.70 | 32.31 | 30.71 | 31.48 | 29.49 | 23.78 | 27.84 | 28.81 |
| | Run3 | 40.00 | 30.63 | 32.53 | 30.54 | 30.09 | 28.91 | 23.60 | 27.95 | 28.90 |

| | Cord 13 | ΔCqsi107 NEU | ΔCqsi124 NEU | ΔCqsi381 NEU | ΔCqsiNEG NEU | ΔΔCqsi107 NEU | ΔΔCqsi124 NEU | ΔΔCqsi381 NEU |
|---|---|---|---|---|---|---|---|---|
| CC | Run1 | 1.42 | 9.12 | 2.16 | 2.22 | 0.80 | -6.90 | 0.06 |
| | Run2 | 1.21 | 8.53 | 2.87 | 2.67 | 1.46 | -5.86 | -0.20 |
| | Run3 | 1.72 | 8.93 | 2.59 | 1.19 | -0.53 | -7.74 | -1.40 |

| | Cord 5 | NTC | Cqsi107 NES | Cqsi124 NES | Cqsi381 NES | CqsiNEG NES | Cqsi07 GAPDH | Cqsi124 GAPDH | Cqsi381 GAPDH | CqsiNEG GAPDH |
|---|---|---|---|---|---|---|---|---|---|---|
| CC-RA | Run1 | 40.00 | 28.98 | 27.89 | 24.03 | 26.16 | 22.82 | 22.40 | 18.68 | 19.92 |
| | Run2 | 40.00 | 28.78 | 27.99 | 23.98 | 25.63 | 23.40 | 22.15 | 18.71 | 19.96 |
| | Run3 | 40.00 | 29.40 | 27.58 | 24.01 | 26.91 | 23.59 | 22.48 | 18.57 | 19.80 |

| | Cord 5 | ΔCqsi107NES | ΔCqsi124 NES | ΔCqsi381 NES | ΔCqsiNEG NES | ΔΔCqsi107 NES | ΔΔCqsi124 NES | ΔΔCqsi381 NES |
|---|---|---|---|---|---|---|---|---|
| CC-RA | Run1 | 6.16 | 5.49 | 5.35 | 6.24 | 0.08 | 0.75 | 0.89 |
| | Run2 | 5.38 | 5.84 | 5.27 | 5.67 | 0.29 | -0.17 | 0.40 |
| | Run3 | 5.81 | 5.10 | 5.44 | 7.11 | 1.30 | 2.01 | 1.67 |

| | Cord 5 | NTC | Cqsi107 TUBB3 | Cqsi124 TUBB3 | Cqsi381 TUBB3 | CqsiNEG TUBB3 | Cqsi07 GAPDH | Cqsi124 GAPDH | Cqsi381 GAPDH | CqsiNEG GAPDH |
|---|---|---|---|---|---|---|---|---|---|---|
| CC-RA | Run1 | 40.00 | 26.86 | 27.18 | 22.65 | 24.63 | 22.82 | 22.40 | 18.68 | 19.92 |
| | Run2 | 40.00 | 26.90 | 26.90 | 22.56 | 24.32 | 23.40 | 22.15 | 18.71 | 19.96 |
| | Run3 | 40.00 | 27.07 | 27.13 | 22.59 | 24.20 | 23.59 | 22.48 | 18.57 | 19.80 |

| | Cord 5 | ΔCqsi107 TUBB3 | ΔCqsi124 TUBB3 | ΔCqsi381 TUBB3 | ΔCqsiNEG TUBB3 | ΔΔCqsi107 TUBB3 | ΔΔCqsi124 TUBB3 | ΔΔCqsi381 TUBB3 |
|---|---|---|---|---|---|---|---|---|
| CC-RA | Run1 | 4.04 | 4.78 | 3.97 | 4.71 | 0.67 | -0.07 | 0.74 |
| | Run2 | 3.50 | 4.75 | 3.85 | 4.36 | 0.86 | -0.39 | 0.51 |
| | Run3 | 3.48 | 4.65 | 4.02 | 4.40 | 0.92 | -0.25 | 0.38 |

| | Cord 5 | NTC | Cqsi107 ND1 | Cqsi124 ND1 | Cqsi381 ND1 | CqsiNEG ND1 | Cqsi07 GAPDH | Cqsi124 GAPDH | Cqsi381 GAPDH | CqsiNEG GAPDH |
|---|---|---|---|---|---|---|---|---|---|---|
| CC-RA | Run1 | 40.00 | 28.09 | 35.15 | 25.88 | 26.96 | 19.31 | 26.96 | 16.51 | 17.52 |
| | Run2 | 40.00 | 27.95 | 35.32 | 25.86 | 27.56 | 19.25 | 26.57 | 16.60 | 17.53 |
| | Run3 | 40.00 | 28.17 | 35.53 | 25.45 | 26.93 | 19.21 | 26.23 | 16.69 | 17.47 |

| | Cord 5 | ΔCqsi107 ND1 | ΔCqsi124 ND1 | ΔCqsi381 ND1 | ΔCqsiNEG ND1 | ΔΔCqsi107 ND1 | ΔΔCqsi124 ND1 | ΔΔCqsi381 ND1 |
|---|---|---|---|---|---|---|---|---|
| CC-RA | Run1 | 8.78 | 8.19 | 9.37 | 9.44 | 0.66 | 1.25 | 0.07 |
| | Run2 | 8.70 | 8.75 | 9.26 | 10.03 | 1.33 | 1.28 | 0.77 |
| | Run3 | 8.96 | 9.30 | 8.76 | 9.46 | 0.50 | 0.16 | 0.70 |

| | Cord 5 | NTC | Cqsi107 MAP2 | Cqsi124 MAP2 | Cqsi381 MAP2 | CqsiNEG MAP2 | Cqsi07 GAPDH | Cqsi124 GAPDH | Cqsi381 GAPDH | CqsiNEG GAPDH |
|---|---|---|---|---|---|---|---|---|---|---|
| CC-RA | Run1 | 40.00 | 28.47 | 26.89 | 23.66 | 24.97 | 22.82 | 22.40 | 18.68 | 19.92 |
| | Run2 | 40.00 | 28.11 | 26.95 | 23.65 | 25.22 | 23.40 | 22.15 | 18.71 | 19.96 |
| | Run3 | 40.00 | 28.37 | 26.21 | 23.62 | 25.15 | 23.59 | 22.48 | 18.57 | 19.80 |

| | Cord 5 | ΔCqsi107 MAP2 | ΔCqsi124 MAP2 | ΔCqsi381 MAP2 | ΔCqsiNEG MAP2 | ΔΔCqsi107 MAP2 | ΔΔCqsi124 MAP2 | ΔΔCqsi381 MAP2 |
|---|---|---|---|---|---|---|---|---|
| CC-RA | Run1 | 5.65 | 4.49 | 4.98 | 5.05 | -0.60 | 0.56 | 0.07 |
| | Run2 | 4.71 | 4.80 | 4.94 | 5.26 | 0.55 | 0.46 | 0.32 |
| | Run3 | 4.78 | 3.73 | 5.05 | 5.35 | 0.57 | 1.62 | 0.30 |

| | Cord 5 | NTC | Cqsi107 NEU | Cqsi124 NEU | Cqsi381 NEU | CqsiNEG NEU | Cqsi07 GAPDH | Cqsi124 GAPDH | Cqsi381 GAPDH | CqsiNEG GAPDH |
|---|---|---|---|---|---|---|---|---|---|---|
| CC-RA | Run1 | 40.00 | 40.00 | 40.00 | 40.00 | 40.00 | 22.82 | 22.40 | 18.68 | 19.92 |
| | Run2 | 40.00 | 40.00 | 40.00 | 40.00 | 40.00 | 23.40 | 22.15 | 18.71 | 19.96 |
| | Run3 | 40.00 | 40.00 | 40.00 | 40.00 | 40.00 | 23.59 | 22.48 | 18.57 | 19.80 |

| | Cord 5 | ΔCqsi107 NEU | ΔCqsi124 NEU | ΔCqsi381 NEU | ΔCqsiNEG NEU | ΔΔCqsi107 NEU | ΔΔCqsi124 NEU | ΔΔCqsi381 NEU |
|---|---|---|---|---|---|---|---|---|
| CC-RA | Run1 | 17.18 | 17.60 | 21.32 | 20.08 | 2.90 | 2.48 | -1.24 |
| | Run2 | 16.60 | 17.85 | 21.29 | 20.04 | 3.44 | 2.19 | -1.25 |
| | Run3 | 16.41 | 17.52 | 21.43 | 20.20 | 3.79 | 2.68 | -1.23 |

| | Cord 6 | NTC | Cqsi107 NES | Cqsi124 NES | Cqsi381 NES | CqsiNEG NES | Cqsi07 GAPDH | Cqsi124 GAPDH | Cqsi381 GAPDH | CqsiNEG GAPDH |
|---|---|---|---|---|---|---|---|---|---|---|
| CC-RA | Run1 | 34.44 | 40.00 | 30.66 | 26.51 | 27.47 | 29.15 | 17.59 | 23.24 | 22.44 |
| | Run2 | 34.82 | 40.00 | 33.04 | 27.27 | 25.54 | 27.64 | 17.23 | 22.84 | 22.37 |
| | Run3 | 34.74 | 38.66 | 22.80 | 26.65 | 24.62 | 27.91 | 17.45 | 22.45 | 21.81 |

| | Cord 6 | ΔCqsi107NES | ΔCqsi124 NES | ΔCqsi381 NES | ΔCqsiNEG NES | ΔΔCqsi107 NES | ΔΔCqsi124 NES | ΔΔCqsi381 NES |
|---|---|---|---|---|---|---|---|---|
| CC-RA | Run1 | 10.85 | 13.07 | 3.27 | 5.03 | -5.82 | -8.04 | 1.76 |
| | Run2 | 12.36 | 15.81 | 4.43 | 3.17 | -9.19 | -12.64 | -1.26 |
| | Run3 | 10.75 | 5.35 | 4.20 | 2.81 | -7.94 | -2.54 | -1.39 |

| | Cord 6 | NTC | Cqsi107 TUBB3 | Cqsi124 TUBB3 | Cqsi381 TUBB3 | CqsiNEG TUBB3 | Cqsi07 GAPDH | Cqsi124 GAPDH | Cqsi381 GAPDH | CqsiNEG GAPDH |
|---|---|---|---|---|---|---|---|---|---|---|
| CC-RA | Run1 | 34.44 | 32.55 | 32.80 | 26.95 | 25.25 | 29.15 | 17.59 | 23.24 | 22.44 |
| | Run2 | 34.82 | 31.73 | 32.68 | 25.56 | 25.65 | 27.64 | 17.23 | 22.84 | 22.37 |
| | Run3 | 34.74 | 31.30 | 33.45 | 25.30 | 24.96 | 27.91 | 17.45 | 22.45 | 21.81 |

| | Cord 6 | ΔCqsi107 TUBB3 | ΔCqsi124 TUBB3 | ΔCqsi381 TUBB3 | ΔCqsiNEG TUBB3 | ΔΔCqsi107 TUBB3 | ΔΔCqsi124 TUBB3 | ΔΔCqsi381 TUBB3 |
|---|---|---|---|---|---|---|---|---|
| CC-RA | Run1 | 3.40 | 15.21 | 3.71 | 2.81 | -0.59 | -12.40 | -0.90 |
| | Run2 | 4.09 | 15.45 | 2.72 | 3.28 | -0.81 | -12.17 | 0.56 |
| | Run3 | 3.39 | 16.00 | 2.85 | 3.15 | -0.24 | -12.85 | 0.30 |

| | Cord 6 | NTC | Cqsi107 ND1 | Cqsi124 ND1 | Cqsi381 ND1 | CqsiNEG ND1 | Cqsi07 GAPDH | Cqsi124 GAPDH | Cqsi381 GAPDH | CqsiNEG GAPDH |
|---|---|---|---|---|---|---|---|---|---|---|
| CC-RA | Run1 | 40.00 | 29.45 | 23.87 | 27.77 | 27.76 | 22.84 | 17.28 | 20.08 | 21.15 |
| | Run2 | 40.00 | 28.70 | 24.08 | 27.01 | 28.70 | 22.74 | 17.16 | 20.08 | 21.02 |
| | Run3 | 40.00 | 30.08 | 23.88 | 27.58 | 28.52 | 22.99 | 17.18 | 20.12 | 21.15 |

| | Cord 6 | ΔCqsi107 ND1 | ΔCqsi124 ND1 | ΔCqsi381 ND1 | ΔCqsiNEG ND1 | ΔΔCqsi107 ND1 | ΔΔCqsi124 ND1 | ΔΔCqsi381 ND1 |
|---|---|---|---|---|---|---|---|---|
| CC-RA | Run1 | 6.61 | 6.59 | 7.69 | 6.61 | 0.00 | 0.02 | -1.08 |
| | Run2 | 5.96 | 6.92 | 6.93 | 7.68 | 1.72 | 0.76 | 0.75 |
| | Run3 | 7.09 | 6.70 | 7.46 | 7.37 | 0.28 | 0.67 | -0.09 |

| | Cord 6 | NTC | Cqsi107 MAP2 | Cqsi124 MAP2 | Cqsi381 MAP2 | CqsiNEG MAP2 | Cqsi07 GAPDH | Cqsi124 GAPDH | Cqsi381 GAPDH | CqsiNEG GAPDH |
|---|---|---|---|---|---|---|---|---|---|---|
| CC-RA | Run1 | 34.44 | 34.13 | 34.00 | 25.27 | 25.91 | 29.15 | 17.59 | 23.24 | 22.44 |
| | Run2 | 34.82 | 40.00 | 31.30 | 26.22 | 24.94 | 27.64 | 17.23 | 22.84 | 22.37 |
| | Run3 | 34.74 | 40.00 | 33.83 | 25.69 | 24.29 | 27.91 | 17.45 | 22.45 | 21.81 |

| | Cord 6 | ΔCqsi107 MAP2 | ΔCqsi124 MAP2 | ΔCqsi381 MAP2 | ΔCqsiNEG MAP2 | ΔΔCqsi107 MAP2 | ΔΔCqsi124 MAP2 | ΔΔCqsi381 MAP2 |
|---|---|---|---|---|---|---|---|---|
| CC-RA | Run1 | 4.98 | 16.41 | 2.03 | 3.47 | -1.51 | -12.94 | 1.44 |
| | Run2 | 12.36 | 14.07 | 3.38 | 2.57 | -9.79 | -11.50 | -0.81 |
| | Run3 | 12.09 | 16.38 | 3.24 | 2.48 | -9.61 | -13.90 | -0.76 |

| | Cord 6 | NTC | Cqsi107 NEU | Cqsi124 NEU | Cqsi381 NEU | CqsiNEG NEU | Cqsi07 GAPDH | Cqsi124 GAPDH | Cqsi381 GAPDH | CqsiNEG GAPDH |
|---|---|---|---|---|---|---|---|---|---|---|
| CC-RA | Run1 | 34.44 | 40.00 | 34.77 | 40.00 | 33.64 | 29.15 | 17.59 | 23.24 | 22.44 |
| | Run2 | 34.82 | 40.00 | 36.38 | 40.00 | 33.45 | 27.64 | 17.23 | 22.84 | 22.37 |
| | Run3 | 34.74 | 40.00 | 37.81 | 40.00 | 33.72 | 27.91 | 17.45 | 22.45 | 21.81 |

| | Cord 6 | ΔCqsi107 NEU | ΔCqsi124 NEU | ΔCqsi381 NEU | ΔCqsiNEG NEU | ΔΔCqsi107 NEU | ΔΔCqsi124 NEU | ΔΔCqsi381 NEU |
|---|---|---|---|---|---|---|---|---|
| CC-RA | Run1 | 10.85 | 17.18 | 16.76 | 11.20 | 0.35 | -5.98 | -5.56 |
| | Run2 | 12.36 | 19.15 | 17.16 | 11.08 | -1.28 | -8.07 | -6.08 |
| | Run3 | 12.09 | 20.36 | 17.55 | 11.91 | -0.18 | -8.45 | -5.64 |

| | Cord 13 | NTC | Cqsi107 NES | Cqsi124 NES | Cqsi381 NES | CqsiNEG NES | Cqsi07 GAPDH | Cqsi124 GAPDH | Cqsi381 GAPDH | CqsiNEG GAPDH |
|---|---|---|---|---|---|---|---|---|---|---|
| CC-RA | Run1 | 39.25 | 25.94 | 27.03 | 26.87 | 26.47 | 17.55 | 16.78 | 17.41 | 17.41 |
| | Run2 | 38.84 | 25.68 | 26.62 | 26.91 | 26.48 | 17.65 | 16.92 | 17.41 | 17.50 |
| | Run3 | 40.00 | 25.62 | 26.82 | 27.06 | 26.25 | 17.83 | 16.97 | 17.36 | 17.74 |

| | Cord 13 | ΔCqsi107NES | ΔCqsi124 NES | ΔCqsi381 NES | ΔCqsiNEG NES | ΔΔCqsi107 NES | ΔΔCqsi124 NES | ΔΔCqsi381 NES |
|---|---|---|---|---|---|---|---|---|
| CC-RA | Run1 | 8.39 | 10.25 | 9.46 | 9.06 | 0.67 | -1.19 | -0.40 |
| | Run2 | 8.03 | 9.70 | 9.50 | 8.98 | 0.95 | -0.72 | -0.52 |
| | Run3 | 7.79 | 9.85 | 9.70 | 8.51 | 0.72 | -1.34 | -1.19 |

| | Cord 13 | NTC | Cqsi107 TUBB3 | Cqsi124 TUBB3 | Cqsi381 TUBB3 | CqsiNEG TUBB3 | Cqsi07 GAPDH | Cqsi124 GAPDH | Cqsi381 GAPDH | CqsiNEG GAPDH |
|---|---|---|---|---|---|---|---|---|---|---|
| CC-RA | Run1 | 39.25 | 26.41 | 33.92 | 24.82 | 25.96 | 17.55 | 16.78 | 17.41 | 17.41 |
| | Run2 | 38.84 | 26.51 | 34.80 | 24.93 | 25.94 | 17.65 | 16.92 | 17.41 | 17.50 |
| | Run3 | 40.00 | 26.23 | 35.87 | 24.91 | 26.16 | 17.83 | 16.97 | 17.36 | 17.74 |

| | Cord 13 | ΔCqsi107 TUBB3 | ΔCqsi124 TUBB3 | ΔCqsi381 TUBB3 | ΔCqsiNEG TUBB3 | ΔΔCqsi107 TUBB3 | ΔΔCqsi124 TUBB3 | ΔΔCqsi381 TUBB3 |
|---|---|---|---|---|---|---|---|---|
| CC-RA | Run1 | 8.86 | 17.14 | 7.41 | 8.55 | -0.31 | -8.59 | 1.14 |
| | Run2 | 8.86 | 17.88 | 7.52 | 8.44 | -0.42 | -9.44 | 0.92 |
| | Run3 | 8.40 | 18.90 | 7.55 | 8.42 | 0.02 | -10.48 | 0.87 |

| | Cord 13 | NTC | Cqsi107 ND1 | Cqsi124 ND1 | Cqsi381 ND1 | CqsiNEG ND1 | Cqsi07 GAPDH | Cqsi124 GAPDH | Cqsi381 GAPDH | CqsiNEG GAPDH |
|---|---|---|---|---|---|---|---|---|---|---|
| CC-RA | Run1 | 40.00 | 18.93 | 18.42 | 19.17 | 18.93 | 15.77 | 15.49 | 16.02 | 15.59 |
| | Run2 | 40.00 | 19.05 | 18.70 | 19.32 | 19.01 | 15.87 | 15.79 | 16.05 | 15.68 |
| | Run3 | 40.00 | 18.83 | 18.27 | 19.02 | 18.73 | 15.93 | 15.61 | 16.00 | 15.64 |

| | Cord 13 | ΔCqsi107 ND1 | ΔCqsi124 ND1 | ΔCqsi381 ND1 | ΔCqsiNEG ND1 | ΔΔCqsi107 ND1 | ΔΔCqsi124 ND1 | ΔΔCqsi381 ND1 |
|---|---|---|---|---|---|---|---|---|
| CC-RA | Run1 | 3.16 | 2.93 | 3.15 | 3.34 | 0.18 | 0.41 | 0.19 |
| | Run2 | 3.18 | 2.91 | 3.27 | 3.33 | 0.15 | 0.42 | 0.06 |
| | Run3 | 2.90 | 2.66 | 3.02 | 3.09 | 0.19 | 0.43 | 0.07 |

| | Cord 13 | NTC | Cqsi107 MAP2 | Cqsi124 MAP2 | Cqsi381 MAP2 | CqsiNEG MAP2 | Cqsi07 GAPDH | Cqsi124 GAPDH | Cqsi381 GAPDH | CqsiNEG GAPDH |
|---|---|---|---|---|---|---|---|---|---|---|
| CC-RA | Run1 | 39.25 | 25.88 | 30.40 | 25.22 | 25.85 | 17.55 | 16.78 | 17.41 | 17.41 |
| | Run2 | 38.84 | 25.95 | 31.38 | 25.54 | 25.82 | 17.65 | 16.92 | 17.41 | 17.50 |
| | Run3 | 40.00 | 26.22 | 31.09 | 25.18 | 25.90 | 17.83 | 16.97 | 17.36 | 17.74 |

| | Cord 13 | ΔCqsi107 MAP2 | ΔCqsi124 MAP2 | ΔCqsi381 MAP2 | ΔCqsiNEG MAP2 | ΔΔCqsi107 MAP2 | ΔΔCqsi124 MAP2 | ΔΔCqsi381 MAP2 |
|---|---|---|---|---|---|---|---|---|
| CC-RA | Run1 | 8.33 | 13.62 | 7.81 | 8.44 | 0.11 | -5.18 | 0.63 |
| | Run2 | 8.30 | 14.46 | 8.13 | 8.32 | 0.02 | -6.14 | 0.19 |
| | Run3 | 8.39 | 14.12 | 7.82 | 8.16 | -0.23 | -5.96 | 0.34 |

| | Cord 13 | NTC | Cqsi107 NEU | Cqsi124 NEU | Cqsi381 NEU | CqsiNEG NEU | Cqsi07 GAPDH | Cqsi124 GAPDH | Cqsi381 GAPDH | CqsiNEG GAPDH |
|---|---|---|---|---|---|---|---|---|---|---|
| CC-RA | Run1 | 39.25 | 35.16 | 35.09 | 36.47 | 34.38 | 17.55 | 16.78 | 17.41 | 17.41 |
| | Run2 | 38.84 | 33.74 | 34.86 | 34.96 | 34.88 | 17.65 | 16.92 | 17.41 | 17.50 |
| | Run3 | 40.00 | 33.84 | 36.44 | 35.19 | 36.01 | 17.83 | 16.97 | 17.36 | 17.74 |

| | Cord 13 | ΔCqsi107 NEU | ΔCqsi124 NEU | ΔCqsi381 NEU | ΔCqsiNEG NEU | ΔΔCqsi107 NEU | ΔΔCqsi124 NEU | ΔΔCqsi381 NEU |
|---|---|---|---|---|---|---|---|---|
| CC-RA | Run1 | 17.61 | 18.31 | 19.06 | 16.97 | -0.64 | -1.34 | -2.09 |
| | Run2 | 16.09 | 17.94 | 17.55 | 17.38 | 1.29 | -0.56 | -0.17 |
| | Run3 | 16.01 | 19.47 | 17.83 | 18.27 | 2.26 | -1.20 | 0.44 |

# Annex IV
# Statistical Analysis

## Neurite Length Statistical Analysis

| Cell Type | Statistic | df | P-value |
|---|---|---|---|
| CC | 0.951 | 25 | 0.262 |
| CC-RA | 0.955 | 25 | 0.319 |

Sharpio-Wilk Test of Normality

| Cell Type | Mean | N | Std. Deviation | Std. Error Mean |
|---|---|---|---|---|
| CC | 3.83 | 25 | 1.55 | 0.31 |
| CC-RA | 15.08 | 25 | 3.64 | 0.73 |

Paired Sample Statistics

| | | | 95% Confidence Interval of the Difference | | | | |
|---|---|---|---|---|---|---|---|
| Mean | Std. Deviation | Std. Error Mean | Lower | Upper | t | df | Sig. (2-tailed) |
| -11.24960 | 4.26542 | .85308 | -13.01028 | -9.48892 | -13.187 | 24 | 0.000 |

Paired Sample T-Test

## RT-qPCR Statistical Analysis

| Marker | Mann-Whitney U | P-value | Z Score |
|---|---|---|---|
| CD73 | 0.000 | 0.000 | -3.576 |
| CD90 | 0.000 | 0.000 | -3.576 |
| CD105 | 0.000 | 0.000 | -3.580 |
| CD34 | 32.500 | 0.480 | -0.707 |
| CD45 | 5.000 | 0.002 | -3.135 |

Mann-Whitney U Analysis CD Marker expression between MSC and CC

| Marker | Mann-Whitney U | P-value | Z Score |
|---|---|---|---|
| CD73 | 9.000 | 0.005 | -2.782 |
| CD90 | 0.000 | 0.000 | -3.576 |
| CD105 | 20.000 | 0.070 | -1.810 |
| CD34 | 40.500 | 1.000 | .000 |
| CD45 | 15.000 | 0.024 | -2.252 |

Mann-Whitney U Analysis CD Marker expression between CC and CC-RA

| Marker | Mann-Whitney U | P-value | Z Score |
|---|---|---|---|
| NES | 0.000 | 0.000 | -3.576 |
| SOX2 | 0.000 | 0.000 | -3.576 |
| OCT4 | 0.000 | 0.000 | -3.576 |
| TUBB3 | 0.000 | 0.000 | -3.576 |
| MASH1 | 14.000 | 0.019 | -2.341 |
| ND1 | 9.000 | 0.005 | -2.782 |
| MAP2 | 0.000 | 0.000 | -3.576 |
| NEU | 0.000 | 0.000 | -3.578 |

Mann-Whitney U Analysis Neural Marker expression between MSC and CC

| Marker | Mann-Whitney U | P-value | Z Score |
|---|---|---|---|
| NES | 18.000 | 0.047 | -1.987 |
| SOX2 | 8.000 | 0.004 | -2.870 |
| OCT4 | 9.000 | 0.005 | -2.782 |
| TUBB3 | 11.000 | 0.009 | -2.605 |
| MASH1 | 0.000 | 0.004 | -2.870 |
| ND1 | 34.000 | 0.566 | -0.574 |
| MAP2 | 28.000 | 0.270 | -1.104 |
| NEU | 27.000 | 0.233 | -1.193 |

Mann-Whitney U Analysis between CC and CC-RA Neural Marker expression

| Cell Type | Target | Mann-Whitney U | P-value | Z Score |
|---|---|---|---|---|
| MSC | DICER | 1.000 | 0.006 | -2.722 |
| | PTP1B | 15.000 | 0.631 | -0.480 |
| | HES1 | 0.000 | 0.004 | -2.882 |
| CC | DICER | 1.000 | 0.000 | -3.488 |
| | PTP1B | 0.000 | 0.000 | -3.576 |
| | HES1 | 30.000 | 0.354 | -0.927 |
| CC-RA | DICER | 22.000 | 0.102 | -1.634 |
| | PTP1B | 15.000 | 0.024 | -2.253 |
| | HES1 | 30.000 | 0.354 | -0.927 |

Mann-Whitney U Analysis for target genes

NES

| Cell Type | siRNA | Mann-Whitney U | P-value | Z Score |
|---|---|---|---|---|
| MSC | siR-107 | 0.000 | 0.004 | -2.882 |
| | siR-124 | 0.000 | 0.004 | -2.882 |
| | siR-381 | 0.000 | 0.004 | -2.882 |
| CC | siR-107 | 36.000 | 0.691 | -0.397 |
| | siR-124 | 11.00 | 0.009 | -2.605 |
| | siR-381 | 31.00 | o.402 | -0.839 |
| CC-RA | siR-107 | 25.000 | 0.171 | -1.369 |
| | siR-124 | 23.000 | 0.122 | -1.545 |
| | siR-381 | 39.000 | 0.895 | -0.132 |

Mann-Whitney U Analysis for NES expression post transfection

TUBB3

| Cell Type | siRNA | Mann-Whitney U | P-value | Z Score |
|---|---|---|---|---|
| MSC | siR-107 | 12.500 | 0.378 | -0.882 |
| | siR-124 | 0.000 | 0.004 | -2.882 |
| | siR-381 | 0.000 | 0.004 | -2.882 |
| CC | siR-107 | 22.000 | 0.102 | -1.634 |
| | siR-124 | 22.000 | 0.102 | -1.634 |
| | siR-381 | 19.500 | 0.064 | -1.855 |
| CC-RA | siR-107 | 39.000 | 0.895 | -0.133 |
| | siR-124 | 10.000 | 0.007 | -2.693 |
| | siR-381 | 31.000 | 0.402 | -0.839 |

Mann-Whitney U Analysis for TUBB3 expression post transfection

ND1

| Cell Type | siRNA | Mann-Whitney U | P-value | Z Score |
|---|---|---|---|---|
| MSC | siR-107 | 6.000 | 0.055 | -1.922 |
| | siR-124 | 7.000 | 0.078 | -1.761 |
| | siR-381 | 17.000 | 0.873 | -0.160 |
| CC | siR-107 | 18.000 | 0.047 | -1.987 |
| | siR-124 | 22.000 | 0.102 | -1.634 |
| | siR-381 | 18.000 | 0.047 | -1.987 |
| CC-RA | siR-107 | 30.500 | 0.377 | -0.883 |
| | siR-124 | 29.000 | 0.310 | -1.015 |
| | siR-381 | 35.000 | 0.627 | -0.486 |

Mann-Whitney U Analysis for ND1 expression post transfection

MAP2

| Cell Type | siRNA | Mann-Whitney U | P-value | Z Score |
|---|---|---|---|---|
| MSC | siR-107 | 0.000 | 0.004 | -2.903 |
| | siR-124 | 0.000 | 0.004 | -2.908 |
| | siR-381 | 6.000 | 0.053 | -1.935 |
| CC | siR-107 | 29.500 | 0.331 | -0.972 |
| | siR-124 | 28.000 | 0.270 | -1.104 |
| | siR-381 | 30.500 | 0.377 | -0.884 |
| CC-RA | siR-107 | 25.000 | 0.171 | -1.369 |
| | siR-124 | 18.000 | 0.47 | -1.987 |
| | siR-381 | 31.500 | 0.427 | -0.795 |

Mann-Whitney U Analysis for MAP2 expression post transfection

NEU

| Cell Type | siRNA | Mann-Whitney U | P-value | Z Score |
|---|---|---|---|---|
| MSC | siR-107 | 0.000 | 0.004 | -2.908 |
| | siR-124 | 0.000 | 0.004 | -2.908 |
| | siR-381 | 0.000 | 0.004 | -2.908 |
| CC | siR-107 | 39.000 | 0.895 | -0.133 |
| | siR-124 | 9.000 | 0.005 | -2.783 |
| | siR-381 | 28.000 | 0.269 | -1.104 |
| CC-RA | siR-107 | 27.000 | 0.233 | -1.192 |
| | siR-124 | 30.000 | 0.354 | -0.927 |
| | siR-381 | 26.000 | 0.200 | -1.2381 |

Mann-Whitney U Analysis for NEU expression post transfection